POINT-OF-CARE TESTING FOR INFECTIOUS AND FOODBORNE PATHOGENS

EDITED BY: Yanbin Li, Hongchao Gou, Yingchun Fu, Jianmin Zhang and Ciprian Iliescu

PUBLISHED IN: Frontiers in Cellular and Infection Microbiology and Frontiers in Bioengineering and Biotechnology

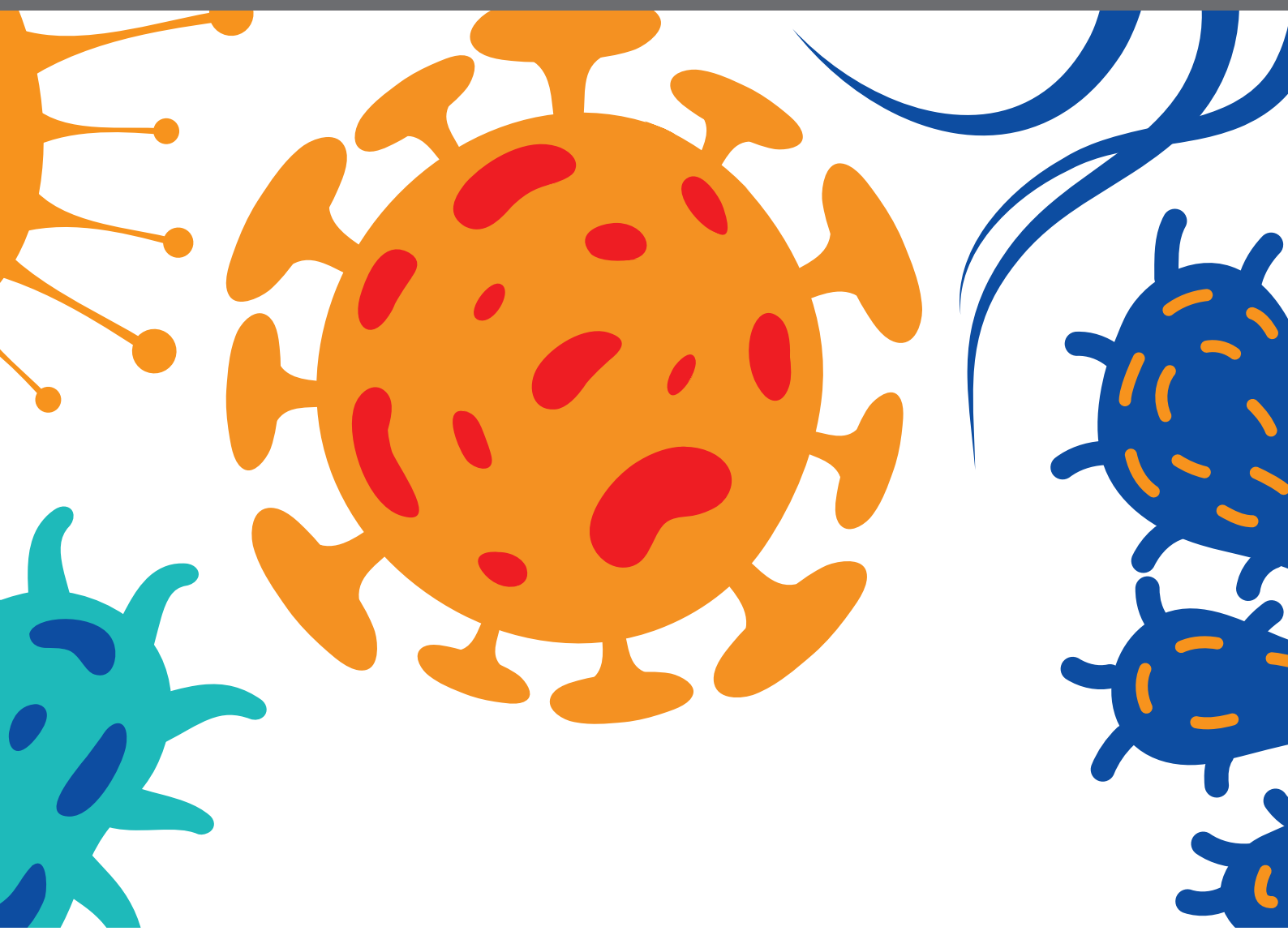

frontiers Research Topics

frontiers

ISSN 1664-8714
ISBN 978-2-88976-890-5
DOI 10.3389/978-2-88976-890-5

About Frontiers

Frontiers is more than just an open-access publisher of scholarly articles: it is a pioneering approach to the world of academia, radically improving the way scholarly research is managed. The grand vision of Frontiers is a world where all people have an equal opportunity to seek, share and generate knowledge. Frontiers provides immediate and permanent online open access to all its publications, but this alone is not enough to realize our grand goals.

Frontiers Journal Series

The Frontiers Journal Series is a multi-tier and interdisciplinary set of open-access, online journals, promising a paradigm shift from the current review, selection and dissemination processes in academic publishing. All Frontiers journals are driven by researchers for researchers; therefore, they constitute a service to the scholarly community. At the same time, the Frontiers Journal Series operates on a revolutionary invention, the tiered publishing system, initially addressing specific communities of scholars, and gradually climbing up to broader public understanding, thus serving the interests of the lay society, too.

Dedication to Quality

Each Frontiers article is a landmark of the highest quality, thanks to genuinely collaborative interactions between authors and review editors, who include some of the world's best academicians. Research must be certified by peers before entering a stream of knowledge that may eventually reach the public - and shape society; therefore, Frontiers only applies the most rigorous and unbiased reviews.
Frontiers revolutionizes research publishing by freely delivering the most outstanding research, evaluated with no bias from both the academic and social point of view. By applying the most advanced information technologies, Frontiers is catapulting scholarly publishing into a new generation.

What are Frontiers Research Topics?

Frontiers Research Topics are very popular trademarks of the Frontiers Journals Series: they are collections of at least ten articles, all centered on a particular subject. With their unique mix of varied contributions from Original Research to Review Articles, Frontiers Research Topics unify the most influential researchers, the latest key findings and historical advances in a hot research area! Find out more on how to host your own Frontiers Research Topic or contribute to one as an author by contacting the Frontiers Editorial Office: frontiersin.org/about/contact

POINT-OF-CARE TESTING FOR INFECTIOUS AND FOODBORNE PATHOGENS

Topic Editors:
Yanbin Li, University of Arkansas, United States
Hongchao Gou, Institute of Animal Health, Guangdong Academy of Agricultural Sciences, China
Yingchun Fu, Zhejiang University, China
Jianmin Zhang, South China Agricultural University, China
Ciprian Iliescu, Regional Institute of Oncology (IRO), Romania

Citation: Li, Y., Gou, H., Fu, Y., Zhang, J., Iliescu, C., eds. (2022). Point-of-Care Testing for Infectious and Foodborne Pathogens. Lausanne: Frontiers Media SA. doi: 10.3389/978-2-88976-890-5

Table of Contents

frontiers | Frontiers in Cellular and Infection Microbiology

TYPE Editorial
PUBLISHED 28 July 2022
DOI 10.3389/fcimb.2022.975449

OPEN ACCESS

EDITED AND REVIEWED BY
Max Maurin,
Université Grenoble Alpes,
France

*CORRESPONDENCE
Jianmin Zhang
junfeng-v@163.com
Ming Liao
mliao@scau.edu.cn

SPECIALTY SECTION
This article was submitted to Clinical Microbiology, a section of the journal Frontiers in Cellular and Infection Microbiology

RECEIVED 22 June 2022
ACCEPTED 13 July 2022
PUBLISHED 28 July 2022

CITATION
Gou H, Zhang J and Liao M (2022) Editorial: Point-of-care testing for infectious and foodborne pathogens. *Front. Cell. Infect. Microbiol.* 12:975449. doi: 10.3389/fcimb.2022.975449

Editorial: Point-of-care testing for infectious and foodborne pathogens

Hongchao Gou[1], Jianmin Zhang[2*] and Ming Liao[1,2*]

[1]Institute of Animal Health, Guangdong Academy of Agricultural Sciences, Guangzhou, China; Guangdong Provincial Key Laboratory of Livestock Disease Prevention, Guangzhou, China; Maoming Branch, Guangdong Laboratory for Lingnan Modern Agriculture, Maoming, China; Scientific Observation and Experiment Station of Veterinary Drugs and Diagnostic Techniques of Guangdong Province, Guangzhou, China, [2]National and Regional Joint Engineering Laboratory for Medicament of Zoonoses Prevention and Control; Key Laboratory of Zoonoses, Ministry of Agriculture; Key Laboratory of Zoonoses Prevention and Control of Guangdong Province; Key Laboratory of Animal Vaccine Development, Ministry of Agriculture; Guangdong Laboratory for Lingnan Modern Agriculture; College of Veterinary Medicine, South China Agricultural University, Guangzhou, China

KEYWORDS

infectious and foodborne pathogens, coronavirus disease 2019 (COVID-19), point-of-care testing (POCT), isothermal amplification, multiplex real-time PCR

Editorial on the Research Topic
Point-of-care testing for infectious and foodborne pathogens

Infectious and foodborne pathogens usually pose emergency threat to the human and animal health. In recent years, they are gaining more attention due to emerging and re-emerging outbreaks, such as Influenza virus, Severe Acute Respiratory Syndromes virus, Ebola virus, Norovirus, *Salmonella Typhimurium*, *Escherichia coli* O157, Hepatitis E Virus, African swine fever virus and so on. Since December 2019, the outbreak of coronavirus disease 2019 (COVID-19) around the world was declared as a disease of "public health emergency of international concern" by the World Health Organization (WHO).

Rapid and early detection of infectious and foodborne pathogens display a dramatic impact in controlling and preventing an outbreak. To face current challenges regarding infectious and foodborne pathogens, a point-of-care testing (POCT) concept has been introduced to detection technologies and devices. Especially for COVID-19, POCT technologies displayed the advance of user-friendly, rapid detection, so they can be directly used on-site or at home. This Research Topic is focused on novel ideas in POCT technologies and devices for infectious and foodborne pathogens, aimed at improving on-site application of rapid diagnostic techniques by detecting analytes including antigens, nucleic acids and specific antibodies for microorganisms.

Of great concern to the increasing incidence of acute respiratory tract infections (RTI), which leads to high mortality in children and adults worldwide in recent years, Gradisteanu Pircalabioru et al. reviewed the advances in microbiological diagnostic of viral RTI in this Research Topic. They provided a non-exhaustive overview of conventional viral detection and infection monitoring methods and technological improvements. Focused on miniaturized systems and evaluating the clinical perspectives for further use as POCT, they discussed the potential of immunoassays and nucleic acid (NA) amplification and the new approaches such as microfluidics and biosensors-based techniques as rapid diagnostic platforms for viral respiratory infections detection methods and monitoring. Since viral infections impose stringent detection and spread monitoring, they presented the emerging Internet-of-Things (IoT) and highlight their potential as a future solution in the virology diagnostic and respiratory infections prophylaxis.

In the face of the sudden outbreak of COVID-19, Daoud et al. validated two commercial kits for the detection of IgM and IgG using lateral flow immunoassay tests and to study the effect of the combination of both serology kits for better detection of immunoglobulins. The results showed sensitivities for IgM detection varying between 58.9 and 66.2% for the kits alone and 87.7% of the combination of both kits. IgG detection was not significantly affected by this combination. Both kits manifested high specificities (99.2–100%). Chen et al. developed a novel molecular diagnosis technique, named multiplex reverse transcription loop-mediated isothermal amplification linked to a nanoparticle-based lateral flow biosensor (mRT-LAMP-LFB). This test was applied to detect SARS-CoV-2 based on the SARS-CoV-2 RdRp and N genes. The full process, including reaction preparation, viral RNA extraction, RT-LAMP, and product identification, could be achieved in 80 min. The mRT-LAMP-LFB detection results were consistent with the Real-Time RT-PCR Kit (Sansure biotech Inc, China) in the evaluation of clinical samples. To identify SARS-CoV-2 variants, Niu et al. established a highly sensitive and portable on-site detection method for the HV69-70del which exist in SARS-CoV-2 Alpha and Omicron variants using a PCR-based CRISPR/Cas13a detection system (PCR-CRISPR). The results showed that the PCR-CRISPR detection method can detect 1 copies/μL SARS-CoV-2 HV69-70del mutant RNA and identify 0.1% of mutant RNA in mixed samples, which was more sensitive than the RT-qPCR based commercial SARS-CoV-2 variants detection kits and sanger sequencing. Additionally, by combining PCR-CRISPR with lateral flow strip, they provided a novel diagnosis tool to identify SARS-CoV-2 variants in primary and resource-limited medical institutions without professional and expensive fluorescent detector.

Hepatitis C virus (HCV) infection is a global public health threat. While immunoassays and qPCR play a significant role in detecting HCV, rapid and accurate point-of-care testing is important for pathogen identification. Wang et al. established a reverse transcription recombinase-aided amplification-lateral flow dipstick (RT-RAA-LFD) assay to detect HCV. Using extracted RNAs from 46 anti-HCV antibody-positive samples, RT-RAA-LFD showed 100% positive and negative concordance rates with qPCR. The RT-RAA-LFD assay established is suitable for the rapid clinical detection of HCV at the community level and in remote areas.

African swine fever (ASF) is a highly contagious and usually deadly porcine infectious disease listed as a notifiable disease by the World Organization for Animal Health (OIE). A sensitive, specific, rapid, and simple molecular point of care testing for African swine fever virus (ASFV) B646L gene in blood samples was established by Zhang et al., including treatment of blood samples with simple dilution and boiling for 5 min, isothermal amplification with recombinase-aided amplification (RAA), and visual readout with lateral flow assay (LFA) at room temperature. Without the need to extract viral DNA in blood samples, the intact workflow from sampling to final diagnostic decision can be completed with minimal equipment requirement in 30 min. Evaluation of clinical blood samples of RAA-LFA showed 100% coincident rate with OIE-recommended PCR, in testing both extracted DNAs and treated bloods. They also found that some components in blood samples greatly inhibited PCR performance, but had little effect on RAA. Inhibitory effect can be eliminated when blood was diluted at least 32-64-fold for direct PCR, while only a 2-4 fold dilution of blood was suitable for direct RAA, indicating RAA is a better choice than PCR when blood was used as detecting sample. Wang et al. established a cleaved probe-based loop-mediated isothermal amplification (CP-LAMP) detection method for ASFV. Based on the original primer sets, they targeted the ASFV 9GL gene sequence to design a probe harboring a ribonucleotide insertion. Ribonuclease H2 (RNase H2) enzyme activity can only be activated when the probe is perfectly complementary, resulting in hydrolytic release of a quencher moiety, and consequent signal amplification. Visualization of the fluorescence product was employed using a self-designed 3D-printed visualization function cassette, and the CP-LAMP method achieved specific identification and visual detection of ASFV. Porcine parvovirus (PPV) is an important cause of pig reproductive diseases. A rapid, visible, and economical clinical diagnostic strategy to detect PPV is necessary. By using three pairs of crRNA primers targeted to the VP2 gene, an ERA-CRISPR/Cas12a system for PPV detection was successfully developed by Wei et al. The approach involved isothermal detection at 37°C, and the method can be used for visual inspection.

For the rapid detection of foodborne pathogens, isothermal real-time recombinase polymerase amplification (RPA) and lateral flow strip detection (LFS RPA) were used. The LFS RPA targeted to the conserved sequence of invasion protein A (invA) to detect Salmonella spp was employed by Zhao et al. To quickly and directly detetct *Mycoplasma bovis* (*M. bovis*) in bovine milk, an RPA assay based on the fluorescence monitoring

(real-time RPA) and an RPA assay combined with a lateral flow strip (LFS RPA) were conducted by Li et al. Lu et al. developed a Cas12a-assisted rapid isothermal detection (CARID) system for the detection of toxigenic *V. cholerae* serogroups O1 and O139 by combining recombinase-aided amplification and CRISPR-Cas (clustered regularly interspaced short palindromic repeats and CRISPR-associated proteins). The results can be determined by fluorescence signal and visualized by lateral flow dipstick. Multiple-CARID was also established for efficiency and economic considerations with an acceptable decrease in sensitivity. Simulated sample tests showed that CARID was suitable for complex samples. The conventional serotyping methods for differentiating *Salmonella* serovars are complicated, time-consuming, laborious, and expensive; therefore, rapid and accurate molecular diagnostic methods are needed for effective detection and prevention of contamination. Xin et al. developed and evaluated a TaqMan multiplex real-time PCR assay for simultaneous detection and differentiation of the *S. Pullorum*, *S. Gallinarum*, *S. Enteritidis*, and *S. Typhimurium*. It achieved comparable results to the traditional bacteriological examination. Meanwhile, a multiplex TaqMan-based real-time PCR assay was developed on the BD MAX platform by Li et al. This assay can simultaneously detect and differentiate *V. cholerae* and *V. parahaemolyticus* directly from human fecal specimens. The BD MAX assay was evaluated for its performance compared with conventional real-time PCR after automated DNA extraction steps, using 164 retrospective stool samples. The overall percent agreement between the BD MAX assay and real-time PCR was ≥ 98.8%.

In this Research Topic, some equipment also showed an advantage on POCT. For example, the Cepheid GeneXpert® (Xpert) CT/NG assay can be performed on the GeneXpert instrument platform in laboratories and is simple to operate. Han et al. reported that the Xpert CT/NG test exhibited high sensitivity and specificity in the detection of *Chlamydia trachomatis* (CT) and *Neisseria gonorrhoeae* (NG) in both urine and cervical samples when compared to the reference results. The 90-min turnaround time for CT and NG detection at the point of care using Xpert may enable patients to receive treatment promptly. Because the emergence and spread of the novel mobile Tet(X) tetracycline destructases confer high-level tigecycline and eravacycline resistance in *Escherichia coli* and *Acinetobacter* spp. and pose serious threats to human and animal health, a rapid and robust Tet(X) detection assay was urgently needed to monitor the dissemination of tigecycline resistance. Based on matrix-assisted laser desorption ionization-time of flight mass spectrometry (MALDI-TOF MS), Cui et al. developed a rapid and simple assay to detect Tet(X) producers in Gram-negative bacteria. This MALDITet(X) test was based on the inactivation of tigecycline by a Tet(X)-producing strain after a 3-h incubation of bacterial cultures with tigecycline. Culture supernatants were analyzed using MALDI-TOF MS to identify peaks corresponding to tigecycline (586 ± 0.2 m/z) and a tigecycline metabolite (602 ± 0.2 m/z). The results were calculated using the MS ratio [metabolite/(metabolite + tigecycline)]. The sensitivity of the MALDITet(X) test with all 216 test strains was 99.19%, and specificity was 100%. The test can be completed within 3 h.

POCT requires that all of the analytical processes, from sample collection to result communication, should be performable in one or a few simple steps to reduce time and costs between the test and treatment. In general, some detection methods and equipment reported in this Research Topic have yet to be fully applied in POCT. They are likely to be improved by combining with microfluidics, biosensors, wireless cell phone based technologies, paper based devices and other advanced techniques in the future.

Author contributions

HG drafted the manuscript. JZ and ML participated the revision of this manuscript. All the authors read and approved the final manuscript.

Funding

This work was supported by grants from the Special fund for scientific innovation strategy-construction of high level Academy of Agriculture Science-Distinguished Scholar (R2020PY-JC001), the Project of Collaborative Innovation Center of GDAAS (XTXM202202), the Scientific innovation strategy-construction of high level Academy of Agriculture Science (202110TD), the Guangzhou Science and Technology Bureau (202103000096 and 202206010192) the Special Fund for Scientific Innovation Strategy-Construction of High Level Academy of Agriculture Science (R2017YJ-YB2005 and R2021PY-QY006) and the Start-up Research Project of Maoming Laboratory (2021TDQD002).

Conflict of interest

The authors declare that the research was conducted in the absence of any commercial or financial relationships that could be construed as a potential conflict of interest.

Publisher's note

frontiers in Cellular and Infection Microbiology

METHODS
published: 25 September 2020
doi: 10.3389/fcimb.2020.583341

Rapid Detection of High-Level Tigecycline Resistance in Tet(X)-Producing *Escherichia coli* and *Acinetobacter* spp. Based on MALDI-TOF MS

Ze-Hua Cui[1,2†], *Zi-Jian Zheng*[1,2†], *Tian Tang*[1,2], *Zi-Xing Zhong*[1,2], *Chao-Yue Cui*[1,2], *Xin-Lei Lian*[1,2], *Liang-Xing Fang*[1,2], *Qian He*[1,2], *Xi-Ran Wang*[1,2], *Chong Chen*[1,2], *Bing He*[1,2], *Min-Ge Wang*[1,2], *Ya-Hong Liu*[1,2,3], *Xiao-Ping Liao*[1,2,3] and *Jian Sun*[1,2,3*]

[1] National Risk Assessment Laboratory for Antimicrobial Resistance of Animal Original Bacteria, South China Agricultural University, Guangzhou, China, [2] Guangdong Provincial Key Laboratory of Veterinary Pharmaceutics Development and Safety Evaluation, South China Agricultural University, Guangzhou, China, [3] Guangdong Laboratory for Lingnan Modern Agriculture, Guangzhou, China

The emergence and spread of the novel mobile Tet(X) tetracycline destructases confer high-level tigecycline and eravacycline resistance in *Escherichia coli* and *Acinetobacter* spp. and pose serious threats to human and animal health. Therefore, a rapid and robust Tet(X) detection assay was urgently needed to monitor the dissemination of tigecycline resistance. We developed a rapid and simple assay to detect Tet(X) producers in Gram-negative bacteria based on matrix-assisted laser desorption ionization–time of flight mass spectrometry (MALDI-TOF MS). This MALDI$^{Tet(X)}$ test was based on the inactivation of tigecycline by a Tet(X)-producing strain after a 3-h incubation of bacterial cultures with tigecycline. Culture supernatants were analyzed using MALDI-TOF MS to identify peaks corresponding to tigecycline (586 ± 0.2 m/z) and a tigecycline metabolite (602 ± 0.2 m/z). The results were calculated using the MS ratio [metabolite/(metabolite + tigecycline)]. The sensitivity of the MALDI$^{Tet(X)}$ test with all 216 test strains was 99.19%, and specificity was 100%. The test can be completed within 3 h. Overall, the MALDI$^{Tet(X)}$ test is an accurate, rapid, cost-effective method for the detection of Tet(X)-producing *E. coli* and *Acinetobacter* spp. by determining the unique peak of an oxygen-modified derivative of tigecycline.

Keywords: rapid detection, MALDI TOF MS, Tet(X), plasmid-mediated, high-level tigecycline resistance

OPEN ACCESS

Edited by:
Hongchao Gou,
Guangdong Academy of Agricultural Sciences, China

Reviewed by:
Lei Lei,
China Agricultural University, China
Zhihai Liu,
Qingdao Agricultural University, China

***Correspondence:**
Jian Sun
jiansun@scau.edu.cn

[†] These authors have contributed equally to this work

Specialty section:
This article was submitted to Clinical Microbiology, a section of the journal Frontiers in Cellular and Infection Microbiology

Received: *14 July 2020*
Accepted: *17 August 2020*
Published: *25 September 2020*

Citation:
Cui Z-H, Zheng Z-J, Tang T, Zhong Z-X, Cui C-Y, Lian X-L, Fang L-X, He Q, Wang X-R, Chen C, He B, Wang M-G, Liu Y-H, Liao X-P and Sun J (2020) Rapid Detection of High-Level Tigecycline Resistance in Tet(X)-Producing Escherichia coli and Acinetobacter spp. Based on MALDI-TOF MS. Front. Cell. Infect. Microbiol. 10:583341. doi: 10.3389/fcimb.2020.583341

INTRODUCTION

Tigecycline is a glycylcycline antibiotic and a last resort for treating serious infections caused by multidrug-resistant (MDR) Gram-negative bacteria and even for extensively drug-resistant Enterobacteriaceae and *Acinetobacter* spp. (Doan et al., 2006). Sporadic cases of tigecycline resistance in recent clinical MDR isolates

have been associated with either ribosomal protection or high-expression antibiotic efflux mechanisms (Linkevicius et al., 2016). These types of resistance affect antibiotic uptake and target interactions and do not affect the concentration or activity of tigecycline. In addition, these types of resistance can only be transferred vertically and not horizontally (Forsberg et al., 2015).

The appearance of the novel mobile Tet(X) tetracycline destructases has altered this situation with tigecycline and the new glycylcyclines, and Tet(X) activity renders these frontline drugs ineffective. The Tet(X) proteins are flavin monooxygenases that catalyze the degradation of tetracyclines and derivatives (Park et al., 2017). There are currently five that have been discovered in different bacterial species, Tet (X3), (X4), (X5), (X6), and (X7), and all confer high-level resistance to all tetracyclines including tigecycline and the newly Food and Drug Administration (FDA)-approved omadacycline and eravacycline; Tet (X), (X1), and (X2) mediate only first-generation and second-generation tetracycline resistance (He et al., 2019; Sun et al., 2019; Wang et al., 2019; Gasparrini et al., 2020). This poses a great threat to the clinical efficacy of the whole family of tetracycline antibiotics (Fang et al., 2020). Therefore, a rapid and robust Tet(X) detection assay is urgently needed to monitor the dissemination of tigecycline resistance.

Following the discovery of Tet(X3/4) in *Escherichia coli* and *Acinetobacter baumannii*, rapid detection methods based on multiplex real-time PCR were developed that could distinguish between *Tet*(X) variants (Ji et al., 2019; Fu et al., 2020). During this period, our laboratory developed a rapid detection method based on microbial growth tetracycline inactivation method (TIM) that could rapidly detect plasmid-mediated high-level tigecycline resistance. However, TIM required 6.5 h that included 3.5 h for the bacterial growth phase (Cui et al., 2020b). To our knowledge, there is currently no detection method for high-level tigecycline resistance bacteria using matrix-assisted laser desorption ionization–time of flight mass spectrometry (MALDI-TOF MS). Herein, we describe a method for rapid detection of Tet(X)-producing *E. coli* and *Acinetobacter* spp. using MALDI-TOF MS that we have named the MALDI$^{Tet(X)}$ test.

MATERIALS AND METHODS

Bacterial Strains

The 221 strains used in this study were isolated between June 2016 and November 2018 as previously described and had been stored in our archived collection (Chen et al., 2019; Sun et al., 2019; Cui et al., 2020a,b). These included 124 Tet(X)-producing *E. coli* and *Acinetobacter* spp. and 92 non-Tet(X) producers. The group included the five *E. coli* JM109 control strains pBAD24, pBAD24-tet(X3), pBAD24-tet(X4), pBAD24-tet(X6), and American Type Culture Collection (ATCC) 25922. The 124 Tet(X) producers consisted of 38 *tet*(X3) *Acinetobacter* spp., 69 *tet*(X4) *E. coli*, one *tet*(X2)-*tet*(X6) *Acinetobacter* spp., and 16 *tet*(X3)-*tet*(X6) *Acinetobacter* spp. There were also 92 Tet(X)-negative strains consisting of 37 *tet*(X)-negative *E. coli* but carrying at least one other tetracycline resistance gene: [19 *tet*(A), five *tet*(B), three *tet*(D), one *tet*(G), one *tet*(M), two *tet*(A)-*tet*(B), two *tet*(B)-*tet*(D), four *tet*(D)-*tet*(M)] as well as 16 *tet*(X)-negative *Salmonella enteritidis* strains that carried at least one other tetracycline resistance gene: [12 *tet*(B), two *tet*(A)-*tet*(B), one *tet*(B)-*tet*(D), one *tet*(B)-*tet*(M)] and 39 *E. coli* that lacked any tetracycline resistance gene. The five control and 154 test strains were used to establish the MALDI$^{Tet(X)}$ test (**Table 1**), and 62 test strains were used to test its sensitivity and specificity (**Table 2**). All strains used to establish and validate the MALDI$^{Tet(X)}$ test were randomly selected based on their species and genotype.

These test strains were isolated from feces (195), dust (three), sewage (eight), flower (one), and soil (nine) samples. The fecal samples were collected from chickens, ducks, geese, pigs, and patients at a tertiary hospital in Guangdong (**Supplementary Tables 1, 2**). All test strains were identified by MALDI-TOF MS (Axima-Assurance-Shimadzu).

Antibiotic Susceptibility Testing

Antimicrobial susceptibility assays were performed and interpreted according to Clinical and Laboratory Standards Institute (CLSI) guidelines (CLSI, 2018). Tetracycline and doxycycline minimum inhibitory concentrations (MICs) were determined using the agar dilution method, and the microdilution broth method was used for tigecycline, eravacycline, and omadacycline MIC determinations (Cui et al., 2020b). Tigecycline breakpoints for *E. coli* and *Acinetobacter* spp. were interpreted according to the FDA criteria as susceptible ($\leq$2 mg/L), intermediate (4 mg/L), and resistant ($\geq$8 mg/L), and eravacycline and omadacycline were uninterpreted with no breakpoint. *E. coli* ATCC 25922 was used as the quality control strain.

Detection of Tetracycline Resistance Genes

The tetracycline resistance genes *tet*(X3), *tet*(X4), *tet*(X6), *tet*(A), *tet*(B), *tet*(D), *tet*(G), and *tet*(M) were identified using PCR as previously described (Tuckman et al., 2007; He et al., 2019; Liu et al., 2020). In addition, a *tet*(X) universal PCR test was designed to examine the potential presence of *tet*(X) variants except for *tet*(X3), *tet*(X4), and *tet*(X6).

The MALDI$^{Tet(X)}$ Test

We used tigecycline as the substrate because Tet (X), (X1), and (X2) mediate tetracycline resistance but not tigecycline resistance (Park et al., 2017; Fang et al., 2020). A 10-μl loopful of an overnight bacterial culture incubated in lysogeny broth agar at 37°C was added to an Eppendorf tube containing 500 μl of 50 mg/L tigecycline (Yuanye, China) and vortexed for 1 min, followed by incubation at 37°C with shaking in the dark for 3 h and was then centrifuged for 3 min at 10,000 × g. A portion (1 μl) of the clear supernatant was spotted onto an MSP 384 target polished steel plate (Shimadzu, Kyoto, Japan) and allowed to dry at room temperature. The matrix (1 μl) α-cyano-4-hydroxycinnamic acid (Sigma-Aldrich, St. Louis, MO, USA) was overlaid onto each target spot. Mass spectra were acquired using a Shimadzu performance mass spectrometer and Shimadzu Biotech MALDI-MS software (Shimadzu) operating in positive linear ion mode between 100 and 1,000 Da. The

TABLE 1 | Characteristics of test strains used to establish the MALDI$^{Tet(X)}$ test.

Species	*n*	Genes	MIC					MS Ratio
			TC(1^{s})[a]	DOX(2^{s})[a]	TGC(3^{s})[a]	ERA(4^{s})[a]	OMA(4^{s})[a]	
Control strains	5							
E. coli-JM109-pBAD24-tet(X3)	1	*tet*(X3)	64	32	4	4	16	0.5 ± 0.09
E. coli-JM109-pBAD24-tet(X4)	1	*tet*(X4)	64	16	8	2	16	0.43 ± 0.11
E. coli-JM109-pBAD24-tet(X6)	1	*tet*(X6)	256	32	2	2	16	0.18 ± 0.01
E. coli-JM109 - pBAD24	1	non-*tet*(X)[b]	2	0.5	0.03	0.008	0.125	0 ± 0
E. coli 25922	1	non-*tet*(X)[b]	2	0.5	0.03	0.06	0.25	0 ± 0
Test strains								
Tet(X) producers	92							
Acinetobacter spp.	30	*tet*(X3)	64–256	1–64	8–64	4–32	8–64	0.03 ± 0.02–0.57 ± 0.14
E. coli	51	*tet*(X4)	32–>256	32–128	1–16	1–16	8–64	0.0067 ± 0.0095–0.48 ± 0.09
Acinetobacter spp.	1	*tet*(X2)- *tet*(X6)	>256	128	32	4	16	0.23 ± 0.12
Acinetobacter spp.	10	*tet*(X3)-*tet*(X6)	128–>256	8–128	32–64	4–16	8–64	0.02 ± 0.02–0.38 ± 0.12
Non-Tet(X) producers	62							
E. coli	19	*tet*(A)	4–256	4–256	0.06–1	0.06–2	0.25–4	0 ± 0
E. coli	5	*tet*(B)	256–>256	32–>256	0.125–2	0.25–1	2–8	0 ± 0
E. coli	1	*tet*(D)	256	32	0.25	0.25	4	0 ± 0
E. coli	1	*tet*(B)- *tet*(D)	256	32	0.25	0.25	4	0.0005 ± 0.0008
S. enteritidis	8	*tet*(B)	64–256	8–64	0.5–2	0.06–0.5	1–4	0 ± 0
S. enteritidis	1	*tet*(A)- *tet*(B)	128	64	0.5	0.06	2	0.0003 ± 0.0005
S. enteritidis	1	*tet*(B)-*tet*(D)	256	64	1	0.25	4	0 ± 0
S. enteritidis	1	*tet*(B)-*tet*(M)	256	64	1	0.125	2	0 ± 0
E. coli	25	non-*tet*(X)[b]	0.5–1	1	0.125–0.5	0.03–0.06	0.25–1	0 ± 0–0.0014 ± 0.0019

TET, tetracycline; DOX, doxycycline; TGC, tigecycline; ERV, eravacycline; OMA, omadacycline; MIC, minimum inhibitory concentration; MS, mass spectrometry.

[a] *The number in parentheses indicates the generation of tetracycline.*

[b] *Non-tet(X) strains lack all tet genes as well as tet(X).*

TABLE 2 | Characteristics of test strains used for test validation.

Species	*n*	Genes	MIC					MS Ratio
			TC(1s)[a]	DOX(2s)[a]	TGC(3s)[a]	ERA(4s)[a]	OMA(4s)[a]	
Tet(X) producers	32							
Acinetobacter spp.	8	*tet*(X3)	128–>256	8–128	16–64	4–16	4–64	0.0134 ± 0.0038–0.32 ± 0.13
E. coli	18	*tet*(X4)	32–>256	32–64	4–32	4–16	16–64	0.0008 ± 0.0011–0.41 ± 0.22
Acinetobacter spp.	6	*tet*(X3)-*tet*(X6)	32–>256	8–128	16–32	4–8	4–16	0.0165 ± 0.0045–0.10 ± 0.02
Non-Tet(X) producers	30							
E. coli	2	*tet*(D)	256	128	4	1–2	8	0 ± 0
E. coli	1	*tet*(G)	256	64	2	0.5	8	0 ± 0
E. coli	1	*tet*(M)	128	64	0.125	0.25	2	0 ± 0
E. coli	2	*tet*(A)- *tet*(B)	128–256	64	0.03–0.125	0.03–0.06	0.25–0.5	0 ± 0
E. coli	1	*tet*(B)-*tet*(D)	>256	>256	4	2	16	0 ± 0
E. coli	4	*tet*(D)-*tet*(M)	128–>256	32–64	0.25–0.5	0.25–0.5	2–4	0 ± 0
S. enteritidis	4	*tet*(B)	2–128	0.06–64	0.5	0.06–0.125	2–4	0 ± 0
S. enteritidis	1	*tet*(A)- *tet*(B)	128	64	1	0.25	2	0.0003 ± 0.0004
E. coli	14	non-*tet*(X)[b]	0.5–1	1	0.125–0.25	0.03–0.06	0.5	0 ±-0.0018 ± 0.0025

TET, tetracycline; DOX, doxycycline; TGC, tigecycline; ERV, eravacycline; OMA, omadacycline; MIC, minimum inhibitory concentration; MS, mass spectrometry.

[a]*The number in parentheses indicates the generation of tetracycline.*

[b]*Non-tet(X) strains lack all tet genes as well as tet(X).*

parameters were set as follows: ion source 1, 20 kV; ion source 2, 2.62 kV; lens, 6 kV; pulsed ion extraction, 114 ns; electronic gain, enhanced; mode, low range; mass range selection, 80–1,120 Da; laser frequency, 60 Hz; digitizer trigger level, 2,500 mV; laser attenuator, 25%; and laser range, 40%. A total of 500 shots were acquired in one position for each spectrum (**Figure 1**).

E. coli strains JM109-pBAD24 and ATCC 25922 served as negative controls, while pBAD24-*tet*(X3), pBAD24-*tet*(X4), and pBAD24-*tet*(X6) cultured in the presence of 0.1% L-arabinose were used as positive controls.

Spectral Analysis

Spectra were analyzed using Shimadzu Biotech MALDI-MS software (Shimadzu). Peaks for tigecycline ($C_{29}H_{39}N_5O_8$) (586 ± 0.2 m/z) and its only known metabolite ($C_{29}H_{39}N_5O_9$) (602 ± 0.2 m/z) were manually labeled, and their intensities noted (Moore et al., 2005). MS ratios of intensities were calculated according to metabolite/(metabolite + tigecycline) [M/(M + T)] and were calculated for the 154 cutoff strains to establish a threshold ratio between Tet(X) producers and non-producers. Strains were classified as Tet(X) producers when this ratio was superior or equal to the cutoff values. All experiments were carried out on three independent bacterial cultures on three different days. MS ratios were calculated as the mean values from three independent experiments.

Statistical Analysis

Descriptive analyses of MS ratios were performed using functions provided in Excel 2010 (Microsoft). A receiver operating characteristic (ROC) curve analysis was used to determine the optimal cutoff value (Hanley and Mcneil, 1982), and the optimal cutoff point was defined by the Youden index (Youden, 1950). The ratio-based model was validated for the results of 62 well-characterized isolates that had been previously identified using PCR.

RESULTS

Antibiotic Susceptibility Testing

Tigecycline MICs for our 221 test strains ranged from 0.03 to 64 mg/L. In the group of strains used to establish the MALDI$^{Tet(X)}$ test, 49/51 *tet*(X4)-positive *E. coli* strains were tigecycline resistant, one was intermediate, and one was tigecycline susceptible. Of the strains used to establish the MALDI$^{Tet(X)}$ test, all the Tet(X)-producing *Acinetobacter* spp. strains were tigecycline resistant, whereas all non-Tet(X) producers were tigecycline susceptible. The strains used for the MALDI$^{Tet(X)}$ test validation included 16/18 of *tet*(X4)-positive *E. coli* strains that were determined tigecycline resistant, one tigecycline intermediate, and one tigecycline susceptible. Of the strains used to validate the MALDI$^{Tet(X)}$ test, all the Tet(X)-producing *Acinetobacter* spp. strains were tigecycline resistant, whereas 28/30 of the non-Tet(X) producers were tigecycline susceptible; the two *E. coli* strains carrying *tet*(D) were tigecycline intermediate (**Tables 1**, **2**).

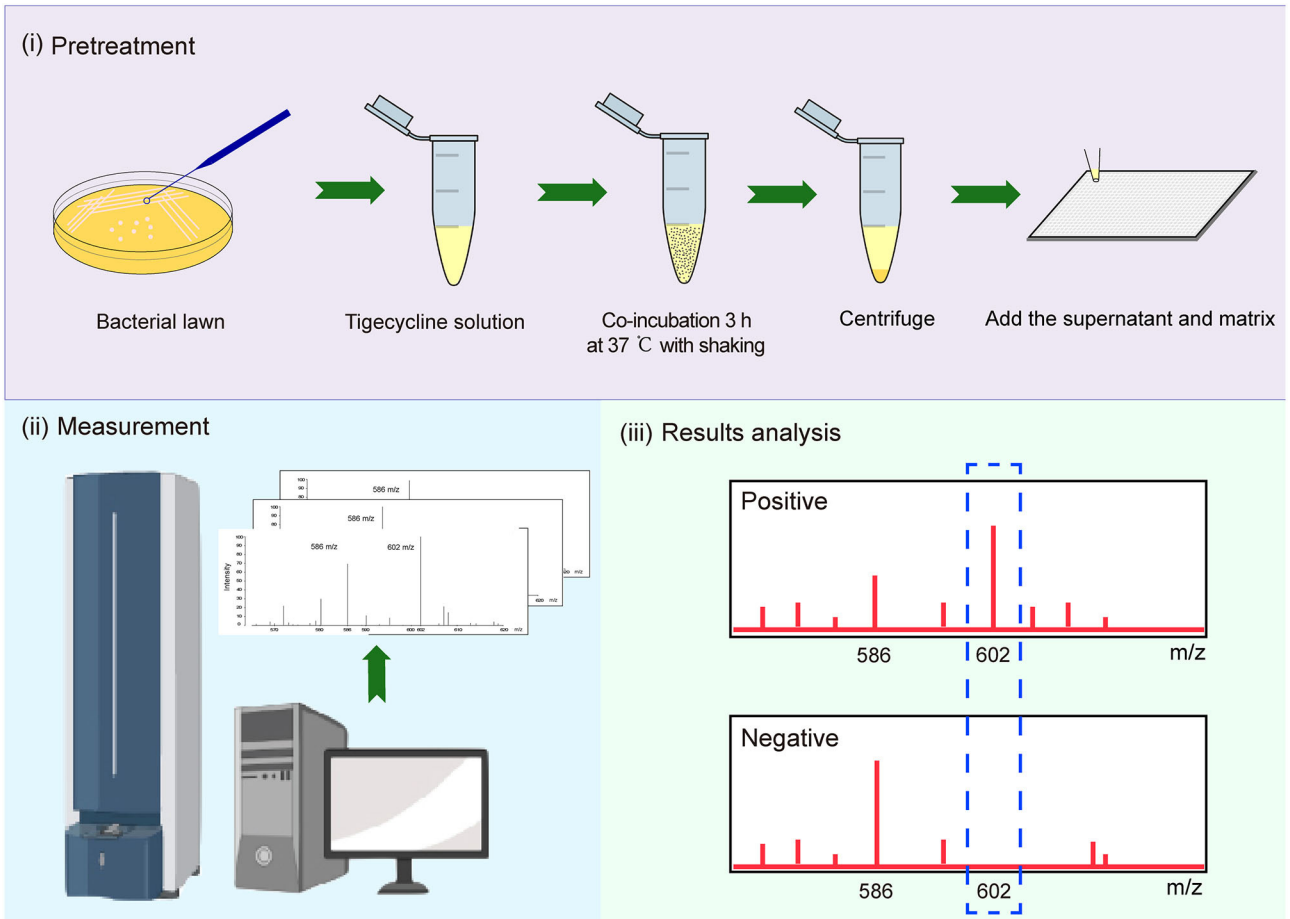

FIGURE 1 | Strategy for identification of Tet(X)-producing *Escherichia coli* (*E. coli*) and *Acinetobacter* spp. using matrix-assisted laser desorption ionization–time of flight mass spectrometry (MALDI-TOF MS).

Detection of Tet(X) Producers Using the MALDI$^{Tet(X)}$ Test

Tigecycline inactivation by Tet(X) occurs *via* covalent modification at C11a of the tetracycline nucleus and results in O addition. The product peak with an m/z of 602 ± 0.2 corresponded to the addition of one oxygen atom to tigecycline (586 ± 0.2 m/z) (**Figure 2A**) (Moore et al., 2005). As expected, the 602 ± 0.2 m/z peak appeared in the mass spectrogram of the Tet(X)-producing *E. coli* and *Acinetobacter* spp. when the MALDI$^{Tet(X)}$ test was used. This peak was lacking in non-Tet(X) producers (**Figure 2B**). We corroborated this by the analysis of 154 test strains that included 92 Tet(X) producers and 62 non-producers. The intensities of the peaks corresponding to tigecycline (586 ± 0.2 m/z) and oxygen-modified tigecycline (602 ± 0.2 m/z) were recorded from three independent experiments. The latter peak corresponded to samples taken from Tet(X) producers (**Table 1**).

The calculation of MS ratios allowed accurate distinction between Tet(X) producers and non-producers. We therefore performed additional tests using the JM109-positive control strains that possessed arabinose-inducible *tet*(X) genes. The MS ratios of pBAD24-*tet*(X3), pBAD24-*tet*(X4), and pBAD24-*tet*(X6) were 0.5 ± 0.09, 0.43 ± 0.11, and 0.18 ± 0.01 m/z, respectively, while the ratios for the two negative controls ATCC 25922 and pBAD24 were 0. Tests of our group of 30 *tet*(X3)-positive *Acinetobacter* spp. included MS ratios that ranged from 0.03 ± 0.02 to 0.57 ± 0.14 and the 51 *tet*(X4)-positive *E. coli* values ranged from 0.0067 ± 0.0095 to 0.48 ± 0.09. However, in three independent experiments, a single isolate in this group had an MS ratio of 0 in two of the experiments. Similarly, 2/11 of the *Acinetobacter* spp. carrying the *tet*(X6) gene presented MS ratios of 0 in 1/3 and 2/3 experiments. The non-Tet(X)-producing *E. coli* and *S. enteritidis* strains had MS ratios of 0 for 57/62 of the samples, and the remaining five strains possessed MS ratios that were not 0 in 1/3 experiments (**Supplementary Table 1**).

The MS ratios of Tet(X)-producing strains ranged from 0.0067 ± 0.0095 to 0.57 ± 0.14, whereas in the non-producers, these ratios ranged from 0 to 0.0014 ± 0.0019 (**Figure 3A**). Receiver operating characteristic (ROC) analysis allowed us to define a cutoff value for the MS ratio at 0.00405 that discriminated Tet(X)

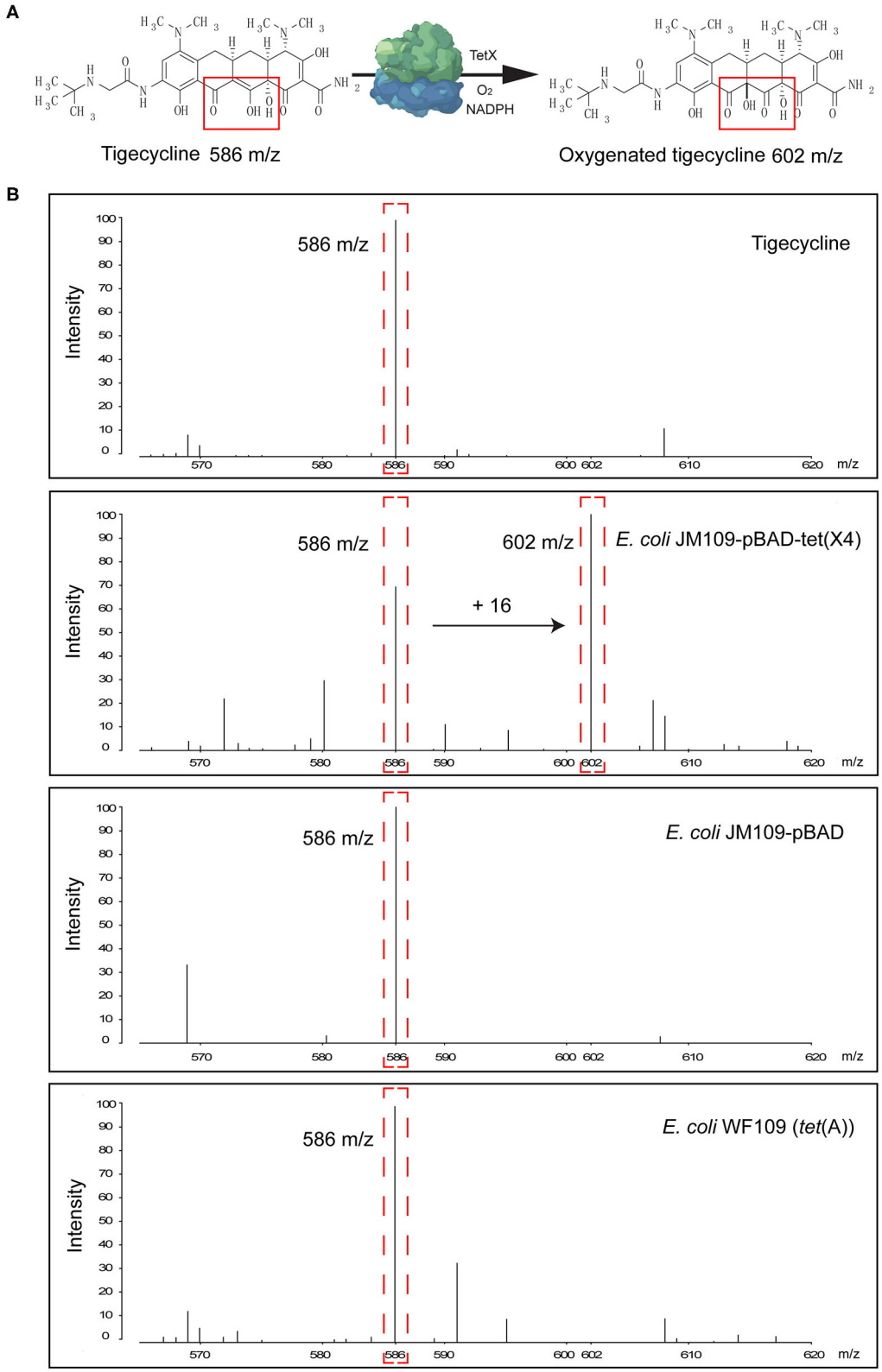

FIGURE 2 | Representative results of the matrix-assisted laser desorption ionization–time of flight mass spectrometry (MALDI-TOF MS) detection of Tet(X) producers and non-producers. **(A)** The structure of tigecycline and the product of the oxygen-modified derivative of tigecycline. Tigecycline and oxygen-modified tigecycline possessed peaks at 586 ± 0.2 and 602 ± 0.2 m/z, respectively. **(B)** Representative MALDI-TOF MS spectra of tigecycline oxygenation assays after a 3-h incubation at 37°C. Peaks of interest are denoted by dashed red lines and represent the tigecycline peak at 586 ± 0.2 m/z and its metabolite at 602 ± 0.2 m/z.

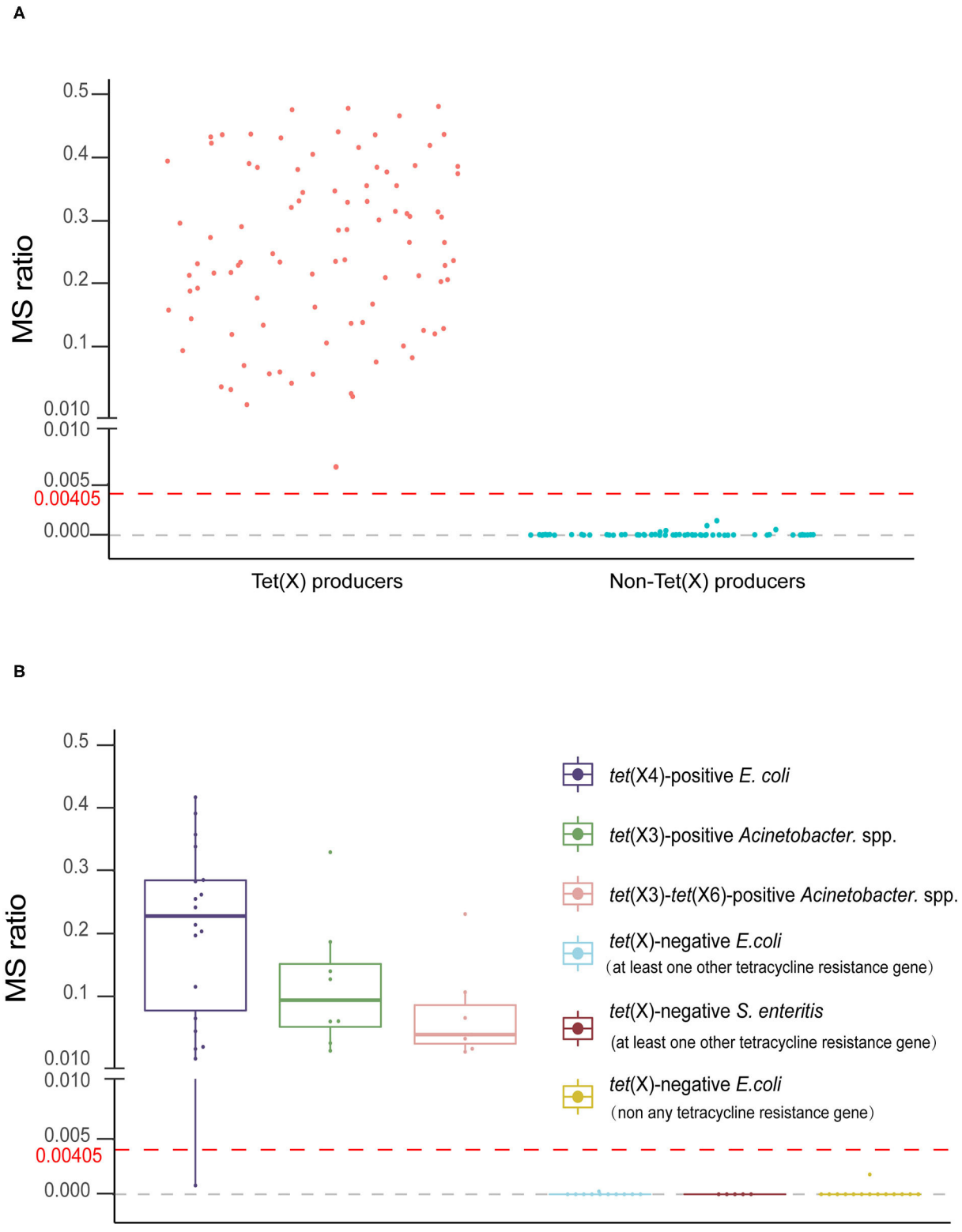

FIGURE 3 | The MALDI$^{Tet(X)}$ test results using test strains. **(A)** Distribution of the mass spectrometry (MS) ratios used to establish the MALDI$^{Tet(X)}$ test. The cutoff value of 0.00405 can clearly distinguish between Tet(X) producers and non-producers **(B)** MS ratio distribution of 32 Tet(X) producers and 30 non-producers used for assay validation. Three independent experiments were performed for each strain.

producers from non-producers. The latter group displayed MS ratios < 0.00405, whereas all Tet(X)-producing strains had MS ratios > 0.00405 (**Figure 3B**).

Model Validation

We validated our model using 62 strains that were blind tested using the calculated cutoff of 0.00405. The 32 Tet(X)-producing *E. coli* and *Acinetobacter* spp. possessed MS ratios that ranged from 0.0008 ± 0.0011 to 0.41 ± 0.22, and only a single *tet*(X4)-positive *E. coli* had an MS ratio below the cutoff value in three independent experiments (0, 0, and 0.0024). Four *tet*(X4)-positive *E. coli* and three *tet*(X3)-*tet*(X6) had MS ratios of 0 in some of the replicates. In the 30 non-Tet(X) producers we examined, the MS ratios ranged from 0 ± 0 to 0.0018 ± 0.0025, and these results were completely consistent with the MALDI$^{Tet(X)}$ test results. Similarly, 2/30 of the non-Tet(X)-producing *E. coli* and *S. enteritidis* strains generated MS ratios that were not 0 in 1/3 experiments (**Supplementary Table 2**).

The group of 62 validation strains yielded only one *tet*(X4)-positive *E. coli* that was incorrect using the MALDI$^{Tet(X)}$ test. The sensitivity and specificity of the MALDI$^{Tet(X)}$ test using the validation group were 96.88 and 100%, respectively, and using all 216 strains, the sensitivity was 99.19% and specificity was 100%.

DISCUSSION

MALDI-TOF MS is an important method for bacterial identification because it is rapid and reliable and therefore is widely deployed in microbiology laboratories around the world (Pan et al., 2007; Stevenson et al., 2010; Huang et al., 2013). In the present study, we developed a MALDI-TOF MS procedure (the MALDI$^{Tet(X)}$ test) to rapidly detect Tet(X) producers in *E. coli* and *Acinetobacter* spp. within 3 h.

There are numerous genotypic and phenotypic methods currently in use for the detection of Tet(X)-producing *E. coli* and *Acinetobacter* spp. Genotypic detection using PCR allows high sensitivity and specificity, but high-throughput detection cannot be achieved due to the lack of universal primers for each gene subtype (Cavanaugh and Bathrick, 2018; Shahi et al., 2018). Multiplex real-time PCR can simultaneously detect multiple gene subtypes but is unable to identify unknown genes (Hawkins and Guest, 2017; Minkus et al., 2019). Since Tet(X) is a tetracycline degradation enzyme, it can be phenotypically detected using tetracycline degradation assays that can be assessed using liquid chromatography–tandem mass spectrometry (LC-MS/MS), but this requires a complex sample pretreatment process (Ji et al., 2010; Palmer et al., 2010). Agar well-diffusion methods are also in use but are time-consuming, although recent modifications using *Bacillus stearothermophilus* as the indicator and color reagent addition have significantly shortened the time required for detection (Mata et al., 2014; Hussein et al., 2015; Balouiri et al., 2016; Galvão et al., 2016; Wu et al., 2019; Cui et al., 2020b). In contrast, the MALDI$^{Tet(X)}$ test is extremely rapid and simple and requires equipment that are now available in many clinical microbiology laboratories. This study is the first to demonstrate the use of MALDI-TOF MS to detect Tet(X)-producing *E. coli* and *Acinetobacter* spp. MALDI-TOF MS has been used for phenotypic characterization of carbapenemase-producing Enterobacteriaceae (CPE) and colistin-resistant Enterobacteriaceae and relies on the detection of carbapenem hydrolysis products in <30 min because of the high catalytic efficiency of carbapenemases (Lasserre et al., 2015). In a similar manner, MALDI-TOF MS has also been used to determine whether a bacterial strain is colistin resistant by the direct measurement of Lipid A modifications, and the process takes only 15 min (Dortet et al., 2018). Our MALDI$^{Tet(X)}$ test identified Tet(X)-producing *E. coli* and *Acinetobacter* spp. at a rate and efficiency to that of the CPE detection method, and both rely on the metabolite identification. However, Tet(X) enzyme efficiency is much lower than for the carbapenemases, and the overall reaction process requires more time (Queenan and Bush, 2007; Park et al., 2017).

Theoretically, the covalent coupling of oxygen to tigecycline occurs only if the test strain is a Tet(X) producer resulting in a 602 ± 0.2 m/z peak. In the group of 124 Tet(X)-producing strains we used for this study, only eight had MS ratios of 0 in 1/3 or 2/3 experiments; these anomalies were most likely the result of a Tet(X) possessing weak activity, and meanwhile, we did identify 7/92 non-Tet(X) producers that possessed low-intensity 602 ± 0.2-m/z peaks. To ensure that the method has higher sensitivity and specificity, we defined a robust cutoff value for the MS ratio of 0.00405, but when coupled with the presence or absence of a 602 ± 0.2-m/z peak, the accuracy of the MALDI$^{Tet(X)}$ test was still very high. The results of the non-Tet(X) producers indicated that the presence of other *tet* genes that mediate tetracycline resistance will not influence the MALDI$^{Tet(X)}$ test results; these results are reasonable and easy to understand, since tigecycline inactivation by Tet(X) occurs *via* covalent modification at C11a of the tetracycline nucleus.

We examined only bacterial strains that possessed the *tet*(X3), *tet*(X4), and tet(X6) genes, although this method can be extended to examine additional isotypes, and specificity and sensitivity should be reexamined. In theory, the MALDI$^{Tet(X)}$ test can detect Tet(X)-producing strains of any species, which will need to be studied in the future. In addition, our method should be extended for the direct detection of these organisms in blood and urine samples (Meier and Hamprecht, 2019), and further evaluation of the MALDI$^{Tet(X)}$ test is worthy of further study.

CONCLUSIONS

We have developed a MALDI-TOF MS-based assay to identify Tet(X)-producing *E. coli* and *Acinetobacter* spp. by determining a unique peak of an oxygen-modified derivative of tigecycline. The overall manipulations were simple and rapid, and this phenotypic detection method is appropriate as a routine test in clinical microbiology laboratories that have access to the MALDI-TOF MS instrumentation. The test is low cost and possesses excellent sensitivity and specificity.

DATA AVAILABILITY STATEMENT

All datasets generated for this study are included in the article/**Supplementary Material**.

ETHICS STATEMENT

Clinical strains isolated from humans in this study were provided by the Third Affiliated Hospital of Sun Yat-sen University. This study was carried out in accordance with the recommendations of ethical guidelines of South China Agricultural University. SCAU Institutional Ethics Committee did not require the study to be reviewed or approved by an ethics committee because we are not involved in the isolation of bacteria.

AUTHOR CONTRIBUTIONS

JS, Y-HL, and X-LL designed the study. Z-HC, Z-JZ, TT, Z-XZ, and C-YC carried out the experiments. JS, X-RW, CC, BH, and M-GW analyzed the data. JS, Z-HC, L-XF, and Z-JZ wrote the draft of the manuscript. All authors read and approved the final manuscript. All authors contributed to the article and approved the submitted version.

FUNDING

This work was supported by the National Key Research and Development Program of China (2016YFD0501300), National Natural Science Foundation of China (31972735), the Program for Innovative Research Team in the University of Ministry of Education of China (IRT_17R39), the 111 Project (D20008).

SUPPLEMENTARY MATERIAL

The Supplementary Material for this article can be found online at: https://www.frontiersin.org/articles/10.3389/fcimb.2020.583341/full#supplementary-material

REFERENCES

Balouiri, M., Sadiki, M., and Ibnsouda, S. K. (2016). Methods for in vitro evaluating antimicrobial activity: a review. *J. Pharm. Anal.* 6, 71–79. doi: 10.1016/j.jpha.2015.11.005

Cavanaugh, S. E., and Bathrick, A. S. (2018). Direct PCR amplification of forensic touch and other challenging DNA samples: a review. *Forensic Sci. Int. Genet.* 32, 40–49. doi: 10.1016/j.fsigen.2017.10.005

Chen, C., Chen, L., Zhang, Y., Cui, C. Y., Wu, X. T., He, Q., et al. (2019). Detection of chromosome-mediated tet(X4)-carrying Aeromonas caviae in a sewage sample from a chicken farm. *J. Antimicrob. Chemother.* 74:3628–30. doi: 10.1093/jac/dkz387

CLSI (2018). *Performance Standards for Antimicrobial Susceptibility Testing, M100, 28th Edn.* Wayne, PA: CLSI.

Cui, C. Y., Chen, C., Liu, B. T., He, Q., Wu, X. T., Sun, R. Y., et al. (2020a). Co-occurrence of plasmid-mediated tigecycline and carbapenem resistance in *Acinetobacter* spp. from waterfowls and their neighboring environment. *Antimicrob. Agents Chemother.* 64:e02502–19. doi: 10.1128/AAC.02502-19

Cui, Z. H., Ni, W. N., Tang, T., He, B., Zhong, Z. X., Fang, L. X., et al. (2020b). Rapid detection of plasmid-mediated high-level tigecycline resistance in *Escherichia coli* and *Acinetobacter* spp. *J. Antimicrob. Chemother.* 75, 1479–1483. doi: 10.1093/jac/dkaa029

Doan, T. L., Fung, H. B., Mehta, D., and Riska, P. F. (2006). Tigecycline: a glycylcycline antimicrobial agent. *Clin. Ther.* 28, 1079–1106. doi: 10.1016/j.clinthera.2006.08.011

Dortet, L., Bonnin, R. A., Pennisi, I., Gauthier, L., Jousset, A. B., Dabos, L., et al. (2018). Rapid detection and discrimination of chromosome- and MCR-plasmid-mediated resistance to polymyxins by MALDI-TOF MS in *Escherichia coli*: the MALDIxin test. *J. Antimicrob. Chemother.* 73, 3359–3367. doi: 10.1093/jac/dky330

Fang, L.-X., Chen, C., Cui, C.-Y., Li, X.-P., Zhang, Y., Liao, X.-P., et al. (2020). Emerging high-level tigecycline resistance: novel tetracycline destructases spread via the mobile Tet(X). *Bioessays.* 42:e2000014. doi: 10.1002/bies.202000014

Forsberg, K. J., Patel, S., Wencewicz, T. A., and Dantas, G. (2015). The tetracycline destructases: a novel family of tetracycline-inactivating enzymes. *Chem. Biol.* 22, 888–897. doi: 10.1016/j.chembiol.2015.05.017

Fu, Y., Liu, D., Song, H., Liu, Z., Jiang, H., and Wang, Y. (2020). Development of a multiplex real-time PCR assay for rapid detection of tigecycline resistance gene tet(X) variants from bacterial, fecal, and environmental samples. *Antimicrob. Agents Chemother.* 64:e02292-19. doi: 10.1128/AAC.02292-19

Galvão, G. V., Saviano, A. M., and Lourenço, F. R. (2016). Reduced incubation time for inhibition zone formation based on diffusion and growth mechanism elucidation. *Anal. Methods* 8, 3885–3891. doi: 10.1039/C6AY00611F

Gasparrini, A. J., Markley, J. L., Kumar, H., Wang, B., Fang, L., Irum, S., et al. (2020). Tetracycline-inactivating enzymes from environmental, human commensal, and pathogenic bacteria cause broad-spectrum tetracycline resistance. *Commun Biol* 3:241. doi: 10.1038/s42003-020-0966-5

Hanley, J. A., and Mcneil, B. J. (1982). The meaning and use of the area under a receiver operating characteristic (Roc) curve. *Radiology* 143, 29–36. doi: 10.1148/radiology.143.1.7063747

Hawkins, S. F., and Guest, P. C. (2017). Multiplex analyses using real-time quantitative PCR. *Methods Mol. Biol.* 1546, 125–133. doi: 10.1007/978-1-4939-6730-8_8

He, T., Wang, R., Liu, D., Walsh, T. R., Zhang, R., Lv, Y., et al. (2019). Emergence of plasmid-mediated high-level tigecycline resistance genes in animals and humans. *Nat Microbiol.* 4, 1450–1456. doi: 10.1038/s41564-019-0445-2

Huang, A. M., Newton, D., Kunapuli, A., Gandhi, T. N., Washer, L. L., Isip, J., et al. (2013). Impact of rapid organism identification via matrix-assisted laser desorption/ionization time-of-flight combined with antimicrobial stewardship team intervention in adult patients with bacteremia and candidemia. *Clin. Infect. Dis.* 57, 1237–1245. doi: 10.1093/cid/cit498

Hussein, A. H., Lisowska, B. K., and Leak, D. J. (2015). The genus Geobacillus and their biotechnological potential. *Adv. Appl. Microbiol.* 92, 1–48. doi: 10.1016/bs.aambs.2015.03.001

Ji, A. J., Saunders, J. P., Amorusi, P., Stein, G., Wadgaonkar, N. D., O'Leary, K. P., et al. (2010). Determination of tigecycline in human skin using a novel validated LC-MS/MS method. *Bioanalysis* 2, 81–94. doi: 10.4155/bio.09.159

Ji, K., Xu, Y., Sun, J., Huang, M., Jia, X., Jiang, C., et al. (2019). Harnessing efficient multiplex PCR methods to detect the expanding Tet(X) family of tigecycline resistance genes. *Virulence* 11, 49–56. doi: 10.1080/21505594.2019.1706913

Lasserre, C., de Saint Martin, L., Cuzon, G., Bogaerts, P., Lamar, E., Glupczynski, Y., et al. (2015). Efficient detection of carbapenemase activity in enterobacteriaceae by matrix-assisted laser desorption ionization-time of flight mass spectrometry in less than 30 minutes. *J. Clin. Microbiol.* 53, 2163–2171. doi: 10.1128/JCM.03467-14

Linkevicius, M., Sandegren, L., and Andersson, D. I. (2016). Potential of tetracycline resistance proteins to evolve tigecycline resistance. *Antimicrob. Agents Chemother.* 60, 789–796. doi: 10.1128/AAC.02465-15

Liu, D., Zhai, W., Song, H., Fu, Y., Schwarz, S., He, T., et al. (2020). Identification of the novel tigecycline resistance gene tet(X6) and its variants in Myroides,

Acinetobacter and Proteus of food animal origin. *J. Antimicrob. Chemother.* 75, 1428–1431. doi: 10.1093/jac/dkaa037

Mata, L., Sanz, D., and Razquin, P. (2014). Validation of the Explorer(R) 2.0 test coupled to e-Reader(R) for the screening of antimicrobials in muscle from different animal species. *Food Addit. Contam. Part A Chem. Anal. Control Expo. Risk Assess.* 31, 1496–1505. doi: 10.1080/19440049.2014.934303

Meier, M., and Hamprecht, A. (2019). Systematic comparison of four methods for the detection of carbapenemase-producing Enterobacterales (CPE) directly from blood cultures. *J. Clin. Microbiol.* 57, e00709-19. doi: 10.1128/JCM.00709-19

Minkus, C. L., Bispo, P. J. M., Papaliodis, G. N., and Sobrin, L. (2019). Real-time multiplex PCR analysis in infectious Uveitis. *Semin. Ophthalmol.* 34, 252–255. doi: 10.1080/08820538.2019.1620803

Moore, I. F., Hughes, D. W., and Wright, G. D. (2005). Tigecycline is modified by the flavin-dependent monooxygenase TetX. *Biochemistry* 44, 11829–11835. doi: 10.1021/bi0506066

Palmer, A. C., Angelino, E., and Kishony, R. (2010). Chemical decay of an antibiotic inverts selection for resistance. *Nat. Chem. Biol.* 6, 105–107. doi: 10.1038/nchembio.289

Pan, C., Xu, S., Zhou, H., Fu, Y., Ye, M., and Zou, H. (2007). Recent developments in methods and technology for analysis of biological samples by MALDI-TOF-MS. *Anal. Bioanal. Chem.* 387, 193–204. doi: 10.1007/s00216-006-0905-4

Park, J., Gasparrini, A. J., Reck, M. R., Symister, C. T., Elliott, J. L., Vogel, J. P., et al. (2017). Plasticity, dynamics, and inhibition of emerging tetracycline resistance enzymes. *Nat. Chem. Biol.* 13, 730–736. doi: 10.1038/nchembio.2376

Queenan, A. M., and Bush, K. (2007). Carbapenemases: the versatile beta-lactamases. *Clin. Microbiol. Rev.* 20, 440–458, table of contents. doi: 10.1128/CMR.00001-07

Shahi, S., Zununi Vahed, S., Fathi, N., and Sharifi, S. (2018). Polymerase chain reaction (PCR)-based methods: promising molecular tools in dentistry. *Int. J. Biol. Macromol.* 117, 983–992. doi: 10.1016/j.ijbiomac.2018.05.085

Stevenson, L. G., Drake, S. K., and Murray, P. R. (2010). Rapid identification of bacteria in positive blood culture broths by matrix-assisted laser desorption ionization-time of flight mass spectrometry. *J. Clin. Microbiol.* 48, 444–447. doi: 10.1128/JCM.01541-09

Sun, J., Chen, C., Cui, C. Y., Zhang, Y., Liu, X., Cui, Z. H., et al. (2019). Plasmid-encoded tet(X) genes that confer high-level tigecycline resistance in *Escherichia coli*. *Nat Microbiol.* 4, 1457–1464. doi: 10.1038/s41564-019-0496-4

Tuckman, M., Petersen, P. J., Howe, A. Y. M., Orlowski, M., Mullen, S., Chan, K., et al. (2007). Occurrence of tetracycline resistance genes among *Escherichia coli* isolates from the phase 3 clinical trials for tigecycline. *Antimicrob. Agents Chemother.* 51, 3205–3211. doi: 10.1128/AAC.00625-07

Wang, L., Liu, D., Lv, Y., Cui, L., Li, Y., Li, T., et al. (2019). Novel plasmid-mediated tet(X5) gene conferring resistance to tigecycline, eravacycline, and omadacycline in a clinical acinetobacter baumannii isolate. *Antimicrob. Agents Chemother.* 64:e01326–19. doi: 10.1128/AAC.01326-19

Wu, Q., Peng, D., Liu, Q., Shabbir, M. A. B., Sajid, A., Liu, Z., et al. (2019). A novel microbiological method in microtiter plates for screening seven kinds of widely used antibiotics residues in milk, chicken egg and honey. *Front. Microbiol.* 10:436. doi: 10.3389/fmicb.2019.00436

Youden, W. J. (1950). Index for rating diagnostic tests. *Cancer* 3, 32–35. doi: 10.1002/1097-0142(1950)3:1<32::AID-CNCR2820030106>3.0.CO;2-3

Conflict of Interest: The authors declare that the research was conducted in the absence of any commercial or financial relationships that could be construed as a potential conflict of interest.

frontiers in Cellular and Infection Microbiology

ORIGINAL RESEARCH
published: 21 October 2020
doi: 10.3389/fcimb.2020.00479

Higher Sensitivity Provided by the Combination of Two Lateral Flow Immunoassay Tests for the Detection of COVID-19 Immunoglobulins

Ziad Daoud[1,2]*, *Jesse McLeod*[1] and *David L. Stockman*[1]

[1] Department of Clinical Microbiology and Infection Prevention, Michigan Health Clinics and Public Health Institute of Science, Epidemiology, and Research, Saginaw, MI, United States, [2] Faculty of Medicine and Medical Sciences, University of Balamand and Clinical Microbiology Division, Saint George Hospital-University Medical Center (UMC), Beirut, Lebanon

OPEN ACCESS

Edited by:
Hongchao Gou,
Guangdong Academy of Agricultural Sciences, China

Reviewed by:
Jing Yuan,
Children's Hospital of Capital Institute of Pediatrics, China
Robert Cody Sharp,
University of Florida Health, United States
Kai Huang,
The University of Texas Medical Branch at Galveston, United States

***Correspondence:**
Ziad Daoud
zdaoud@mihealthclinic.com

Specialty section:
This article was submitted to Clinical Microbiology, a section of the journal Frontiers in Cellular and Infection Microbiology

Received: 03 June 2020
Accepted: 03 August 2020
Published: 21 October 2020

Citation:
Daoud Z, McLeod J and Stockman DL (2020) Higher Sensitivity Provided by the Combination of Two Lateral Flow Immunoassay Tests for the Detection of COVID-19 Immunoglobulins. Front. Cell. Infect. Microbiol. 10:479. doi: 10.3389/fcimb.2020.00479

SARS-Cov-2 was identified in Wuhan, China in December 2019. The World Health Organization (WHO) declared it a pandemic in March of 2020. COVID-19 has now been reported on every continent. In the United States, the total number of confirmed reported cases of COVID-19 has exceeded 1.8 million with the total death exceeding 100,000 people. The most common investigational diagnostics of this disease are RT-PCR and serology testing. The objective of this work was to validate two commercial kits for the detection of IgM and IgG using lateral flow immunoassay tests and to study the effect of the combination of both serology kits for better detection of immunoglobulins. A total of 195 patients presenting with respiratory symptoms suggestive of infection with SARS-Cov-2 were subject to serology and molecular testing. Two lateral flow immunochromatographic assay kits were used: the Healgen Scientific for SARS-CoV-2 IgM/IgG and the Raybiotech for SARS-CoV-2 IgM/IgG. Sensitivity and specificity of each kit alone and in combination were determined and compared. The limit of detection, inter and intra test variations, as well interfering substances and cross reactivity were also studied for both kits. The results show sensitivities for IgM detection varying between 58.9 and 66.2% for the kits alone and 87.7% of the combination of both kits. IgG detection was not significantly affected by this combination. Both kits manifested high specificities (99.2–100%). Both kits showed high clinical performance in terms of cross reactivity and interfering substances. Our results suggest using combinatory testing for the serology of COVID-19 after a full evaluation study, assessing all the parameters affecting their clinical performance before deciding on this combination.

Keywords: SARS-CoV-2, IgM, IgG, sensitivity, specificity, serology

INTRODUCTION

Severe acute respiratory syndrome coronavirus 2 (SARS-CoV-2) is the virus responsible for the coronavirus disease of 2019 (COVID-19). This virus was first identified in Wuhan, China in December 2019, it has since been declared a pandemic by the World Health Organization (WHO) in March of 2020 (Coronavirus disease (COVID-19) pandemic- 2020 https://www.who.int/emergencies/diseases/novel-coronavirus-2019. Coronavirus disease 2019 (COVID-19):

situation summary (2020). https://www.cdc.gov/coronavirus/2019-ncov/cases-updates/summary.html). The disease caused by this virus, COVID-19, has now been reported on every continent. In the United States, the total number of confirmed reported cases of Covid-19 has exceeded 1.8 million with total death exceeding 100,000 people. (https://www.worldometers.info/coronavirus/). The World Health Organization (WHO) has criticized countries that have not prioritized testing. The chief executive of the WHO has highlighted the importance of testing on several occasions (WHO, 2020).

The tests most commonly used now for the diagnosis of COVID-19 are RT-PCR and serology testing. Other techniques such as the detection of the viral antigen are also used. The RT-PCR looks for the virus itself (viral RNA) in the nose, throat, or other areas in the respiratory tract to determine if there is an active infection with SARS-CoV-2 (Liua et al., 2020). A positive PCR test suggests that the person being tested has an active COVID-19 infection.

PCR testing only helps determine whether a person has an active infection at the time of testing (Tahamtan and Ardebili, 2020). Unfortunately, it does not help determine who had an infection in the past. It also does not help determine which people who have been exposed to COVID-19 will develop active infection during the two weeks after exposure. In some people, the virus can only be found by PCR for a few days at the beginning of the infection, so the test might not find the virus if the swab is taken more than a few days after the illness starts. Lateral flow immunoassay (LFIA) testing of SARS-Cov-2 (IgM/IgG) is intended for use as a screening test helping in the identification and diagnosis of human subjects who developed antibodies as a result of SARS-CoV-2 infection or exposure. Any reactive specimen with the IgM-SARS-Cov-2 or IgG-SARS-Cov-2 must be confirmed with alternative testing method(s). It is not yet confirmed if the antibodies produced during this infection will be enough to yield immunity and whether this immunity is long or short. The serology testing should not be used alone to diagnose acute SARS-CoV-2 infection. Antibodies against SARS-CoV-2 can be detected in blood a few days after the infection. The production of IgM typically happens 3–5 days post infection, IgG of course are produced at a later stage; this is known as seroconversion. Negative results do not exclude the possibility of a SARS-CoV-2 infection. For this reason, the combination of both serologic and molecular testing to detect the virus is necessary. Cross reactivity of IgM and/or IgG may occur as a result of a previous exposure to other SARS viruses. The serology testing of SARS-CoV-2 (IgM/IgG) is currently permitted only for use under the Food and Drug Administration's emergency use authorization (EUA) (https://www.cdc.gov/coronavirus/2019-ncov/cases-in-us.html).

As an effective point-of-care tool, paper-based assays offer the advantage of providing supporting results in a timely manner. In addition, these tests are not expensive and allow for faster treatment decisions (Yager et al., 2006). Paper assays have been used in many diagnostic areas. In view of their complexity, many differences can occur between different kits from different manufacturers.

On April 16, 2020, the White House released a document: "Opening Up America Again Guidelines." This constitutes a road map based on three phases for reopening the society in the States. The Blueprint document released by the White House demonstrates "how the use of two antibody tests rather than one dramatically improves the predictive value of a testing program, particularly in low prevalence environments." By definition, higher positive predictive values (PPV) are mostly associated with people who contracted the disease and responded with the production of antibodies. Higher negative predictive values (NPV), on the other hand, commonly suggest that one does not have the disease and did not produce the corresponding antibodies (Blueprint for testing plans and rapid response programs- partnering with states to put America back to work https://www.whitehouse.gov/wp-content/uploads/2020/04/Testing-Blueprint.pdf).

In this paper, our intention was to validate two commercial kits for the detection of IgM and IgG using lateral flow immunoassay tests. Based on our results, we propose to combine two serology kits for better detection of immunoglobulins.

MATERIALS AND METHODS

Patients and patient sampling: 195 patients presenting with respiratory symptoms suggestive of an infection with SARS-Cov-2 were subject to serology and molecular testing. For serology testing, venous blood was withdrawn by phlebotomy. Blood was collected in EDTA tubes and separated by centrifugation at 2,500 g for 5 min, and plasma was obtained. For molecular testing, a nasopharyngeal swab was obtained from the same patient. RT-PCR experiments were not performed in our lab, they were sent to a reference lab and results were communicated within 24 h.

Lateral flow immunoassay testing: Two different rapid tests were used for the detection IgM and IgG in human plasma. Both test devices utilize lateral flow immunoassay technology that is used for the qualitative, differential detection of both anti-SARS-CoV-2 IgM and IgG antibodies: 1- Healgen Scientific for SARS-CoV-2 IgM/IgG and 2- Raybiotech for SARS-CoV-2 IgM/IgG.

For both kits, the separation of components was performed using capillary force and the specific and rapid binding of an antibody to its antigen. Each cassette consists of a dry medium coated with novel coronavirus N protein and goat anti-chicken IgY antibody (control). Two free colloidal gold-labeled antibodies, mouse anti-human immunoglobulin and chicken IgY, were included in the release pad section. After the addition of plasma, the Ig will bind to coronavirus Ig antibodies if they are present, forming an IgM-IgM complex. The sample and antibodies will then move across the cassette's medium *via* capillary action. If the coronavirus IgM antibody is present in the

sample, the IgM-IgM complex will bind to the test line and develop color.

For the Healgen kit, the test cassette was provided in a sealed foil pouch and laid on a flat surface. Using the plastic dropper provided, 5 μl of plasma specimen was transferred into the sample well (S). Immediately 50 μL of sample buffer was added to the buffer well (B) ensuring that the buffer vial tip did not touch the sample, air bubbles were avoided. After, the control line (C) changed from blue to red in color. One additional drop of sample buffer may be added to the buffer well if migration of the sample has not moved across the test window. The results were read in 10 min, no reading was allowed after 15 min. Both IgM and IgG were reported in the following way: 1- Positive for anti-SARS-CoV-2 immunoglobulins when both the control line (C) and the test line (T) were dark or light pink. 2- Negative for anti-SARS-CoV-2 immunoglobulins when the control line (C) was dark pink and the test line (T) did not develop color or had a faint gray band. 3- Invalid: there was no colored control line (C). Image 1 represents the possible lateral flow device results for the IgM and IgG cassette.

For the Raybiotech kit, one test cassette for each immunoglobulin was provided in a sealed foil pouch (One cassette for IgM and another for IgG). For both immunoglobulins, 25 ul of patient plasma were added to a diluent tube that was mixed by gentle inversion. Using the pipette provided with the cassette, 2–3 drops of the prepared diluent/plasma were added to the release pad of the cassette. If there is no movement of the liquid in the first 30 s, an additional drop may be added to the release pad. Plasma from patients with PCR confirmed positive and negative SARS-CoV-2 infection were used as controls. Positive and negative control plasma were frozen at −20°C for up to 3 months in 35 ul aliquots in labeled plastic bullets. For longer storage periods, controls were frozen at −80°C. These were tested with every new kit lot received, after receipt of a new shipment of the same lot, and on daily basis when running tests from patients. Results were read within 10 min, and no reading was done after 15 min. Both IgM and IgG were reported in the following way: 1- Positive for anti-SARS-CoV-2 immunoglobulins: both the control line (C) and the test line (T) were dark or light pink. 2- Negative for anti-SARS-CoV-2 immunoglobulins: the control line (C) was dark pink and the test line (T) did not develop color or had a faint gray band. 3- Invalid: there was no colored control line (C).

When both tests were combined for interpretation, the following rule was implemented for both IgM and IgG: in the case of agreement between both kits (Raybiotech and Healgen), the agreed upon result was reported. In the case of disagreement between both kits (positive for one kit and negative for the other), the result was reported as positive for the immunoglobulin in question.

Performance parameters

1. Sensitivity or PPA (positive coincidence rate) and specificity or NPA (negative coincidence rate) of the separate and combined kits' results were calculated according to the following formulas:

$$\text{Sensitivity \%} = 100 \times [\text{True Positive}/(\text{True Positive} + \text{False Negative})]$$
$$\text{Specificity \%} = 100 \times [\text{True Negative}/(\text{True Negative} + \text{False Positive})]$$

The total agreement with PCR results was calculated in percent of the total coincidence between serology and molecular tests.
2. Accuracy and limit of detection (LoD) for IgM and IgG: three serial dilutions from three different patients' plasma were prepared separately. The dilution interval from one dilution to another was the double leading to decreasing concentrations by half. Detection of IgM tests were performed on all the dilutions and results were recorded.
3. Intra-assay validation (intra-assay repeatability): intra-assay validation shows the reproducibility between the tubes within one testing time. Data resulting from intra-assay validation helps ensure that samples run in different tubes of the same experiment will give comparable results. Eight plasma samples were run in five repetitions each.
4. Cross-reactivity: we evaluated the cross-reactivity of the SARS-Cov-2 detection rapid test using plasma samples from patients with documented antibodies against the below listed pathogens. Human Coronavirus 229 E, Human Coronavirus NL63 (alpha coronavirus, Human Coronavirus, Respiratory Syncytial Virus, Human Coronavirus NL63+RSV, Human Coronavirus 229+RSV, Human Metapneumovirus (hMPV, Parainfluenza virus (1,3,), Influenza A, Influenza B, Hepatitis C Virus, Hepatitis B Virus, Hemophilus influenzae, Chlamydia pneumoniae, HPV, HIV.
5. Class specificity: we evaluated the potential for: (a) human IgM (0.4 mg/ml of human IgM purified immunoglobulin-Biorad) to cross react and produce false positive results for IgG: using five patients' plasma with IgG negative. Each sample was tested in duplicate, (b) human IgG (8 mg/ml of natural human IgG - Biorad) to cross react and produce false positive results for IgM: using five patients' plasma with IgM negative. Each sample was tested in duplicate, and (c) human IgM 0.4 mg/ml and human IgG 8 mg/ml to compete and produce false negative results for IgM or IgG using five patients' plasma (IgM positive IgG positive). Each sample was tested in duplicate.
6. Potential interfering substances: we prepared low titer SARS-CoV-2 antibody positive serum samples, and SARS-CoV-2 antibody negative serum samples. Then we spiked aliquots of both preparations with one of the below substances to approximate the indicated concentrations and tested triplicates. Hemoglobin (10–20 mg/mL), Bilirubin Conjugated <1 mg/mL, Bilirubin Unconjugated <1 mg/mL, Ciprofloxacin 200 mg/L, Cefotaxime 500 mg/L, Meropenem 200 mg/L, Imipenem 200 mg/L, Amikacin 10 mg/L, and Amphotericin B 200 mg/L.
7. Statistical methods: for the comparison of sensitivity and specificity, the Fisher-Exact test was used for the sample population analysis using a two sided p. Significance was determined according to the value of p.

TABLE 1 | Detection of IgM by Raybiotech alone, Healgen alone, Raybiotech + Healgen combined.

Patient plasma	RT-PCR	IgM Raybio	IgM Healgen	Comparison RT-PCR/ IgM Raybio	Comparison RT-PCR/ IgM Healgen	Comparison RT-PCR-IgM Raybio+Healgen
CP1	Neg	Neg	Neg	A	A	A
CP2	Pos	Pos	Pos	A	A	A
CP3	Pos	Neg	Pos	F-	A	AC
CP4	Neg	Neg	Neg	A	A	A
CP5	Neg	Neg	Neg	A	A	A
CP6	Neg	Neg	Neg	A	A	A
CP7	Pos	Neg	Pos	F-	A	AC
CP8	Pos	Neg	Neg	F-	F-	F-
CP9	Pos	Neg	Neg	F-	F-	F-
CP10	Neg	Neg	Neg	A	A	A
CP11	Neg	Neg	Neg	A	A	A
CP12	Neg	Neg	Neg	A	A	A
CP13	Pos	Neg	Neg	F-	F-	F-
CP14	Neg	Neg	Neg	A	A	A
CP15	Neg	Neg	Neg	A	A	A
CP16	Pos	Pos	Neg	A	F-	AC
CP17	Pos	Pos	Pos	A	A	A
CP18	Pos	Pos	Pos	A	A	A
CP19	Neg	Neg	Neg	A	A	A
CP20	Pos	Pos	Pos	A	A	A
CP21	Neg	Pos	Neg	F+	A	F+-
CP22	Neg	Neg	Neg	A	A	A
CP23	Neg	Neg	Neg	A	A	A
CP24	Pos	Pos	Neg	A	F-	AC
CP25	Neg	Neg	Neg	A	A	A
CP26	Pos	Pos	Pos	A	A	A
CP27	Pos	Neg	Pos	F-	A	AC
CP28	Pos	Pos	Neg	A	F-	AC
CP29	Pos	Neg	Pos	F-	A	AC
CP30	Pos	Neg	Pos	F-	A	AC
CP31	Pos	Pos	Neg	A	F-	AC
CP32	Pos	Pos	Pos	A	A	A
CP33	Pos	Pos	Pos	A	A	A
CP34	Pos	Pos	Neg	A	F-	AC
CP35	Pos	Neg	Neg	F-	F-	F-
CP36	Pos	Neg	Pos	F-	A	AC
CP37	Pos	Pos	Pos	A	A	A
CP38	Pos	Pos	Neg	A	F-	AC
CP39	Pos	Pos	Neg	A	F-	AC
CP40	Pos	Pos	Pos	A	A	A
CP41	Pos	Neg	Neg	F-	F-	F-
CP42	Pos	Neg	Neg	F-	F-	F-
CP43	Pos	Pos	Pos	A	A	A
CP44	Neg	Neg	Neg	A	A	A
CP45	Pos	Pos	Pos	A	A	A
CP46	Pos	Neg	Pos	F-	A	AC
CP47	Pos	Pos	Pos	A	A	A
CP48	Pos	Pos	Pos	A	A	A
CP49	Pos	Neg	Pos	F-	A	AC
CP50	Pos	Neg	Neg	F-	F-	F-

(Continued)

TABLE 1 | Continued

Patient plasma	RT-PCR	IgM Raybio	IgM Healgen	Comparison RT-PCR/ IgM Raybio	Comparison RT-PCR/ IgM Healgen	Comparison RT-PCR-IgM Raybio+Healgen
CP51	Neg	Neg	Neg	A	A	A
CP52	Neg	Neg	Neg	A	A	A
CP53	Neg	Neg	Neg	A	A	A
CP54	Neg	Neg	Neg	A	A	A
CP55	Neg	Neg	Neg	A	A	A
CP56	Neg	Neg	Neg	A	A	A
CP57	Neg	Neg	Neg	A	A	A
CP58	Neg	Neg	Neg	A	A	A
CP59	Neg	Neg	Neg	A	A	A
CP60	Neg	Neg	Neg	A	A	A
CP61	Pos	Pos	Pos	A	A	A
CP62	Pos	Pos	Pos	A	A	A
CP63	Neg	Neg	Neg	A	A	A
CP64	Pos	Pos	Pos	A	A	A
CP65	Neg	Neg	Neg	A	A	A
CP66	Neg	Neg	Neg	A	A	A
CP67	Pos	Pos	Pos	A	A	A
CP68	Neg	Neg	Neg	A	A	A
CP69	Neg	Neg	Neg	A	A	A
CP70	Neg	Neg	Neg	A	A	A
CP71	Pos	Pos	Pos	A	A	A
CP72	Neg	Neg	Neg	A	A	A
CP73	Neg	Neg	Neg	A	A	A
CP74	Neg	Neg	Neg	A	A	A
CP75	Neg	Neg	Neg	A	A	A
CP76	Pos	Pos	Neg	A	F-	AC
CP77	Pos	Pos	Neg	A	F-	AC
CP78	Pos	Neg	Pos	F-	A	AC
CP79	Neg	Neg	Neg	A	A	A
CP80	Neg	Neg	Neg	A	A	A
CP81	Pos	Neg	Pos	F-	A	AC
CP82	Neg	Neg	Neg	A	A	A
CP83	Pos	Pos	Pos	A	A	A
CP84	Neg	Neg	Neg	A	A	A
CP85	Pos	Pos	Pos	A	A	A
CP86	Pos	Pos	Pos	A	A	A
CP87	Pos	Pos	Pos	A	A	A
CP88	Pos	Pos	Pos	A	A	A
CP89	Pos	Pos	Pos	A	A	A
CP90	Pos	Pos	Pos	A	A	A
CP91	Pos	Neg	Neg	F-	F-	A
CP92	Pos	Neg	Neg	F-	F-	A
CP93	Pos	Neg	Pos	F-	A	AC
CP94	Pos	Neg	Neg	F-	F-	A
CP95	Pos	Pos	Neg	A	F-	AC
CP96	Pos	Neg	Neg	F-	F-	F-
CP97	Pos	Neg	Neg	F-	F-	F-
CP98	Pos	Pos	Pos	A	A	A
CP99	Pos	Neg	Pos	F-	A	AC
CP100	Pos	Neg	Pos	F-	A	AC

(Continued)

TABLE 1 | Continued

Patient plasma	RT-PCR	IgM Raybio	IgM Healgen	Comparison RT-PCR/ IgM Raybio	Comparison RT-PCR/ IgM Healgen	Comparison RT-PCR-IgM Raybio+Healgen
CP101	Neg	Neg	Neg	A	A	A
CP102	Neg	Neg	Neg	A	A	A
CP103	Neg	Neg	Neg	A	A	A
CP104	Neg	Neg	Neg	A	A	A
CP105	Neg	Neg	Neg	A	A	A
CP106	Neg	Neg	Neg	A	A	A
CP107	Neg	Neg	Neg	A	A	A
CP108	Neg	Neg	Neg	A	A	A
CP109	Pos	Pos	Pos	A	A	A
CP110	Pos	Pos	Pos	A	A	A
CP111	Pos	Pos	Neg	A	F-	AC
CP112	Pos	Neg	Pos	F-	A	AC
CP113	Pos	Neg	Pos	F-	A	AC
CP114	Pos	Pos	Pos	A	A	A
CP115	Pos	Pos	Pos	A	A	A
CP116	Pos	Neg	Pos	F-	A	AC
CP117	Pos	Neg	Neg	F-	F-	A
CP118	Pos	Pos	Pos	A	A	A
CP119	Pos	Pos	Pos	A	A	A
CP120	Pos	Neg	Pos	F-	A	AC
CP121	Neg	Neg	Neg	A	A	A
CP122	Neg	Neg	Neg	A	A	A
CP123	Neg	Neg	Neg	A	A	A
CP124	Neg	Neg	Neg	A	A	A
CP125	Neg	Neg	Neg	A	A	A
CP126	Neg	Neg	Neg	A	A	A
CP127	Neg	Neg	Neg	A	A	A
CP128	Neg	Neg	Neg	A	A	A
CP129	Neg	Neg	Neg	A	A	A
CP130	Neg	Neg	Neg	A	A	A
CP131	Neg	Neg	Neg	A	A	A
CP132	Neg	Neg	Neg	A	A	A
CP133	Neg	Neg	Neg	A	A	A
CP134	Neg	Neg	Neg	A	A	A
CP135	Neg	Neg	Neg	A	A	A
CP136	Neg	Neg	Neg	A	A	A
CP137	Neg	Neg	Neg	A	A	A
CP138	Neg	Neg	Neg	A	A	A
CP139	Neg	Neg	Neg	A	A	A
CP140	Neg	Neg	Neg	A	A	A
CP141	Neg	Neg	Neg	A	A	A
CP142	Neg	Neg	Neg	A	A	A
CP143	Neg	Neg	Neg	A	A	A
CP144	Neg	Neg	Neg	A	A	A
CP145	Neg	Neg	Neg	A	A	A
CP146	Neg	Neg	Neg	A	A	A
CP147	Neg	Neg	Neg	A	A	A
CP148	Neg	Neg	Neg	A	A	A
CP149	Neg	Neg	Neg	A	A	A
CP150	Neg	Neg	Neg	A	A	A

(Continued)

TABLE 1 | Continued

Patient plasma	RT-PCR	IgM Raybio	IgM Healgen	Comparison RT-PCR/ IgM Raybio	Comparison RT-PCR/ IgM Healgen	Comparison RT-PCR-IgM Raybio+Healgen
CP151	Neg	Neg	Neg	A	A	A
CP152	Neg	Neg	Neg	A	A	A
CP153	Neg	Neg	Neg	A	A	A
CP154	Neg	Neg	Neg	A	A	A
CP155	Neg	Neg	Neg	A	A	A
CP156	Neg	Neg	Neg	A	A	A
CP157	Neg	Neg	Neg	A	A	A
CP158	Neg	Neg	Neg	A	A	A
CP159	Neg	Neg	Neg	A	A	A
CP160	Neg	Neg	Neg	A	A	A
CP161	Neg	Neg	Neg	A	A	A
CP162	Neg	Neg	Neg	A	A	A
CP163	Neg	Neg	Neg	A	A	A
CP164	Neg	Neg	Neg	A	A	A
CP165	Neg	Neg	Neg	A	A	A
CP166	Neg	Neg	Neg	A	A	A
CP167	Neg	Neg	Neg	A	A	A
CP168	Neg	Neg	Neg	A	A	A
CP169	Neg	Neg	Neg	A	A	A
CP170	Neg	Neg	Neg	A	A	A
CP171	Neg	Neg	Neg	A	A	A
CP172	Neg	Neg	Neg	A	A	A
CP173	Neg	Neg	Neg	A	A	A
CP174	Neg	Neg	Neg	A	A	A
CP175	Neg	Neg	Neg	A	A	A
CP176	Neg	Neg	Neg	A	A	A
CP177	Neg	Neg	Neg	A	A	A
CP178	Neg	Neg	Neg	A	A	A
CP179	Neg	Neg	Neg	A	A	A
CP180	Neg	Neg	Neg	A	A	A
CP181	Neg	Neg	Neg	A	A	A
CP182	Neg	Neg	Neg	A	A	A
CP183	Neg	Neg	Neg	A	A	A
CP184	Neg	Neg	Neg	A	A	A
CP185	Neg	Neg	Neg	A	A	A
CP186	Neg	Neg	Neg	A	A	A
CP187	Neg	Neg	Neg	A	A	A
CP188	Neg	Neg	Neg	A	A	A
CP189	Neg	Neg	Neg	A	A	A
CP190	Neg	Neg	Neg	A	A	A
CP191	Neg	Neg	Neg	A	A	A
CP192	Neg	Neg	Neg	A	A	A
CP193	Neg	Neg	Neg	A	A	A
CP194	Neg	Neg	Neg	A	A	A
CP195	Neg	Neg	Neg	A	A	A

Neg, Negative; Pos, Positive; F-, False negative; F+, False positive; A, Agreement with PCR result; AC, Agreement of combined testing.

RESULTS

The results of the detection of IgM and IgG of 195 tests performed by LFIA using the Raybiotech kit and or the Healgen kit are shown in **Tables 1**, **2**. Concerning IgM detection, **Tables 3–5** show that the sensitivity of Raybiotech alone was 58.9%, and Healgen alone was 66.2% (p-value for IgM RayBio vs. IgM Healgen = 0.3969). When the rule about disagreement was implemented (refer to Material and Methods), the sensitivity of the combined kits reached 87.7% (p-value for IgM RayBio vs.

TABLE 2 | Detection of IgG by Raybiotech alone, Healgen alone, Raybiotech + Healgen combined.

Patient plasma	RT-PCR	IgG RayBio	IgG Healgen	Comparison RT-PCR/IgG Raybio	Comparison RT-PCR/ IgG Healgen	Comparison RT-PCR/ IgG Raybio+Healgen
CP1	Neg	Neg	Neg	A	A	A
CP2	Pos	Pos	Pos	A	A	A
CP3	Pos	Pos	Pos	A	A	A
CP4	Neg	Neg	Neg	A	A	A
CP5	Neg	Neg	Neg	A	A	A
CP6	Neg	Neg	Neg	A	A	A
CP7	Pos	Neg	Neg	F-	F-	F-
CP8	Pos	Neg	Neg	F-	F-	F-
CP9	Pos	Neg	Neg	F-	F-	F-
CP10	Neg	Neg	Neg	A	A	A
CP11	Neg	Neg	Neg	A	A	A
CP12	Neg	Neg	Neg	A	A	A
CP13	Pos	Neg	Neg	F-	F-	F-
CP14	Neg	Neg	Neg	A	A	A
CP15	Neg	Neg	Neg	A	A	A
CP16	Pos	Pos	Pos	A	A	A
CP17	Pos	Pos	Pos	A	A	A
CP18	Pos	Neg	Neg	F-	F-	F-
CP19	Neg	Neg	Neg	A	A	A
CP20	Pos	Pos	Pos	A	A	A
CP21	Neg	Neg	Neg	A	A	A
CP22	Neg	Neg	Neg	A	A	A
CP23	Neg	Neg	Neg	A	A	A
CP24	Pos	Neg	Neg	F-	F-	F-
CP25	Neg	Neg	Neg	A	A	A
CP26	Pos	Pos	Pos	A	A	A
CP27	Pos	Neg	Neg	F-	F-	F-
CP28	Pos	Neg	Neg	F-	F-	F-
CP29	Pos	Pos	Pos	A	A	A
CP30	Pos	Pos	Pos	A	A	A
CP31	Pos	Neg	Neg	F-	F-	F-
CP32	Pos	Pos	Pos	A	A	A
CP33	Pos	Pos	Pos	A	A	A
CP34	Pos	Neg	Neg	F-	F-	F-
CP35	Pos	Neg	Neg	F-	F-	F-
CP36	Pos	Neg	Pos	F-	A	AC
CP37	Pos	Pos	Pos	A	A	A
CP38	Pos	Neg	Neg	F-	F-	F-
CP39	Pos	Neg	Neg	F-	F-	F-
CP40	Pos	Pos	Pos	A	A	A
CP41	Pos	Neg	Neg	F-	F-	F-
CP42	Pos	Neg	Neg	F-	F-	F-
CP43	Pos	Pos	Pos	A	A	A
CP44	Neg	Neg	Neg	A	A	A
CP45	Pos	Pos	Pos	A	A	A
CP46	Pos	Pos	Pos	A	A	A
CP47	Pos	Neg	Neg	F-	F-	F-
CP48	Pos	Pos	Pos	A	A	A
CP49	Pos	Pos	Pos	A	A	A
CP50	Pos	Neg	Neg	F-	F-	F-

(Continued)

TABLE 2 | Continued

Patient plasma	RT-PCR	IgG RayBio	IgG Healgen	Comparison RT-PCR/IgG Raybio	Comparison RT-PCR/ IgG Healgen	Comparison RT-PCR/ IgG Raybio+Healgen
CP51	Neg	Neg	Neg	A	A	A
CP52	Neg	Neg	Neg	A	A	A
CP53	Neg	Neg	Neg	A	A	A
CP54	Neg	Neg	Neg	A	A	A
CP55	Neg	Neg	Neg	A	A	A
CP56	Neg	Neg	Neg	A	A	A
CP57	Neg	Neg	Neg	A	A	A
CP58	Neg	Neg	Neg	A	A	A
CP59	Neg	Neg	Neg	A	A	A
CP60	Neg	Neg	Neg	A	A	A
CP61	Pos	Pos	Pos	A	A	A
CP62	Pos	Pos	Pos	A	A	A
CP63	Neg	Neg	Neg	A	A	A
CP64	Pos	Pos	Pos	A	A	A
CP65	Neg	Neg	Neg	A	A	A
CP66	Neg	Neg	Neg	A	A	A
CP67	Pos	Pos	Pos	A	A	A
CP68	Neg	Neg	Neg	A	A	A
CP69	Neg	Neg	Neg	A	A	A
CP70	Neg	Neg	Neg	A	A	A
CP71	Pos	Neg	Pos	F-	A	AC
CP72	Neg	Neg	Neg	A	A	A
CP73	Neg	Neg	Neg	A	A	A
CP74	Neg	Neg	Neg	A	A	A
CP75	Neg	Neg	Neg	A	A	A
CP76	Pos	Pos	Pos	A	A	A
CP77	Pos	Pos	Pos	A	A	A
CP78	Pos	Pos	Pos	A	A	A
CP79	Neg	Neg	Neg	A	A	A
CP80	Neg	Neg	Neg	A	A	A
CP81	Pos	Pos	Pos	A	A	A
CP82	Neg	Neg	Neg	A	A	A
CP83	Pos	Pos	Pos	A	A	A
CP84	Neg	Neg	Neg	A	A	A
CP85	Pos	Pos	Pos	A	A	A
CP86	Pos	Neg	Pos	F-	A	AC
CP87	Pos	Pos	Pos	A	A	A
CP88	Pos	Pos	Pos	A	A	A
CP89	Pos	Pos	Pos	A	A	A
CP90	Pos	Pos	Pos	A	A	A
CP91	Pos	Pos	Pos	A	A	A
CP92	Pos	Pos	Pos	A	A	A
CP93	Pos	Pos	Pos	A	A	A
CP94	Pos	Pos	Pos	A	A	A
CP95	Pos	Neg	Neg	F-	F-	F-
CP96	Pos	Pos	Pos	A	A	A
CP97	Pos	Pos	Pos	A	A	A
CP98	Pos	Pos	Pos	A	A	A
CP99	Pos	Pos	Pos	A	A	A
CP100	Pos	Pos	Pos	A	A	A

(Continued)

TABLE 2 | Continued

Patient plasma	RT-PCR	IgG RayBio	IgG Healgen	Comparison RT-PCR/IgG Raybio	Comparison RT-PCR/ IgG Healgen	Comparison RT-PCR/ IgG Raybio+Healgen
CP101	Neg	Neg	Neg	A	A	A
CP102	Neg	Neg	Neg	A	A	A
CP103	Neg	Neg	Neg	A	A	A
CP104	Neg	Neg	Neg	A	A	A
CP105	Neg	Neg	Neg	A	A	A
CP106	Neg	Neg	Neg	A	A	A
CP107	Neg	Neg	Neg	A	A	A
CP108	Neg	Neg	Neg	A	A	A
CP109	Pos	Pos	Pos	A	A	A
CP110	Pos	Pos	Pos	A	A	A
CP111	Pos	Pos	Pos	A	A	A
CP112	Pos	Pos	Pos	A	A	A
CP113	Pos	Pos	Pos	A	A	A
CP114	Pos	Pos	Pos	A	A	A
CP115	Pos	Pos	Pos	A	A	A
CP116	Pos	Pos	Pos	A	A	A
CP117	Pos	Neg	Neg	F-	F-	F-
CP118	Pos	Pos	Pos	A	A	A
CP119	Pos	Pos	Pos	A	A	A
CP120	Pos	Pos	Pos	A	A	A
CP121	Neg	Neg	Neg	A	A	A
CP122	Neg	Neg	Neg	A	A	A
CP123	Neg	Neg	Neg	A	A	A
CP124	Neg	Neg	Neg	A	A	A
CP125	Neg	Neg	Neg	A	A	A
CP126	Neg	Neg	Neg	A	A	A
CP127	Neg	Neg	Neg	A	A	A
CP128	Neg	Neg	Neg	A	A	A
CP129	Neg	Neg	Neg	A	A	A
CP130	Neg	Neg	Neg	A	A	A
CP131	Neg	Neg	Neg	A	A	A
CP132	Neg	Neg	Neg	A	A	A
CP133	Neg	Neg	Neg	A	A	A
CP134	Neg	Neg	Neg	A	A	A
CP135	Neg	Neg	Neg	A	A	A
CP136	Neg	Neg	Neg	A	A	A
CP137	Neg	Neg	Neg	A	A	A
CP138	Neg	Neg	Neg	A	A	A
CP139	Neg	Neg	Neg	A	A	A
CP140	Neg	Neg	Neg	A	A	A
CP141	Neg	Neg	Neg	A	A	A
CP142	Neg	Neg	Neg	A	A	A
CP143	Neg	Neg	Neg	A	A	A
CP144	Neg	Neg	Neg	A	A	A
CP145	Neg	Neg	Neg	A	A	A
CP146	Neg	Neg	Neg	A	A	A
CP147	Neg	Neg	Neg	A	A	A
CP148	Neg	Neg	Neg	A	A	A
CP149	Neg	Neg	Neg	A	A	A
CP150	Neg	Neg	Neg	A	A	A

(Continued)

TABLE 2 | Continued

Patient plasma	RT-PCR	IgG RayBio	IgG Healgen	Comparison RT-PCR/IgG Raybio	Comparison RT-PCR/ IgG Healgen	Comparison RT-PCR/ IgG Raybio+Healgen
CP151	Neg	Neg	Neg	A	A	A
CP152	Neg	Neg	Neg	A	A	A
CP153	Neg	Neg	Neg	A	A	A
CP154	Neg	Neg	Neg	A	A	A
CP155	Neg	Neg	Neg	A	A	A
CP156	Neg	Neg	Neg	A	A	A
CP157	Neg	Neg	Neg	A	A	A
CP158	Neg	Neg	Neg	A	A	A
CP159	Neg	Neg	Neg	A	A	A
CP160	Neg	Neg	Neg	A	A	A
CP161	Neg	Neg	Neg	A	A	A
CP162	Neg	Neg	Neg	A	A	A
CP163	Neg	Neg	Neg	A	A	A
CP164	Neg	Neg	Neg	A	A	A
CP165	Neg	Neg	Neg	A	A	A
CP166	Neg	Neg	Neg	A	A	A
CP167	Neg	Neg	Neg	A	A	A
CP168	Neg	Neg	Neg	A	A	A
CP169	Neg	Neg	Neg	A	A	A
CP170	Neg	Neg	Neg	A	A	A
CP171	Neg	Neg	Neg	A	A	A
CP172	Neg	Neg	Neg	A	A	A
CP173	Neg	Neg	Neg	A	A	A
CP174	Neg	Neg	Neg	A	A	A
CP175	Neg	Neg	Neg	A	A	A
CP176	Neg	Neg	Neg	A	A	A
CP177	Neg	Neg	Neg	A	A	A
CP178	Neg	Neg	Neg	A	A	A
CP179	Neg	Neg	Neg	A	A	A
CP180	Neg	Neg	Neg	A	A	A
CP181	Neg	Neg	Neg	A	A	A
CP182	Neg	Neg	Neg	A	A	A
CP183	Neg	Neg	Neg	A	A	A
CP184	Neg	Neg	Neg	A	A	A
CP185	Neg	Neg	Neg	A	A	A
CP186	Neg	Neg	Neg	A	A	A
CP187	Neg	Neg	Neg	A	A	A
CP188	Neg	Neg	Neg	A	A	A
CP189	Neg	Neg	Neg	A	A	A
CP190	Neg	Neg	Neg	A	A	A
CP191	Neg	Neg	Neg	A	A	A
CP192	Neg	Neg	Neg	A	A	A
CP193	Neg	Neg	Neg	A	A	A
CP194	Neg	Neg	Neg	A	A	A
CP195	Neg	Neg	Neg	A	A	A

Neg, Negative; Pos, Positive; F-, False negative; F+, False positive; A, Agreement with PCR result; AC, Agreement of combined testing.

combination of tests = 0.0001 and *p*-value for IgM Healgen vs. combination of tests = 0.0003). These results show a clear significance and beneficial added value for the combination of both kits in detecting IgM.

Concerning IgG, as shown in **Tables 6–8**, it was noted that the sensitivity of Raybiotech alone was 68.9%, and Healgen alone was 74.0% (*p*-value for IgG RayBio vs. IgG Healgen = 0.5847). When the rule about disagreement was implemented (refer to Material

TABLE 3 | Sensitivity, specificity, and agreement of Raybiotech LFIA IgM with RT-PCR results.

		LFIA IgM (Raybio)		Total
		+	-	
RT-PCR	+	43	30	73
	-	1	121	122
	Total	44	151	195
	Sensitivity	Specificity	Agreement	
	58.9%	99.2%	84.1%	

TABLE 4 | Sensitivity, specificity, and agreement of Healgen LFIA IgM with RT-PCR results.

		LFIA IgM (Healgen)		Total
		+	-	
RT-PCR	+	49	25	74
	-	0	121	121
	Total	49	146	195
	Sensitivity	Specificity	Agreement	
	66.2%	100.0%	87.7%	

TABLE 5 | Sensitivity, specificity, and agreement of combined Raybiotech+Healgen LFIA IgM with RT-PCR results.

		LFIA IgM combined		Total
		+	-	
RT-PCR	+	64	9	73
	-	1	121	122
	Total	65	130	195
	Sensitivity	Specificity	Agreement	
	87.7%	99.2%	94.9%	

and Methods), the sensitivity of the combined kits was 74.0% (p-value of IgG Raybio vs. combination of both tests = 0.5847). This result does not suggest an added value for the combination of both kits in detecting IgG. The very low number of false positive results (only one patient) resulted in a high specificity varying between 99.2 and 100% for both kits.

The results of limit of detection show a better detection of IgG at higher dilutions of the sample in both kits than for IgM (**Tables 9**, **10**).

For both tested kits, no cross-reactivity of the SARS-CoV-2 detection rapid tests using plasma samples from patients with documented antibodies against the below listed pathogens was seen: Human Coronavirus 229 E, Human Coronavirus NL63 (alpha coronavirus, Human Coronavirus, Respiratory Syncytial Virus, Human Coronavirus NL63+RSV, Human Coronavirus 229+RSV, Human Metapneumovirus (hMPV, Parainfluenza virus (1,3,), Influenza A, Influenza B, Hepatitis C Virus, Hepatitis B Virus, Hemophilus influenzae, Chlamydia pneumoniae, HPV, HIV.

No class specificity interference with both kits was found using human IgM and human IgG. No false positive or false negative results were recorded.

None of the tested substances (Hemoglobin, Bilirubin Conjugated, Bilirubin Unconjugated, Ciprofloxacin, Cefotaxime, Meropenem, Imipenem, Amikacin, and Amphotericin) were found to interfere with the ability of IgM and IgG detection in both kits. No changes in results were recorded for the inter- and intra-assay tests. All replicates of the same samples in the same experiment as well as the same samples in different experiments yielded the same results.

DISCUSSION

The pandemic caused by SARS-CoV-2 has been ongoing since the end of 2019. Unfortunately, in the absence of a successful vaccine and a standard efficient treatment, this virus remains invincible in many ways. Lockdown of societies and prevention measures only hope to contain the transmission of the disease until further notice. In this context, massive testing remains a good strategy to identify carriers of the virus. In view of the shortage of material and resources, RT-PCR tests should be part of the algorithm of testing and not the only test. Serology tests investigating the development of IgG and IgM in patients who have been potentially infected is another good addition to the algorithm. Unfortunately, many parameters including the onset of the disease, incubation period, symptomatology, and immunity status of the patient put some limitations on these serological tests regarding their sensitivity and specificity (Haveri et al., 2020). A negative IgM, negative IgG test can be interpreted as no evidence of an increase in human IgM and IgG production against SARS-CoV-2. This negative or non-reactive result might indicate a state of no infection or an incubation period of the virus. In the case of suspicious exposure, the patient should be advised to repeat the test in 7–10 days (Pal et al., 2020). A negative result can also be due to a delayed immune response by the patient. A test showing positive IgM and negative or non-reactive IgG can indicate an early stage of a SARS-CoV-2 infection. The absence of IgG indicates that the patient had not developed acquired immunity yet. A positive IgM and IgG result suggests either an active or an early recovery stage of the infection with SARS-CoV-2. A negative IgM and positive IgG generally indicates a late stage or a past infection with SARS-CoV-2. This suggests that an acquired immunity has developed to the virus.

The detection of immunoglobulins (M and G) is based on immunochromatography where the separation of components in a mixture is accomplished based on the capillary force and the highly specific antigen-antibody binding. IgM antibodies to SARS-CoV-2 generally become positive (detectable in serum) between day 5 and 7 following infection but may occur later. This is the same for IgG antibodies to SARS-CoV-2 that generally become detectable 10–14 days following infection (Huang et al., 2020).

In this work, we have shown that the combination of two lateral flow immunochromatographic tests increase the sensitivity of the assay in detecting IgM, however, this was not

TABLE 6 | Sensitivity, specificity, and agreement of Raybiotech LFIA IgG with RT-PCR results.

		LFIA IgG (Raybio)		Total
		+	-	
RT-PCR	+	51	23	74
	-	0	121	121
	Total	51	144	195
		Sensitivity	Specificity	Agreement
		68.9%	100.0%	88.7%

TABLE 7 | Sensitivity, specificity, and agreement of Healgen LFIA IgG with RT-PCR results.

		LFIA IgG (Healgen)		Total
		+	-	
RT-PCR	+	54	19	73
	-	0	122	122
	Total	54	141	195
		Sensitivity	Specificity	Agreement
		74.0%	100.0%	90.3%

TABLE 8 | Sensitivity, specificity, and agreement of combined Raybiotech+Healgen LFIA IgG with RT-PCR results.

		LFIA IgG combined		Total
		+	-	
RT-PCR	+	54	19	73
	-	0	122	122
	Total	54	141	195
		Sensitivity	Specificity	Agreement
		74.0%	100.0%	90.3%

TABLE 9 | Limit of detection for IgM and IgG by Healgen kit.

	Dilutions of the plasma of patients CP2, CP17, and CP64						
CP2	**D0**	**D1**	**D2**	**D3**	**D4**	**D5**	**D6**
Concentration	1	D0/2	D0/4	D0/8	D0/16	D0/32	D0/64
Band control	+	+	+	+	+	+	-
Band IgM	+	+	+	-	-	-	-
Band IgG	+	+	+	+	+	+	-
CP17	**D0**	**D1**	**D2**	**D3**	**D4**	**D5**	**D6**
Concentration	1	D0/2	D0/4	D0/8	D0/16	D0/32	D0/64
Band control	+	+	+	+	+	+	-
Band IgM	+	+	+	-	-	-	-
Band IgG	+	+	+	+	+	+	-
CP64	**D0**	**D1**	**D2**	**D3**	**D4**	**D5**	**D6**
Concentration	1	D0/2	D0/4	D0/8	D0/16	D0/32	D0/64
Band control	+	+	+	+	+	+	-
Band IgM	+	+	+	-	-	-	-
Band IgG	+	+	+	+	+	+	-

TABLE 10 | Limit of detection for IgM and IgG by Raybiotech kit.

	Dilutions of the plasma of patients CP2, CP17, and CP64						
CP2	**D0**	**D1**	**D2**	**D3**	**D4**	**D5**	**D6**
Concentration	1	D0/2	D0/4	D0/8	D0/16	D0/32	D0/64
Band control	+	+	+	+	+	+	+
Band IgM	+	+	+	-	-	-	-
Band IgG	+	+	+	+	+	+	-
CP17	**D0**	**D1**	**D2**	**D3**	**D4**	**D5**	**D6**
Concentration	1	D0/2	D0/4	D0/8	D0/16	D0/32	D0/64
Band control	+	+	+	+	+	+	+
Band IgM	+	+	+	+	+	+	-
Band IgG	+	+	+	+	+	+	+
CP64	**D0**	**D1**	**D2**	**D3**	**D4**	**D5**	**D6**
Concentration	1	D0/2	D0/4	D0/8	D0/16	D0/32	D0/64
Band control	+	+	+	+	+	+	+
Band IgM	+	+	+	+	+	-	-
Band IgG	+	+	+	+	+	+	+

the case for IgG. As well as any other testing, the sensitivity and specificity of paper-based assays determines their performance (Tan et al., 1999). Sensitivity assesses and measures the ability of the test to correctly detect the target-substrate. In this context, it is very important to determine the limit of detection (LoD) which can directly affect positively or negatively the sensitivity of the test in question (Wang et al., 2013; Farka et al., 2017). The LoD corresponds to the lowest concentration associated with a positive detectable signal. Several parameters can influence the LoD, such as the affinity of the antigen and antibody, as well as the physical properties of these molecules. In addition, the paper substrate properties, number, printed detector molecules, immunoprobe stability, readout method, and competition with free target molecules are all parameters that can influence the quality of the lateral flow immunochromatography test.

On the other hand, the specificity of a technique relates to the probability of yielding a false positive result. Similar to sensitivity, it is defined by many parameters and factors including the cross-reactivity and nonspecific binding to the immunoprobe. On the other hand, fluidic properties of the paper strip as well as sample preparation are important parameters affecting paper assay performance (Hristov et al., 2019).

It is expected that different manufacturers will produce different products with different performances. When two tests are used for the same sample, there is the possibility of agreement or disagreement on the result. While agreement between tests is considered to "dramatically improve the predictive value of a testing program, particularly in low

prevalence environments" (Blueprint for testing plans and rapid response programs- partnering with states to put America back to work https://www.whitehouse.gov/wp-content/uploads/2020/04/Testing-Blueprint.pdf), the disagreement can also be used to dramatically improve the agreement of LFIA with RT-PCT tests, as shown in our paper. This effect has been significantly high with IgM (**Tables 3–8**) and was insignificant with IgG. Our results suggest that in view of the differences in material and production, and in view of the high specificity of immunoglobulin detection (yielding low levels of false positive results), it is to our advantage to use more than one kit for the detection of immunoglobulins and consider the positive result where the disagreement occurs. The reason why this is true for IgM and not for IgG might be due to the high specificity, smaller size, and higher number of IgGs as compared to IgMs. In any case, the combination of more than one kit should be only advised if this is confirmed by method evaluation and validation.

Regarding the evaluation of LFIA for SARS-CoV-2 detection by Raybiotech and Healgen, our results have shown particularly good performance in terms of the limit of detection, interfering substances, and inter and intra assay variation. These parameters are extremely important in the evaluation process, not only for their direct significance, but also for their influence on the sensitivity and specificity of the tests.

In conclusion, our results are in agreement with others suggesting the use of combinatory testing for the serology of COVID-19 and suggest a full evaluation study including all the parameters affecting their clinical performance before deciding on this combination.

DATA AVAILABILITY STATEMENT

All datasets generated for this study are included in the article/supplementary material.

ETHICS STATEMENT

The studies involving human participants were reviewed and approved by Institution Review Board waived- Michigan Health Clinics IRB approval waived- Only plasma samples previously collected from the patients were used. Written informed consent to participate in this study was provided by the participants' legal guardian/next of kin.

AUTHOR CONTRIBUTIONS

ZD designed the study, participated in the experiments, data analysis, and manuscript writing. JM participated in the experiments and data analysis. DS participated in the study design, data analysis, and manuscript writing. All authors contributed to the article and approved the submitted version.

REFERENCES

Farka, Z. K., Jurík, T. S., Kovár, D., Trnková, L. E., and Skládal, P. (2017). Nanoparticle-based immunochemical biosensors and assays: recent advances and challenges. *Chem. Rev*. 117, 9973–10042. doi: 10.1021/acs.chemrev.7b00037

Haveri, A., Smura, T., Kuivanen, S., Österlund, P., Hepojoki, J., Ikonen, N., et al. (2020). Serological and molecular findings during SARS-CoV-2 infection: the first case study in Finland, January to February 2020. *Euro. Surveill*. 25:2000266. doi: 10.2807/1560-7917.ES.2020.25.11.2000266

Hristov, D. R., Rodriguez-Quijada, C., Gomez-Marquez, J., and Hamad-Schifferli, K. (2019). Designing paper-based immunoassays for biomedical applications. *Sensors* 19:554. doi: 10.3390/s19030554

Huang, C., Wen, T., Shi, F. J., Zeng, X. Y., and Jiao, Y. J. (2020). Rapid detection of IgM antibodies against the SARS-CoV-2 virus via colloidal gold nanoparticle-based lateral-flow assay. *ACS Omega* 21, 12550–12556. doi: 10.1021/acsomega.0c01554

Liua, R., Hana, H., Liubc, F., Lva, Z., Wub, K., and Liub, Y. (2020). Positive rate of RT-PCR detection of SARS-CoV-2 infection in 4880 cases from one hospital in Wuhan, China, from Jan to Feb 2020. *Clin. Chim. Acta* 505, 172–175. doi: 10.1016/j.cca.2020.03.009

Pal, M., Berhanu, G., Desalegn, C., and Kandi, V. (2020). Severe acute respiratory syndrome coronavirus-2 (SARS-CoV-2): an update. *Cureus* 12:e7423. doi: 10.7759/cureus.7423

Tahamtan, A., and Ardebili, A. (2020). Real-time RT-PCR in COVID-19 detection: issues affecting the results. *Expert. Rev. Mol. Diagn*. 20, 453–454. doi: 10.1080/14737159.2020.1757437

Tan, E. M., Smolen, J. S., McDougal, J., Butcher, B. T., Conn, D., Dawkins, R., et al. (1999). A critical evaluation of enzyme immunoassays for detection of antinuclear autoantibodies of defined specificities: I. Precision, sensitivity, and specificity. *Arthritis Rheum*. 42, 455–464.

Wang, Y., Salehi, M., Schütz, M., Rudi, K., and Schlücker, S. (2013). Microspectroscopic SERS detection of interleukin-6 with rationally designed gold/silver nanoshells. *Analyst* 138, 1764–1771. doi: 10.1039/c3an36610c

WHO (2020). WHO Director-General's opening remarks at the media briefing on COVID-19 - 16March2020. [Online]. Available: https://www.who.int/dg/speeches/detail/who-director-general-s-opening-remarks-at-the-mediabriefing-on-covid-19 (accessed 16-march, 2020).

Yager, P., Edwards, T., Fu, E., Helton, K., Nelson, K., Tam, M. R., et al. (2006). Microfluidic diagnostic technologies for global public health. *Nature* 442:412. doi: 10.1038/nature05064

Conflict of Interest: The authors declare that the research was conducted in the absence of any commercial or financial relationships that could be construed as a potential conflict of interest.

frontiers in Cellular and Infection Microbiology

ORIGINAL RESEARCH
published: 25 February 2021
doi: 10.3389/fcimb.2021.639473

Development of a Rapid and Fully Automated Multiplex Real-Time PCR Assay for Identification and Differentiation of *Vibrio cholerae* and *Vibrio parahaemolyticus* on the BD MAX Platform

*Zhenpeng Li[1], Hongxia Guan[2], Wei Wang[1], He Gao[1], Weihong Feng[2], Jie Li[1], Baowei Diao[1], Hongqun Zhao[1], Biao Kan[1,3] and Jingyun Zhang[1]**

[1] State Key Laboratory of Infectious Disease Prevention and Control, National Institute for Communicable Disease Control and Prevention, Chinese Center for Disease Control and Prevention, Beijing, China, [2] Wuxi Center for Disease Control and Prevention, Wuxi, China, [3] Collaborative Innovation Center for Diagnosis and Treatment of Infectious Diseases, Hangzhou, China

OPEN ACCESS

Edited by:
Hongchao Gou,
Guangdong Academy of Agricultural Science, China

Reviewed by:
Li Bsn,
Guangdong Provincial Center for Disease Control and Prevention, China
Yajun Song,
Beijing Institute of Microbiology and Epidemiology, China

***Correspondence:**
Jingyun Zhang
zhangjingyun@icdc.cn

Specialty section:
This article was submitted to Clinical Microbiology, a section of the journal Frontiers in Cellular and Infection Microbiology

Received: 09 December 2020
Accepted: 21 January 2021
Published: 25 February 2021

Citation:
Li Z, Guan H, Wang W, Gao H, Feng W, Li J, Diao B, Zhao H, Kan B and Zhang J (2021) Development of a Rapid and Fully Automated Multiplex Real-Time PCR Assay for Identification and Differentiation of Vibrio cholerae and Vibrio parahaemolyticus on the BD MAX Platform. Front. Cell. Infect. Microbiol. 11:639473. doi: 10.3389/fcimb.2021.639473

Vibrio cholerae and *Vibrio parahaemolyticus* are common diarrheal pathogens of great public health concern. A multiplex TaqMan-based real-time PCR assay was developed on the BD MAX platform; this assay can simultaneously detect and differentiate *V. cholerae* and *V. parahaemolyticus* directly from human fecal specimens. The assay includes two reactions. One reaction, BDM-VC, targets the gene *ompW*, the cholera toxin (CT) coding gene *ctxA*, the O1 serogroup specific gene *rfbN*, and the O139 serogroup specific gene *wbfR* of *V. cholerae*. The other, BDM-VP, targets the gene *toxR* and the toxin coding genes *tdh* and *trh* of *V. parahaemolyticus*. In addition, each reaction contains a sample process control. When evaluated with spiked stool samples, the detection limit of the BD MAX assay was 195–780 CFU/ml for *V. cholerae* and 46–184 CFU/ml for *V. parahaemolyticus*, and the amplification efficiency of all genes was between 95 and 115%. The assay showed 100% analytical specificity, using 63 isolates. The BD MAX assay was evaluated for its performance compared with conventional real-time PCR after automated DNA extraction steps, using 164 retrospective stool samples. The overall percent agreement between the BD MAX assay and real-time PCR was ≥ 98.8%; the positive percent agreement was 85.7% for *ompW*, 100% for *toxR*/*tdh*, and lower (66.7%) for *trh* because of a false negative. This is the first report to evaluate the usage of the BD MAX open system in detection and differentiation of *V. cholerae* and *V. parahaemolyticus* directly from human samples.

Keywords: *Vibrio cholerae*, *Vibrio parahaemolyticus*, multiplex, real-time PCR, BD MAX

INTRODUCTION

Vibrio cholerae is the etiological pathogen of cholera, an acute watery diarrheal disease. Researchers have estimated that in endemic countries globally, there are approximately 1.3 billion people at risk for cholera, 1.3–4.0 million cholera cases occurring annually, and 21,000–143,000 deaths among these cases (Ali et al., 2015). In 2017, more than 1.2 million cases and 5,654 deaths were reported from 34 countries (WHO, 2018). The current seventh cholera pandemic continues to be a major public health threat for countries in Asia, Africa, and the Americas (WHO, 2018). With more than 220 serogroups of *V. cholerae*, only the O1 and O139 serogroups have been associated with epidemics and pandemics (Reidl and Klose, 2002; Mahapatra et al., 2014; Bonnin-Jusserand et al., 2019). Cholera toxin (CT) encoded by *ctxA* and *ctxB* is responsible for severe, cholera-like diseases in epidemic and sporadic forms (Holmgren, 1981; Wernick et al., 2010). In assessing the public health significance of an isolate of *V. cholerae*, the possession of the O1 or O139 antigen is a marker of epidemic or pandemic potential (Kaper et al., 1995), and the production of CT is one of the most important properties to be determined.

V. parahaemolyticus causes acute gastroenteritis mostly associated with the consumption of raw or improperly cooked contaminated seafood (Daniels et al., 2000). It often leads to sporadic cases or outbreaks in coastal areas during warm seasons (Baker-Austin et al., 2017) and has been a major seafood-borne pathogen and a global public health concern. Thermostable direct hemolysin (TDH, encoded by the gene *tdh*) and TDH-related hemolysin (TRH, encoded by the gene *trh*) are considered to be the main pathogenic factors of *V. parahaemolyticus* (Shinoda, 2011). The genes *tdh* and *trh* exist in most clinical isolates and are relatively rare in environmental isolates (Theethakaew et al., 2013).

Timely detection of *V. cholerae* and *V. parahaemolyticus* infection in patients with diarrhea, as well as identification of serogroups and virulence factors, is of great significance for patient treatments and controlling disease spread. With the development of molecular detection technology, various PCR-based detection methods have been developed and applied, including conventional PCR, real-time PCR, and multiplex PCR (Tada et al., 1992; Rivera et al., 2003; Jeyasekaran et al., 2011; Tebbs et al., 2011; Tall et al., 2012). These methods require that before amplification, nucleic acids be extracted independently, which is time-consuming and labor-intensive. Therefore, there is an urgent need for an automated and integrated platform to complete the molecular detection of *Vibrios* directly from infected patients' specimens.

The BD MAX system (Becton Dickinson Inc., Maryland, USA) is a fully automated molecular platform for *in vitro* diagnostic, as well as in-house-developed tests. The platform extracts DNA or RNA using specific extraction reagents, followed by real-time PCR amplification and detection of fluorescence in up to five channels. The system can be run in an open mode that allows adding any user-specific primers and PCR reagents. In this study, we developed a multiplex real-time PCR assay on a BD MAX open system for detection and differentiation of *V. cholerae* and *V. parahaemolyticus* directly from human fecal specimens.

MATERIALS AND METHODS

Strains and Samples

V. cholerae strains N16961 (O1 serogroup, CT positive) (Heidelberg et al., 2000) and ATCC 51394 (O139 serogroup, CT positive), and *V. parahaemolyticus* strain VP8 (a clinical strain, *tdh* and *trh* positive) were used as positive reference strains for the establishment of the real-time PCR assay. The 63 strains (**Table 1**) used for specificity evaluation included 22 V. *cholerae* strains (11 O1 serogroup and 11 O139 serogroup), 19 V. *parahaemolyticus* strains, 8 diarrheagenic *Escherichia coli* (DEC), 6 *Salmonella* spp., 2 *Shigella* spp., 1 V. *mimicus*, 1 V. *fluvialis*, 1 V. *vulnificus*, 1 V. *anguillarum*, 1 *Plesinomonas shigelloides*, and 1 *Aeromonas hydrophila.* The *ctxA* gene of *V. cholerae* and the *tdh*/*trh* genes of *V. parahaemolyticus* were screened and determined by singleplex real-time PCR assays as described in the "analysis of clinical samples" section below with primers/probes listed in **Table 2**.

To evaluate the effectiveness of the assay on the detection of actual diarrhea samples, based on the detection results in other studies, we retrospectively selected 164 fecal samples from outpatients with diarrhea from 2016 to 2018 in Wuxi, Jiangsu Province. One to two grams of fecal samples were added to 5 ml of liquid Carry-Blair transport medium and mixed. The samples were delivered to the laboratory at room temperature and frozen to -80°C within 24 hours.

Primers and Probes

The primers/probes designed for *V. cholerae* (the reaction BDM-VC) targets the genes *ompW*, *ctxA*, *rfbN* (specific for the O1 serogroup), and *wbfR* (specific for the O139 serogroup). The reaction for *V. parahaemolyticus* (BDM-VP) targets the gene *toxR* and the toxin coding genes *tdh* and *trh.* In addition, each reaction contained a pair of primers and a probe targeting *yaiO* gene of *E. coli* as a sample process control (SPC).

All the targeted gene sequences were based on alignments of available sequences deposited in nr database of NCBI (https://www.ncbi.nlm.nih.gov/nucleotide/). All primers and probes were designed using Beacon Designer V8.20, and were synthesized by Sangon Biotech (Shanghai, China). The NCBI BLASTn was used to check the in silico specificity and sensitivity.

Testing Procedures on the BD MAX Open System Platform

During sample processing, 50 µl of each sample was added into the sample buffer tubes (SBTs) of the BD MAX ExK TNA-2 extraction kit (IDS, BD). SBTs were covered with a cap, vortexed, and placed into the sample rack. Extraction reagent strips of the ExK TNA-2 kit were supplemented with the 2 × PCR master mix of BDM-VC in position 2, 2 × PCR master mix of BDM-VP in position 4, and 25 µl of deionized water in position 3. The positions 2, 3, and 4 are specified in the product manual of ExK TNA-2 kit. The 2 × PCR master mix contained 600 nM of each

TABLE 1 | Strains used in the study.

	Strain	Year	Description
***Vibrio cholerae* (n = 22)**	N16961	1975	O1 Inaba, reference strain, *ctxA*+
	ICDC-VC4679	1977	O1 Ogawa, clinical strain, *ctxA*+
	ICDC-VC4684	1978	O1 Ogawa, clinical strain, *ctxA*+
	ICDC-VC4685	1978	O1 Ogawa, clinical strain, *ctxA*+
	ICDC-VC4689	1978	O1 Ogawa, clinical strain, *ctxA*+
	ICDC-VC4692	1980	O1 Inaba, clinical strain, *ctxA*+
	ICDC-VC4696	1991	O1 Inaba, clinical strain, *ctxA*+
	ICDC-VC4879	1988	O1 Ogawa, *ctxA*+
	ICDC-VC4981	1982	O1 Inaba, clinical strain, *ctxA*+
	ICDC-VC4670	2008	O1 Inaba, estuarine water, *ctxA*-
	ICDC-VC4876	1987	O1 Ogawa, clinical strain, *ctxA*-
	ATCC 51394	1992	O139, reference strain, *ctxA*+
	ICDC-VC206	2001	O139, clinical strain, *ctxA*+
	ICDC-VC213	2003	O139, clinical strain, *ctxA*+
	ICDC-VC495	2005	O139, clinical strain, *ctxA*+
	ICDC-VC818	2003	O139, clinical strain, *ctxA*+
	ICDC-VC1193	1997	O139, clinical strain, *ctxA*+
	ICDC-VC1662	2006	O139, clinical strain, *ctxA*+
	ICDC-VC2384	2009	O139, clinical strain, *ctxA*+
	ICDC-VC2650	1994	O139, clinical strain, *ctxA*+
	ICDC-VC207	2002	O139, clinical strain, *ctxA*-
	ICDC-VC3768	1993	O139, clinical strain, *ctxA*-
***V. parahaemolyticus* (n = 19)**	VP8	1984	Clinical strain, *tdh*+, *trh*+
	VP6-1	1984	Clinical strain, *tdh*+, *trh*-
	VP649	2010	Clinical strain, *tdh*+, *trh*-
	VP669	2011	Clinical strain, *tdh*+, *trh*-
	VP651	2010	Clinical strain, *tdh*+, *trh*-
	VP652	2010	Clinical strain, *tdh*+, *trh*-
	VP667	2011	Clinical strain, *tdh*+, *trh*-
	VP668	2011	Clinical strain, *tdh*+, *trh*-
	VP670	2011	Clinical strain, *tdh*+, *trh*-
	VP674	2011	Clinical strain, *tdh*+, *trh*-
	VP686	2011	Clinical strain, *tdh*+, *trh*-
	VP654	2010	Aquatic product, *tdh*-, *trh*-
	VP656	2010	Aquatic product, *tdh*-, *trh*-
	VP660	2010	Aquatic product, *tdh*-, *trh*-
	VP661	2010	Aquatic product, *tdh*-, *trh*-
	VP678	2011	Aquatic product, *tdh*-, *trh*-
	VP680	2011	Aquatic product, *tdh*-, *trh*-
	ATCC17802	NA	Reference strain, *tdh*-, *trh*-
	Vp-8411	NA	Environmental strain, *tdh*-, *trh*-
Non-target species			
V. mimicus (n = 1)	SX-4	2009	Clinical strain, *ctxA*+
V. fluvialis (n = 1)	CICC21612	NA	Reference strain
V. vulnificus (n = 1)	ATCC27562	1979	Estuarine. Reference strain
V. anguillarum (n = 1)	ATCC17749	NA	Clinical strain
Plesinomonas shigelloides (n = 1)	PS6	2012	Clinical strain
Aeromonas hydrophila (n = 1)	AH1	2012	Clinical strain
diarrheagenic *Escherichia coli* (n = 8)	EPEC49	2013	Clinical strain
	EPEC51	2013	Clinical strain
	EPEC87	2013	Clinical strain
	EAEC68	2013	Clinical strain
	EAEC73	2013	Clinical strain
	ETEC42	2013	Clinical strain
	EIEC9	2013	Clinical strain
	CN-ETEC-16	2016	Clinical strain
Salmonella (n = 6)	St1787	2002	*S. typhi*, clinical strain
	CT18	1993	*S. typhi*, clinical strain. Reference strain
	St1806	2016	*S. typhi*, clinical strain
	St1866	2016	*S. typhi*, Sewage
	St1868	2016	*S. typhi*, clinical strain
	Sa10387	2013	*S. enteritidis*, clinical strain
Shigella (n = 2)	4153-6	2012	Clinical strain
	CN-Shigella-2	2016	Clinical strain

TABLE 2 | Primers and probes for detection of virulence genes in strains and clinical samples.

Target genes	Code	Sequence (5'-3')	size (bp)
ctxA	CT1 F	CTTCCCTCCAAGCTCTATGCTC	114
	CT1 R	TACATCGTAATAGGGGCTACAGAG	
	CT1 P	FAM-ACCTGCCAATCCATAACCATCTGCTGCTG-BHQ1	
tdh	TDH F	AATGGTTGACATCCTACATGACTG	100
	TDH R	TTTACGAACACAGCAGAATGACC	
	TDH P	FAM-TATAGCCAGACACCGCTGCCATTGTATAGT-BHQ1	
trh	TRH F	GATTGCGTTAACTGGTGATTCAG	105
	TRH R	GCGATTGATCTACCATCCATACC	
	TRH P	HEX-TTCCTTCTCCAGGTTCGGATGAGCTACT-BHQ1	

primer, 200 nM of each probe, 5 µl of 5 × HR qPCR Master Mix (Huirui, Shanghai, China), and deionized water to complete a 12.5 µl final volume. The extraction strip was placed into the testing rack and then the test started running. Nucleic acid from 600 µl of liquid in the SBT was extracted and added to the conical tube containing 25 µl of deionized water at position 3; 12.5 µl of the mixture at position 3 were added into the conical tubes at positions 2 and 4, respectively. Cycling conditions were as follows: 95°C for 5 min and 40 cycles of 95°C for 15 s, 60°C for 43 s.

For SPC and all targets, the result was considered positive when the cycle threshold (Ct) value was ≤ 35. As long as SPC or any target gene was positive, the test was considered valid; if SPC and all target genes were negative, the test was considered invalid, and repeated testing was required.

Analytical Test

The analytical sensitivity was evaluated using the positive reference strains *V. cholerae* N16961, ATCC 51394, and *V. parahaemolyticus* VP8. Strains were cultured on LB agar and incubated overnight at 37°C. The bacterial lawn was picked into a centrifuge tube with a pipette tip, washed twice with 0.9% sodium chloride solution (normal saline), and then made into a 2.5 McFarland (BD PhoenixSpec, NJ, USA) suspension with normal saline. This was followed by the preparation of six 10-fold dilutions. Ten microliters of each dilution was mixed into 40 µl of healthy human stool samples, which were then transferred to the SBT of the ExK TNA-2 kit for detection on the BD MAX platform. The bacterial concentration of each dilution was calculated by colony count on LB agar. When a standard curve was plotted, Ct values obtained from each dilution were graphed on the y-axis versus the log of the bacterial concentration in artificially spiked stools on the x-axis. The amplification efficiency (E) was calculated from the slope of the standard curve according to the equation: $E = 10^{-1/slope}-1$.

When determining the limit of detection (LoD) of the established assay for each target gene, the 10^{-4} dilution of the bacterial suspension was serially diluted twice in normal saline. As above, 50 µl of artificially spiked stools (containing 10 µl of diluted bacterial solution and 40 µl of healthy human stool) was added to the SBTs and tested on the BD MAX platform. Each dilution was repeated 10 times. When all 10 replicates could be detected, the lowest bacterial concentration in the spiked stool was recorded as the LoD value of the target.

Analysis of Clinical Samples

Cryopreserved fecal samples, which were collected from diarrheal patients from 2016 to 2018 in Wuxi, Jiangsu Province, were melted at room temperature, and 50 µl of each sample was added into SBT for detection with both BDM-VC and BDM-VP on the BD MAX platform. When the internal control SPC and all target genes were negative, the test was invalid and needed to be repeated. In the repeated detection of invalid samples, three tests were performed in parallel to detect samples, *E. coli* ATCC25922 which could be used as the SPC template, and the mixture of samples and *E. coli* ATCC25922; if the Ct value of SPC increased with the addition of sample in SBT, it was speculated that there is an amplification inhibitor in the nucleic acid of the sample.

Clinical samples were detected in parallel with conventional singleplex real-time PCR assays. The template nucleic acids were extracted from 200 µl of fecal samples using a bacterial genomic DNA extraction kit on the automatic purification system NP968 (Tianlong, Xi'an, China). Species-specific genes of *V. cholerae* and *V. parahaemolyticus* were detected using commercial real-time PCR kits (X-ABT, Beijing, China) in accordance with the manufacturer's instructions. The virulence genes (*ctxA*, *tdh*, and *trh*) were screened with the primers and probes in **Table 2** in a 20 µl of reaction mixture containing 1 µl of DNA template, 200 nM primers, and 200 nM probes under the following conditions: 95°C for 30 s; 40 cycles of 95°C for 5 s, and 60°C for 40 s. The tests were carried out with a CFX96 system (Bio-Rad, Hercules, CA). Results were considered positive when Ct ≤ 35.

Statistical Analysis

The overall percent agreement (OPA), positive percent agreement (PPA), and negative percent agreement (NPA) were calculated (Institute, 2008) to evaluate the consistency between the results of BDM-VC/VP and the real-time PCR assays. Cohen's unweighted *kappa* (Kundel and Polansky, 2003) and the 95% confidence intervals (95% CIs) of the *kappa* value were calculated with SPSS version 23.0 (IBM Corp., Armonk, NY, USA).

RESULTS

Analytical Sensitivity and Specificity

The amplification efficiency and sensitivity of the BD MAX assay for each target gene were evaluated with healthy human stools

spiked with serial dilutions of positive reference strains. When the concentration of the strains in the spiked stool samples was 10^2–10^7 CFU/ml for *V. cholerae* (N16961 or ATCC51394) and 10^1–10^6 CFU/ml for *V. parahaemolyticus*, the standard curves showed good linearity (**Figure 1**), the coefficients of determination R^2 were all above 0.99, and the amplification efficiency of each target gene was 95.0–115.3% (**Table 3**). Spiked stools with higher and lower bacterial concentrations were not analyzed.

The LoD of BDM-VC for target genes of *V. cholerae* was 328–655 CFU/ml and 195–780 CFU/ml when analyzed with stools spiked with N16961 (O1 serogroup) and ATCC51394 (O139 serogroup), respectively. The BDM-VP reaction was more sensitive, and the LoD of the three target genes was 46–184 CFU/ml.

Specificity of the BD MAX assay was confirmed by testing a panel of strains (**Table 1**). All 22 V. *cholerae* isolates were *ompW* positive by BDM-VC; 11 of these were positive for *rfbN*, 11 were positive for *wbfR*, and 18 were *ctxA* positive. In the detection of 19 V. *parahaemolyticus* and 22 non-target strains, no amplification of BDM-VC was observed except for *ctxA* positive in *V. mimicus* SX-4. All 19 V. *parahaemolyticus* isolates were *toxR* positive by BDM-VP; 10 of these were positive for *tdh*, and one was positive for both *tdh* and *trh*. In the detection of 22 V. *cholerae* and 22 non-target strains, no amplification of BDM-VP was observed. The detection results of BDM-VC/VP were consistent with the singleplex real-time PCR assays (**Table 1**) and showed high specificity.

Clinical Validation of the BD MAX Assay

In order to evaluate the detection efficiency of the established method for clinical samples, 164 diarrheal fecal samples were selected and detected by the BD MAX assay and conventional real-time PCR respectively, and the results were compared (**Table 4**). BDM-VC detected 7 samples positive for non-O1/non-O139 and non-toxigenic *V. cholerae*. The real-time PCR assays detected 7 samples positive for non-O1/non-O139 and non-toxigenic *V. cholerae*. However, there were two samples with inconsistent results; one was positive by real-time PCR but negative by BDM-VC, and the other was just the opposite, resulting in a *kappa* value of 0.85 (95% CIs, 0.65–1.06) for *V. cholerae*. The *ompW* gene of the former (negative by BDM-VC) was sequenced, and a point mutation was found at the binding site of the BDM-VC probe. The latter was *ompW* positive with a Ct value of 34.4 by BDM-VC. In

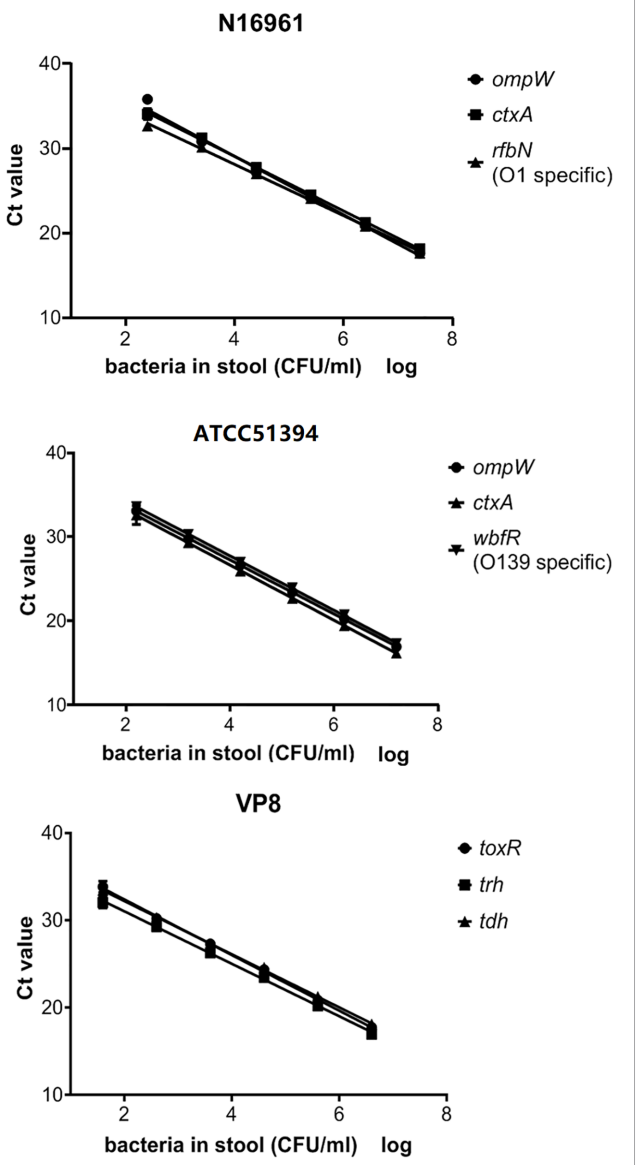

FIGURE 1 | The standard curve of the BD MAX assay for the detection of each gene in artificial samples. Ct values obtained from each dilution were graphed on the y-axis versus the log of the bacterial concentration in artificially spiked stools on the x-axis.

TABLE 3 | The amplification efficiency and sensitivity of the BD Max assay for each target gene.

Reaction	Strains spiked in stool	Targeted genes	R^2	Amplification efficiency	LoD (CFU/ml stool)
BDM-VC	N16961	*ompW*	0.993	95.0%	327.5
		ctxA	0.998	104.2%	655
		rfbN	0.998	113.8%	655
BDM-VC	ATCC51394	*ompW*	0.999	104.6%	195
		ctxA	0.996	101.8%	195
		wbfR	1.000	103.7%	780
BDM-VP	VP8	*toxR*	0.998	106.1%	46
		trh	0.998	115.3%	46
		tdh	0.999	112.8%	184

R^2, coefficient of determination; LoD, Limit of Detection.

the repeated real-time PCR tests for *V. cholerae*, the Ct values were 36.1 and 37.1, which were considered negative because they were higher than the threshold of Ct 35. Considering that a strain of *V. cholerae* was isolated from this sample, the false negative of real-time PCR might be mainly due to the low concentration of the strain in the feces.

BDM-VP detected 29 V. *parahaemolyticus* positive samples, 27 positive for *toxR/tdh* and two positive for *toxR/tdh/trh*. The same 29 positive samples were detected by real-time PCR assays, but the results of *trh* in one sample were different: BDM-VP was negative and real-time PCR was positive. By sequencing the amplified products of real-time PCR, it was confirmed that the sample was *trh* positive. Because the target fragments of BDM-VP and real-time PCR on *trh* gene did not overlap each other and the sequence of BDM-VP target fragment was not obtained, it could not be determined whether the false negative was caused by mutations in primers or probe binding sites. The *kappa* values of BDM-VP and the real-time PCR assays were 1.00 (95% CIs, 1.00–1.00) for *V. parahaemolyticus* and *tdh*, and 0.98 (95% CIs, 0.94–1.02) for *trh* (**Table 4**).

Eight of the 164 samples were negative for all targets including SPC by BDM-VC and BDM-VP, and the results were the same in repeated tests. They were also negative by conventional real-time PCR. The template of SPC (that is, the nucleic acid of *E. coli*) was directly added to the reactions of BDM-VC and BDM-VP. When the nucleic acid of the sample was not included in the reaction (control), the Ct value of SPC was 26.4–26.8. When the nucleic acid of the sample was contained in the reaction, the Ct value of SPC was (1) 25.9–27.4 in six samples, close to the control; (2) significantly increased in one sample, 36.2 in BDM-VC and 35.9 in BDM-VP; and (3) still negative in one sample. It was suggested that there were amplification inhibition factors in the nucleic acids extracted from the last two samples.

DISCUSSION

V. cholerae and *V. parahaemolyticus* are important intestinal pathogens of public health concern. In this study, an automated multiplex assay was established on a BD MAX platform to detect *V. cholerae* and *V. parahaemolyticus* as well as their important virulence genes and serogroup-related genes directly from clinical human fecal specimens. We evaluated the sensitivity and specificity of this assay and evaluated its application in clinical diarrhea samples.

In the analytical performance evaluation, the developed assay showed high sensitivity and specificity. The analytical specificity of the assay was established using a group of *Vibrio* isolates from different species as well as other organisms. No cross-reactivity, false positives, or false negatives were observed, even when species closely related to *V. cholerae* and *V. parahaemolyticus* were tested. The assay was shown to be very sensitive with a LoD as low as 46–780 CFU/ml and to have high PCR efficiency between 95.0 and 115.3% with spiked fecal samples. The sensitivity of this assay was close to the real-time PCR methods used to screen other pathogens in fecal samples (Raphael and Andreadis, 2007; Lin et al., 2008; Luna et al., 2011; Kouhsari et al., 2019).

In the detection of 164 retrospective stool samples, the developed assay on BD MAX achieved results comparable to the conventional real-time PCR assays. The inconsistent results of the two samples in the detection of *V. cholerae* showed that the BD MAX assay was more sensitive, but also revealed the defect that the probe sequence does not match the target sequence occasionally. BD MAX was also found to have an occasional false negative in the detection of the *trh* gene, which was speculated to be related to the diversity of *trh* sequences (Kishishita et al., 1992). In addition to the detection of *V. cholerae* and *V. parahaemolyticus* in clinical samples, the BD MAX assay screened important virulence genes and serogroup-specific genes, providing more information in one test regarding pathogens of interest than the comparison conventional assays.

The BD MAX assay contains an internal control SPC (a pair of primers and a probe designed according to the sequence of *E. coli* gene *yaiO*), which can monitor the processes of fecal nucleic acid extraction and PCR amplification. The failure of the SPC detection (unresolved results) could be caused by inhibitory substances in the stool

TABLE 4 | Consistency of the BD Max assay and conventional real time PCR results.

		Conventional real-time PCR assay		Consistency between the results			
		+	-	OPA	PPA	NPA	*kappa* (95% CIs)
BDM-VC							
ompW	+	6	1	98.8%	85.7%	99.4%	0.85 (0.65-1.06)
	–	1	156				
ctxA, *rfbN* and wbfR	+	0	0	100.0%	NA	100.0%	NA
	–	0	164				
BDM-VP							
toxR & *tdh*	+	29	0	100.0%	100.0%	100.0%	1.00 (1.00-1.00)
	–	0	135				
trh	+	2	0	99.4%	66.7%	100.0%	0.80 (0.40-1.19)
	–	1	161				

OPA, overall percent agreement; PPA, positive percent agreement; NPA, negative percent agreement; 95% CIs, 95% confidence intervals; NA, not available.

samples or reagent, or potential instrument failure. Evaluation of the commercially available BD MAX EBP assay revealed the rate of unresolved results was 2.4–8.03% (Harrington et al., 2015; Knabl et al., 2016; Simner et al., 2017). In this study, eight samples (4.9%) were unresolved. This proportion is consistent with literature reports. The negative of SPC in two samples (1.2% of the total and 25% of the unsolved) was due to the existence of amplification inhibition factors, while in other samples it might be due to the low concentration of *E. coli*, which might be caused by insufficient preservation of fecal samples when collected or during transportation, or by the degradation of nucleic acid during long-term preservation. When the developed assay was used for sample detection in this study, no exogenous SPC template was added to the samples or reaction system, which could monitor not only the amplification inhibitory factors in the sample but also the quality of the sample.

This assay has several limitations. The assay is incapable of detecting pathogens with mutations in the sequence of the binding sites of primers and probes. Like other PCR-based methods, the assay can amplify the DNA of dead bacteria in the sample, so a positive result does not necessarily indicate an active infection.

This multiplex assay was carried out on a BD MAX open system, a fully integrated sample-to-answer platform that performs both nucleic acid extraction and real-time PCR. Twenty-four samples can be detected at the same time. It took no more than 15 min hands-on time and less than 3 h for results, compared to conventional culture methods that would take days. Minimum manual operation can reduce potential human error, contamination, and potential biohazard to laboratory workers. This developed assay demonstrates potential promise to be useful in clinical settings routinely for detecting two of the most clinically important *V. cholerae* and *V. parahaemolyticus* species in public health.

DATA AVAILABILITY STATEMENT

The original contributions presented in the study are included in the article/supplementary material. Further inquiries can be directed to the corresponding author.

ETHICS STATEMENT

The studies involving human participants were reviewed and approved by Ethics Committee of National Institute for Communicable Disease Control and Prevention, China CDC. Written informed consent to participate in this study was provided by the participants' legal guardian/next of kin.

AUTHOR CONTRIBUTIONS

ZL: paper writing and data analysis. HXG: the test of clinical diarrheal samples. WW: evaluation of the analytical sensitivity and specificy of the multiplex assay. HG and WF: the collection of clinical diarrheal samples. JL, BD, and HZ: the identification of strains used in the study. BK: study design. JZ: study design, data analysis, and paper review. All authors contributed to the article and approved the submitted version.

FUNDING

This study was supported by National Science and Technology Major Project of China from the Ministry of Science and Technology of the People's Republic of China (2018ZX10712001-014 and 2018ZX10305409-003-003) and Wuxi Health Commission (T202017). The BD MAX instrument was provided by BD China free of charge, and no financial support was received from BD or any other commercial entities.

REFERENCES

Ali, M., Nelson, A. R., Lopez, A. L., and Sack, D. A. (2015). Updated Global Burden of Cholera in Endemic Countries. *PLoS Negl. Trop. Dis.* 9 (6), e0003832. doi: 10.1371/journal.pntd.0003832

Baker-Austin, C., Trinanes, J., Gonzalez-Escalona, N., and Martinez-Urtaza, J. (2017). Non-Cholera *Vibrios*: The Microbial Barometer of Climate Change. *Trends Microbiol.* 25 (1), 76–84. doi: 10.1016/j.tim.2016.09.008

Bonnin-Jusserand, M., Copin, S., Le Bris, C., Brauge, T., Gay, M., Brisabois, A., et al. (2019). *Vibrio* species involved in seafood-borne outbreaks (*Vibrio cholerae*, *V. parahaemolyticus* and *V. vulnificus*): review of microbiological *versus* recent molecular detection methods in seafood products. *Crit. Rev. Food Sci. Nutr.* 59 (4), 597–610. doi: 10.1080/10408398.2017.1384715

Daniels, N. A., MacKinnon, L., Bishop, R., Altekruse, S., Ray, B., Hammond, R. M., et al. (2000). *Vibrio parahaemolyticus* infections in the United States 1973-1998. *J. Infect. Dis.* 181 (5), 1661–1666. doi: 10.1086/315459

Harrington, S. M., Buchan, B. W., Doern, C., Fader, R., Ferraro, M. J., Pillai, D. R., et al. (2015). Multicenter evaluation of the BD max enteric bacterial panel PCR assay for rapid detection of *Salmonella* spp., *Shigella* spp., *Campylobacter* spp. (*C. jejuni* and *C. coli*), and *Shiga toxin 1* and *2* genes. *J. Clin. Microbiol.* 53 (5), 1639–1647. doi: 10.1128/JCM.03480-14

Heidelberg, J. F., Eisen, J. A., Nelson, W. C., Clayton, R. A., Gwinn, M. L., Dodson, R. J., et al. (2000). DNA sequence of both chromosomes of the cholera pathogen *Vibrio cholerae*. *Nature* 406 (6795), 477–483. doi: 10.1038/35020000

Holmgren, J. (1981). Actions of cholera toxin and the prevention and treatment of cholera. *Nature* 292 (5822), 413–417. doi: 10.1038/292413a0

Institute, C.A.L.S (2008). *User Protocol for Evaluation of Qualitative Test Performance; Approved Guideline—Second Edition* (940 West Valley Road, Suite 1400, Wayne, Pennsylvania 19087-1898 USA: Clinical and Laboratory Standards Institute).

Jeyasekaran, G., Raj, K. T., Shakila, R. J., Thangarani, A. J., and Sukumar, D. (2011). Multiplex polymerase chain reaction-based assay for the specific detection of toxin-producing *Vibrio cholerae* in fish and fishery products. *Appl. Microbiol. Biotechnol.* 90 (3), 1111–1118. doi: 10.1007/s00253-011-3175-9

Kaper, J. B., Morris, J. G.Jr., and Levine, M. M. (1995). Cholera. *Clin. Microbiol. Rev.* 8 (1), 48–86 doi: 10.1128/CMR.8.1.48-86.1995

Kishishita, M., Matsuoka, N., Kumagai, K., Yamasaki, S., Takeda, Y., and Nishibuchi, M. (1992). Sequence variation in the thermostable direct hemolysin-related hemolysin (*trh*) gene of *Vibrio parahaemolyticus*. *Appl. Environ. Microbiol.* 58 (8), 2449–2457 doi: 10.1128/AEM.58.8.2449-2457.1992

Knabl, L., Grutsch, I., and Orth-Holler, D. (2016). Comparison of the BD MAX$^{(R)}$ Enteric Bacterial Panel assay with conventional diagnostic procedures in diarrheal stool samples. *Eur. J. Clin. Microbiol. Infect. Dis.* 35 (1), 131–136. doi: 10.1007/s10096-015-2517-4

Kouhsari, E., Douraghi, M., Barati, M., Yaseri, H. F., Talebi, M., Abbasian, S., et al. (2019). Rapid Simultaneous Molecular Stool-Based Detection of Toxigenic *Clostridioides difficile* by Quantitative TaqMan Real-Time PCR Assay. *Clin. Lab.* 65 (4). doi: 10.7754/Clin.Lab.2018.180735

Kundel, H. L., and Polansky, M. (2003). Measurement of observer agreement. *Radiology* 228 (2), 303–308. doi: 10.1148/radiol.2282011860

Lin, S., Wang, X., Zheng, H., Mao, Z., Sun, Y., and Jiang, B. (2008). Direct detection of *Campylobacter jejuni* in human stool samples by real-time PCR. *Can. J. Microbiol.* 54 (9), 742–747. doi: 10.1139/w08-064

Luna, R. A., Boyanton, B. L.Jr., Mehta, S., Courtney, E. M., Webb, C. R., Revell, P. A., et al. (2011). Rapid stool-based diagnosis of *Clostridium difficile* infection by real-time PCR in a children's hospital. *J. Clin. Microbiol.* 49 (3), 851–857. doi: 10.1128/JCM.01983-10

Mahapatra, T., Mahapatra, S., Babu, G. R., Tang, W., Banerjee, B., Mahapatra, U., et al. (2014). Cholera outbreaks in South and Southeast Asia: descriptive analysis 2003-2012. *Jpn. J. Infect. Dis.* 67 (3), 145–156 doi: 10.7883/yoken.67.145

Raphael, B. H., and Andreadis, J. D. (2007). Real-time PCR detection of the nontoxic nonhemagglutinin gene as a rapid screening method for bacterial isolates harboring the botulinum neurotoxin (A-G) gene complex. *J. Microbiol. Methods* 71 (3), 343–346. doi: 10.1016/j.mimet.2007.09.016

Reidl, J., and Klose, K. E. (2002). *Vibrio cholerae* and cholera: out of the water and into the host. *FEMS Microbiol. Rev.* 26 (2), 125–139. doi: 10.1111/j.1574-6976.2002.tb00605.x

Rivera, I. N., Lipp, E. K., Gil, A., Choopun, N., Huq, A., and Colwell, R. R. (2003). Method of DNA extraction and application of multiplex polymerase chain reaction to detect toxigenic *Vibrio cholerae* O1 and O139 from aquatic ecosystems. *Environ. Microbiol.* 5 (7), 599–606. doi: 10.1046/j.1462-2920.2003.00443.x

Shinoda, S. (2011). Sixty years from the discovery of *Vibrio parahaemolyticus and* some recollections. *Biocontrol Sci.* 16 (4), 129–137 doi: 10.4265/bio.16.129

Simner, P. J., Oethinger, M., Stellrecht, K. A., Pillai, D. R., Yogev, R., Leblond, H., et al. (2017). Multisite Evaluation of the BD Max Extended Enteric Bacterial Panel for Detection of *Yersinia enterocolitica*, Enterotoxigenic *Escherichia coli*, *Vibrio*, and *Plesiomonas shigelloides* from Stool Specimens. *J. Clin. Microbiol.* 55 (11), 3258–3266. doi: 10.1128/JCM.00911-17

Tada, J., Ohashi, T., Nishimura, N., Shirasaki, Y., Ozaki, H., Fukushima, S., et al. (1992). Detection of the thermostable direct hemolysin gene (*tdh*) and the thermostable direct hemolysin-related hemolysin gene (*trh*) of *Vibrio parahaemolyticus* by polymerase chain reaction. *Mol. Cell Probes* 6 (6), 477–487. doi: 10.1016/0890-8508(92)90044-x

Tall, A., Teillon, A., Boisset, C., Delesmont, R., Touron-Bodilis, A., and Hervio-Heath, D. (2012). Real-time PCR optimization to identify environmental *Vibrio* spp. strains. *J. Appl. Microbiol.* 113 (2), 361–372. doi: 10.1111/j.1365-2672.2012.05350.x

Tebbs, R. S., Brzoska, P. M., Furtado, M. R., and Petrauskene, O. V. (2011). Design and validation of a novel multiplex real-time PCR assay for *Vibrio* pathogen detection. *J. Food Prot.* 74 (6), 939–948. doi: 10.4315/0362-028X.JFP-10-511

Theethakaew, C., Feil, E. J., Castillo-Ramirez, S., Aanensen, D. M., Suthienkul, O., Neil, D. M., et al. (2013). Genetic relationships of *Vibrio parahaemolyticus* isolates from clinical, human carrier, and environmental sources in Thailand, determined by multilocus sequence analysis. *Appl. Environ. Microbiol.* 79 (7), 2358–2370. doi: 10.1128/AEM.03067-12

Wernick, N. L., Chinnapen, D. J., Cho, J. A., and Lencer, W. I. (2010). Cholera toxin: an intracellular journey into the cytosol by way of the endoplasmic reticulum. *Toxins (Basel)* 2 (3), 310–325. doi: 10.3390/toxins2030310

World Health Organization (2018). Cholera 2017. *Wkly. Epidemiol. Rec.* 93 (38), 489–500. Available at: https://apps.who.int/iris/handle/10665/274654

Conflict of Interest: A PCT patent application has been filed in China.

The authors declare that the research was conducted in the absence of any commercial or financial relationships that could be construed as a potential conflict of interest.

frontiers in Cellular and Infection Microbiology

ORIGINAL RESEARCH
published: 25 February 2021
doi: 10.3389/fcimb.2021.639083

Direct and Rapid Detection of *Mycoplasma bovis* in Bovine Milk Samples by Recombinase Polymerase Amplification Assays

Ruiwen Li[1†], *Jinfeng Wang*[2†], *Xiaoxia Sun*[2], *Libing Liu*[2], *Jianchang Wang*[2*] *and Wanzhe Yuan*[1*]

[1] College of Veterinary Medicine, Hebei Agricultural University, Baoding, China, [2] Food Microbiology and Animal Quarantine Laboratory, Technology Center of Shijiazhuang Customs District, Shijiazhuang, China

OPEN ACCESS

Edited by:
Hongchao Gou,
Guangdong Academy of Agricultural Sciences, China

Reviewed by:
Baozheng Luo,
Technology Center of Gongbei Customs District, China
Jun Zhao,
Henan Agricultural University, China

***Correspondence:**
Wanzhe Yuan
yuanwanzhe2015@126.com
Jianchang Wang
jianchangwang1225@126.com

[†]These authors have contributed equally to this work

Specialty section:
This article was submitted to Clinical Microbiology, a section of the journal Frontiers in Cellular and Infection Microbiology

Received: 08 December 2020
Accepted: 19 January 2021
Published: 25 February 2021

Citation:
Li R, Wang J, Sun X, Liu L, Wang J and Yuan W (2021) Direct and Rapid Detection of Mycoplasma bovis in Bovine Milk Samples by Recombinase Polymerase Amplification Assays. Front. Cell. Infect. Microbiol. 11:639083. doi: 10.3389/fcimb.2021.639083

This study aimed to detetct *Mycoplasma bovis* (*M. bovis*) in bovine milk quickly and directly by developing and validating isothermal recombinase polymerase amplification (RPA) assays. Targeting the *uvrC* gene of *M. bovis*, an RPA assay based on the fluorescence monitoring (real-time RPA) and an RPA assay combined with a lateral flow strip (LFS RPA) were conducted. It took 20 min for the real-time RPA to finish in a Genie III at 39°C, and 15 min were required to perform the LFS RPA in an incubator block at 39°C, followed by the visualization of the products on the lateral flow strip within 5 min. Both of the two assays showed high specificity for *M. bovis* without any cross-reaction with the other tested pathogens. With the standard recombinant plasmid pMbovis-uvrC serving as a template, both RPA assays had a limit of detcion of 1.0×10^1 copies per reaction, equivalent to that of a real-time PCR assay. In the 65 milk samples collected from cattle with mastitis, the *M. bovis* genomic DNA was detected in 24 samples by both the real-time RPA and the LFS RPA assays. The developed RPA assays could detect *M. bovis* in bovine milk in an efficient, convenient, and credible manner as attractive and promising tools, and the assays would be helpful in the rapid response to *M. bovis* infection causing bovine mastitis.

Keywords: *Mycoplasma bovis*, *uvrC* gene, real-time RPA, LFS RPA, isothermal amplification

INTRODUCTION

As a major etiological agent of bovine mycoplasmosis globally, *Mycoplasma bovis* (*M. bovis*) causes various clinical symptoms in cattle, including pneumonia, arthritis, and mastitis (Nicholas and Ayling, 2003). Consequently, in addition to being recognized as a major pathogen in bovine respiratory disease complex (BRDC), *M. bovis* has also been found to cause cattle mastitis (Nicholas, 2011; Gioia et al., 2016). More importantly, infections with *M. bovis* cause considerable economic loss in the beef and dairy cattle industry, approximately 150 million euros across Europe as well as over $100 million per year in the United States (Nicholas and Ayling, 2003). However, it is difficult for *M. bovis* to be eradicated from a farm after an outbreak, and one infected cattle could be an infection source for months or even years (Burki et al., 2015).

As mentioned, rapid and accurate detection of *M. bovis* is imperative for effective prevention and control of the disease. Although bacteriological culture is considered to be the gold standard for the diagnosis of infection, routine diagnosis is not prioritized in practice. The culture method tends to be laborious, time-consuming, and lacks sensitivity and specificity owing to the fastidious nature of *M. bovis*, overgrowth of other contaminant bacteria, and subsequent difficulties in species identification (Khodakaram-Tafti and Lopez, 2004; Caswell and Archambault, 2007). Serological methods are typically used as a herd-level disease diagnostic test, and a variety of commercial *M. bovis* ELISA tests have been developed to detect antibodies in the milk and serum (Heller et al., 1993; Le et al., 2002; Nicholas and Ayling, 2003). However, they are not ideally suited for *M. bovis* infection investigations with individual animals, as a misdiagnosis may occur due to the delayed seroconversion after natural infection (Calcutt et al., 2018). Moreover, the high level of seroprevalence in many cattle herds restricts their routine use for diagnosis (Calcutt et al., 2018).

In efforts to avoid such disadvantages, diverse nucleic acid amplification approaches have been reported to sensitively, specifically, and immediately detect *M. bovis* from clinical samples, including milk (Clothier et al., 2010; Higa et al., 2016; Ashraf et al., 2018; Zhao et al., 2018). Dubbed the prime choice for molecular detection, PCR assays have been well established in the clinical diagnosis of cattle herds with BRDC and/or mastitis (Parker et al., 2018). However, compared with PCR assays, isothermal nucleic acid amplification assays, which are comparable to PCR and have a faster time-to-result in many cases, are more approporiate for the small-footprint devices in low-resource settings (Craw and Balachandran, 2012).

Among the recent isothermal nucleic acid amplification technologies, RPA has come into the spotlight because of its simplicity to design and optimize and its speed to obtain results. Thus, RPA technology has been widely utilized to explore different pathogens, as it tends to be fast, easy, and accurate (Piepenburg et al., 2006; Daher et al., 2016). In this paper, an exo probe-based real-time RPA and an nfo probe-based LFS RPA assays were developed and analyzed for their sensitivity and specificity for the direct detection of *M. bovis* in milk samples from cattle with mastitis.

MATERIALS AND METHODS

Bacteria Strains and Clinical Samples

M. bovis (strain PG45), Mycoplasma agalactiae (strain PG2), Mycoplasma ovipneumoniae (strain Y98), Mycoplasma hyopneumoniae (strain 168), Mycoplasma capricolum subsp. capripneumoniae (strain F38), Pasteurella multocida (strain F91G3), Staphylococcus aureus (ATCC 6538), and Pseudomonas aeruginosa (ATCC 9027) were reserved in our laboratory.

Sixty-five individual bovine milk samples were collected from eight different dairy farms in Baoding and Hengshui, Hebei Province, from July 2018 to December 2020. The samples were all gathered from cattle with mastitis.

DNA Extraction

The mycoplasma and bacterial genomic DNA were extracted with the TIANamp Bacteria DNA kit (Tiangen, Beijing, China), following the manufacturer's instructions. First, 1 ml of each milk sample was centrifuged at 12,000 g for 10 min at 4°C, the supernatant containing the fat and excess liquid was removed, and the pellet was washed twice with phosphate-buffered saline (PBS, pH 7.4). The washed pellet was resuspended in 200 µl of PBS and then the DNA was extracted with the TIANamp Bacteria DNA kit. The extracted DNA was eluted in 50 µl of nuclease-free water, and the DNA was quantified with an ND-2000c spectrophotometer (NanoDrop, Wilmington, USA) and stored at −80°C until use.

Generation of Standard DNA

Aimed to generate a *M. bovis*-standard DNA for the RPA assays, a PCR product with 1,908 bp covering the region of interest of *uvrC* gene, was amplified from the *M. bovis* DNA using uvrC-F and uvrC-R as primers (**Table 1**) and cloned into the pMD19-T (Takara, Dalian, China) for standards. The generating plasmid, pMbovis-uvrC, was transformed into *Escherichia coli* DH5α cells and the positive clones were identified by sequencing with M13

TABLE 1 | Sequences of the primers and probes used in this study.

Assay	Primers and probes	Sequence 5′-3′	Amplicon size (bp)	Reference
Real-time RPA	uvrC-exo-F	GAGTTTCACAAAACCAAAGCCTTAATTGACCT	180	This study
	uvrC-exo-R	TCCTTTTATGTTTCTTAGTTTGCCTTCTAGTG		
	uvrC-exo-P	CTTAGTTCAAATTCAAGTTGACCGG (FAM-dT) (THF)(BHQ1-dT) GCAAAGTCGCACTT-C3-spacer		
LFS RPA		GAGTTTCACAAAACCAAAGCCTTAATTGACCT biotin-TCCTTTTATGTTTCTTAGTTTGCCTTCTAGTG FAM-CTTAGTTCAAATTCAAGTTGACCGGT(THF)TGCAAAGTCGCACTT-C3-spacer	180	This study
Real-time PCR	Mbov F2024	TCTAATTTTTTCATCATCGCTAATGC	112	Clothier et al., 2010
	Mbov R2135	TCAGGCCTTTGCTACAATGAAC		
	Mbov uvrC	FAM-AACTGCATCATATCACATACT-MGB		
PCR	uvrC-F	GCAAAGAATTTACGCAAGAG	1908	This study
	uvrC-F	GACTTTGAAATAACTAGACCAGT		

primers (Invitrogen®, Carlsbad, CA, USA). pMbovis-uvrC was purified with the SanPrep Plasmid MiniPrep Kit (Sangon Biotech, Shanghai, China) and quantified with a ND-2000c spectrophotometer. The copy number of DNA molecules was calculated according to the formula as follows: amount (copies/μl) = [DNA concentration (g/μl)/(plasmid length in base pairs × 660)] × 6.02×10^{23}. Aliquots of the standard DNA were prepared in 10-fold serial dilutions from 1.0×10^7 to 1.0×10^0 copies/μl in nuclease-free water and stored at −80°C until use.

RPA Primers and Probes

Nucleotide sequence data for different *M. bovis* strains available in GenBank were aligned to identify the conserved regions in the *uvrC* gene, which was determined as the amplification target for RPA. Basing on the reference sequences of *M. bovis* (Acession number: AF003959, KX772801, KX772803, CP045797, KU168366, KP099619), the primers, exo probe and LF probe were designed following the RPA manufacturer guidelines (TwistDx. Cambridge, UK). Primers and probes are presented in **Table 1** and were synthesized by Sangon Biotech Co., Shanghai, China.

Real-Time RPA Assay

A commercial ZC BioScience™ exo kit (ZC BioScience, Hangzhou, China) was employed in the *M. bovis* real-time RPA assay. The reaction volume was 50 μl including 40.9 μl of Buffer A (rehydration buffer), 2.0 μl of each RPA primer (uvrC-exo-F and uvrC-exo-R, 10 μmol/L), 0.6 μl of exo probe (uvrC-exo-P, 10 μmol/L), and 2.5 μl of Buffer B (magnesium acetate, 280 mmol/L). Additionally, 1 μl of bacterial genomic DNA or standard DNA was used for the specificity and sensitivity analysis, while 2 μl of sample DNA was used for the clinical sample diagnosis. Real-time RPA reactions were performed at 39°C for 20 min in a Genie III (OptiGene Limited, West Sussex, UK).

LFS RPA Assay

A commercial TwistAmp™ nfo kit (TwistDX, Cambridge, UK) and lateral flow strip (USTAR, Hangzhou, China) were utilized in the *M. bovis* LFS RPA assay. The reaction volume was 50 μl including 29.5 μl of rehydration buffer, 2.1 μl of each RPA primer (uvrC-nfo-F and uvrC-nfo-R, 10 μmol/L), 0.6 μl of exo probe (uvrC-nfo-P, 10 μmol/L), and 2.5 μl of magnesium acetate (280 mmol/L). In addition, 1 μl of bacterial genomic DNA or standard DNA was used for the specific and sensitive analysis, while 2 μl of sample DNA was used for the clinical sample diagnosis. The LFS RPA reactions were incubated in an incubator block at 39°C for 5, 10, 15, and 20 min. The lateral flow strips were used to recognize the amplicons dual-labeled with FAM and biotin. The LFS RPA products were identified visually by using lateral flow strips according to the manufacturer's instructions.

Analytical Specificity and Sensitivity Analysis

The specificity of the developed real-time RPA and LFS RPA assays was assessed using the genomic DNA of a panel of pathogens, including *M. bovis*, *M. agalactiae*, *M. ovipneumoniae*, *M. hyopneumoniae*, *M. capricolum subsp. capripneumoniae*, *P. multocida*, *S. aureus*, and *P. aeruginosa*. Five of these were closely related Mycoplasma species, and the other three could potentially be associated with mastitis in cattle. The assays were conducted independently in triplicate.

Aliquots of the *M. bovis* standard DNA ranging from 1.0×10^7 to 1.0×10^0 copies/μl were used to analyze the RPA analytical sensitivity. One microliter of each dilution was amplified by both RPA assays, and the limit of detection (LOD) was determined as the highest dilution of the virus detectable by the assays. The real-time RPA was additionally tested using the standard DNA in eight replicates, the threshold time was plotted against the molecules identified, and a semilog regression was calculated by Prism software 5.0 (GraphPad Software Inc., San Diego, CA, USA). Furthermore, in the LFS RPA, three independent reactions proceeded separately.

Validation With Clinical Samples

The developed assays were directly applied to DNA extracted from 65 bovine milk samples to confirm the applicability of the *M. bovis*-specific real-time RPA and LFS RPA assays in clinical diagnosis,. Then, the results were compared with those obtained with real-time PCR described previously (Clothier et al., 2010), which was run in parallel for the above clinical samples.

RESULTS

Performance of the Real-Time RPA Assay

In the analytical specificity analysis, only the *M. bovis* DNA was amplified with the development of a typical fluorescence curve, and none of the other pathogens were amplified (**Figure 1A**), suggesting that the real-time RPA assay was highly specific to *M. bovis*. Similar results were observed in three repeats, demonstrating the good repeatability of the assays.

The real-time RPA assay was conducted eight times, in which 1.0×10^7–1.0×10^1 copies of standard plasmid were detected in 8/8 runs, and 1.0×10^0, 0/8 (**Figure 1B**). From these results, what have been exhibited is the LOD for the real-time RPA was 1.0×10^1 copies/reaction. Moreover, the dynamic detection range of the real-time RPA spans seven logs ranging from seven to one log copies per reaction, with the corresponding threshold time ranging from 2 min at 1.0×10^7 copies/reaction to 12 min at 1.0×10^1 copies/reaction, which revealed that the *M. bovis* real-time RPA assay has a wide dynamic range to detect the target DNA (**Figure 1C**).

Performance of the LFS RPA Assay

The optimal reaction time of the LFS RPA assay was evaluated by testing the results at 5, 10, 15, and 20 min with 1.0×10^5 copies standard plasmids as the template, and the results are presented in **Figure 2A**. A very weak red band was observed after 5 min of incubation, and no distinct differences were observed among the products after 10, 15, and 20 min of incubation. Similar results were obtained from three repeats. Based on the above results, 15 min was selected as the best incubation time for the *M. bovis* LFS RPA assay.

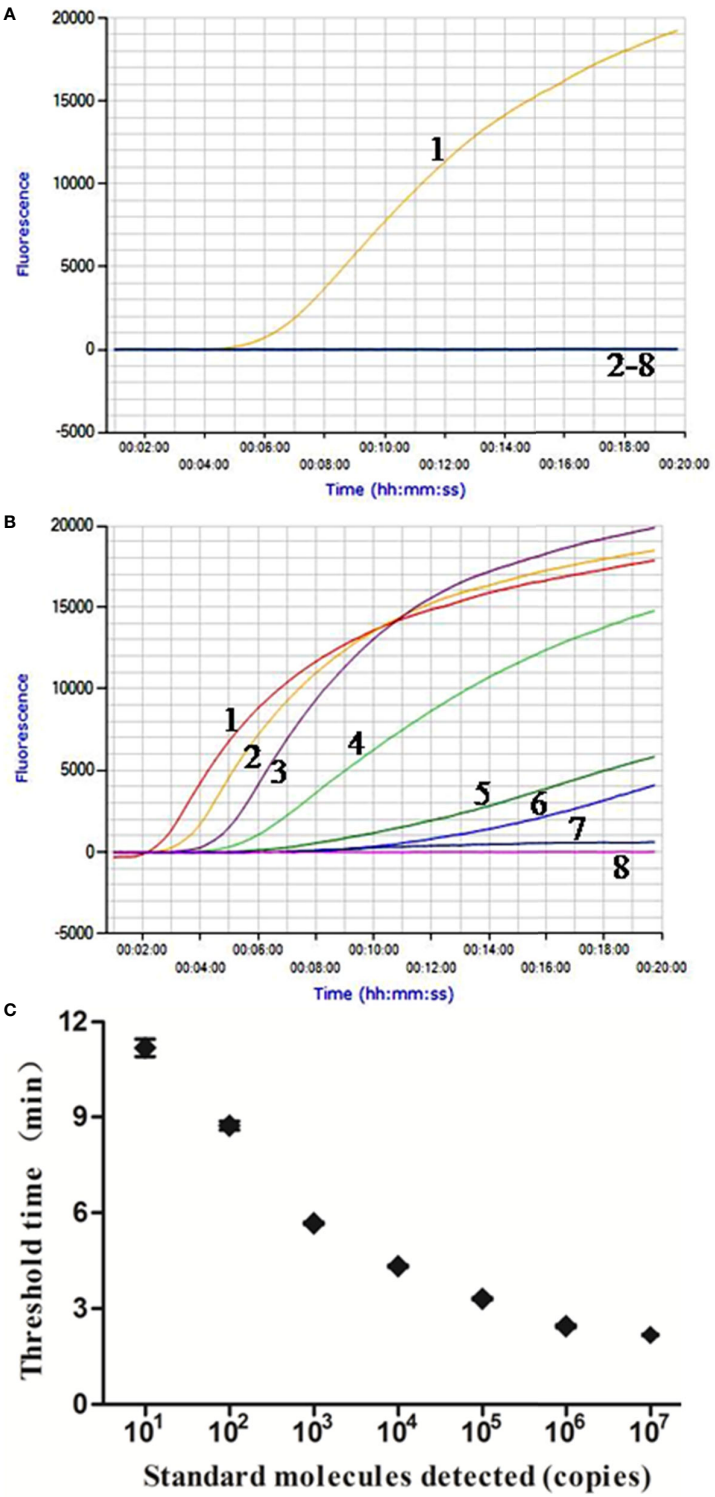

FIGURE 1 | Performance of *M. bovis* real-time RPA assay. **(A)** Analytical specificity of the real-time RPA assay. Only the *M. bovis* was amplified and there were no cross-reactions with other pathogens tested. Line 1, *M. bovis*; line 2, *M. agalactiae*; line 3, *M. ovipneumoniae*; line 4, *M. hyopneumoniae*; line 5, *M. capricolum subsp. capripneumoniae*; line 6, *P. multocida*; line 7, *S. aureus*; line 8, *P. aeruginosa*. **(B)** Fluorescence development over time using a dilution range of 1.0×10^7–1.0×10^0 copies of *M. bovis* standard recombinant plasmid. Line 1, 1.0×10^7 copies; line 2, 1.0×10^6 copies; line 3, 1.0×10^5 copies; line 4, 1.0×10^4 copies; line 5, 1.0×10^3 copies; line 6, 1.0×10^2 copies; line 7, 1.0×10^1 copies; line 8, 1.0×10^0 copies. **(C)** Reproducibility of *M. bovis* real-time RPA assay. The data collected from *M. bovis* real-time RPA tests and the semi-log regression was calculated using Prism Software. The run time of the real-time RPA was between 2 min and 12 min for 1.0×10^7 and 1.0×10^1 copies.

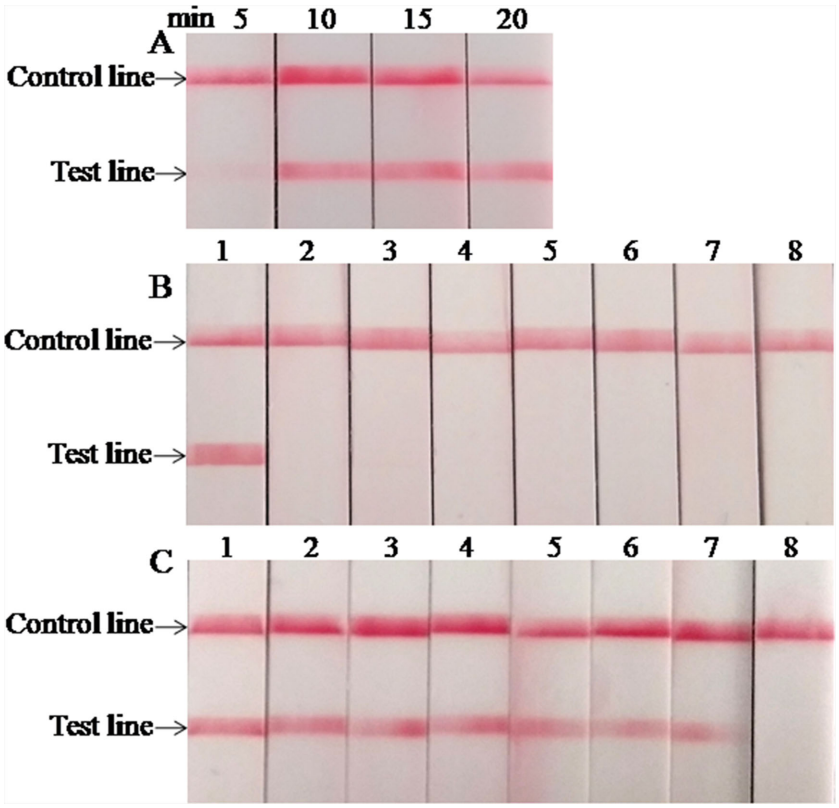

FIGURE 2 | Performance of *M. bovis* LFS RPA assay. **(A)** Optimization of LFS RPA reaction time. The test line was clearly visible when the amplification time was longer than 10 min. **(B)** Analytical specificity of the LFS RPA assay. Only the *M. bovis* was amplified, but not other pathogens tested. Line 1, *M. bovis*; line 2, *M. agalactiae*; line 3, *M. ovipneumoniae*; line 4, *M. hyopneumoniae*; line 5, *M. capricolum subsp. capripneumoniae*; line 6, *P. multocida*; line 7, *S. aureus*; line 8, *P. aeruginosa*. **(C)** Analytical sensitivity of the LFS RPA assay. Line 1, 1.0×10^7 copies; line 2, 1.0×10^6 copies; line 3, 1.0×10^5 copies; line 4, 1.0×10^4 copies; line 5, 1.0×10^3 copies; line 6, 1.0×10^2 copies; line 7, 1.0×10^1 copies; line 8, 1.0×10^0 copies.

When the analytical specificity analysis was conducted, the red band was only observed in the test line on the strip when the DNA of *M. bovis* was used as the template (**Figure 2B**), and the same results were seen in three independent reactions that the same results were received. As mentioned above, these results revealed that the LFS RPA assay was highly specific for detecting *M. bovis* and showed no cross-reactions with the other pathogens tested. As the analytical sensitivity analysis proceeded, red bands could be observed in the test line on the strips with 1.0×10^7–1.0×10^1 copies of standard plasmid serving as the template (**Figure 2C**), and all three independent reactions showed identical results. Thus, the LOD of the LFS RPA was 1.0×10^1 copies/reaction.

Validation of the RPA Assays on Clinical Samples

The real-time RPA, LFS RPA, and real-time PCR all had identical results for the 65 milk samples from eight farms, in which 24 samples from four farms tested positive for *M. bovis* (**Table 2**). Using the real-time PCR as the reference, the diagnostic specificity (DSp) and diagnostic sensitivity (DSe) of the real-time RPA and LFS RPA assays were 100%. The threshold time (TT) and cycle threshold (Ct) values of the real-time RPA and real-time PCR were good at an R^2 value of 0.951 (**Figure 3**).

DISCUSSION

M. bovis is the most prevalent agent of mycoplasma mastitis in dairy cattle (Gioia et al., 2016). It can survive in the milk of asymptomatically infected and clinically healthy cows, and ingestion of milk from cows with mastitis is one of the primary modes of transmission (Maunsell et al., 2011). Both bovine individual and bulk tank milk samples have been applied to recognize *M. bovis* in daily surveillance and eradication efforts (Passchyn et al., 2012; Pinho et al., 2013). Concerning the *uvrC* gene, this paper proposed and demonstrated that real-time RPA and LFS RPA assays could directly identify *M. bovis* in milk samples, and the tests were proven to be rapid, sensitive, and specific.

Selecting the target gene is critical for the application of nucleic acid amplification. A series of PCR and LAMP assays targeting various genes, such as *uvrC*, *oppD/F*, *polC*, gyrB, and *16S rRNA*, have been conducted for the species-specific detection of *M. bovis* in diverse clinical samples from cattle herds with

TABLE 2 | Detection results of *M. bovis* in milk samples from cattle with mastitis in the developed real-time RPA, LFS RPA, and real-time PCR assays.

Origin	Location	Number	Real-time RPA		LFS RPA		Real-time PCR	
			P	N	P	N	P	N
Farm 1	Baoding	17	10	7	10	7	10	7
Farm 2	Baoding	2	2	0	2	0	2	0
Farm 3	Baoding	11	5	6	5	6	5	6
Farm 4	Baoding	6	0	6	0	6	0	6
Farm 5	Hengshui	2	0	2	0	2	0	2
Farm 6	Hengshui	7	0	7	0	7	0	7
Farm 7	Hengshui	11	7	4	7	4	7	4
Farm 8	Hengshui	9	0	9	0	9	0	9
	T	65	24	41	24	41	24	41

P, positive; N, negative; T, total.

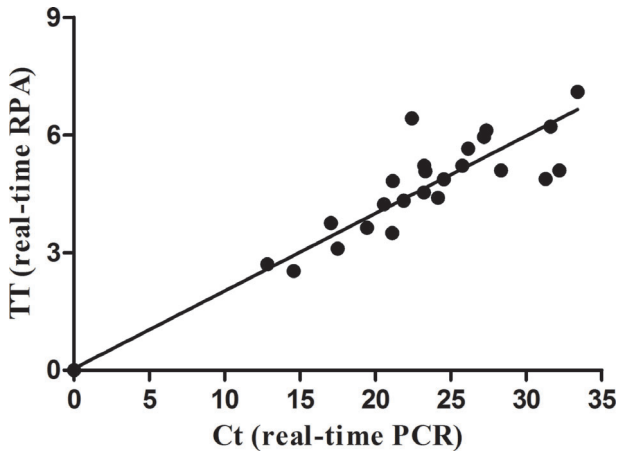

FIGURE 3 | Comparison between performances of the real-time RPA and real-time PCR on the milk samples. DNA extracts of the positive milk samples were screened. Linear regression analysis of real-time RPA threshold time (TT) values (y axis) and real-time PCR cycle threshold (Ct) values (x axis) were determined by Prism software, and the R^2 value was 0.951.

BRDC and/or mastitis (Clothier et al., 2010; Rossetti et al., 2010; Ashraf et al., 2018). A study indicated that most PCR assays targeting different genes performed comparatively (Wisselink et al., 2019). Nevertheless, all the sequences of the 16S rRNA genes of *M. bovis* and *M. agalactiae* are extremely similar (>99.8%) (Pettersson et al., 1996; Konigsson et al., 2002), the available *M. bovis* PCR and LAMP assays targeting the *16S rRNA* gene exhibited cross-reactivity with *M. agalactiae* (Ashraf et al., 2018; Wisselink et al., 2019). The *uvrC* gene is a highly conserved housekeeping gene specific for each of *Mycoplasma* species that is highly stable within a species, and it differs considerably between the two phylogenetically closely related *Mycoplasma* species, *M. bovis* and *M. agalactiae* (Subramaniam et al., 1998; Konigsson et al., 2002). Several previous studies have revealed that the *uvrC* gene is universally deemed to be the preferred target for *M. bovis* in the nucleic acid amplification assays (Clothier et al., 2010; Ashraf et al., 2018; Zhao et al., 2018; Wisselink et al., 2019). As a result, the *M. bovis* RPA primers and probes were designed to target the conserved region of the *uvrC* gene in this study. Through *in silico* analysis, there was no mismatch in the primers and probes with the currently circulating strains available in GenBank. For the specificity analysis, both the real-time RPA and the LFS RPA could only amplify the genomic DNA of *M. bovis* but not the other mycoplasmas, including *M. agalactiae*. With the recombinant plasmid being the standard, the LOD of both RPA assays was 1.0×10^1 copies per reaction. Unfortunately, only one *M. bovis* strain and one *M. agalactiae* stain were considered in the analysis, which may be a shortcoming of this study. The developed assays should be further confirmed by testing more *M. bovis* and *M. agalactiae* DNA extracts in the future.

Directly detecting *M. bovis* in milk samples has the potential to be of great significance for the control of *M. bovis*-causing bovine mastitis. Fortunately, the developed real-time RPA and LFS RPA assays could detect the *M. bovis* in a direct and efficient way from clinical bovine milk samples. In this study, the *M. bovis* positive rate at the farm level and at the individual level reached 50.0% (4/8) and 36.92% (24/65), respectively. Compared with a real-time PCR assay, the real-time RPA and LFS RPA assays showed DSp and Dse values of 100%. The RPA assays showed positive results within 20 min, demonstrating Ct values varying from 12.83 to 33.40 for the real-time PCR. The diagnostic performances of the developed RPA assays were the same as that of the real-time PCR assay, while the RPA assays demonstrated two distinct merits, rapidness and convenience. Although the above results are inspiring, RPA assays still require further validation by testing additional types of *M. bovis* DNA-positive clinical samples, such as nasal swabs and lungs. Overall, our results demonstrated that the performance of the RPA assays was comparable to that of real-time PCR, but the RPA assays were relatively faster.

Considered the prime assay in the realm of molecular detection, the PCR assays are, however, limited in underequipped laboratories and at point-of-need (PON) diagnosis owing to the demands of expensive thermocyclers and centralized laboratory facilities (Clothier et al., 2010; Rossetti et al., 2010). The recently developed LAMP assays do not require a specialized instrument, but the reaction time is 60 or 120 min (Higa et al., 2016; Ashraf et al., 2018). In this study, the developed real-time RPA assay and LFS RPA assay were performed on the portable tube scanner Genie III and in a metal bath incubator, respectively. Both of these devices are portable and can be charged by a battery, allowing

them to work for an entire day with no need for an electrical outlet. Combined with the time needed for DNA extraction, the developed RPA assays require less than 50 min to obtain results. Moreover, RPA reagents are cold chain independent and RPA is tolerant to common PCR inhibitors (Daher et al., 2016; Lillis et al., 2016). These advantages make the developed RPA assays perfect for detecting *M. bovis* in the field.

Similar to the PCR and LAMP assays, DNA extraction by commercial nucleic acid extraction kits is still necessary for the RPA assays developed in this study. Currently, numerous simple and rapid nucleic acid extraction methods that do not require complex instruments are being evaluated in our laboratory, including the innuPREP MP basic kit A (Jena Analytik, Jena, Germany), Punch-it™ NA-Sample Kit (NanoHelix, Daejeon, South Korea), and other commercial reagents. Combining the DNA extracted by those simple methods with comparable performance to routine commercial nucleic acid extraction kits has the potential to allow the recentlyl developed RPA assays for *M. bovis* to be applied in the field.

In summary, the developed *M. bovis* real-time RPA and LFS RPA assays could be performed in the laboratory as routine diagnostic assays, and they have substantial potential as uncomplicated, rapid, and reliable methods for directly detecting *M. bovis* in bovine milk on farm.

DATA AVAILABILITY STATEMENT

The original contributions presented in the study are included in the article/supplementary material. Further inquiries can be directed to the corresponding authors.

AUTHOR CONTRIBUTIONS

Among the authors, RL and JFW were responsible for sampling, sample testing, and writing the paper. XS and LL were responsible for data statistics and analysis. JCW and WY were responsible for editing the paper. All authors contributed to the article and approved the submitted version.

FUNDING

This work was supported by the Project for Key Common Technologies for High Quality Agricultural Development of Hebei Province (19226636D), the Research Programm of General Administration of Customs (2020HK170).

REFERENCES

Ashraf, A., Imran, M., Yaqub, T., Tayyab, M., Shehzad, W., Mingala, C. N., et al. (2018). Development and validation of a loop-mediated isothermal amplification assay for the detection of Mycoplasma bovis in mastitic milk. *Folia Microbiol. (Praha)* 63, 373–380. doi: 10.1007/s12223-017-0576-x

Burki, S., Frey, J., and Pilo, P. (2015). Virulence, persistence and dissemination of Mycoplasma bovis. *Vet. Microbiol.* 179, 15–22. doi: 10.1016/j.vetmic.2015.02.024

Calcutt, M. J., Lysnyansky, I., Sachse, K., Fox, L. K., Nicholas, R. A. J., and Ayling, R. D. (2018). Gap analysis of Mycoplasma bovis disease, diagnosis and control: An aid to identify future development requirements. *Transbound. Emerg. Dis.* 65 (Suppl 1), 91–109. doi: 10.1111/tbed.12860

Caswell, J. L., and Archambault, M. (2007). Mycoplasma bovis pneumonia in cattle. *Anim. Health Res. Rev.* 8, 161–186. doi: 10.1017/S1466252307001351

Clothier, K. A., Jordan, D. M., Thompson, C. J., Kinyon, J. M., Frana, T. S., and Strait, E. L. (2010). Mycoplasma bovis real-time polymerase chain reaction assay validation and diagnostic performance. *J. Vet. Diagn. Invest.* 22, 956–960. doi: 10.1177/104063871002200618

Craw, P., and Balachandran, W. (2012). Isothermal nucleic acid amplification technologies for point-of-care diagnostics: a critical review. *Lab. Chip.* 12, 2469–2486. doi: 10.1039/c2lc40100b

Daher, R. K., Stewart, G., Boissinot, M., and Bergeron, M. G. (2016). Recombinase Polymerase Amplification for Diagnostic Applications. *Clin. Chem.* 62, 947–958. doi: 10.1373/clinchem.2015.245829

Gioia, G., Werner, B., Nydam, D. V., and Moroni, P. (2016). Validation of a mycoplasma molecular diagnostic test and distribution of mycoplasma species in bovine milk among New York State dairy farms. *J. Dairy. Sci.* 99, 4668–4677. doi: 10.3168/jds.2015-10724

Heller, M., Berthold, E., Pfutzner, H., Leirer, R., and Sachse, K. (1993). Antigen capture ELISA using a monoclonal antibody for the detection of Mycoplasma bovis in milk. *Vet. Microbiol.* 37, 127–133. doi: 10.1016/0378-1135(93)90187-C

Higa, Y., Uemura, R., Yamazaki, W., Goto, S., Goto, Y., and Sueyoshi, M. (2016). An improved loop-mediated isothermal amplification assay for the detection of Mycoplasma bovis. *J. Vet. Med. Sci.* 78, 1343–1346. doi: 10.1292/jvms.15-0459

Khodakaram-Tafti, A., and Lopez, A. (2004). Immunohistopathological findings in the lungs of calves naturally infected with Mycoplasma bovis. *J. Vet. Med. A Physiol. Pathol. Clin. Med.* 51, 10–14. doi: 10.1111/j.1439-0442.2004.00596.x

Konigsson, M. H., Bolske, G., and Johansson, K. E. (2002). Intraspecific variation in the 16S rRNA gene sequences of Mycoplasma agalactiae and Mycoplasma bovis strains. *Vet. Microbiol.* 85, 209–220. doi: 10.1016/S0378-1135(01)00517-X

Le, G. D., Calavas, D., Brank, M., Citti, C., Rosengarten, R., Bezille, P., et al. (2002). Serological prevalence of Mycoplasma bovis infection in suckling beef cattle in France. *Vet. Rec.* 150, 268–273. doi: 10.1136/vr.150.9.268

Lillis, L., Siverson, J., Lee, A., Cantera, J., Parker, M., Piepenburg, O., et al. (2016). Factors influencing Recombinase polymerase amplification (RPA) assay outcomes at point of care. *Mol. Cell Probes* 30, 74–78. doi: 10.1016/j.mcp.2016.01.009

Maunsell, F. P., Woolums, A. R., Francoz, D., Rosenbusch, R. F., Step, D. L., Wilson, D. J., et al. (2011). Mycoplasma bovis infections in cattle. *J. Vet. Intern. Med.* 25, 772–783. doi: 10.1111/j.1939-1676.2011.0750.x

Nicholas, R. A., and Ayling, R. D. (2003). Mycoplasma bovis: disease, diagnosis, and control. *Res. Vet. Sci.* 74, 105–112. doi: 10.1016/S0034-5288(02)00155-8

Nicholas, R. A. (2011). Bovine mycoplasmosis: silent and deadly. *Vet. Rec.* 168, 459–462. doi: 10.1136/vr.d2468

Parker, A. M., Sheehy, P. A., Hazelton, M. S., Bosward, K. L., and House, J. K. (2018). A review of mycoplasma diagnostics in cattle. *J. Vet. Intern. Med.* 32, 1241–1252. doi: 10.1111/jvim.15135

Passchyn, P., Piepers, S., De Meulemeester, L., Boyen, F., Haesebrouck, F., and De Vliegher, S. (2012). Between-herd prevalence of Mycoplasma bovis in bulk milk in Flanders, Belgium. *Res. Vet. Sci.* 92, 219–220. doi: 10.1016/j.rvsc.2011.03.016

Pettersson, B., Uhlen, M., and Johansson, K. E. (1996). Phylogeny of some mycoplasmas from ruminants based on 16S rRNA sequences and definition of a new cluster within the hominis group. *Int. J. Syst. Bacteriol.* 46, 1093–1098. doi: 10.1099/00207713-46-4-1093

Piepenburg, O., Williams, C. H., Stemple, D. L., and Armes, N. A. (2006). DNA detection using recombination proteins. *PLoS Biol.* 4, e204. doi: 10.1371/journal.pbio.0040204

Pinho, L., Thompson, G., Machado, M., and Carvalheira, J. (2013). Management practices associated with the bulk tank milk prevalence of Mycoplasma spp. in dairy herds in Northwestern Portugal. *Prev. Vet. Med.* 108, 21–27. doi: 10.1016/j.prevetmed.2012.07.001

Rossetti, B. C., Frey, J., and Pilo, P. (2010). Direct detection of Mycoplasma bovis in milk and tissue samples by real-time PCR. *Mol. Cell Probes* 24, 321–323. doi: 10.1016/j.mcp.2010.05.001

Subramaniam, S., Bergonier, D., Poumarat, F., Capaul, S., Schlatter, Y., Nicolet, J., et al. (1998). Species identification of Mycoplasma bovis and Mycoplasma agalactiae based on the uvrC genes by PCR. *Mol. Cell Probes* 12, 161–169. doi: 10.1006/mcpr.1998.0160

Wisselink, H. J., Smid, B., Plater, J., Ridley, A., Andersson, A. M., Aspan, A., et al. (2019). A European interlaboratory trial to evaluate the performance of different PCR methods for Mycoplasma bovis diagnosis. *BMC Vet. Res.* 15, 86. doi: 10.1186/s12917-019-1819-7

Zhao, G., Hou, P., Huan, Y., He, C., Wang, H., and He, H. (2018). Development of a recombinase polymerase amplification combined with a lateral flow dipstick assay for rapid detection of the Mycoplasma bovis. *BMC Vet. Res.* 14, 412. doi: 10.1186/s12917-018-1703-x

Conflict of Interest: The authors declare that the research was conducted in the absence of any commercial or financial relationships that could be construed as a potential conflict of interest.

frontiers in Cellular and Infection Microbiology

ORIGINAL RESEARCH
published: 25 February 2021
doi: 10.3389/fcimb.2021.631921

Development and Evaluation of the Rapid and Sensitive RPA Assays for Specific Detection of *Salmonella* spp. in Food Samples

Liwei Zhao[1†], *Jianchang Wang*[2†], *Xiao Xia Sun*[2], *Jinfeng Wang*[2], *Zhimin Chen*[2], *Xiangdong Xu*[3], *Mengyuan Dong*[1], *Ya-nan Guo*[1], *Yuanyuan Wang*[1], *Pingping Chen*[1], *Weijuan Gao*[1*] *and Yunyun Geng*[1*]

[1] Heibei Key Laboratory of Chinese Medicine Research on Cardiocerebrovascular Disease, Hebei University of Chinese Medicine, Shijiazhuang, China, [2] Food Microbiology and Animal Quarantine Laboratory, Technology Center of Shijiazhuang Customs, Shijiazhuang, China, [3] School of Public Health, Key Laboratory of Environment and Human Health, Hebei Medical University, Shijiazhuang, China

OPEN ACCESS

Edited by:
Jianmin Zhang,
South China Agricultural University, China

Reviewed by:
Jun Tang,
China Agricultural University, China
Qianru Yang,
United States Food and Drug Administration, United States
Baowei Yang,
Northwest A and F University, China

***Correspondence:**
Weijuan Gao
502678560@qq.com
Yunyun Geng
gengyunyun2015@126.com

[†]These authors have contributed equally to this work

Specialty section:
This article was submitted to Clinical Microbiology, a section of the journal Frontiers in Cellular and Infection Microbiology

Received: 21 November 2020
Accepted: 19 January 2021
Published: 25 February 2021

Citation:
Zhao L, Wang J, Sun XX, Wang J, Chen Z, Xu X, Dong M, Guo Y-n, Wang Y, Chen P, Gao W and Geng Y (2021) Development and Evaluation of the Rapid and Sensitive RPA Assays for Specific Detection of Salmonella spp. in Food Samples. Front. Cell. Infect. Microbiol. 11:631921. doi: 10.3389/fcimb.2021.631921

Salmonella spp. is among the main foodborne pathogens which cause serious foodborne diseases. An isothermal real-time recombinase polymerase amplification (RPA) and lateral flow strip detection (LFS RPA) were used to detect *Salmonella* spp. targeting the conserved sequence of invasion protein A (*invA*). The Real-time RPA was performed in a portable florescence scanner at 39°C for 20 min. The LFS RPA was performed in an incubator block at 39°C for 15 min, under the same condition that the amplifications could be inspected by the naked eyes on the LFS within 5 min. The detection limit of *Salmonella* spp. DNA using real-time RPA was 1.1×10^1 fg, which was the same with real-time PCR but 10 times higher than that of LFS RPA assay. Moreover, the practicality of discovering *Salmonella* spp. was validated with artificially contaminated lamb, chicken, and broccoli samples. The analyzing time dropped from 60 min to proximately 5–12 min on the basis of the real-time and LFS RPA assays compared with the real-time PCR assay. Real-time and LFS RPA assays' results were equally reliable. There was no cross-reactivity with other pathogens in both assays. In addition, the assays had good stability. All of these helped to show that the developed RPA assays were simple, rapid, sensitive, credible, and could be a potential point-of-need (PON) test required mere resources.

Keywords: *Salmonella*, *invA* gene, real-time RPA, lateral flow strip (LFS), isothermal amplification

INTRODUCTION

Salmonella spp. is a Gram-negative bacterium belonging to the family of *Enterobacteriaceae*. *Salmonella* spp. is a major cause of the foodborne pathogen around the world (Nassib et al., 2003). It is widespread in nature and proliferates under ambient temperature with low nutritional demands (Li et al., 2013). *Salmonella* spp. infections attract much attention in public health especially in food safety. *Salmonella* spp. causes food poisoning, typhoid fever, gastrointestinal inflammation, and septicemia for both humans and animals (McGuinness et al., 2009; Rukambile et al., 2019).

Currently, there are over 80 million cases of foodborne salmonellosis in the world (Li et al., 2019). Additionally, reports revealed that outbreaks caused by *Salmonella* spp. were largely associated with animal derived products such as poultry, egg, and chicken, and contamination is common in retail raw meats (Nassib et al., 2003; Foley and Lynne, 2008; Foley et al., 2008). An accurate and fast diagnosis is needed in order to prevent *Salmonella* spp. infections.

Salmonella spp. is currently detected in foods primarily through traditional laboratory methods. These traditional laboratory methods are inconvenient, time-consuming and takes over 3 days to obtain the result following multiple analytical steps (Li et al., 2019; Hong et al., 2020). Moreover, the complexity of the samples had a great effect on the bacterial morphology colony. The cross-reactivity among bacteria in *Enterobacteriaceae* restricted the specificity and sensitivity of the test (Nassib et al., 2003; Li et al., 2019). Upgrading molecular diagnostics provides powerful means for detecting *Salmonella* spp. in light of sensitivity and specificity. Currently, many nucleic acid amplification-based assays have gained popularity such as polymerase chain reaction (PCR), real-time PCR, multiplex PCR, reverse transcriptase PCR (RT-PCR), and loop-mediated isothermal amplification (LAMP) (Hirose et al., 2002; Yeh et al., 2002; Techathuvanan et al., 2010; Domesle et al., 2018). Real-time PCR is extensively applied for the quantitative detection of *Salmonella* spp. However, PCR requires sophisticated thermal cyclers with trained personnel which makes its use difficult in underequipped laboratories and low-resource field settings (Techathuvanan et al., 2011). PCR assays' application is limited within the walls of the laboratories (Techathuvanan et al., 2011). In addition to the PCR assays, state-of-the-art isothermal amplification technologies such as LAMP, have been used for early and rapid detection of *Salmonella* spp. Simpler and more convenient techniques are required imperatively for the point-of-need (PON) diagnosis of *Salmonella* spp. in field conditions.

Recombinase polymerase amplification (RPA) acts as one of isothermal gene amplification techniques. RPA has the merit of amplification at a relatively low temperature (37–42°C) within 10–20 min (Piepenburg et al., 2006; Geng et al., 2018). The use of RPA-based methods has been proved to be a success in detecting pathogenic bacteria and viruses in clinical and food samples (Euler et al., 2012; Abd El Wahed et al., 2015; Wang et al., 2020). RPA-based methods have been designed to be a miniaturized diagnostic device that includes all the components for the RPA assay (Asiello and Baeumner, 2011). RPA assay was a rapid, stable, and promising assay for the on-site detection. The objective of the study was to develop the real-time and LFS RPA assays using the exo probe and nfo probe combined with lateral flow strip respectively as a way of rapidly detecting *Salmonella* spp. in food samples.

TABLE 1 | Bacterial strains and analytical specificity results for real-time RPA and LFS RPA assays.

Strain Name	Origin[1]	Real-time RPA[2]	LFS RPA[2]	Real-time PCR[2]
Salmonella	CICC 22956	+	+	+
Salmonella aberdeen	CMCC50786	+	+	+
Salmonella dublin	CMCC50761	+	+	+
Salmonella taksony	CMCC50359	+	+	+
Salmonella typhimurium	Isolated by lab	+	+	+
Salmonella enteritidis	Isolated by lab	+	+	+
Salmonella paratyphi	Isolated by lab	+	+	+
Salmonella enterica	Isolated by lab	+	+	+
Enterobacter sakazakii	ATCC 29544	–	–	–
Staphylococcus aureus	ATCC 6538	–	–	–
Campylobacter jejuni	ATCC 33291	–	–	–
Vibrio parahaemolyticus	ATCC 17802	–	–	–
Pseudomonas aeruginosa	ATCC 9027	–	–	–
Vibrio vulnificus	ATCC 27562	–	–	–
Pseudomonas aeruginosa	ATCC 9027	–	–	–
Bacillus cereus	CMCC 63301	–	–	–
Listeria monocytogenes	ATCC 19114	–	–	–
Proteus mirabilis	ATCC 35659	–	–	–
Enterobacter aerogenes	ATCC 13048	–	–	–
Shigella sonnei	ATCC 51592	–	–	–
Bacillus licheniformis	ATCC 14580	–	–	–
Proteus pneumonia	CMCC 49027	–	–	–
Shigella boydii	CMCC 51250	–	–	–
Shigella flexneri	CMCC51105	–	–	–
Shigella flexneri	CICC 21678	–	–	–
Escherichia coli O157:H7	CICC 21530	–	–	–
Mannheimia haemolytica	Isolated by lab	–	–	–
Enterobacter cloacae	Isolated by lab	–	–	–
Citrobacter freundii	Isolated by lab	–	–	–
Streptococcus	Isolated by lab	–	–	–
Bacillus subtilis	Isolated by lab	–	–	–
Pseudomonas aeruginosa	Isolated by lab	–	–	–
Staphylococcus pasteuri	Isolated by lab	–	–	–
Escherichia coli	Isolated by lab	–	–	–

[1]*ATCC, American Type Culture Collection; CICC, China Center of Industrial Culture Collection; CMCC, China Center for Medical Culture Collection.*
[2]*+, positive results; –, negative results.*

MATERIALS AND METHODS

Bacterial Strains and DNA Extraction

A total of 34 common pathogenic bacteria strains were used to validate the techniques employed in this study (**Table 1**). These pathogenic bacteria were purchased from the American Type Culture Collection (ATCC), China Center of Industrial Culture Collection (CICC), China Center for Medical Culture Collection (CMCC) or isolated in the lab. All strains were reserved in the lab. Stock cultures were stored at −80°C in 0.8 ml of Nutrient broth (Beijing Land Bridge Technology Co., Ltd., Beijing, China) and 0.2 ml of 80% glycerol. The DNA templates were extracted using the TIANamp Bacteria DNA Kit (Tiangen, Beijing, China). These DNA samples were stored at −20°C before the assays.

RPA Primers and Probe

Nucleotide sequence data for *Salmonella* spp. strains from GenBank were aligned to identify conserved regions. Based on the reference sequences of different *Salmonella* spp. genotypes (accession numbers: AY594273, AY594271, DQ644632, DQ644633, EU348367, EU348368, JF951188, and JN982040), three pairs of primers targeting the conserved region of *invA* were designed (Rahn et al., 1992; Gonzalez-Escalona et al., 2009). RPA, Real-time RPA primers, and probes were then selected through testing the combination that yielded the highest sensitivity (**Table 2**). Primers and exo probes were synthesized by Sangon (Sangon, Shanghai, China).

Real-Time RPA Assay

Real-time RPA was accomplished in the tube with 50 µl reaction volume, including 40.9 µl of Buffer A (rehydration buffer), 2.0 µl of each RPA primers (***Sa***-exo-F and ***Sa***-exo-R, 10 µmol/L), 0.6 µl of exo probe (***Sa***-exo-P,10 µmol/L), and 2.5 µl of Buffer B (magnesium acetate, 280 mmol/L). Furthermore, 1 µl of genomic DNA was used for the specificity and sensitivity analysis, or 2 µl of sample DNA was used for the clinical sample diagnosis. In the process, the Genie III scanner device (OptiGene Limited, West Sussex, UK) and TwistAmpTM exo kit (TwistDX, Cambridge, UK) were applied.

LFS RPA Assay

Moreover, the LFS RPA assay was performed according to the given instructions. The commercial TwistAmp™ nfo kit (TwistDX, Cambridge, UK) was used in the LFS RPA. The reactions were performed in a 50 µl volume with 29.5 µl of rehydration buffer with 2.5 µl of magnesium acetate (280 mM) included. Other components contained 420 nM RPA primer, 120 nM exo probe, and 1 µl of bacterial genomic DNA or 5 µl of sample DNA. The assay was performed in an incubator block at 39°C for 15 min and the lateral flow strips (Ustra Biotec GmbH, Germany) were employed to discover the RPA amplicons dual-labeled with FAM and biotin. Testing samples were considered positive when both the test line and the control line were visible. The testing sample was considered negative when the control line was visible. However, the sample was considered invalid when the control line was invisible.

Real-Time PCR

Real-time PCR was performed on the ABI 7500 instrument in which premix Ex Taq TM (Takara Co., Ltd., Dalian, China) was employed (Geng et al., 2019). The reaction was performed as follows: 95°C for 30 s, followed by 35 cycles of 95°C for 10 s and then 60°C for 34 s. The sequences of the primers and probes used for real-time PCR were listed in **Table 2**. The reporter and fluorescence quencher were marked with 6-FAM (6-CarboxyFluorescein) and BHQ1 (Black Hole Quencher 1) respectively.

Analytical Specificity and Analytical Sensitivity Analysis

For the food security, the real-time RPA and LFS RPA assays were evaluated to amplify the nucleic acid of some important pathogens. Five independent reactions were performed.

The genomic DNA of *Salmonella* spp. varying from 1.1×10^8 to 1.1×10^0 fg was diluted in nuclease-free water for the analytical sensitivity analysis of the RPA. One microliter of each DNA dilution was amplified by both RPA assays to determine the limit of detection (LOD). The culture of *Salmonell*a spp. was diluted in sterile water (ranging from 1.4×10^7 to 1.4×10^0 CFU) and counted by plate counting in 37°C overnight. The sensitivity of the real-time RPA and LFS RPA method were assessed with *Salmonella* spp. in pure culture. The analytical sensitivity analysis was repeated for five times.

Validation With Artificially Contaminated Samples

The pure colony of *Salmonella* spp. was picked into a tube containing 1 ml sterile saline. The solution was vortexed for 30 s and the turbidity was measured to 1.00 using a turbidimeter. Sterile saline was used for 10-fold gradient dilution until it attained 10^{-8} dilution. With 10^{-5}, 10^{-6}, and 10^{-7} diluents of 200 µl on the chromogenic medium of *Salmonella* spp., the initial concentration of the pure culture bacteria was calculated using three parallels.

Commercially available chicken/lamb/broccoli were purchased from a local supermarket free of *Salmonella* spp. to assess the potential use and suitability of the developed RPA assays. Testing of the samples was done according to the Chinese national standard (GB 4789.4-2016). A total of 4, 14, and 59 CFU/25g of *Salmonella* spp. with chicken, lamb, and broccoli respectively, were added into a sterile stomaching bag containing 225 ml Nutrient broth. These samples were mixed well to get homogenous samples and incubated for 6 or 8 h at 37°C to increase the bacterial concentrations to attain detectable levels. The Bacterial genomic DNA extraction, the real-time RPA, and

TABLE 2 | Primer and probe sequences for *Salmonella* spp. Real-time PCR, RPA, real-time RPA and LFS RPPA assays.

Method	Name[1]	Sequence 5′-3′Amplication	Size(bp)
Real-time RPA	RPA-FP	GTCATTCCATTACCTACCTATCTGGTTGATTTCC	200
LFS-RPA	RPA-RP	GCATCGGCTTCAATCAAGATAAGACGACTGGT	
	exo Probe	GTACTGGCGATATTGGTGTTTATGGGGTCGT-(FAM-dT)-THF-(BHQ1-dT)-ACATTGACAGAATCC-C3-spacer	
	nfo Probe	FAM-GTACTGGCGATATTGGTGTTTATGGGGTCGTT-THF-T-ACATTGACAGAATCC-C3-spacer	
Real-time PCR	PCR-FP	GAAGTTGAGGATGTTATTCGCAAAG	68
	PCR-RP	GGAGGCTTCCGGGTCAAG	
	Probe	JOE-CCGTCAGACCTCTGGCAGTACCTTCCTC-Eclipse	

[1]*FP, Forward primer; RP, Reverse primer.*

LFS RPA reactions were performed, and each experiment was repeated for no less than three times to attain results.

RESULTS

Analytical Specificity and Sensitivity of the Real-Time RPA and LFS-RPA Assay

The *invA* gene coding of the invasion protein of *Salmonella* spp. is the most used specific gene for the discovery of many different *Salmonella* spp. serotypes. The RPA primers and probes were designed according to the *invA* gene of *Salmonella* spp. in this study. Both RPA assays provide excellent results at 39°C within 20 min. This was faster than any other common nucleic acid amplification method. The analytical sensitivity of RPA methods was evaluated by employing *Salmonella* spp. genomic DNA and bacterial pure culture as templates from 1.1×10^8 to 1.1×10^0 fg and from 1.4×10^7 to 1.4×10^0 CFU. The data on the analytical sensitivity of RPA methods was presented in **Figures 1A**, **2A**. The detection limit (LOD) of real-time RPA was 1.1×10^1 fg similar to that of real-time PCR (the data was not shown) (**Figure 1A**). The limit of detection of the LFS RPA method was 1.1×10^2 fg for genomic DNA (**Figure 2A**), 10-times lower compared with the real-time PCR. The LOD of the real-time RPA and LFS RPA was 1.4×10^2 CFU for bacteria in pure culture (shown in **Figures 1B**, **2B**).

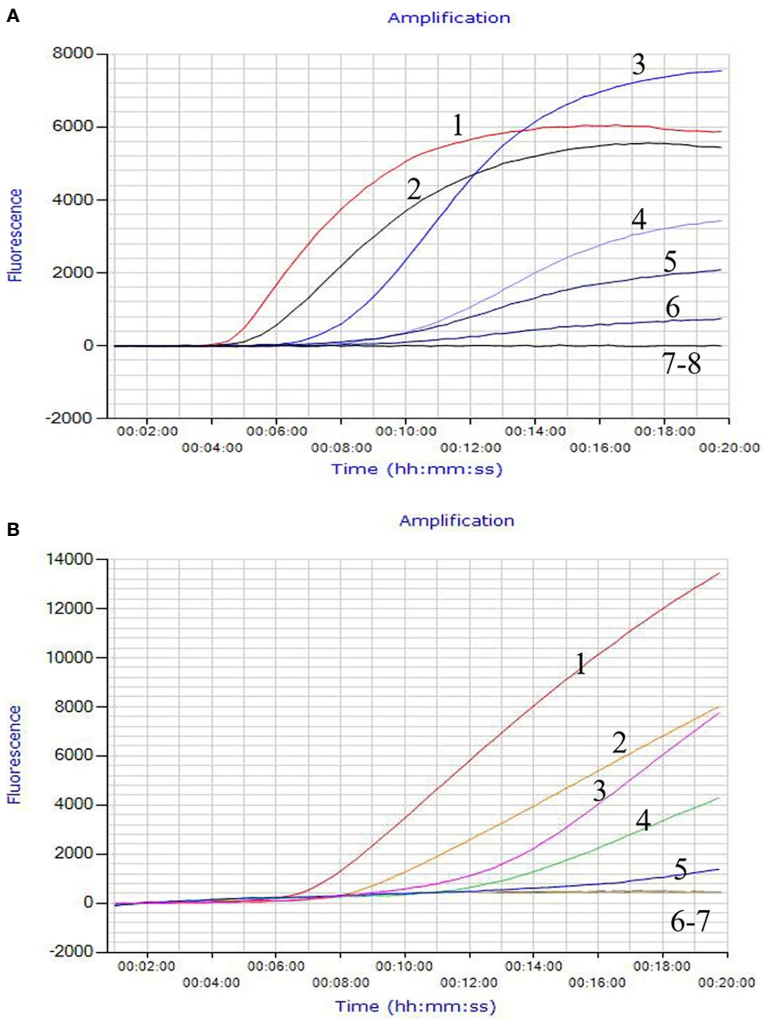

FIGURE 1 | Analytical Sensitivity of the real-time RPA assay. The LOD of the real-time RPA was 1.1×10^1 fg/µl of *Salmonella* spp. standard DNA and 1.4×10^2 CFU/ml for bacteria in pure culture. Fluorescence development over time using a dilution range of 1.1×10^6–1.1×10^0 fg of *Salmonella* spp. genomic DNA. For **(A)**: Curve 1, 1.1×10^6 fg; Curve 2, 1.1×10^5 fg; Curve 3, 1.1×10^4 fg; Curve 4, 1.0×10^3 fg; Curve 5, 1.1×10^2 fg; Curve 6, 1.1×10^1 fg; Curve 7, 1.1×10^0 fg; Curve 8, ddH_2O. For **(B)**: Curve 1, 1.4×10^6 CFU; Curve 2, 1.4×10^5 CFU; Curve 3, 1.4×10^4 CFU; Curve 4, 1.4×10^3CFU; Curve 5, 1.4×10^2 CFU; Curve 6, 1.4×10^1CFU; Curve 7, 1.4×10^0 CFU.

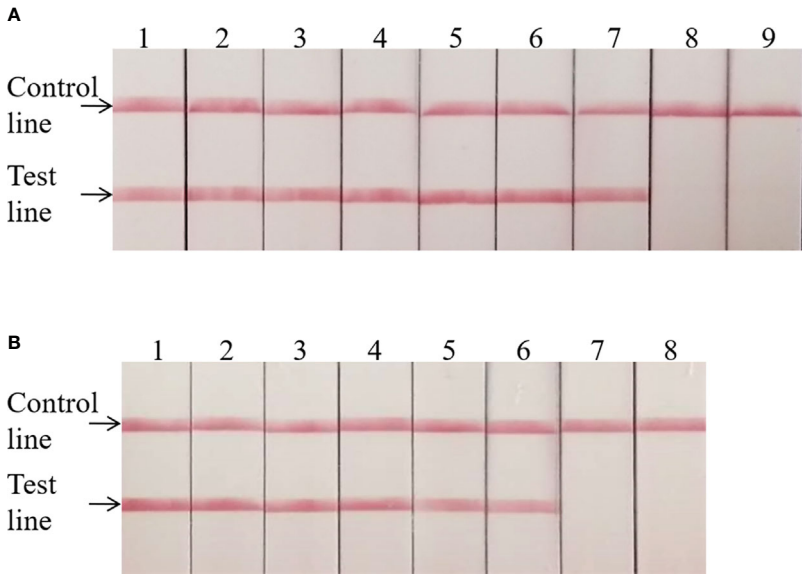

FIGURE 2 | Analytical sensitivity of the LFS RPA assay. The LOD of the LFS RPA method was 1.1×10^2 fg for genomic DNA and 1.4×10^2 CFU/ml for bacteria in pure culture. For **(A)**: Sample 1, 1.1×10^8 fg; Sample 2, 1.1×10^7fg; Sample 3, 1.1×10^6 fg; Sample 4, 1.1×10^5 fg; Sample 5, 1.1×10^4 fg; Sample 6, 1.1×10^3 fg; Sample 7, 1.1×10^2 fg; Sample 8, 1.1×10^1 fg; Sample 9, 1.1×10^0 fg. For **(B)**: Sample 1, 1.4×10^7 CFU; Sample 2, 1.4×10^6 CFU; Sample 3, 1.4×10^5 CFU; Sample 4, 1.4×10^4 CFU; Sample 5, 1.4×10^3 CFU; Sample 6, 1.4×10^2 CFU; Sample 7, 1.4×10^1 CFU; Sample 8, 1.4×10^0 CFU.

Regarding specificity, only amplification signal was observed at the control line with *Salmonella* spp. and no cross-detection of other pathogens were shown in both real-time RPA and LFS-RPA assays (**Table 1**). Five independent reactions were repeated and similar results were obtained. This manifests the high specificity of the assays.

Evaluation With Artificially Contaminated Samples After Enrichment

The diagnostic performance of the developed RPA assays was compared with other detection approaches and was shown in **Table 3**. This was done while detecting *Salmonella* spp. in artificially contaminated food samples. The National Standard

TABLE 3 | The comparison of reaction time of different methods in contaminated foods.

Food samples	Spiked samples[1] (CFU/25g)	Enrichment time(h)	Real-time RPA (min:ss)	LFS-RPA[2] (min)	Real-timePCR[3] (Ct)	GB4789.4-2016	Viable cell counts (CFU/g)
Lamb	4	6	–	–	–	–	0
		8	12:18	15(+)	33.24	+	4.7×10^3
	14	6	–	–	–	–	0
		8	11:44	15(+)	33.38	+	5.1×10^3
	59	6	12:04	15(+)	33.78	+	4.6×10^3
		8	10:15	15(+)	30.58	+	7.8×10^3
Broccoli	4	6	–	–	–	–	0
		8	10:09	15(+)	30.02	+	6.2×10^3
	14	6	6:55	15(+)	28.47	+	1.3×10^3
		8	5:16	15(+)	19.34	+	5.3×10^5
	59	6	6:33	15(+)	25.46	+	1.8×10^4
		8	5:39	15(+)	20.58	+	1.8×10^5
Chicken	4	6	–	–	–	–	0
		8	11:54	15(+)	33.49	+	3.8×10^4
	14	6	12:06	15(+)	34.01	+	6.3×10^3
		8	6:14	15(+)	25.18	+	2.8×10^5
	59	6	11:22	15(+)	33.28	+	3.9×10^4
		8	5:54	15(+)	22.39	+	3.7×10^5

[1]CFU, colony-forming units; [2]Ct, Cycle threshold; [3]+, detected; –, not detected.
Total bacterial count, 1.5×10^7 CFU/g and coliform group, 3.1×10^4 CFU/g in Lamb;
Total bacterial count, <1.0 × 10 CFU/g and coliform group, <1.0 × 10 CFU/g in Broccoli;
Total bacterial count, 3.7×10^2 CFU/g and coliform group, <1.0 × 10 CFU/g in Chicken.

GB 4789.4-2016 method was used as a reference to guarantee that the food samples were successfully contaminated. However, after 6-h enrichment of food samples contaminated with 4 CFU/25 g of *Salmonella* spp., no *Salmonella* spp. was discovered through any of the detection methods. This signaled no false-positive results from samples containing low levels of *Salmonell*a spp. All contaminated food samples were detected and showed increasing values of CFU/25 g of spiked samples and enrichment time. However, lamb contaminated with 14 CFU/25 g of *Salmonella* spp. was different from the other contaminated food samples and was enriched for 6 h. Furthermore, a diagnostic agreement of 100% with real-time PCR and the traditional method was indicated in the developed real-time RPA and LFS RPA assays. Moreover, the speed of the RPA assays outstripped. The time required to attain positive results with real-time RPA and LFS RPA was 5–12 min and 15 min respectively. Real-time PCR with CT values at 19.34–34.01 required approximately 20–35 min. Therefore, the results demonstrated that, with the equal sensitivity, the real-time and LFS RPA assays was faster than the real-time PCR.

DISCUSSION

The disease induced by foodborne pathogens remains a major public health issue worldwide despite ongoing measurements to ensuring food safety. *Salmonella* spp. frequently leads to infections and worldwide outbreaks accounting for huge economic costs and life loss every year (Foley and Lynne, 2008). Rapid and reliable diagnostic techniques play an important part to efficiently detect *Salmonella* spp. from contaminated specimens and make appropriate measures for preventing and controlling the risk of *Salmonella* spp. infection as early as possible.

The real-time RPA and LFS RPA assays are good choices for detecting *Salmonella* spp. as demonstrated in this report. These assays are specific, sensitive, and simple to perform. In the specificity analysis, both the real-time RPA and LFS RPA only amplified the genomic DNA of *Salmonella* spp. used in the study. This indicated high specificity of these assays. However, other more *Salmonella* strains are needed to further examine the cross-reactivity of these RPA assays. The real-time RPA had equal sensitivity (limit of detection) as real-time PCR in this study. This was 10 times higher than the LFS assay. However, it is possible for a varied reaction mechanism and enzyme kinetics between the different methods. The reaction time of RPA assays was much shorter than real-time PCR. The diagnostic performances of the developed real-time RPA and LFS RPA assays has been further assessed. These assays were proved to be a success in the detection of the artificially contaminated food samples, and performed better than the real-time PCR in light of the detecting speed. However, a pre-enrichment step was necessary when the level of pathogen contamination was low. A similar ideal result was obtained using the direct water boiling method to extract the bacterial DNA as the template of RPA reaction. Direct boiling method was used to extract the *Salmonella* spp. genomic DNA as the template of the RPA reaction. The LFS strip were combined to facilitate the detection of *Salmonella* spp. at quarantine stations, ports, or the site of outbreak by the PRA assay based on nfo-probe.

RPA was first introduced in 2006 and represented an innovative DNA isothermal detecting technology beyond the reach of PCR or traditional culture-based methods (Piepenburg et al., 2006; James and Macdonald, 2015). RPAs have successfully been practiced in the discovery of pathogenic bacteria (Hong et al., 2020), fungus (Ahmed et al., 2014), and viruses (Boyle et al., 2013). The reagents in RPA are available in lyophilized form for long-term storage and are conveniently transported even without cold-chain (Wang et al., 2020). Moreover, under the prerequisite that the testing results were visible, the real-time RPA assay was accomplished on the user-friendly PON (point of need) detection platform (Genie III) with battery power. The developed LFS RPA assay only needed a simple incubator block. Therefore, these two pieces of equipment were portable, lightweight, and less expensive than the equipment for LAMP/PCR. As other isothermal DNA amplification methods, Loop-mediated isothermal amplification (LAMP) and the cross-priming amplification assay (CPA) have been adopted for rapidly and sensitively detecting *Salmonella* spp. Both RPA assays have the merits of amplification at a relatively lower temperature and within shorter time than that of LAMP and CPA assays. Both RPA reactions could be done at 37–42°C within 10–20 min. However, the optimum time and temperature were approximately 60 min and above 60°C respectively which were required for LAMP and CPA (Domesle et al., 2018; Wang et al., 2018). Moreover, several reports have shown that RPA is tolerant to mismatches, background DNA, and most of PCR inhibitors (Daher et al., 2016; Li et al., 2019; Liu et al., 2019). All of these outstanding characteristics make the assays readily suitable for the field, PON (point-of-need), or diagnosis of infectious diseases with poor environmental resources.

In conclusion, the current study proved that, the developed RPA assays with high specificity and sensitivity was convenient, rapid, and reliable for *Salmonella* spp. detection. In addition, the simple devices and easy operation protocol helped to improve the efficiency of detection. Among the isothermal amplification techniques, real-time RPA and LFS RPA assays play an outstanding role in preventing and controlling of *Salmonella* spp. especially in the settings with limited resources.

DATA AVAILABILITY STATEMENT

The datasets presented in this study can be found in online repositories. The names of the repository/repositories and accession number(s) can be found in the article/supplementary material.

AUTHOR CONTRIBUTIONS

YG, JCW, and WG designed and conducted the experiment. LZ, XS, JFW, XX, MD, Y-nG, YW, and PC performed the experiments and analyzed the data. YG drafted the manuscript. All authors contributed to the article and approved the submitted version.

FUNDING

This work was supported by the program of Traditional Chinese Medicine Scientific Research foundation in Hebei Administration of Traditional Chinese Medicine (2020142, Hebei, China), the Project of Excellent Young Teacher Fundamental Research (YQ2019003) and Doctoral Foundation (BSZ2019009) of Hebei University of Chinese Medicine.

REFERENCES

Abd El Wahed, A., Weidmann, M., and Hufert, F. T. (2015). Diagnostics-in-a-Suitcase: Development of a portable and rapid assay for the detection of the emerging avian influenza A (H7N9) virus. *J. Clin. Virol.* 69, 16–21. doi: 10.1016/j.jcv.2015.05.004

Ahmed, A., van der Linden, H., and Hartskeerl, R. A. (2014). Development of a recombinase polymerase amplification assay for the detection of pathogenic Leptospira. *Int. J. Environ. Res. Public Health* 11, 4953–4964. doi: 10.3390/ijerph110504953

Asiello, P. J., and Baeumner, A. J. (2011). Miniaturized isothermal nucleic acid amplification, a review. *Lab. Chip.* 11, 1420–1430. doi: 10.1039/c0lc00666a

Boyle, D. S., Lehman, D. A., Lillis, L., Peterson, D., Singhal, M., Armes, N., et al. (2013). Rapid detection of HIV-1 proviral DNA for early infant diagnosis using recombinase polymerase amplification. *mBio.* 4, e00135-13. doi: 10.1128/mBio.00135-13

Daher, R. K., Stewart, G., Boissinot, M., and Bergeron, M. G. (2016). Recombinase Polymerase Amplification for Diagnostic Applications. *Clin. Chem.* 62, 947–958. doi: 10.1373/clinchem.2015.245829

Domesle, K. J., Yang, Q., Hammack, T. S., and Ge, B. (2018). Validation of a Salmonella loop-mediated isothermal amplification assay in animal food. *Int. J. Food Microbiol.* 264, 63–76. doi: 10.1016/j.ijfoodmicro.2017.10.020

Euler, M., Wang, Y., Otto, P., Tomaso, H., Escudero, R., Anda, P., et al. (2012). Recombinase polymerase amplification assay for rapid detection of Francisella tularensis. *J. Clin. Microbiol.* 50, 2234–2238. doi: 10.1128/JCM.06504-11

Foley, S. L., and Lynne, A. M. (2008). Food animal-associated Salmonella challenges: pathogenicity and antimicrobial resistance. *J. Anim. Sci.* 86, E173–E187. doi: 10.2527/jas.2007-0447

Foley, S. L., Lynne, A. M., and Nayak, R. (2008). Salmonella challenges: prevalence in swine and poultry and potential pathogenicity of such isolates. *J. Anim. Sci.* 86, E149–E162. doi: 10.2527/jas.2007-0464

Geng, Y., Liu, S., Wang, J., Nan, H., Liu, L., Sun, X., et al. (2018). Rapid Detection of Staphylococcus aureus in Food Using a Recombinase Polymerase Amplification-Based Assay. *Food Anal. Methods* 11, 2847–2856. doi: 10.1016/j.mimet.2018.12.017

Geng, Y., Liu, G., Liu, L., Deng, Q., Zhao, L., Sun, X. X., et al. (2019). Real-time recombinase polymerase amplification assay for the rapid and sensitive detection of Campylobacter jejuni in food samples. *J. Microbiol. Methods* 157, 31–36. doi: 10.1007/s12161-018-1267-1

Gonzalez-Escalona, N., Hammack, T. S., Russell, M., Jacobson, A. P., De Jesus, A. J., Brown, E. W., et al. (2009). Detection of live Salmonella sp. cells in produce by a TaqMan-based quantitative reverse transcriptase real-time PCR targeting invA mRNA. *Appl. Environ. Microbiol.* 75, 3714–3720. doi: 10.1128/AEM.02686-08

Hirose, K., Itoh, K., Nakajima, H., Kurazono, T., Yamaguchi, M., Moriya, K., et al. (2002). Selective amplification of tyv (rfbE), prt (rfbS), viaB, and fliC genes by multiplex PCR for identification of Salmonella enterica serovars Typhi and Paratyphi A. *J. Clin. Microbiol.* 40, 633–636. doi: 10.1128/jcm.40.02.633-636.2002

Hong, H., Sun, C., Wei, S., Sun, X., Mutukumira, A., and Wu, X. (2020). Development of a real-time recombinase polymerase amplification assay for rapid detection of Salmonella in powdered infant formula. *Int. Dairy J.* 102. doi: 10.1016/j.idairyj.2019.104579

James, A., and Macdonald, J. (2015). Recombinase polymerase amplification: Emergence as a critical molecular technology for rapid, low-resource diagnostics. *Expert Rev. Mol. Diagn.* 15, 1475–1489. doi: 10.1586/14737159.2015.1090877

Li, R., Lai, J., Wang, Y., Liu, S., Li, Y., Liu, K., et al. (2013). Prevalence and characterization of Salmonella species isolated from pigs, ducks and chickens in Sichuan Province, China. *Int. J. Food Microbiol.* 163, 14–18. doi: 10.1016/j.ijfoodmicro.2013.01.020

Li, J., Ma, B., Fang, J., Zhi, A., Chen, E., Xu, Y., et al. (2019). Recombinase Polymerase Amplification (RPA) Combined with Lateral Flow Immunoassay for Rapid Detection of Salmonella in Food. *Foods.* 9, 27. doi: 10.3390/foods9010027

Liu, L., Li, R., Zhang, R., Wang, J., An, Q., Han, Q., et al. (2019). Rapid and sensitive detection of Mycoplasma hyopneumoniae by recombinase polymerase amplification assay. *J. Microbiol. Methods* 159, 56–61. doi: 10.1016/j.mimet.2019.02.015

McGuinness, S., McCabe, E., O'Regan, E., Dolan, A., Duffy, G., Burgess, C., et al. (2009). Development and validation of a rapid real-time PCR based method for the specific detection of Salmonella on fresh meat. *Meat Sci.* 83, 555–562. doi: 10.1016/j.meatsci.2009.07.004

Nassib, T. A., El-Din, M. Z., and El-Sharoud, W. M. (2003). Assessment of the presence of Salmonella spp. in Egyptian dairy products using various detection media. *Lett. Appl. Microbiol.* 37, 405–409. doi: 10.1046/j.1472-765X.2003.01420.x

Piepenburg, O., Williams, C. H., Stemple, D. L., and Armes, N. A. (2006). DNA detection using recombination proteins. *PLoS Biol.* 4, e204. doi: 10.1371/journal.pbio.0040204

Rahn, K., De Grandis, S. A., Clarke, R. C., McEwen, S. A., Galan, J. E., Ginocchio, C., et al. (1992). Amplification of an invA gene sequence of Salmonella typhimurium by polymerase chain reaction as a specific method of detection of Salmonella. *Mol. Cell Probes.* 6, 271–279. doi: 10.1016/0890-8508(92)90002-f

Rukambile, E., Sintchenko, V., Muscatello, G., Kock, R., and Alders, R. (2019). Infection, colonization and shedding of Campylobacter and Salmonella in animals and their contribution to human disease: A review. *Zoonoses Public Health* 66, 562–578. doi: 10.1111/zph.12611

Techathuvanan, C., Draughon, F. A., and D'Souza, D. H. (2010). Real-time reverse transcriptase PCR for the rapid and sensitive detection of Salmonella typhimurium from pork. *J. Food Prot.* 73, 507–514. doi: 10.4315/0362-028x-73.3.507

Techathuvanan, C., Draughon, F. A., and D'Souza, D. H. (2011). Comparison of reverse transcriptase PCR, reverse transcriptase loop-mediated isothermal amplification, and culture-based assays for Salmonella detection from pork processing environments. *J. Food Prot.* 74, 294–301. doi: 10.4315/0362-028X.JFP-10-306

Wang, Y. X., Zhang, A. Y., Yang, Y. Q., Lei, C. W., Cheng, G. Y., Zou, W. C., et al. (2018). Sensitive and rapid detection of Salmonella enterica serovar Indiana by cross-priming amplification. *J. Microbiol. Methods* 153, 24–30. doi: 10.1016/j.mimet.2018.08.003

Wang, J., Li, R., Sun, X., Liu, L., Hao, X., Wang, J., et al. (2020). Development and validation of the isothermal recombinase polymerase amplification assays for rapid detection of Mycoplasma ovipneumoniae in sheep. *BMC Vet. Res.* 16, 172. doi: 10.1186/s12917-020-02387-3

Yeh, K. S., Chen, T. H., Liao, C. W., Chang, C. S., and Lo, H. C. (2002). PCR amplification of the *Salmonella typhimurium* fimY gene sequence to detect the Salmonella species. *Int. J. Food Microbiol.* 78, 227–234. doi: 10.1016/s0168-1605(02)00115-0

Conflict of Interest: The authors declare that the research was conducted in the absence of any commercial or financial relationships that could be construed as a potential conflict of interest.

frontiers in Cellular and Infection Microbiology

ORIGINAL RESEARCH
published: 17 March 2021
doi: 10.3389/fcimb.2021.633763

An Isothermal Molecular Point of Care Testing for African Swine Fever Virus Using Recombinase-Aided Amplification and Lateral Flow Assay Without the Need to Extract Nucleic Acids in Blood

*Yuhang Zhang[1], Qingmei Li[2], Junqing Guo[2], Dongliang Li[1], Li Wang[2], Xun Wang[1], Guangxu Xing[2], Ruiguang Deng[2] and Gaiping Zhang[1,2,3]**

[1] College of Veterinary Medicine, Henan Agricultural University, Zhengzhou, China, [2] Key Laboratory of Animal Immunology, Henan Academy of Agricultural Sciences, Zhengzhou, China, [3] Jiangsu Co-Innovation Center for Prevention and Control of Important Animal Infectious Disease and Zoonose, Yangzhou University, Yangzhou, China

African swine fever (ASF) is a highly contagious and usually deadly porcine infectious disease listed as a notifiable disease by the World Organization for Animal Health (OIE). It has brought huge economic losses worldwide, especially since 2018, the first outbreak in China. As there are still no effective vaccines available to date, diagnosis of ASF is essential for its surveillance and control, especially in areas far from city with limited resources and poor settings. In this study, a sensitive, specific, rapid, and simple molecular point of care testing for African swine fever virus (ASFV) *B646L* gene in blood samples was established, including treatment of blood samples with simple dilution and boiling for 5 min, isothermal amplification with recombinase-aided amplification (RAA) at 37°C in a water bath for 10 min, and visual readout with lateral flow assay (LFA) at room temperature for 10–15 min. Without the need to extract viral DNA in blood samples, the intact workflow from sampling to final diagnostic decision can be completed with minimal equipment requirement in 30 min. The detection limit of RAA-LFA for synthesized *B646L* gene-containing plasmid was 10 copies/μl, which was 10-fold more sensitive than OIE-recommended PCR and quantitative PCR. In addition, no positive readout of RAA-LFA was observed in testing classical swine fever virus, porcine reproductive and respiratory syndrome virus, porcine epidemic diarrhea virus, pseudorabies virus and porcine circovirus 2, exhibiting good specificity. Evaluation of clinical blood samples of RAA-LFA showed 100% coincident rate with OIE-recommended PCR, in testing both extracted DNAs and treated bloods. We also found that some components in blood samples greatly

OPEN ACCESS

Edited by:
Jianmin Zhang, South China Agricultural University, China

Reviewed by:
Yuan Sun, Chinese Academy of Agricultural Sciences, China
Rongliang Hu, Academy of Military Medical Science, China

***Correspondence:**
Gaiping Zhang
zhanggaip@126.com

Specialty section:
This article was submitted to Clinical Microbiology, a section of the journal Frontiers in Cellular and Infection Microbiology

Received: *26 November 2020*
Accepted: *08 February 2021*
Published: *17 March 2021*

Citation:
Zhang Y, Li Q, Guo J, Li D, Wang L, Wang X, Xing G, Deng R and Zhang G (2021) An Isothermal Molecular Point of Care Testing for African Swine Fever Virus Using Recombinase-Aided Amplification and Lateral Flow Assay Without the Need to Extract Nucleic Acids in Blood. Front. Cell. Infect. Microbiol. 11:633763. doi: 10.3389/fcimb.2021.633763

inhibited PCR performance, but had little effect on RAA. Inhibitory effect can be eliminated when blood was diluted at least 32–64-fold for direct PCR, while only a 2–4 fold dilution of blood was suitable for direct RAA, indicating RAA is a better choice than PCR when blood is used as detecting sample. Taken together, we established an sensitive, specific, rapid, and simple RAA-LFA for ASFV molecular detection without the need to extract viral DNA, providing a good choice for point of care testing of ASF diagnosis in the future.

Keywords: point of care testing, African swine fever, isothermal molecular diagnosis, recombinase-aided amplification, lateral flow assay, blood

INTRODUCTION

African swine fever (ASF) is an infectious disease of domestic pigs and wild boars of all breeds and ages, usually showing symptoms like high fever and hemorrhages with a high mortality rate. It endangers swine industries and brings huge economic losses each year, and thus is listed as a reportable disease by the World Organization for Animal Health (OIE) (Penrith and Vosloo, 2009). African swine fever virus (ASFV), the causative agent of ASF, is a large enveloped double-stranded DNA virus. It is the only member of the *Asfarviridae* family, *Asfivirus* genus, with a large viral genome around 170–194 kb, encoding at least 125 viral proteins (Dixon et al., 2013). Based on sequencing of the 3' terminal end of the *B646L* that encodes the p72 protein major capsid protein, ASFV can be divided up to 24 distinct genotypes (I-XXIV), of which only genotypes I and II have been found outside of African continent (Bastos et al., 2003; Quembo et al., 2018). ASFV is extremely resistant to heat, desiccation, putrefaction, and varified pH conditions, especially in environments with proteins and low temperature, making ASF a highly contagious disease that can be transmitted not only by infected pigs or tampans, but also by contaminated materials such as meat, blood, feces, urine, or saliva from infected pigs (Brown and Bevins, 2018). ASFV can even remain infectivity over 75 weeks at 4°C in blood (Plowright and Parker, 1967). High stability of ASFV makes eradication and prevention of ASF a challenging work during live pig production.

ASF was first reported in Kenya in 1921 and circulated only in Sub-Saharan Africa for decades. In 1957, an outbreak of ASF from African continent invaded Portugal and Spain, resulting in an ASF epidemic within European countries until its eradication in 1990s. In 2007, another outbreak of ASF started from Georgia and rapidly spread across Eastern Europe (Costard et al., 2013). The first case of ASF in China was reported on August 3, 2018 (Zhou et al., 2018). Since then, ASF cases were continuously reported from all provinces of China and neighboring Asian countries, including Mongolia (January 2019), Vietnam (February 2019), Cambodia (March 2019), Korea (May 2019), Laos (June 2019), Myanmar (August 2019), Philippines (July 2019), Timor-Leste (September 2019), Indonesia (November 2019), Papua New Guinea (March 2020), and India (May 2020). To date, ASF is mainly distributed in Africa, Europe, and Asia, revealing a serious deterioration. ASF has led to a total of 8,202,702 pigs lost since 2018, of which Asia accounts for 82% (OIE, 2020).

Though efforts have been put in developing ASF vaccines with varying levels of success, there is still no vaccine available to date (Bosch-Camos et al., 2020). Control and prevention of ASF are mainly based on animal slaughter and strict sanitation strategies, in the aid of early detection and surveillance of the disease. However, sensitive, specific clinical diagnosis of ASF is hard to make, due to its non-specific symptoms which are similar to some common porcine diseases such as classical swine fever. Traditional OIE recommended diagnostic methods for ASF include virus isolation, antigen identification (hemadsorption test and fluorescent antibody test) and serological tests (enzyme-linked immunosorbent assay, indirect fluorescent antibody test, indirect immunoperoxidase test and immunoblotting test) (OIE, 2019). All these methods need to be performed by skilled technicians with expensive equipments under laboratory condition, often leading to diagnosis delay and virus transmission, especially in areas far from city with limited resources and poor settings.

With a short incubation time from 4 to 19 days, some ASF cases even show no clinical signs and antibody responses before pig death and virus spread. In addition, ASFV genomic DNA can be detected in blood as early as 56 h post-infection (Wang X. et al., 2020) and stably exist up to 78 days (Gallardo et al., 2019), making it an ideal choice for ASFV early and bioptic molecular detection. Current ASFV molecular detection methods used in laboratory mainly rely on OIE recommended PCR and real-time PCR. However, it is well known that some components in blood have the inhibitory effects on PCR, which limits its performance on blood samples (Zhang et al., 1995; Klein et al., 1997; Fredricks and Relman, 1998). PCR-based technologies also cannot avoid sophisticated instruments such as thermal cycler and fluorescent devices, making them not suitable for point of care testing (POCT).

Recently, the isothermal amplification techniques have become an alternative way to PCR for ASFV molecular detection, including polymerase cross-linking spiral reaction (PCLSR) (Woźniakowski et al., 2017), isothermal cross-priming amplification (CPA) (Frączyk et al., 2016; Gao et al., 2018), loop-mediated isothermal amplification (LAMP) (James et al., 2010; Atuhaire et al., 2014; Wang D. et al., 2020), and recombinase based isothermal amplification assays (Wang et al., 2017; Miao et al., 2019; Fan et al., 2020; Zhai et al., 2020). With simple primer requirement and high amplification efficiency, recombinase based isothermal amplification assays, including recombinase polymerase amplification (RPA) and recombinase-aided amplification (RAA) display various advantages for POCT. Both RPA and RAA can be

completed within 30 min at a constant temperature from 37 to 42°C under the action of recombinase, single-stranded DNA binding protein and polymerase (**Figure 1**). Combined with lateral flow assay (LFA) for readout (**Figure 2**) or portable fluorescent detection devices, RPA and RAA has been applied for many infectious diseases as a powerful in-field diagnostic tool for POCT (James and Macdonald, 2015; Daher et al., 2016; Moore and Jaykus, 2017; Lobato and O'Sullivan, 2018).

In this study, we established a rapid RAA-LFA dignostic platform of ASFV and evaluated the sensitivity, specificity, repeatability, and stability. A simple treatment of clinical blood samples for virus inactivation and nucleic acids release was also investigated. Blood samples can be directly used for RAA-LFA after simply boiled, without the need to extract viral DNA. With minimal requirements for equipment and reagent, a complete POCT workflow for ASF from sampling to final decision within 30 min at a relative constant temperature was presented in this study (**Figure 3**).

MATERIALS AND METHODS

Clinical Samples and Ethics Statement

A total of 37 clinical blood samples were collected from a pig farm that suffered from an ASF epidemic in Henan, China. Blood sampling was performed under licenses granted by Henan Academy of Agricultural Sciences (Approval number SYXK 2014-0007) with the animal welfare guidelines of the Institutional Animal Care and Use Committee. All sample treatments were performed at the infected farm, strictly in accordance with the standard operation for ASFV by OIE.

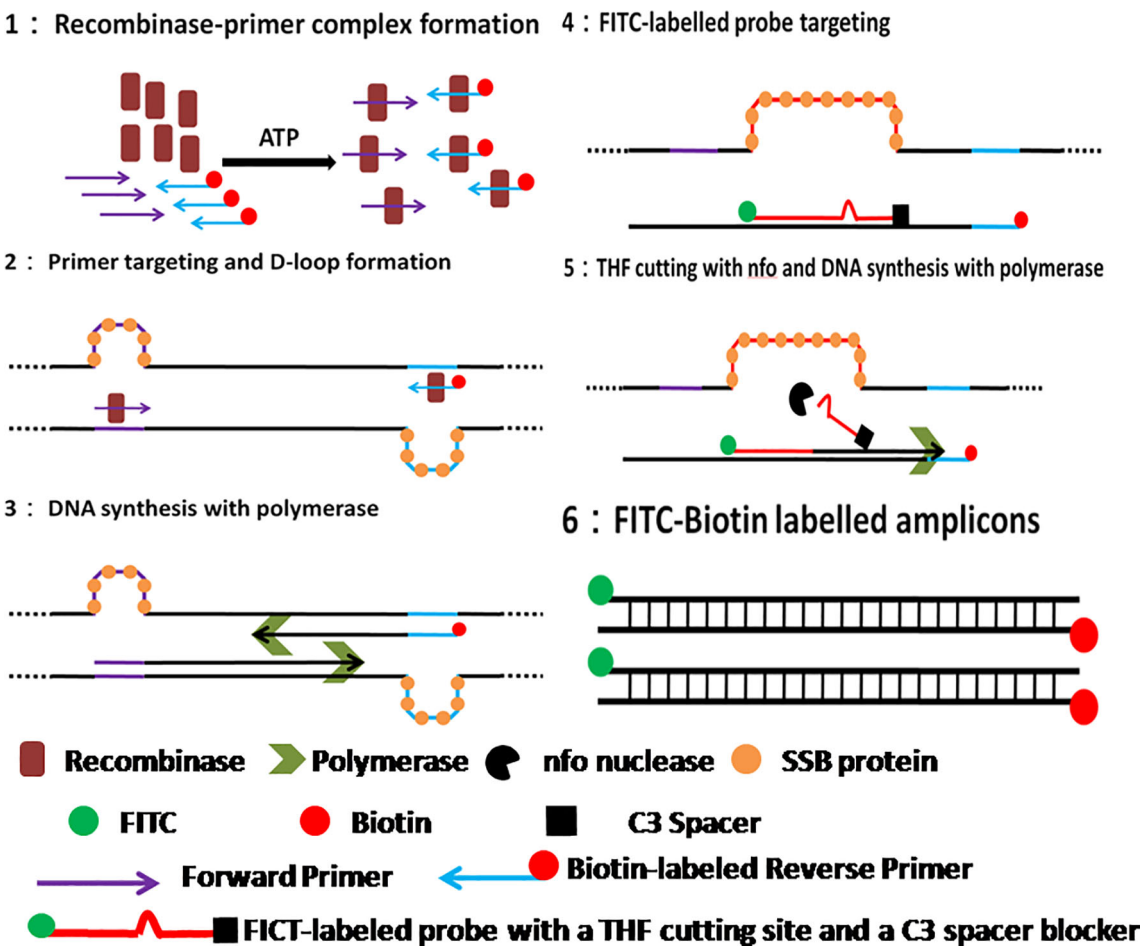

FIGURE 1 | Schematic of RAA reaction. 1. Recombinase-primer complex scans the duplex DNA and locates homologous sequence; 2. D-loop structure formation, with one chain hybridizing with primer and the other chain being stabilized by SSB protein. 3. Recombinase breaks away for the next round RAA reaction, leaving the free 3'-OH of primer behind for the initiation of DNA synthesis with Polymerase; 4. RAA probe labeled with 5'-FITC and 3'-C3 spacer hybridizes target DNA and forms double stranded structure; 5. Nfo nucleases cleaves probe at the THF cutting site, leaving a free 3'-OH for DNA synthesis by Polymerase; 6. RAA amplicon formation, with a 5'-FITC group and a 3'-biotin group.

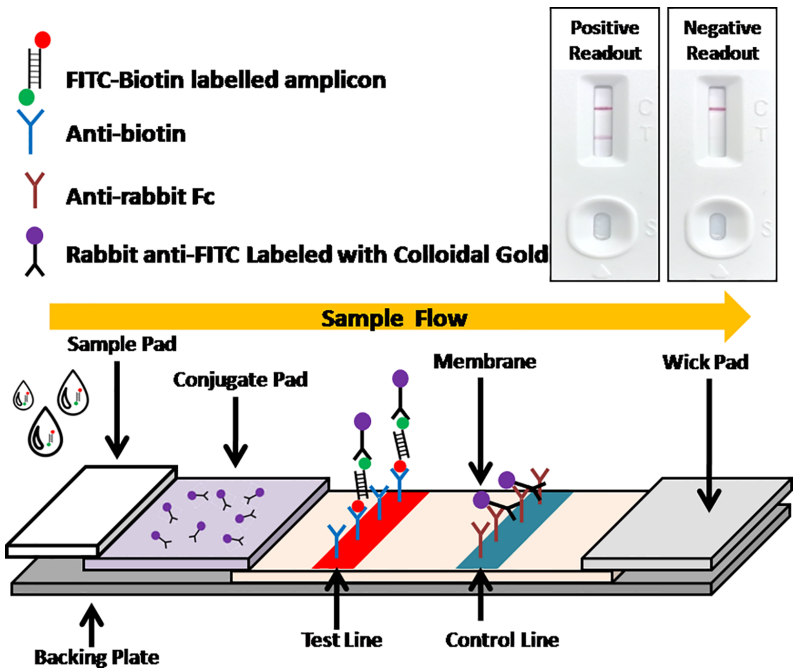

FIGURE 2 | Schematic of LFA visual readout. Biotin-FITC-labeled RAA amplificons firstly conjugate with colloidal gold labeled anti-FITC antibodies. As the conjugate flowing, streptavidins can capture the conjugate at test line, while anti-mouse antibodies can capture free excess colloidal gold labeled anti-FITC antibodies at control line. Visual bands at both test line and control lines indicates a positive readout while only a single band at control line indicates a negative readout.

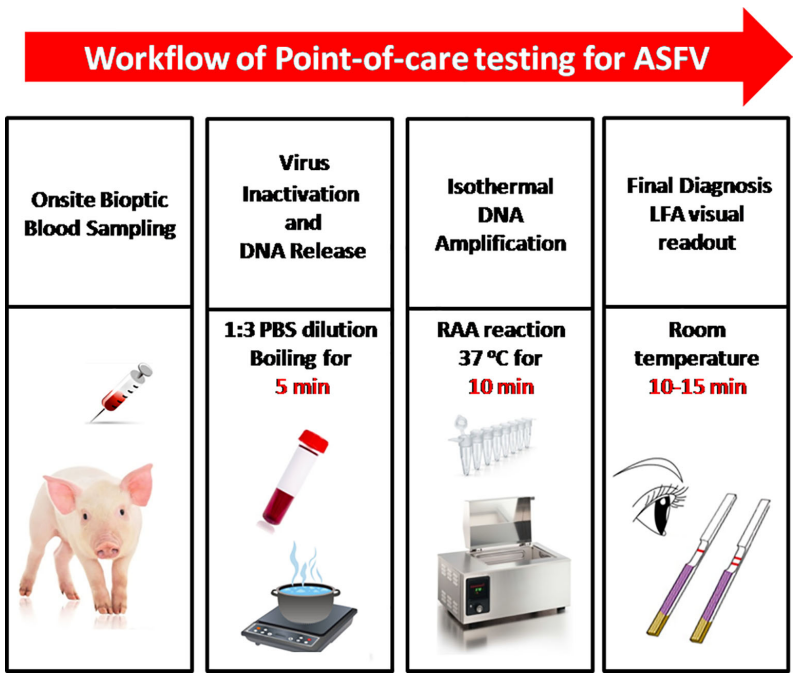

FIGURE 3 | The intact point of care testing workflow for ASF from sampling to final diagnosis. Blood dilution and boiling for 5 min; RAA reaction for 10 min; LFA visual readout for 10–15 min. All work can be done within 30 min, with minimal equipment requirement.

Other viral cell cultures used in this study, including classical swine fever virus (CSFV) Shimen strain, porcine reproductive and respiratory syndrome virus (PRRSV) HN07-1 strain, porcine epidemic diarrhea virus (PEDV) Hubei2016 strain, pseudorabies virus (PRV) HeNLH/2017 strain, and porcine circovirus 2 (PCV 2) HN-LB-2016 strain, are provided by Key Laboratory of Animal Immunology, Henan Academy of Agricultural Sciences.

Nucleic Acid

Primers, probe, and a standard plasmid pUC57-p72 that contains ASFV Pig/HLJ/2018 strain p72-encoding gene *B646L* (GenBank: MK333180.1) used in this study were all synthesized by Sangon Biotech (Shanghai, China).

Viral DNA from clinical blood samples were extracted with MiniBEST Viral RNA/DNA Extraction Kit Ver.5.0 (Takara, Dalian, China). Briefly, 200 µl whole blood was used for extraction procedure according to manufacturer's instruction. The total viral genomic DNA was eluted with 50 µl DEPC water and stored at -80°C for further PCR and RAA assays in this study.

OIE Recommended PCR

According to OIE Terrestrial Manual 2019 (chapter 3.8.1 African swine fever), the recommanded PCR was performed with some modifications. A 25 µl PCR reaction contains 2×ExTaq 12.5 µl, 10 µM forward and reverse primer 0.5 µl each (OIEPCR-F and OIEPCR-R, **Table 1**), double distilled water 9 µl and DNA template 2.5 µl. The following thermal programs were: one cycle at 95°C for 10 min; 40 cycles at 95°C for 15 s, 62°C for 30 s and 72°C for 30 s; one cycle at 72°C for 7 min. PCR results were analyzed by agarose gel electrophoresis.

Quantitative Real-Time PCR

A commercial ASFV nucleic acid fluorescence PCR detection kit (MingRiDa, Beijing, China), approved by the Ministry of Agriculture and Rural Affairs of the People's Republic of China (010688870), was used for quantitative real-time PCR (qPCR). A 25 µl qPCR reaction contains 20 µl fluorescent PCR reaction mix and 5 µl DNA template. Amplification was performed using an ABI 7500 thermocycler (Life Technologies, USA) with thermal profile as follows: one cycle at 50°C for 2 min, one cycle at 95°C for 3 min, and 40 cycles at 95°C for 10 s and 60°C for 30 s. The fluorescence signal was collected in FAM channel at the end of each cycle. It was determined positive if Ct value was less than 40 with a sigmoid-shaped amplification curve. It was determined negative if Ct value was reported as undetermined with fluorescent signal maintained at background level.

TABLE 1 | Primer and probe sequences used in this study.

Oligo Name	Sequence
OIEPCR-F	5'-AGTTATGGGAAACCCGACCC-3'
OIEPCR-R	5'-CCCTGAATCGGAGCATCCT-3'
RAA-1F	5'-CCCGTTACGTATCCGATCACATTACCTATT-3'
RAA-2F	5'-TCAAAGTTCTGCAGCTCTTACATACCCTTCC-3'
RAA-3F	5'-TTCTGCAGCTCTTACATACCCTTCCACTAC-3'
RAA-4F	5'-TCTTACATACCCTTCCACTACGGAGGCAAT-3'
RAA-1R	5'-GTTAATAGCAGATGCCGATACCACAAGATCAG-3'
RAA-2R	5'-CGATACCACAAGATCAGCCGTAGTGATAGA-3'
RAALFA-F	5'-CCCGTTACGTATCCGATCACATTACCTATT-3'
RAALFA-R	5'-biotin-CGATACCACAAGATCAGCCGTAGTGATAGA-3'
RAALFA-Probe	5'-FITC-CAATGCGATTAAAACCCCCGATGATCCGGGTGCGA[THF]TGATGATTACCTTTGCT-C3-3'

Basic RAA Assay

RAA primers were designed in conserved regions of ASFV Pig/HLJ/2018 strain p72-encoding gene *B646L*. Four candidate forward primers (RAA-1F, RAA-2F, RAA-3F, and RAA-4F) and two candidate reverse primers (RAA-1R and RAA-2R) were screened in pairs for the best primer combination (**Table 1**). Basic RAA assay was performed at 37°C in a water bath for 30 min with basic RAA kit (Zhongce, Hangzhou, China). A 50 µl volume RAA reaction mixture included rehydration buffer (Buffer A) 41.5 µl, 20 µM forward and reverse primer 1 µl each, DNA template 4 µl and 280 mM MgOAc (Buffer B) 2.5 µl. Once RAA was completed, 50 µl DNA extraction regent (phenol:chloroform:isopropanol=25:24:1, v/v/v) was mixed with 50 µl RAA reaction and centrifuged at 10,000 rpm for 15 min. The supernatant that contained RAA amplicon was then analyzed by agarose gel electrophoresis.

RAA Visual Readout With Lateral Flow Assay

RAA visual readout with LFA was performed with RAA nfo kit (Zhongce, Hanhzhou, China) and RAA lateral flow dipstick (Jishi, Zhengzhou, China). Primers and probe used in RAA-LFA (**Table 1**) included a common forward primer (LFA-F), a 5'-biotin-labeled reverse primer (LFA-R) and a FITC-labeled probe (LFA-probe). A 50 µl volume RAA reaction mixture included rehydration buffer (Buffer A) 40.9 µl, 20 µM forward and reverse primer 1 µl each, 10 µM probe 0.6 µl, DNA template 4 µl and 280 mM MgOAc (Buffer B) 2.5 µl. Optimal reaction temperature and time for RAA-LFA were achieved by individually performing RAA reaction at constant temperatures (room temperature, 37 or 41°C) in a water bath for 5, 10, or 15 min. After amplification, 20 µl RAA reaction was then immediately diluted with 80 µl PBST (1 x phosphate buffered saline with 0.1% Tween-20) and added to RAA lateral flow dipstick for visual readout after 10–15 min development at room temperature.

With optimal reaction condition, the sensitivity of RAA-LFA was evaluated. Decimal serial dilutions of pUC57-p72 from 10^8 to 1 copies/µl were assayed by RAA-LFA and compared with OIE recommended PCR and commercial qPCR kit. In addition, the specificity of RAA-LFA were estimated using cell cultures of common porcine diseases, including CSFV, PRRSV, PEDV, PRV, and PCV 2.

The repeatability and stability of RAA-LFA were also evaluated. The experimental materials used for sensitivity and specificity assays were stored under the required conditions. RAA regents, primers, probe, and standard plasmid pUC57-p72 decimal serial dilutions were stored at -20°C. RAA lateral flow dipsticks were stored at room temperature under drying condition. Considering the shelf-life of RAA regents was one year, the repeatability and stability assay of RAA-LFA was

performed at 0, 4, 8, 12 months after sensitivity assay, in testing 10^5 copies/μl (strong positive sample, +++), 10^3 copies/μl (moderate positive sample, ++), 10 copies/μl (weak positive sample, +) of standard plasmid pUC57-p72 and double distilled water (negative sample, -). All tests at each time point were repeated three times and the relative optical density (ROD) values of lateral flow dipstick's test lines were recorded by TSR3000 membrane strip reader (BioDot manufactures, USA). Coefficient of variations (Cv) values of RAA-LFA in testing each sample were individually calculated as the ratio of standard deviation to average value among four experiments at each time point.

Treatment of Blood Sample for Virus Inactivation and Nucleic Acid Release

To achieve both virus inactivation and nucleic acids release purposes, 2-fold serial dilutions of an ASFV positive whole blood sample were prepared with PBS and then heated in boiling water for 5 min. Optimal dilution was determined by basic RAA and compared with OIE recommended PCR. In addition, a total of 17 clinical blood samples were directly assayed with RAA-LFA after dilution and boiling, and compared with results tested with extracted viral DNAs by RAA-LFA.

RESULTS

Optimization of RAA-LFA

The optimal primer combination was determined by agarose gel electrophoresis of basic RAA. As shown in **Figure 4A**, among 8 primer combinations, the best RAA performance was achieved with RAA-1F and RAA-2R. Thus, these two primers were chosen as forward and reverse primers for RAA in this study.

To achieve best RAA-LFA performance, RAA reaction temperatures and times were also investigated. Three groups of RAA reactions in testing 10^5 copies/μl standard plasmid pUC57-p72 were individually incubated at either room temperature, 37°C or 42°C for 5, 10, and 15 min. RAA performances were then analyzed with lateral flow dipstick. As shown in **Figure 4B**, RAA was not efficient at room temperature, resulting in weak positive LFA visual readout. In contrast, RAA showed good performances at both 37 and 42°C with an incubating time of 10 or 15 min. Thus, the RAA-LFA used in this study was optimized as performing RAA reaction at 37°C for 10 min, followed by LFA readout at room temperature for 10–15 min.

Sensitivity and Specificity of RAA-LFA

Though the detection limit of basic RAA alone was 10^3 copies/μl (**Figure 5A**), the detection limit of RAA-LFA reached 10 copies/μl (**Figure 5B**), which is 10 fold more sensitive than both OIE recommended PCR (10^2 copies/μl) (**Figure 5C**) and qPCR with commercial kit (10^2 copies/μl) (**Figure 5D**).

In specificity tests, no positive readout was observed for both basic RAA and RAA-LFA in testing CSFV, PRRSV, PEDV, PRV, and PCV 2 (**Figure 6**), showing good specificity of RAA-LFA established in this study.

Repeatability and Stability of RAA-LFA

In repeatability and stability assay, the intensity of three repeated lateral flow dipstick's test lines in testing strong positive sample,

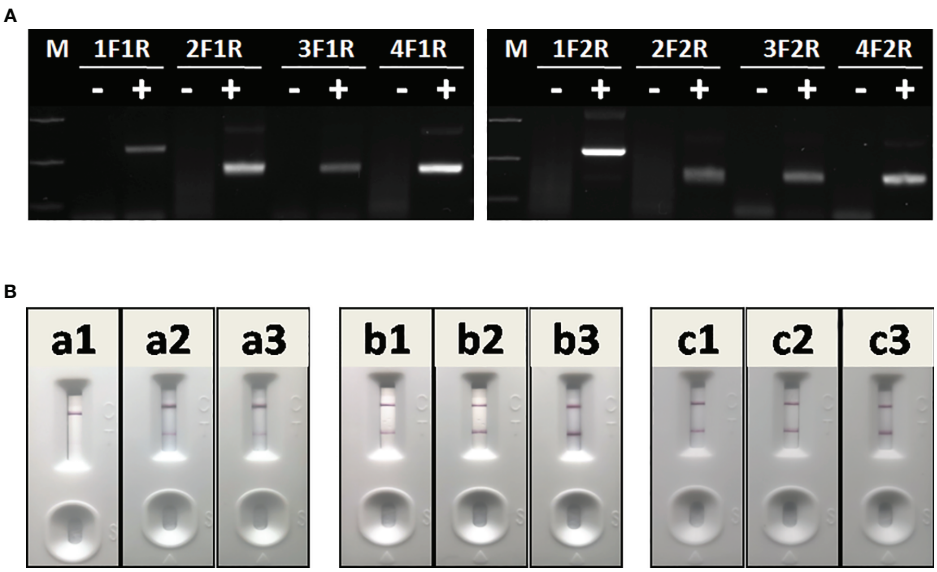

FIGURE 4 | Optimization of RAA-LFA. **(A)** Optimization of primer combination. 1F1R: the combination of RAA-1F and RAA-1R; 2F1R: the combination of RAA-2F and RAA-1R. 3F1R: the combination of RAA-3F and RAA-1R; 4F1R: the combination of RAA-4F and RAA-1R. 1F2R: the combination of RAA-1F and RAA-2R; 2F2R: the combination of RAA-2F and RAA-2R. 3F1R: the combination of RAA-3F and RAA-2R; 4F2R: the combination of RAA-4F and RAA-2R. **(B)** Optimization of amplification temperature and time. a1, a2, a3: RAA was performed at room temperature for 5, 10, 15 min. b1, b2, b3: RAA was performed at 37°C for 5, 10, 15 min. c1, c2, c3: RAA was performed at 42°C for 5, 10, 15 min.

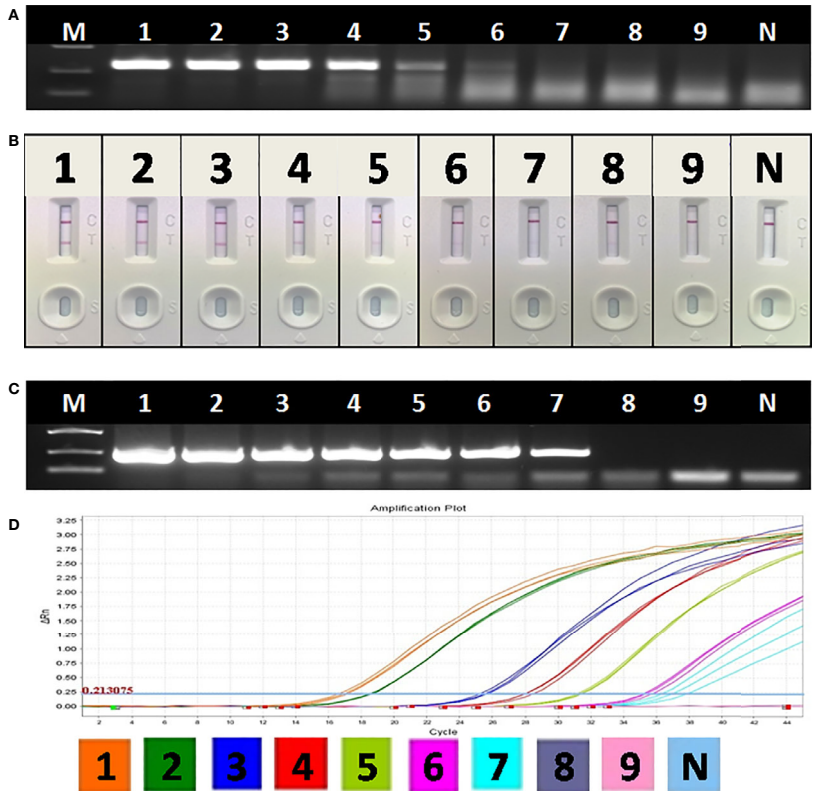

FIGURE 5 | Sensitivity of OIE-recommended PCR, basic RAA and RAA-LFA for plasmid pUC57-p72. **(A)** Agarose gel electrophoresis of basic RAA. M: DL2000 DNA marker; 1–9: Decimal dilutions of plasmid pUC57-p72 from 108–100 copies/μL. N, negative control with double distilled water. **(B)** RAA-LFA visual readout. 1–9: Decimal dilutions of plasmid pUC57-p72 from 108–100 copies/μL. N, negative control with double distilled water. **(C)** Agarose gel electrophoresis of OIE-recommended PCR. M: DL2000 DNA marker; 1–9: Decimal dilutions of plasmid pUC57-p72 from 108–100 copies/μL. N, negative control with double distilled water. **(D)** qPCR amplification plot. 1–9: Decimal dilutions of plasmid pUC57-p72 from 108–100 copies/μL. N, negative control with double distilled water.

FIGURE 6 | Specificity of basic RAA and RAA-LFA for common porcine diseases. **(A)** Agarose gel electrophoresis of basic RAA. M: DL 2000 DNA marker; 1: ASFV; 2: CSFV; 3: PRRSV; 4: PRV; 5: PCV 2; 6: PEDV. **(B)** RAA-LFA visual readout. 1: ASFV; 2: CSFV; 3: PRRSV; 4: PRV; 5: PCV 2; 6: PEDV.

moderate positive sample, weak positive sample, and negative sample at 0, 4, 8, 12 months were analyzed (**Figure 7**). As shown in **Table 2**, except for the Cv value in testing marginal weak positive sample (10.45%), the Cv values of four individual experiments in testing strong positive sample (2.73%), moderate positive sample (4.01%), and negative sample (8.76%) were all less than 10%, indicating good repeatability and stability of RAA-LFA established in this study within one year.

Evaluation of RAA-LFA in Detecting Extracted DNA From Blood Samples

To evaluate the performance of RAA-LFA on detection of clinical samples, nucleic acids extracted from 37 blood samples were firstly tested by basic RAA, RAA-LFA and OIE recommended PCR in parallel. Initial results showed that 20 samples were tested positive and 8 samples were tested negative by all three methods. However, 9 samples were tested positive by both basic RAA and RAA-LFA (**Figures 8B, C**), but tested negative by OIE recommended PCR (**Figure 8A**).

Interestingly, even though extracted nucleic acids from blood samples were purified with commercial kits, some eluted DNA

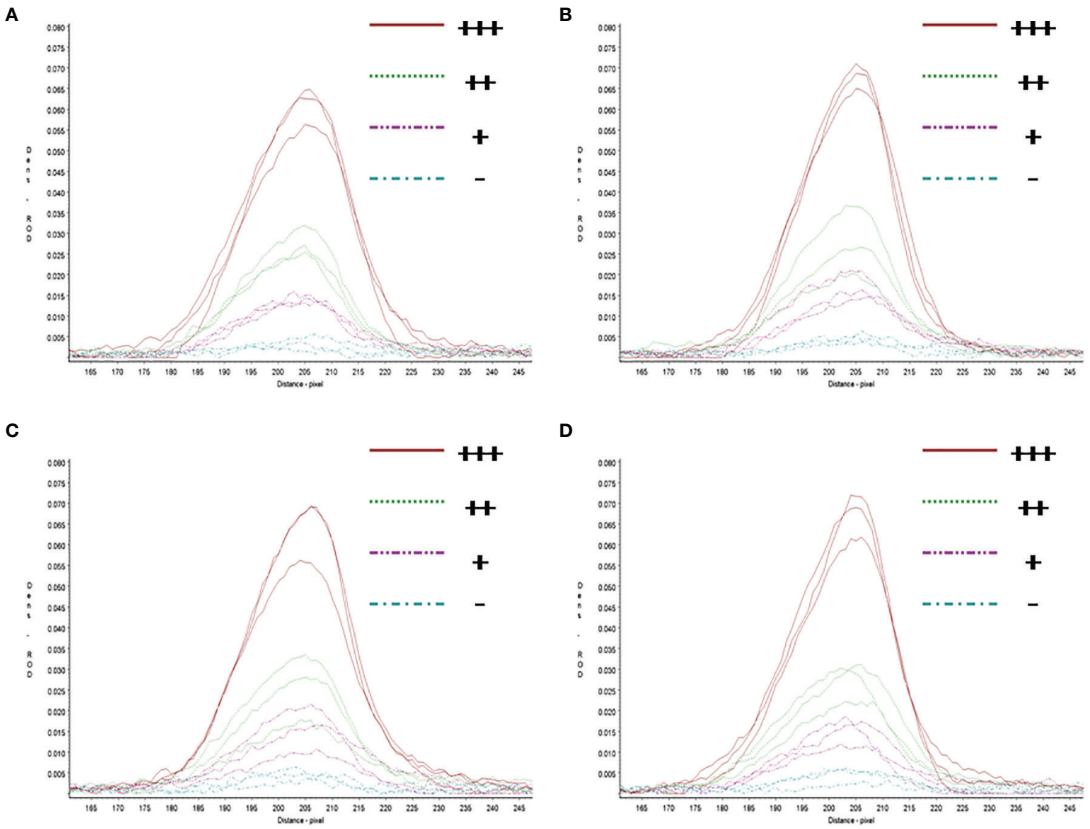

FIGURE 7 | Repeatability and stability of RAA-LFA. **(A)** Screening of lateral flow dipstick's test lines at 0 month after sensitivity and specificity assays with TSR3000 membrane strip reader. +++, strong positive sample, 10^5 copies/μl; ++, moderate positive sample 10^3 copies/μl; +, weak positive sample 10 copies/μl; -, negative sample, double distilled water. **(B)** Screening of lateral flow dipstick's test lines at 4 months after sensitivity and specificity assays with TSR3000 membrane strip reader. +++, strong positive sample, 10^5 copies/μl; ++, moderate positive sample 10^3 copies/μl; +, weak positive sample 10 copies/μl; -, negative sample, double distilled water. **(C)** Screening of lateral flow dipstick's test lines at 8 months after sensitivity and specificity assays with TSR3000 membrane strip reader. +++, strong positive sample, 10^5 copies/μl; ++, moderate positive sample 10^3 copies/μl; +, weak positive sample 10 copies/μl; -, negative sample, double distilled water. **(D)** Screening of lateral flow dipstick's test lines at 12 months after sensitivity and specificity assays with TSR3000 membrane strip reader. +++, strong positive sample, 10^5 copies/μl; ++, moderate positive sample 10^3 copies/μl; +, weak positive sample 10 copies/μL; -, negative sample, double distilled water.

TABLE 2 | Readability and stability assay of RAA-LFA.

Time point (Month) Sample	0	4	8	12	Cv Value
	Average ROD of three repeat tests ± SD				
10^5 copies/μl, +++	106.2016 ± 6.9602	106.8246 ± 3.0436	112.7224 ± 9.8524	109.4778 ± 9.4636	2.73%
10^3 copies/μl, ++	46.4175 ± 4.3735	49.12173 ± 10.1194	48.98073 ± 12.0557	51.2038 ± 8.6220	4.0%
10 copies/μl, +	25.90397 ± 2.3371	31.94877 ± 5.7289	30.20243 ± 8.5297	26.21923 ± 1.7925	10.45%
double distilled water, -	7.657333 ± 1.9936	9.1572 ± 1.2772	8.5984 ± 3.0125	9.357833 ± 3.6918	8.76%

samples might still contain soluble colored contaminants, probably due to inappropriate blood sampling procedure. In this study, all the 9 DNA samples tested with contrary results by RAA and PCR were such cases. To verify whether these 9 DNA samples were tested false positive by RAA, or tested false negative by PCR, a serial dilutions (1/10, 1/20, 1/40, 1/80 and 1/160) of these DNA samples were prepared and tested by PCR again. Results showed that all these 9 samples were tested positive by PCR with various degrees of dilution (**Figure 9**), probably due to a reduced inhibitory effect with decreased concentration of blood contaminants. This indicated that the blood soluble colored contaminants strongly inhibited PCR but show little effect on RAA.

To verify the accuracy of RAA-LFA in testing clinical samples, a commercial ASFV qPCR kit was also used and compared with RAA-LFA and OIE recommended PCR results (**Table 3**). Taken together, RAA-LFA showed 100%

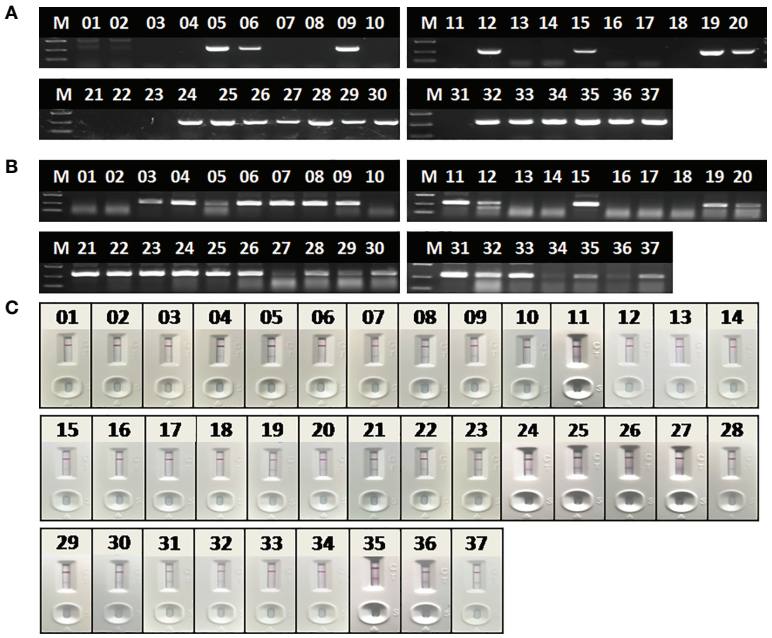

FIGURE 8 | Evaluation of OIE-recommended, basic RAA and RAA-LFA in testing extracted DNA from blood samples. **(A)** Agarose gel electrophoresis of OIE-recommended PCR. M, DL2000 DNA marker; 1–37, blood sample number. **(B)** Agarose gel electrophoresis of basic RAA. M, DL2000 DNA marker; 1–37, blood sample number. **(C)** RAA-LFA visual readout. 1–37, blood sample number.

positive coincident rate and 100% negative coincident rate with both OIE recommended PCR and commercial qPCR (**Table 4**).

Blood Significantly Inhibits PCR, but Slightly Inhibits RAA

To further confirm the inhibitory effect of blood on PCR, as well as to establish a simple and rapid blood sample treatment procedure for RAA, a positive blood sample was diluted with PBS in a two-fold ratio from 1:2 to 1:16. For virus inactivation and nucleic acids release, the effect of boiling on RAA performance was also studied. Agarose gel electrophoresis showed that blood had to be diluted to at least 32–64-fold to remove the inhibitory effect on PCR (**Figure 10A**), while a 2–4-fold dilution of blood can be directly used for RAA (**Figure 10B**). In addition, the RAA performance will be further improved if blood sample was boiled for 5 min with proper dilution (**Figure 10B**), probably because that heating facilitates viral DNA release from virus particles.

Direct Detection of ASFV From Blood Samples With RAA-LFA

Without nucleic acids extraction and purification, a positive whole blood sample and a negative one were directly assayed with RAA-LFA after being diluted with PBS in a ratio of 1:3 and boiled for 5 min. Results showed that blood treated with PBS dilution and boiling was perfectly applicable for RAA isothermal amplification and LFA visual readout (**Figure 10C**). The whole procedure can be completed within 30 min, with minimal requirements for complicated regents and expensive instruments.

Fourteen positive whole blood samples and three negative ones, which had been confirmed in section 3.2 by RAA-LFA, OIE recommended PCR and qPCR, were also direct tested by RAA-LFA after being 1:3 diluted with PBS and boiled for 5 min without viral DNA extraction. Results showed both 100% positive and negative coincident rates with former results (**Figure 11**).

DISCUSSION

In this study, we established the RAA-LFA for ASFV with high sensitivity and good specificity. The detection limit in testing synthesized plasmids reached 10 copies/μl, which is 10-fold more sensitive than OIE recommended PCR and commercial qPCR tested in parallel. In addition, no positive band was observed in testing CSFV, PCV 2, PRRSV, PEDV, and PRV by RAA-LFA. The RAA reaction can be completed at constant 37°C just in a water bath in for 10 min, followed by LFA visual readout at room temperature for 10–15 min, avoiding expensive thermal cycling and fluorescent instruments. Even though an initial evaluation of RAA-LFA and PCR on extracted DNAs from clinical blood samples showed unexpected coincident rate, we confirmed it was due to the false negative results given by PCR with some low-

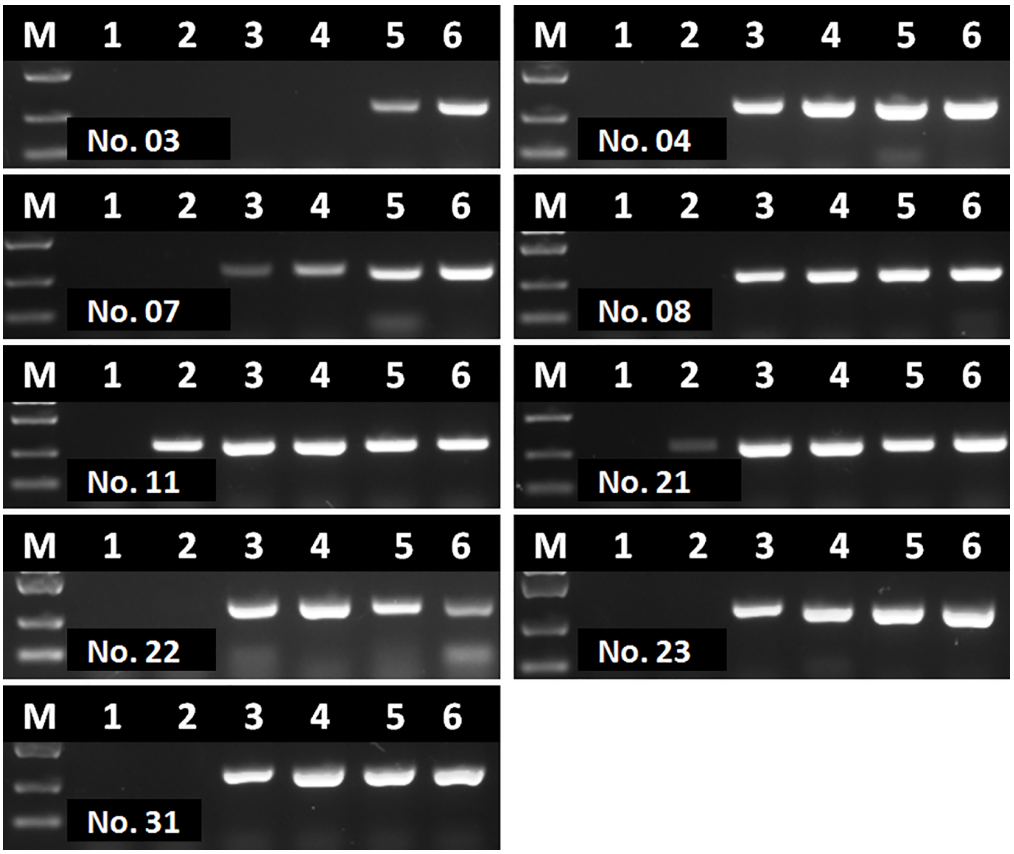

FIGURE 9 | Agarose gel electrophoresis of basic RAA in testing dilutions of blood DNA with poor quality. M, DL2000 DNA maker; 1, initial DNA preparation with no dilution; 2–6, DNA dilutions with double distilled water in a ratio of 1:10, 1:20, 1:40, 1:80, and 1:160. The number of blood sample are indicated in gel electrophoresis picture, which are consistent with **Figure 8**.

TABLE 3 | qPCR results in testing DNA samples extracted from clinical blood.

Sample No.	Ct value ± SD	Sample No.	Ct value ± SD	Sample No.	Ct value ± SD
1	Undetermined	**14**	Undetermined	**27**	28.84 ± 0.22
2	Undetermined	**15**	20.14 ± 0.18	**28**	21.41 ± 0.056
3	20.15 ± 0.02	**16**	Undetermined	**28**	28.03 ± 0.15
4	23.92 ± 0.33	**17**	Undetermined	**30**	24.14 ± 0.26
5	23.90 ± 0.58	**18**	Undetermined	**31**	19.07 ± 0.02
6	21.56 ± 0.14	**19**	21.47 ± 0.90	**32**	25.23 ± 0.06
7	20.43 ± 0.07	**20**	28.47 ± 0.26	**33**	20.11 ± 0.15
8	18.99 ± 0.07	**21**	18.49 ± 0.01	**34**	21.42 ± 0.10
9	25.02 ± 0.03	**22**	24.65 ± 0.01	**35**	18.96 ± 0.05
10	Undetermined	**23**	19.63 ± 0.24	**36**	20.07 ± 0.34
11	19.65 ± 0.11	**24**	22.78 ± 0.02	**37**	19.46 ± 0.10
12	24.46 ± 0.21	**25**	21.59 ± 0.13		
13	Undetermined	**26**	27.10 ± 0.20		

TABLE 4 | Comparison of RAA-LFA with OIE recommended PCR and Commercial ASFV qPCR kit.

RAA-LFA	OIE recommeded PCR		Commercial ASFV qPCR kit	
+	–	+	–	
+	29	0	29	0
–	0	8	0	8

quality DNA preparation cases. A later PCR with serial dilutions of these low-quality DNAs preparation showed all of them were ASFV positive. Many studies have confirmed the presence of PCR-inhibitory substances in blood, such as heme, leukocyte DNA and immunoglobulin G. Single-stranded DNA binding protein gp32, one of the key enzymes involved in RAA reaction, has been shown the ability to reduce the inhibitory effects of hemoglobin and lactoferrin on polymerase activity (Akane et al., 1994; Al-Soud and Rådström, 2001). This may be a potential reason for different performances of RAA and PCR in detecting blood samples.

In combination with either portable devices for fluorescence detection or with lateral flow assay for visual readout, there has been studies using recombinase based isothermal amplification assays for POCT of ASF diagnosis (Miao et al., 2019; Zhai et al., 2020). However, all published RAA/RPA protocols to date start with the extraction of viral genomic DNA with commercial nucleic acids

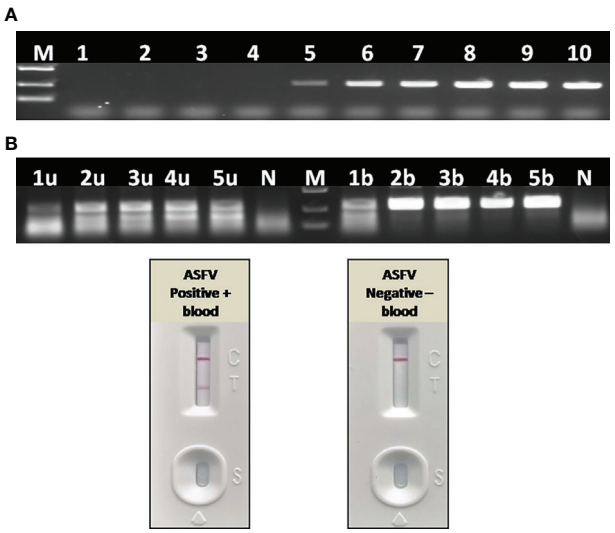

FIGURE 10 | Effect of blood on the performance of PCR and RAA. **(A)** Agarose gel electrophoresis of PCR on blood samples. M, DL2000 DNA marker; 1–10, ASFV positive blood dilutions with double distilled water in a ratio of 1:2, 1:4, 1:8, 1:16, 1:32, 1:64, 1:128, 1:256, 1:512, and 1:1,024. **(B)** Agarose gel electrophoresis of RAA on blood samples. M, DL2000 DNA marker; N, negative control with double distilled water; 1u–5u, ASFV positive blood dilutions with double distilled water in a ratio of 1:2, 1:4, 1:8, 1:16, 1:32, without boiling and directly used for RAA; 1b–5b, ASFV positive blood dilutions with double distilled water in a ratio of 1:2, 1:4, 1:8, 1:16, 1:32, boiling for 5 min and used for RAA. **(C)** LFA-RAA for a positive blood samples and a negative one. Blood samples were diluted with PBS in a ratio of 1:3 and boiled for 5 min, follow by RAA reaction. Correct LFA readout indicate blood treatment used in this study was applicable for RAA isothermal amplification and LFA visual readout.

extraction kit. This is a considerable cost in sample preparation and also needs inconvenient and expensive instruments such as centrifuge and automatic DNA extraction machine. Considering genomic DNA of ASFV is detectable in the quite early infection stage and very stable in blood of infected animals, it is significant and possible to develop a blood sample treatment procedure compatible with RAA-LFA for POCT of ASF diagnosis, avoiding the extraction of viral DNA. In this study, we verified some components in blood samples greatly inhibited PCR performance, but has little effect on RAA. Inhibitory effect can be eliminated when blood was diluted at least 32–64-fold for directly PCR, while only a 2–4-fold dilution of blood was suitable for directly RAA, indicating RAA is a better choice that PCR when blood is used as detecting sample.

In addition, boiling was not only a reliable strategy for virus inactivation, but was also essential for direct RAA with blood. We found an improved performance when diluted blood samples was boiled, probably due to a better viral genomic DNA release from virus particles. With PBS dilution and boiling for 5 min, blood can be directly used for RAA-LFA, with 100% coincident rate with results given by RAA-LFA with extracted DNA.

CONCLUSION

Taken together, we established a sensitive, specific, and rapid POCT protocol of ASF diagnosis, including a blood sample treatment procedure with dilution and boiling, an isothermal amplification with RAA and visual readout with LFA. Besides common advantages shared by other POCT methods, this

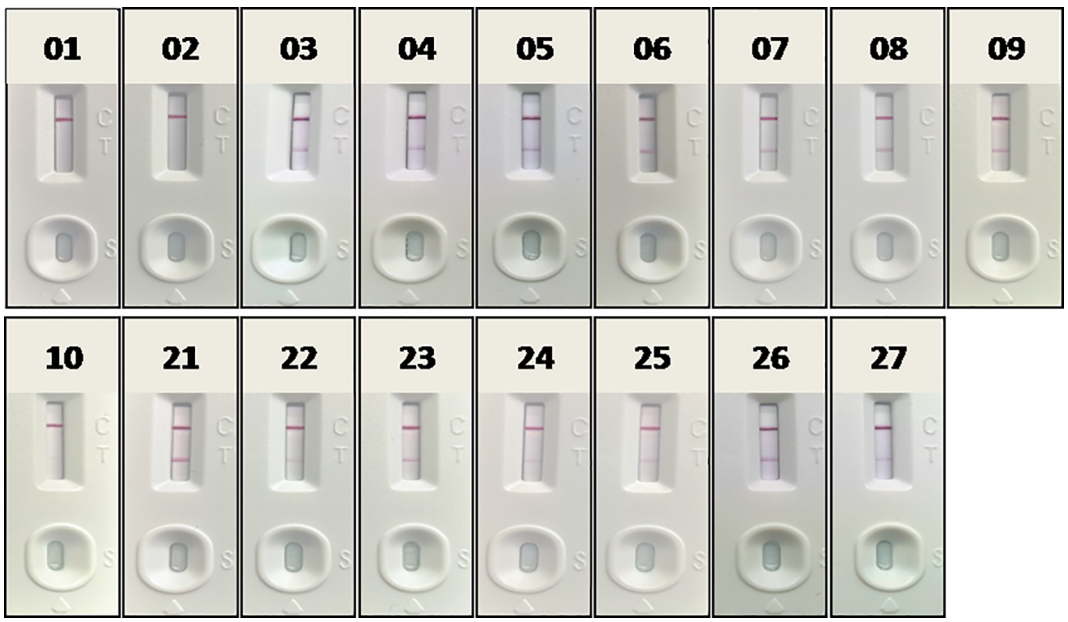

FIGURE 11 | Evaluation RAA-LFA readout for detect testing blood samples without DNA extraction. The number of blood sample are indicated in gel electrophoresis picture, which are consistent with **Figures 8** and **9**.

protocol also meets the demands for on-site virus inactivation and bioptic purposes, providing a good choice for screening and surveillance of ASF in the future.

DATA AVAILABILITY STATEMENT

The original contributions presented in the study are included in the article/supplementary material. Further inquiries can be directed to the corresponding author.

ETHICS STATEMENT

The animal study was reviewed and approved by Henan Academy of Agricultural Sciences (Approval number SYXK 2014-0007).

AUTHOR CONTRIBUTIONS

All authors contributed to the article and approved the submitted version. YZ, JG and GZ designed the research and analyzed the data. JG, GX, RD and GZ provided resources. YZ, QL, DL, LW and XW performed the experiments and wrote the manuscript.

FUNDING

This work was supported by grants from the National Key Research and Development Program of China (2016YFD0500701), the Earmarked Fund for Modern Agro-Industry Technology Research System of China (CARS-35), the Special Fund for Henan Agriculture Research System (S2012-06-02), and the Key Scientific and Technological Research Projects of Henan Province (192102110007).

REFERENCES

Akane, A., Matsubara, K., Nakamura, H., Takahashi, S., and Kimura, K. (1994). Identification of the heme compound copurified with deoxyribonucleic acid (DNA) from bloodstains, a major inhibitor of polymerase chain reaction (PCR) amplification. *J. Forensic Sci.* 39 (2), 362–372. doi: 10.1007/BF01371342

Al-Soud, W. A., and Rådström, P. (2001). Purification and characterization of PCR-inhibitory components in blood cells. *J. Clin. Microbiol.* 39 (2), 485–493. doi: 10.1128/JCM.39.2.485-493.2001

Atuhaire, D. K., Afayoa, M., Ochwo, S., Katiti, D., Mwiine, F. N., Nanteza, A., et al. (2014). Comparative detection of African swine fever virus by loop-mediated isothermal amplification assay and polymerase chain reaction in domestic pigs in uganda. *Afr. J. Microbiol. Res.* 8 (23), 9. doi: 10.5897/AJMR2014.6848

Bastos, A. D., Penrith, M. L., Crucière, C., Edrich, J. L., Hutchings, G., Roger, F., et al. (2003). Genotyping field strains of African swine fever virus by partial p72 gene characterisation. *Arch. Virol.* 148 (4), 693–706. doi: 10.1007/s00705-002-0946-8

Bosch-Camós, L., López, E., and Rodriguez, F. (2020). African swine fever vaccines: a promising work still in progress. *Porcine Health Manag.* 6, 17. doi: 10.1186/s40813-020-00154-2

Brown, V. R., and Bevins, S. N. (2018). A review of African swine fever and the potential for introduction into the United States and the possibility of subsequent establishment in feral swine and native ticks. *Front. Vet. Sci.* 5, 11. doi: 10.3389/fvets.2018.00011

Costard, S., Mur, L., Lubroth, J., Sanchez-Vizcaino, J. M., and Pfeiffer, D. U. (2013). Epidemiology of African swine fever virus. *Virus Res.* 173 (1), 191–197. doi: 10.1016/j.virusres.2012.10.030

Daher, R. K., Stewart, G., Boissinot, M., and Bergeron, M. G. (2016). Recombinase Polymerase Amplification for Diagnostic Applications. *Clin. Chem.* 62 (7), 947–958. doi: 10.1373/clinchem.2015.245829

Dixon, L. K., Chapman, D. A., Netherton, C. L., and Upton, C. (2013). African swine fever virus replication and genomics. *Virus Res.* 173 (1), 3–14. doi: 10.1016/j.virusres.2012.10.020

Fan, X., Li, L., Zhao, Y., Liu, Y., Liu, C., Wang, Q., et al. (2020). Clinical validation of two recombinase-based isothermal amplification assays (RPA/RAA) for the rapid detection of African swine fever virus. *Front. Microbiol.* 11, 1696. doi: 10.3389/fmicb.2020.01696

Frączyk, M., Woźniakowski, G., Kowalczyk, A., Niemczuk, K., and Pejsak, Z. (2016). Development of cross-priming amplification for direct detection of the African swine fever virus, in pig and wild boar blood and sera samples. *Lett. Appl. Microbiol.* 62 (5), 386–391. doi: 10.1111/lam.12569

Fredricks, D. N., and Relman, D. A. (1998). Improved amplification of microbial DNA from blood cultures by removal of the PCR inhibitor sodium polyanetholesulfonate. *J. Clin. Microbiol.* 36 (10), 2810–2816. doi: 10.1128/JCM.36.10.2810-2816.1998

Gallardo, C., Fernández-Pinero, J., and Arias, M. (2019). African swine fever (ASF) diagnosis, an essential tool in the epidemiological investigation. *Virus Res.* 271, 197676. doi: 10.1016/j.virusres.2019.197676

Gao, Y., Meng, X. Y., Zhang, H. W., Luo, Y. Z., Sun, Y., Li, Y. F., et al. (2018). Cross-priming amplification combined with immunochromatographic strip for rapid on-site detection of African swine fever virus. *Sensor Actuators B Chem.* 274, 304–309. doi: 10.1016/j.snb.2018.07.164

James, A., and Macdonald, J. (2015). Recombinase polymerase amplification: Emergence as a critical molecular technology for rapid, low-resource diagnostics. *Expert Rev. Mol. Diagn.* 15 (11), 1475–1489. doi: 10.1586/14737159.2015.1090877

James, H. E., Ebert, K., McGonigle, R., Reid, S. M., Boonham, N., Tomlinson, J. A., et al. (2010). Detection of African swine fever virus by loop-mediated isothermal amplification. *J. Virol. Methods* 164 (1-2), 68–74. doi: 10.1016/j.jviromet.2009.11.034

Klein, A., Barsuk, R., Dagan, S., Nusbaum, O., Shouval, D., and Galun, E. (1997). Comparison of methods for extraction of nucleic acid from hemolytic serum for PCR amplification of hepatitis B virus DNA sequences. *J. Clin. Microbiol.* 35 (7), 1897–1899. doi: 10.1128/JCM.35.7.1897-1899.1997

Lobato, I. M., and O'Sullivan, C. K. (2018). Recombinase polymerase amplification: Basics, applications and recent advances. *Trends Analyt. Chem.* 98, 19–35. doi: 10.1016/j.trac.2017.10.015

Miao, F., Zhang, J., Li, N., Chen, T., Wang, L., Zhang, F., et al. (2019). Rapid and sensitive recombinase polymerase amplification combined with lateral flow strip for detecting African swine fever virus. *Front. Microbiol.* 10, 1004. doi: 10.3389/fmicb.2019.01004

Moore, M. D., and Jaykus, L. A. (2017). Development of a recombinase polymerase amplification assay for detection of epidemic human Noroviruses. *Sci. Rep.* 7, 40244. doi: 10.1038/srep40244

OIE (2019). "African swine fever (Infection with Africa swine fever virus)," in *OIE terrestrial manual 2019. Chapter 3.8.1.* Paris: World organization for animal health.

OIE (2020).ASF. Available at: https://www.oie.int/fileadmin/Home/eng/Animal-Health-in-the-World/docs/pdf/Disease-cards/ASF/Report-47-Global-situation-ASF.pdf (Accessed November 24, 2020).

Penrith, M. L., and Vosloo, W. (2009). Review of African swine fever: transmission, spread and control. *J. S. Afr. Vet. Assoc.* 80 (2), 58–62. doi: 10.4102/jsava.v80i2.172

Plowright, W., and Parker, J. (1967). The stability of African swine fever virus with particular reference to heat and pH inactivation. *Arch. Gesamte Virusforsch.* 21 (3), 383–402. doi: 10.1007/BF01241738

Quembo, C. J., Jori, F., Vosloo, W., and Heath, L. (2018). Genetic characterization of African swine fever virus isolates from soft ticks at the wildlife/domestic interface in Mozambique and identification of a novel genotype. *Transbound Emerg. Dis.* 65 (2), 420–431. doi: 10.1111/tbed.12700

Wang, D., Yu, J., Wang, Y., Zhang, M., Li, P., Liu, M., et al. (2020). Development of a real-time loop-mediated isothermal amplification (LAMP) assay and visual LAMP assay for detection of African swine fever virus (ASFV). *J. Virol. Methods* 276, 113775. doi: 10.1016/j.jviromet.2019.113775

Wang, J., Wang, J., Geng, Y., and Yuan, W. (2017). A recombinase polymerase amplification-based assay for rapid detection of African swine fever virus. *Can. J. Vet. Res.* 81 (4), 308–312.

Wang, X., Ji, P., Fan, H., Dang, L., Wan, W., Liu, S., et al. (2020). CRISPR/Cas12a technology combined with immunochromatographic strips for portable detection of African swine fever virus. *Commun. Biol.* 3 (1), 62. doi: 10.1038/s42003-020-0796-5

Woźniakowski, G., Frączyk, M., Kowalczyk, A., Pomorska-Mól, M., Niemczuk, K., and Pejsak, Z. (2017). Polymerase cross-linking spiral reaction (PCLSR) for detection of African swine fever virus (ASFV) in pigs and wild boars. *Sci. Rep.* 7, 42903. doi: 10.1038/srep42903

Zhai, Y., Ma, P., Fu, X., Zhang, L., Cui, P., Li, H., et al. (2020). A recombinase polymerase amplification combined with lateral flow dipstick for rapid and specific detection of African swine fever virus. *J. Virol. Methods* 285, 113885. doi: 10.1016/j.jviromet.2020.113885

Zhang, Y., Isaacman, D. J., Wadowsky, R. M., Rydquist-White, J., Post, J. C., and Ehrlich, G. D. (1995). Detection of Streptococcus pneumoniae in whole blood by PCR. *J. Clin. Microbiol.* 33 (3), 596–601. doi: 10.1128/JCM.33.3.596-601.1995

Zhou, X., Li, N., Luo, Y., Liu, Y., Miao, F., Chen, T., et al. (2018). Emergence of African swine fever in China 2018. *Transbound Emerg. Dis.* 65, 1482–1484. doi: 10.1111/tbed.12989

Conflict of Interest: The authors declare that the research was conducted in the absence of any commercial or financial relationships that could be construed as a potential conflict of interest.

frontiers in Cellular and Infection Microbiology

ORIGINAL RESEARCH
published: 14 July 2021
doi: 10.3389/fcimb.2021.581239

Rapid and Visual Detection of SARS-CoV-2 Using Multiplex Reverse Transcription Loop-Mediated Isothermal Amplification Linked With Gold Nanoparticle-Based Lateral Flow Biosensor

Xu Chen[1,2,3†], Qingxue Zhou[4†], Shijun Li[3], Hao Yan[5], Bingcheng Chang[1,2], Yuexia Wang[6] and Shilei Dong[7*]*

[1] The Second Clinical College, Guizhou University of Traditional Chinese Medicine, Guiyang, China, [2] Central Laboratory of the Second Affiliated Hospital, Guizhou University of Traditional Chinese Medicine, Guiyang, China, [3] Laboratory of Bacterial Infectious Disease of Experimental Centre, Guizhou Provincial Centre for Disease Control and Prevention, Guiyang, China, [4] Clinical Laboratory, Hangzhou Women's Hospital, Hangzhou, China, [5] Department of Microbiology, Zhejiang Provincial Center for Disease Control and Prevention, Hangzhou, China, [6] TCM Research Institute, Zhejiang Chinese Medical University, Hangzhou, China, [7] Department of Clinical Laboratory, Zhejiang Hospital, Hangzhou, China

OPEN ACCESS

Edited by:
Nahed Ismail,
University of Illinois at Chicago,
United States

Reviewed by:
Guillaume Tresset,
Université Paris-Saclay, France
Nathan A. Tanner,
New England Biolabs, United States

***Correspondence:**
Xu Chen
xuchen1220@126.com
Shilei Dong
dsl166@126.com

†These authors have contributed equally to this work

Specialty section:
This article was submitted to Clinical Microbiology, a section of the journal Frontiers in Cellular and Infection Microbiology

Received: 08 July 2020
Accepted: 29 June 2021
Published: 14 July 2021

Citation:
Chen X, Zhou Q, Li S, Yan H, Chang B, Wang Y and Dong S (2021) Rapid and Visual Detection of SARS-CoV-2 Using Multiplex Reverse Transcription Loop-Mediated Isothermal Amplification Linked With Gold Nanoparticle-Based Lateral Flow Biosensor. Front. Cell. Infect. Microbiol. 11:581239. doi: 10.3389/fcimb.2021.581239

Background: Severe acute respiratory syndrome coronavirus 2 (SARS-CoV-2) is a novel coronavirus that has caused the outbreak of coronavirus disease 2019 (COVID-19) all over the world. In the absence of appropriate antiviral drugs or vaccines, developing a simple, rapid, and reliable assay for SARS-CoV-2 is necessary for the prevention and control of the COVID-19 transmission.

Methods: A novel molecular diagnosis technique, named multiplex reverse transcription loop-mediated isothermal amplification, that has been linked to a nanoparticle-based lateral flow biosensor (mRT-LAMP-LFB) was applied to detect SARS-CoV-2 based on the SARS-CoV-2 *RdRp* and *N* genes, and the mRT-LAMP products were analyzed using nanoparticle-based lateral flow biosensor. The mRT-LAMP-LFB amplification conditions, including the target RNA concentration, amplification temperature, and time were optimized. The sensitivity and specificity of the mRT-LAMP-LFB method were tested in the current study, and the mRT-LAMP-LFB assay was applied to detect the SARS-CoV-2 virus from clinical samples and artificial sputum samples.

Results: The SARS-CoV-2 specific primers based on the *RdRp* and *N* genes were valid for the establishment of mRT-LAMP-LFB assay to detect the SARS-CoV-2 virus. The multiple-RT-LAMP amplification condition was optimized at 63°C for 30 min. The full process, including reaction preparation, viral RNA extraction, RT-LAMP, and product identification, could be achieved in 80 min. The limit of detection (LoD) of the mRT-LAMP-LFB technology was 20 copies per reaction. The specificity of mRT-LAMP-LFB detection was 100%, and no cross-reactions to other respiratory pathogens were observed.

Conclusion: The mRT-LAMP-LFB technique developed in the current study is a simple, rapid, and reliable method with great specificity and sensitivity when it comes to identifying SARS-CoV-2 virus for prevention and control of the COVID-19 disease, especially in resource-constrained regions of the world.

Keywords: lateral flow biosensor, reverse transcription-loop-mediated isothermal amplification, limit of detection, COVID-19, SARS-CoV-2

INTRODUCTION

Severe acute respiratory syndrome coronavirus 2 (SARS-CoV-2), a non-segmented positive-sense RNA genome virus, is a novel coronavirus that causes the outbreak of respiratory disease (COVID-19) all over the world (Bao et al., 2020; Zhang, 2020). In the 21st century, two important coronaviruses, severe acute respiratory syndrome coronavirus (SARS-CoV) and Middle East respiratory syndrome coronavirus (MERS-CoV), have severely threatened public health (in 2003 and 2012, respectively) (Chen, 2020; Wang et al., 2020). Since December 2019, the novel SARS-CoV-2 coronavirus has been found in many countries around the world and was declared as a disease of "public health emergency of international concern" by the World Health Organization (WHO) (Rothe et al., 2020). Most patients infected with SARS-CoV-2, present with acute onset of fever, cough, dyspnea, and radiological evidence of ground-glass lung opacities compatible with atypical pneumonia (Tu et al., 2020). Not only that, asymptomatic or mildly symptomatic cases have also been reported (Coronaviridae Study Group of the International Committee on Taxonomy of Viruses, 2020; Jiang et al., 2020). Owning to the current disease situation, the SARS-CoV-2 virus has been becoming the third coronavirus posing significant threats to public health worldwide. In the absence of appropriate antiviral drugs or vaccines, developing a reliable, simple, and rapid assay for SARS-CoV-2 is necessary for the prevention and control of the COVID-19 transmission.

The size of SARS-CoV-2 genome is ~30 kilobases and encodes ~9860 amino acids, which has been classified as a beta coronavirus (Ji, 2020; Younes et al., 2020). The genome of SARS-CoV-2 is arranged in the order of 5'-untranslated region (UTR), replicase complex (*ORF1a/b*), spike gene (*S* gene), *E* gene, *M* gene, *N* gene, 3' UTR, and several unidentified non-structural open reading frames (van Kasteren et al., 2020; Younes et al., 2020). Since the outbreak of COVID-19, real-time reverse transcription-polymerase chain reaction (RT-PCR) is the most robust and widely used technology for the detection of SARS-CoV-2 in hospitals and other medical institutions (Corman et al., 2020; Tahamtan and Ardebili, 2020; Zhen et al., 2020). However, RT-PCR assays require special experimental instruments, are time-consuming, and require skilled personnel, which may not be readily available in many resource-poor settings. Therefore, a cost-effective, simple, reliable, rapid, sensitive, and specific assay for the identification of SARS-CoV-2 is urgently developed to improve the detection capability and prevent the spread of COVID-19.

To overcome the drawbacks of RT-PCR detection, a wide variety of isothermal amplification-based methods have been developed for use in molecular identification (Wang et al., 2015; Wang et al., 2017). Loop-mediated isothermal amplification (LAMP), as a reliable, sensitive, and rapid assay with low equipment cost, has been widely applied to detect many pathogens, including SARS-CoV, MERS-CoV, and influenza virus (Huang et al., 2018; Kim et al., 2019; Ravina et al., 2020). LAMP products have been analyzed by various methods, including visual inspection of color changes, turbidimetry changes, and fluorescence dye (Notomi et al., 2000; Wang et al., 2019; Lu et al., 2020). However, these detection techniques require special apparatus and reagents. To overcome this defect, a target-specific, visual and simple nanoparticle-based lateral flow biosensor (LFB) detection method was successfully designed and applied to analyze mRT-LAMP products (Jiao et al., 2019; Li et al., 2019; Wang et al., 2019). In this study, a multiplex reverse transcription LAMP technique linked to an LFB detector (mRT-LAMP-LFB) was developed for the simple, specific, reliable, sensitive, and visual identification of SARS-CoV-2 by targeting the RNA-dependent RNA polymerase gene (*RdRp* gene) and nucleocapsid protein gene (*N* gene) (Chen et al., 2020; Huang et al., 2020). The optimal amplification conditions and feasibility of the mRT-LAMP-LFB assay were confirmed with SARS-CoV-2 pseudo-virus, clinical samples, and artificial sputum samples.

Abbreviations: SARS-CoV-2, severe acute respiratory syndrome coronavirus 2; SARS-CoV, severe acute respiratory syndrome coronavirus; MERS-CoV, Middle East respiratory syndrome coronavirus; RT-PCR, real-time reverse transcription-polymerase chain reaction; LAMP, loop-mediated isothermal amplification; LFB, nanoparticle-based lateral flow biosensor; LoD, limit of detection; WHO, World Health Organization; NCBI, National Centre for Biotechnology Information; MG, malachite green; 2nd GZUTCM, Second Affiliated Hospital, Guizhou University of Traditional Chinese Medicine; ZJH, Zhejiang Hospital; GZCDC, Guizhou Provincial Center for Disease Control and Prevention; ZJCDC, Zhejiang Provincial Center for Disease Control and Prevention; 1st ZJUSM, The First Affiliated Hospital, Zhejiang University School of Medicine; Dig, digoxigenin; FAM, 6-carboxy-fluorescein; nt, nucleotide; mer, monomeric unit; TL1, test line 1; TL2, test line 2; CL, control line; NC, negative control; BC, blank control; DW, distilled water; POCT, Point-of-Care testing.

MATERIALS AND METHODS

Materials Instruments

Viral RNA extraction kits (QIAamp Viral RNA minikits; Qiagen, Hilden, Germany) (Cat NO. 52906) were purchased from Qiagen (Beijing, China). Universal isothermal amplification kits, AMV Reverse Transcriptase, colorimetric indicator (malachite green, MG), and biotin-14-dCTP were obtained from Bei-Jing HaiTaiZhengYuan. Co., Ltd. (Beijing, China). The LFB

materials, including the backing card, sample pad, absorbent pad, conjugate pad, and nitrocellulose membrane (NC), were purchased from Jie-Yi Biotechnology. Co., Ltd. (Shanghai, China). Anti-FAM (rabbit anti-fluorescein antibody) and biotin-BSA (biotinylated bovine serum albumin) were purchased from Abcam. Co., Ltd. (Shanghai, China). Dye (Crimson red) streptavidin-coated polymer nanoparticles (129 nm, 10 mg ml^{-1}; 100 mM borate, pH 8.5, with 0.1% BSA, 0.05% Tween 20 and 10 mM EDTA) were purchased from Bangs Laboratories, Inc. (Indiana, USA).

Design of RT-LAMP Primers

Based on the reaction mechanism of LAMP, two sets of specific primers were designed according to the target genes *RdRp* and *N* (GenBank Accession No. NC_045512.2), respectively. The primers were designed with Primer Explorer V5 (http://primerexplorer.jp/e/; Eiken Chemical Co., Ltd., Tokyo, Japan) online primer design software and checked with the basic local alignment search tool (BLAST). The primer positions are shown in **Figure 1**, and the *RdRp* and *N* genes sequence alignment among seven human coronaviruses (SARS-CoV-2, SARS-CoV, MERS-CoV, HCoV-HKU-1, HCoV-NL63, HCoV-OC43, and HCoV-229E) are shown in **Supplementary Figure 1**. The primer sequences and modifications are shown in **Table 1**. All of the primers were synthesized by TsingKe Biotech Co., Ltd. (Beijing, China) with HPLC purification grade.

SARS-CoV-2 RNA Standard and Artificial SARS-CoV-2 Virus Preparation

The SARS-CoV-2 RNA standard material was obtained from the Chinese Academy of Metrology (Code NO. GBW (E) 091089). The RNA transcripts contained *ORF1ab* gene segment (13201-15600), complete *E* gene, and *N* gene (GenBank NO. NC_045512), and the concentration of RNA was measured by absolute quantitative digital PCR.

FIGURE 1 | Sequence and location of the *RdRp* **(A)** and *N* **(B)** genes used to design SARS-CoV-2 mRT-LAMP primers. The nucleotide sequence of the sense strand of the *RdRp* and *N* is shown in the diagram. Right arrows and left arrows indicate sense and complementary sequences which were used in the current study, respectively.

TABLE 1 | The primers used in the present study.

Primer name	Sequence and modifications	Length	Gene
F3	5′-CACCTTATGGGTTGGGAT-3′	18 nt	*RdRp*
B3	5′-AACATATAGTGAACCGCCA-3′	19 nt	
FIP	5′-GCAAGAACAAGTGAGGCCATA-ATCCTAAATGTGATAGAGCCA-3′	42 mer	
BIP	5′-ACATACAACGTGTTGTAGCTTGTC-CACATGACCATTTCACTCAA-3′	44 nt	
FIP*	5′-FAM-GCAAGAACAAGTGAGGCCATA-ATCCTAAATGTGATAGAGCCA-3′	42 mer	
LF	5′-ATTCTAAGCATGTTAGGCA-3′	19 nt	
LB	5′-ATTAGCTAATGAGTGTGCTCAAGT-3′	24 nt	
LF*	5′-Biotin-ATTCTAAGCATGTTAGGCA-3′	19 nt	
F3	5′-TGGCTACTACCGAAGAGCT-3′	19 nt	*N*
B3	5′-TGCAGCATTGTTAGCAGGAT-3′	20 nt	
FIP	5′-TCTGGCCCAGTTCCTAGGTAGT-CCAGACGAATTCGTGGTGG-3′	41 nt	
BIP	5′-AGACGGCATCATATGGGTTGCA-CGGGTGCCAATGTGATCT-3′	40 nt	
FIP*	5′-Dig-TCTGGCCCAGTTCCTAGGTAGT-CCAGACGAATTCGTGGTGG-3′	41 nt	
LF	5′-AAATACCATCTTGGACTGAGATC-3′	23 nt	
LB	5′-AGGGAGCCTTGAATACACCAA-3′	21 nt	
LF*	5′-Biotin-AAATACCATCTTGGACTGAGATC-3′	23 nt	

RdRp-FIP, 5′-labeled with FAM when used in LAMP-LFB assay; RdRp-LF*, 5′-labeled with biotin when used in LAMP-LFB assay; N-FIP*, 5′-labeled with Dig when used in the LAMP-LFB assay; N-LF*, 5′-labeled with biotin when used in the LAMP-LFB assay. FAM, 6-carboxy-fluorescein; Dig, digoxigenin; nt, nucleotide; mer, monomeric unit.*

The pseudo-virus for the positive quality control agent was obtained from TsingKe Biotech Co., Ltd. (Beijing, China) (Cat NO. TSV2614), which was made with 293T cell cultures and included segments of the ORF1a/b gene (genome coordinates: 13237-13737, 15231-15729), M Gene (genome coordinates: 26523-27191), E Gene (genome coordinates: 26245-26472), and N Gene (genome coordinates: 28274-29533). The pseudo-virus of SARS-CoV and MERS-CoV were obtained from TsingKe Biotech Co., Ltd. (Cat NO. TSV2589; Cat NO.TSV2575).

RNA Template Preparation

In the current study, the viral RNA comes from both pseudo-virus (TsingKe Biotech Co., Ltd) and clinical samples were obtained using Viral RNA Extraction Kits (Qiagen, Hilden, Germany) in accordance with the manufacturer's instructions. The RNA templates were stored at -80°C before use. The concentration was assayed using quantitative PCR with RNA standard. Then, 10-fold serial dilutions of the pseudo-viruses ranging from 1×10^4copies/μl to 1 copy/μl were prepared.

Gold Nanoparticle-Based Lateral Flow Biosensor Preparation

The LFB platform was prepared according to a previous report (Cheng et al., 2019). Briefly, the LFB contained four components: an absorbent pad, NC membrane, sample pad, and conjugate pad (Jie-Yi Biotechnology. Co., Ltd.). The components were assembled orderly on a backing card. The capture reagents, including anti-FAM, anti-Dig, and biotin-BSA (Abcam. Co., Ltd.), were immobilized by physical adsorption on the reaction regions. Then, anti-FAM was immobilized at test line 1 (TL1) (*RdRp*), and anti-Dig was immobilized at test line 2 (TL2) (*N*), while biotin-BSA was immobilized at the control line (CL); each line was separated by 5 mm. SA-PNPs (dye streptavidin-coated polymer nanoparticles) were gathered on the conjugate pad. The prepared biosensors were preserved in a plastic box with a desiccant gel at room temperature before use.

The Standard RT-LAMP Reaction

The single RT-LAMP reactions for *RdRp* or *N* were performed in 25 μl reaction systems as previously described. Briefly, 0.4 μM of each outer primer (F3 and B3), 0.8 μM of each loop primer (LF* and LB), 1.6 μM of each inner primer (FIP* and BIP), 0.4 mM of biotin-14-dCTP, 1 μl (8 U) of *Bst* DNA polymerase (New England Biolabs, USA), 1 μl (10 U) of AMV Reverse Transcriptase (New England Biolabs, USA), 12.5 μl of 2 × reaction buffer [40 mM Tris-HCl (pH 8.8), 40 mM of KCl, 16 mM of $MgSO_4$, 20 mM of $(NH_4)_2SO_4$, 2 M of betaine, and 0.2% Tween-20] (HuiDeXin Bio-technique, Tianjin, China), and 1×10^4 copies of the RNA template were added to a tube. The mixtures were incubated at 63°C for 1 h. Viral RNA from SARS-CoV (pseudo-virus), MERS-CoV (pseudo-virus), and double distilled water (DW) were used as negative controls (NCs). The mRT-LAMP reaction was performed in a one-step reaction in a 25 μl reaction system containing 12.5 μl of 2 × reaction buffer; 0.2 μM each outer primer, *RdRp*-F3, *RdRp*-B3, *N*-F3, and *N*-B3; 0.4 μM each loop primer, *RdRp*-LF*, *RdRp*-LB, *N*-LF* and *N*-LB; 0.8 μM each inner primer, *RdRp*-FIP*, *RdRp*-BIP, *N*-FIP* and *N*-BIP; 0.4 mM biotin-14-dCTP; 1 μl (8 U) of *Bst* DNA polymerase (New England Biolabs, USA); 1 μl (8 U) of AMV Reverse Transcriptase (New England Biolabs, USA); and 1×10^4 copies of RNA template. The reaction conditions were carried out as described above.

RT-LAMP Products Detection

The monitoring techniques, including 2% agarose gel electrophoresis, visual detection reagents MG (VDR, Haitai-Zhengyuan biotech, Co. Ltd. Beijing, China), and lateral flow biosensor (LFB) methods, were applied for the determination and verification of the *RdRp*-RT-LAMP, *N*-RT-LAMP, and mRT-LAMP products. For the products amplified effectively, the agarose gel presented ladder-like bands, and the color changed from colorless to light green in the MG assay. However, there have no bands in gel electrophoresis, and the

color remains colorless in negative and blank controls. The strategy of visualization of RT-LAMP products with LFB was as previously described (Gong et al., 2019).

Temperature Optimization of the RT-LAMP Assays

To confirm the optimal amplification temperature for *RdRp*-RT-LAMP and *N*-RT-LAMP, the pseudo-virus of SARS-CoV-2-*RdRp-N* was used as a positive control at a concentration of 1×10^4 copies per reaction, and the RT-LAMP amplifications were monitored by a real-time turbidity technique. Reaction temperatures ranging from 60 to 67°C with 1°C intervals were tested. The curves of DNA concentrations of each amplified product were exhibited in the graph. Turbidity > 0.1 was considered as positive. Three replicates were tested for each temperature.

Optimization of the Amplification Time for the mRT-LAMP-LFB Assay

To optimize the reaction time of mRT-LAMP-LFB, four amplification times (20, 30, 40, and 50 min) were evaluated. The mRT-LAMP-LFB reactions were carried out as described above, and the results were tested by LFB. Each reaction time was tested at least three times.

Analytical Sensitivity of mRT-LAMP-LFB Assays

The sensitivity of each RT-LAMP-LFB reaction (*RdRp*-RT-LAMP-LFB, *N*-RT-LAMP-LFB, and mRT-LAMP-LFB) was determined using pseudo-virus of SARS-CoV-2 with ten-fold serial dilutions range from 1×10^4 copies to 1 copy. The RT-LAMP reactions were carried out as described above, and the results were tested using visual detection reagents (MG) and LFB. The limit of detection (LoD) of single and multiplex reactions was verified as the last dilution of each positive test. The LoD of RT-PCR technology using Applied Biosystems™ 7500 Real-Time PCR System (Life Technologies, Singapore) with Novel Coronavirus Nucleic Acid Diagnostic Real-Time RT-PCR Kit (Sansure biotech Inc, China) was also tested in the current study. Three replicates were tested for each dilution.

Specificity Analysis of mRT-LAMP-LFB Detection

To evaluate the specificity of the mRT-LAMP-LFB assay, pseudo-viruses of SARS-CoV-2, SARS-CoV-2 positive clinical samples, and other pathogens (**Table 2**) were used for mRT-LAMP detection, and all of the results were tested using the LFB method. All examinations were confirmed at least three times.

Application of the mRT-LAMP-LFB Method to Analyze the Clinical Samples and Artificial Sputum Samples

To verify the applicability of the mRT-LAMP-LFB assay for detecting SARS-CoV-2, one hundred and ten clinical nasopharyngeal swab specimens were collected from suspected SARS-CoV-2 infected patients, and sixty artificial sputum samples (randomly added 100 copies of SARS-CoV-2 pseudo-viruses in each 200 μl artificial sputum sample) were used in the current study. The artificial sputum samples were pretreated with N-acetyl-L-cysteine-2% NaOH. The initial process of all specimens was handled in a validated biological safety cabinet, and performed by staff trained with appropriate personal protective equipment. The clinical samples and artificial sputum samples were detected for SARS-CoV-2 using RT-PCR and mRT-LAMP-LFB methods. The mRT-LAMP detection was as described above. The Novel Coronavirus Nucleic Acid Diagnostic Real-Time RT-PCR Kit (Sansure biotech Inc, China) was used as the reference standard, which was recommended by the Chinese Center for Disease Control and Prevention. The RT-PCR detection was performed with Applied Biosystems™ 7500 Real-Time PCR System (Life Technologies, Singapore). A threshold cycle (Ct value) < 38 was determined to indicate a positive result. The mRT-LAMP-LFB and RT-PCR assays were performed simultaneously in a biosafety level 2 laboratory, as detailed in the WHO Laboratory biosafety manual, third edition. The mRT-LAMP-LFB detection was performed as described above.

RESULTS

COVID-19 is a newly emerging, life-threatening respiratory disease caused by a novel coronavirus SARS-CoV-2, and it has had a significant impact on public health and the economy worldwide (Bao et al., 2020; She et al., 2020). The purpose of the current study is to develop a reliable, rapid, sensitive, and easy-to-use assay for SARS-CoV-2.

Verification and Analysis of RT-LAMP Products

To confirm the amplification with the two sets of LAMP primers, the *RdRp*-, *N*-, or mRT-LAMP mixtures were incubated at a constant temperature of 65°C for 1 h. Then, the *RdRp*-, *N*-, and mRT-LAMP products were analyzed with 2% agarose gel electrophoresis, colorimetric indicator (MG), and lateral flow biosensor (LFB), respectively. The ladder-liker bands of agarose gel were observed in the positive amplification, but not in the negative controls (**Figures 2A, D, G**). The color of the positive results in the *RdRp*-, *N*-, and mRT-LAMP reactions changed from colorlessness to bright green, while the negative reactions remained colorless (**Figures 2B, E, H**). LFB was used for further confirmation of *RdRp*-, *N*-, and mRT-LAMP. For *RdRp*-RT-LAMP detection, two crimson red bands (CL and TL1) appeared, indicating positive results, CL and TL2 were visible for *N*-RT-LAMP, indicating successful amplification, while the negative controls only appeared as a crimson red line (CL) in the biosensor (**Figures 2C, F, I**). Therefore, the results suggested that the two sets of RT-LAMP primers for *RdRp* and *N* detection were valid for the development of the mRT-LAMP assay.

Optimal Reaction Temperature for *RdRp*-RT-LAMP and *N*-RT-LAMP Amplification

The reaction temperature is crucial for RT-LAMP amplification. In this study, the reaction temperature of *RdRp*- and *N*-LAMP

TABLE 2 | Pathogens used in the current study.

No.	Pathogen species	Pathogen name	Source of pathogens[a]	No. of strains	RT-LAMP-LFB result[b]	
					RdRp	*N*
	Coronavirus					
1	SARS-CoV-2 (pseudo-virus)	2019-nCoV-ab II EMN	TsingKe Biotech Co., Ltd. (Beijing, China)	1	P	P
2	SARS-CoV-2 (nucleic acid samples)	ZJCDC-2019-nCoV-52; -85;-86;-90-120;-123; -134;-152;-189;-190; ZJ-2019-nCoV-304;-305	ZJCDC and 1st ZJUSM	12	P	P
3	SARS-CoV (pseudo-virus)	SARS-ORF1a-N	TsingKe Biotech Co., Ltd. (Beijing, China)	1	N	N
4	MERS-CoV (pseudo-virus)	MERS-abEN	TsingKe Biotech Co., Ltd. (Beijing, China)	1	N	N
5	Human coronavirus HKU1	Quality control sample	DAAN Gene Co., Ltd. (Guangzhou, China)	1	N	N
6	Human coronavirus HCoV-NL63	Quality control sample	DAAN Gene Co., Ltd. (Guangzhou, China)	1	N	N
7	Human coronavirus OC43	Quality control sample	DAAN Gene Co., Ltd. (Guangzhou, China)	1	N	N
8	Human coronavirus 229E	Quality control sample	DAAN Gene Co., Ltd. (Guangzhou, China)	1	N	N
	Other pathogens					
9	H1N1	ZJH-H1N1-57	Zhejiang Hospital	1	N	N
10	H3N2 (nucleic acid sample)	GZCDC-H3N2-14	GZCDC	1	N	N
11	H5N1 (nucleic acid sample)	GZCDC-11-H5N1	GZCDC	1	N	N
12	H7N9 (nucleic acid sample)	GZCDC-5-H7N9	GZCDC	1	N	N
13	Influenza B	ZJH Influenza B-115	Zhejiang Hospital	1	N	N
14	Respiratory syncytial virus type A	Quality control sample	DAAN Gene Co., Ltd. (Guangzhou, China)	1	N	N
15	Respiratory syncytial virus type B	Quality control sample	DAAN Gene Co., Ltd. (Guangzhou, China)	1	N	N
16	Human rhinovirus	Quality control sample	DAAN Gene Co., Ltd. (Guangzhou, China)	1	N	N
17	Adenoviruses	Quality control sample	DAAN Gene Co., Ltd. (Guangzhou, China)	1	N	N
18	*Mycoplasma pneumoniae*	ZJH-MP-594	Zhejiang Hospital	1	N	N
19	*Mycobacterium tuberculosis*	GZCDC-MTB-564	GZCDC	1	N	N
20	*Pseudomonas aeruginosa*	ATCC 27853	ATCC	1	N	N
21	*Klebsiella pneumonia*	ZJH-KP-104	Zhejiang Hospital	1	N	N
22	*Streptococcus pneumoniae*	ZJH-SP-016	Zhejiang Hospital	1	N	N
23	*Mycoplasma pneumonia* M129/FH	2nd GZUTCM-MP-102	2nd GZUTCM	1	N	N
24	*Haemophilus influenza*	ATCC49247	ATCC	1	N	N
25	*Streptococcus pyogenes*	ZJH-SP-1087	Zhejiang Hospital	1	N	N
26	*Acinetobacter baumannii*	ZJH-AB-984	Zhejiang Hospital	1	N	N
27	*Staphylococcus aureus*	ZJH-SA-065	Zhejiang Hospital	1	N	N
28	*Cryptococcus neoformans*	ATCC14053	ATCC	1	N	N
29	*Candida glabrata*	ZJH-CG-057	Zhejiang Hospital	1	N	N
30	*Hemophililus parainfluenza*	GZCDC-HP-045	GZCDC	1	N	N
31	*Shigella boydii*	GZCDC-SB-107	GZCDC	1	N	N
32	Enteropathogenic *Escherichia coli*	GZCDC-EPEC-045	GZCDC	1	N	N
33	*Bordetella pertussis*	GZCDZ-BP-052	GZCDC	1	N	N
34	*Bordetella parapertussis*	GZCDC-BP-0094	GZCDC	1	N	N
35	*Bacillus cereus*	2nd GZUTCM-BC-037	2nd GZUTCM	1	N	N
36	*Listeria monocytogenes*	2nd GZUTCM-LM-025	2nd GZUTCM	1	N	N
37	*Shigella flexneri*	2nd GZUTCM-SF-018	2nd GZUTCM	1	N	N
38	*Leptospira interrogans*	GZCDC-LI-005	GZCDC	1	N	N

[a] *ZJCDC, Zhejiang Provincial Center for Disease Control and Prevention; 1st ZJUSM, The First Affiliated Hospital, Zhejiang University School of Medicine; ZJCCL, Zhejiang Center for Clinical Laboratories; 2nd GZUTCM, The Second Affiliated Hospital, Guizhou University of Traditional Chinese Medicine; GZCDC, Guizhou Provincial Center for Disease Control and Prevention; ATCC, American Type Culture Collection.*

[b] *P, Positive; N, Negative.*

amplification was tested at different temperatures (60 to 67°C with 1°C intervals) with genomic templates (1×10^4 copies) from the pseudo-virus of SARS-CoV-2. The RT-LAMP amplification protocol was as described above, the *RdRp*- and *N*-LAMP amplification were monitored by means of real-time turbidity technique, and the kinetics graphs were recorded from all temperatures. The results showed that the faster amplifications of *RdRp*-RT-LAMP were obtained for detection temperature range from 63 to 64°C, and 62 to 63°C for the *N*-RT-LAMP reactions (**Figure 3**). Hence, the amplification temperature of

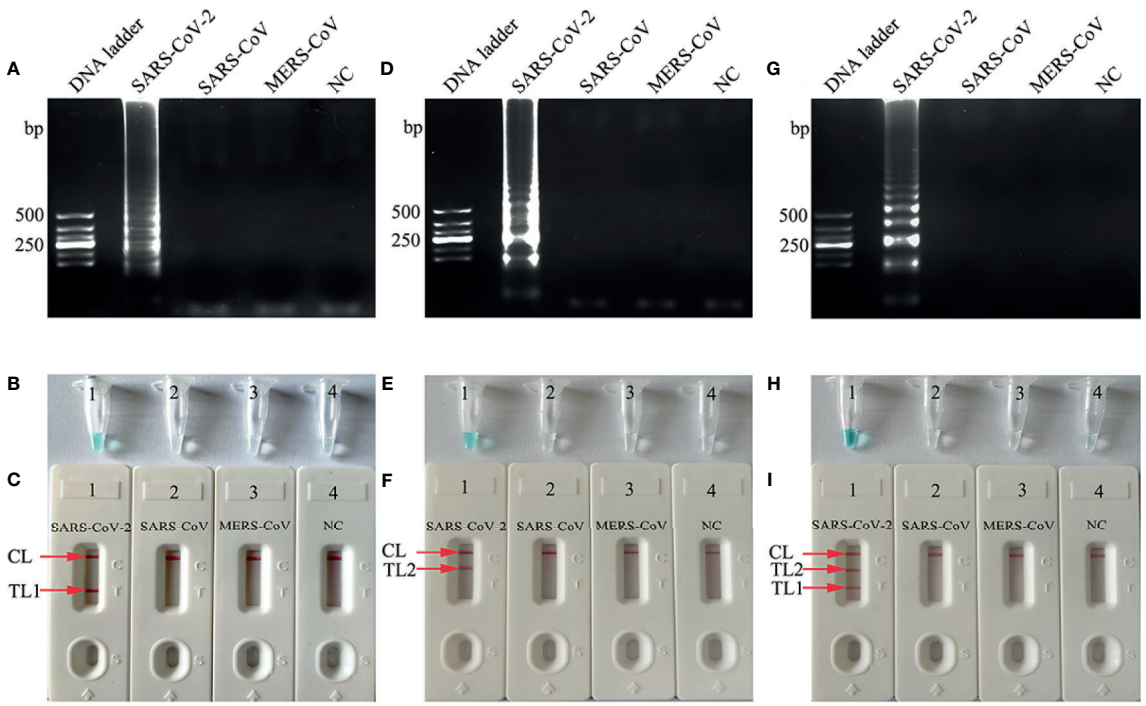

FIGURE 2 | Determination and verification of mRT-LAMP products. The *RdRp*-, *N*-, or mRT-LAMP mixtures, containing 1×10^4 copies of the RNA template, were incubated at a constant temperature of 65°C for 1 h, and the RT-LAMP products were identified with 2% agarose gel electrophoresis **(A, D, G)**, visual detection reagents **(B, E, H)** and lateral flow biosensor **(C, F, I)**. Viral RNA from pseudo-virus SARS-CoV, pseudo-virus MERS-CoV, and double distilled water (DW) were used as negative controls (NCs). Lane DNA ladder: 500 bp DNA ladder, the ladder-like bands indicate positive RT-LAMP amplification, the color changed from colorlessness to bright green indicates positive nucleic acid amplification. CL and TL1 appeared crimson red bands, indicating positive results of *RdRp*-RT-LAMP products, CL and TL2 presented crimson red bands, indicating positive results of *N*-RT-LAMP products, three crimson red bands (CL, TL1, and TL2) appeared indicating positive results of mRT-LAMP amplification.

63°C was considered as optimal temperature for the rest of multiple-RT-LAMP reactions in the current study.

Optimization of Amplification Time for mRT-LAMP-LFB Assay

To obtain an optimal reaction time for mRT-LAMP, four amplification times (20, 30, 40, and 50 min) were tested at the 63° C amplification temperature. The results showed that the LoD of the genomic RNA templates (20 copies) was detected when the mRT-LAMP amplification lasted 30 min (**Figure 4**). Hence, a reaction time of 30 min was considered the optimal amplification time for mRT-LAMP detection. In summary, the whole detection procedure, including reaction preparation (approximately 10 min), target genomic RNA preparation (30 min), mRT-LAMP (30 min), and analysis of results (approximately 2 min), could be completed within 80 min.

Sensitivity of *RdRp*-, *N*-, and mRT-LAMP Detection

The sensitivity of *RdRp*-, *N*-, and mRT-LAMP detection was evaluated with serially diluted pseudo-virus RNA range from 1×10^4 copies to 1 copy. The RT-LAMP amplification products were analyzed by visual inspection with MG reagents and lateral flow biosensors. The CL and TL1 lines appeared on the biosensor, showing positive results for the *RdRp*-RT-LAMP assay, and two crimson lines (CL and TL2) were observed on the biosensor, indicating positive results for *N*-RT-LAMP detection. The CL, TL1, and TL2 bands simultaneously became crimson on the biosensor, reporting positive results for the *RdRp* and *N* genes. For the negative controls, only the CL line appeared on the biosensors. The results showed that the LoD of mRT-LAMP was 20 copies per reaction, which was the same as the LoD of the *RdRp*- and *N*-RT-LAMP assay (**Figures 5A, B, D, E, G, H**). Meanwhile, the sensitivity of RT-PCR technique was also tested in the current study, the results indicated that the LoD of RT-PCR was 100 copies per reaction (**Figures 5C, F, I**).

Specificity of the mRT-LAMP Assay

The specificity of mRT-LAMP detection was confirmed with pseudo-viruses of SARS-CoV-2, 12 clinical SARS-CoV-2-positive samples, and 36 other pathogens (**Table 2**). The process of mRT-LAMP amplification, as described above. The genomic RNA extracted from SARS-CoV-2 presented positive results. Other pathogens and the blank control showed negative results (**Table 2**). Hence, the results confirmed that the mRT-

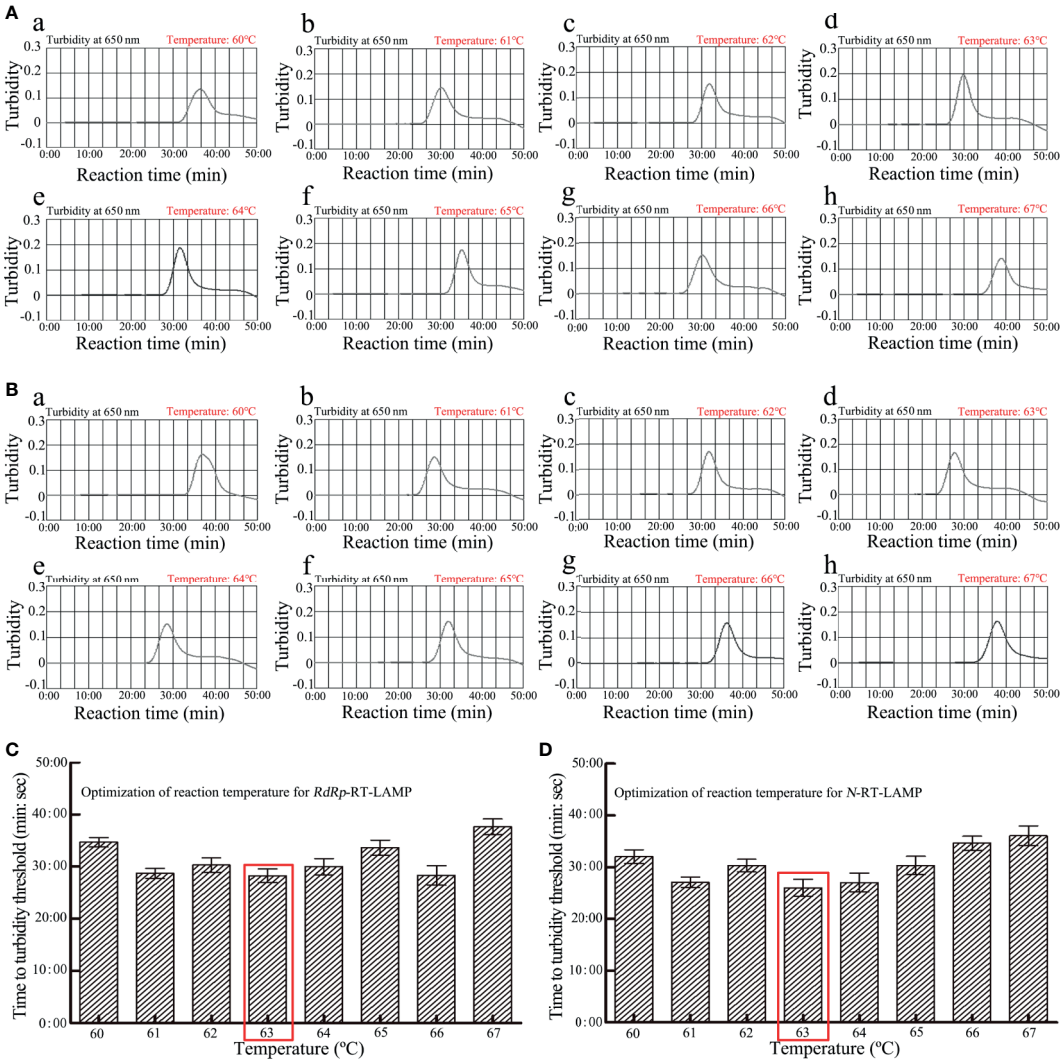

FIGURE 3 | Optimization of amplification temperature for *RdRp* -LAMP **(A)** and *N*-LAMP **(B)** primer sets. The LAMP amplifications for detection of *RdRp* **(A)** and *N* **(B)** were monitored through real-time turbidity and the corresponding curves of amplicons were displayed in the graphs. The threshold value was 0.1 and the turbidity>0.1 was considered as positive. 8 kinetic graphs were obtained at different temperatures (60-67°C, 1°C intervals) with 1×10^4 copies target genomic RNA per reaction. **(C)** Optimization of reaction temperature for *RdRp*-RT-LAMP; **(D)** Optimization of reaction temperature for *N*-RT-LAMP.

LAMP-LFB method could accurately identify SARS-CoV-2 from other pathogens.

Feasibility of the mRT-LAMP-LFB Method Using Clinical Samples

To further demonstrate the feasibility of mRT-LAMP-LFB as a valuable method for the detection of SARS-CoV-2, 110 clinical nasopharyngeal swab specimens and 60 artificial sputum samples (randomly added 100 copies of SARS-CoV-2 pseudo-viruses in each 200 μl artificial sputum sample) were simultaneously tested by mRT-LAMP-LFB and RT-PCR. Among them, 12 clinical samples and 35 artificial sputum samples had been confirmed as SARS-CoV-2 through RT-PCR and mRT-LAMP-LFB, respectively (**Table 3**). The Cq values of RT-PCR and mRT-LAMP-LFB detection results were shown in **Supplementary Table 1**. These results suggested that the mRT-LAMP-LFB assay established in the current study could be used as an advanced tool to detect SARS-CoV-2.

DISCUSSION

SARS-CoV-2 is the seventh coronavirus that causes human infections. Like SARS-CoV and MERS-CoV, this virus has the ability to cause lethal pneumonia (Chiappelli, 2020). Moreover, it has a stronger human-to-human transmission capacity than the above two coronaviruses (Ki, 2020; Wilson and Chen, 2020). Until now, up to 140 million COVID-19 cases have been confirmed, including more than 3 million deaths (www.who.int/emergencies/diseases/novel-coronavirus-2019).

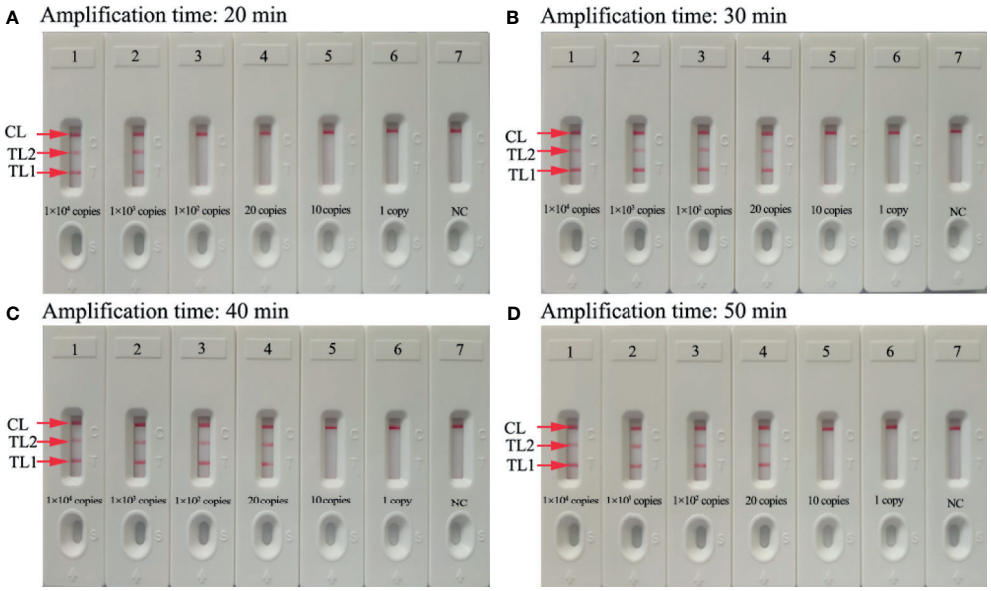

FIGURE 4 | Optimization of the amplification time for mRT-LAMP-LFB detection. Different amplification times (**A**, 20 min, **B**, 30 min, **C**, 40 min, **D**, 50 min) were tested at 63°C. Biosensors 1-7 represent SARS-CoV-2 genomic RNA levels of 1×10^4 copies, 1×10^3 copies, 1×10^2 copies, 20 copies, 10 copies, and 1 copy per reaction and blank control (DW), respectively. The best sensitivity was observed when the amplification lasted for 30 min **(B)**.

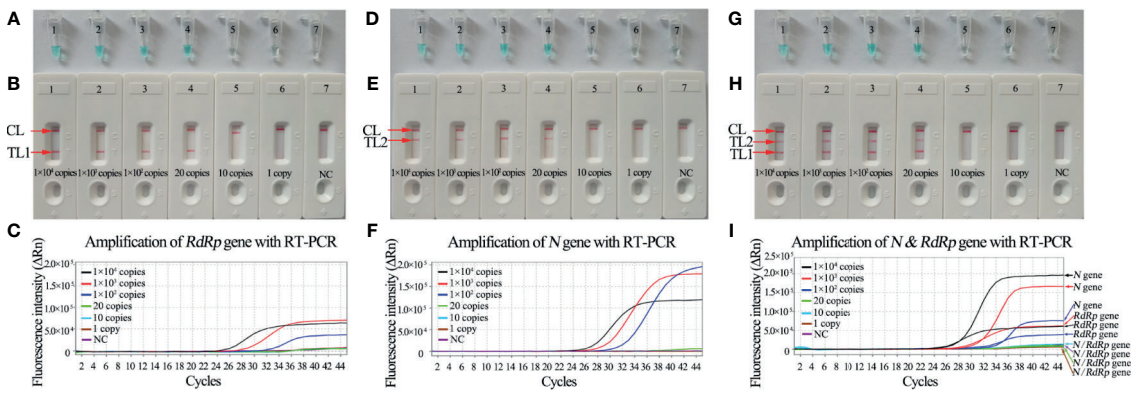

FIGURE 5 | Sensitivity analysis of *RdRp*-, *N*-, and mRT-LAMP detection with serial dilutions of RNA extracted from pseudo-virus SARS-CoV-2. The LoD of RT-LAMP for detecting SARS-CoV-2 was analyzed with visual detection reagents (MG) and lateral flow biosensors. **(A, B)** Sensitivity analysis of *RdRp*-RT-LAMP reaction. Tubes A1-A7 (Biosensors B1-B7) represent the genomic RNA amounts of 1×10^4 copies, 1×10^3 copies, 1×10^2 copies, 20 copies, 10 copies, and 1 copy per reaction and blank control (DW), respectively. The LoD of *RdRp*-RT-LAMP detection was 20 copies of RNA template per reaction. **(C)** Sensitive of *RdRp*-RT-PCR detection (1×10^4 copies to 1 copy). The LoD of *RdRp*-RT-PCR detection was 100 copies of RNA template per reaction. **(D, E)** Sensitivity analysis of *N*-RT-LAMP reaction. Tubes D1-D7 (Biosensors E1-E7) represent the genomic RNA amounts of 1×10^4 copies, 1×10^3 copies, 1×10^2 copies, 20 copies, 10 copies, and 1 copy per reaction and blank control (DW), respectively. The LoD of *N*-RT-LAMP detection was 20 copies of RNA template per reaction. **(F)** Sensitive of *N*-RT-PCR detection (1×10^4 copies -1 copy). The LoD of *N*-RT-PCR detection was 100 copies of RNA template per reaction. **(G, H)** Tubes G1-G7 (Biosensors H1-H7) represent the genomic RNA amounts of 1×10^4 copies, 1×10^3 copies, 1×10^2 copies, 20 copies, 10 copies, and 1 copy per reaction and blank control (DW), respectively. The LoD of the mRT-LAMP assay for *RdRp* and *N* detection was 20 copies of RNA template per reaction. **(I)** Sensitive of mRT-PCR detection (1×10^4 copies to 1 copy). The LoD of mRT-PCR detection was 100 copies of RNA template per reaction.

The main findings of the current study are that we established a simple, sensitive, reliable, and rapid assay with great specificity and low equipment cost for SARS-CoV-2 by mRT-LAMP-LFB. To avoid false-positive or -negative results, we chose the two target genes, *RdRp* and *N*, to detect viral RNA in clinical samples (Chen et al., 2020; Huang et al., 2020; Pang et al., 2020). To reduce the amplification time, we designed the loop primers. Briefly, six primers targeting eight regions generated a self-priming dumbbell-shaped template upon isothermal incubation with strand-displacing polymerase, resulting in the

TABLE 3 | Comparison of RT-PCR and mRT-LAMP-LFB methods to identify SARS-CoV-2 in clinical samples and artificial sputum samples.

Detection method	Clinical samples (n = 110)			Artificial sputum samples (n = 60)		
	Positive	Negative	Time consumption	Positive	Negative	Time consumption
RT-PCR	12 (Ct<38)	98	~150 min	35 (Ct<38)	25	~150 min
mRT-LAMP-LFB	12	98	Within 80 min	35	25	Within 80 min

rapid production of large quantities of the complex amplicon. The specificity of the mRT-LAMP assay was confirmed with genomic RNA from pseudo-viruses of SARS-CoV-2, clinical samples, and other pathogens. The mRT-LAMP detection of the *RdRp* and *N* genes identified SARS-CoV-2 with 100% specificity (**Table 2**).

In previous studies, there have some reports on a molecular diagnostic test for SARS-CoV-2 using RT-LAMP technology. Most of them have used visual inspection of color changes, turbidimetry, and fluorescence dye to analyze RT-LAMP products (Huang et al., 2020; Lu et al., 2020; Park et al., 2020; Yan et al., 2020). However, these techniques have to rely on special instruments and expensive reagents, such as colorimetric indicator, turbidimeter, and fluorescence detector, which may not be readily available in many resource-poor settings. To overcome these drawbacks, a target-specific visual nanoparticle-based lateral flow biosensor (LFB) detection method of easy operation and low-cost (approximately $2 USD) was successfully designed and applied to analyze mRT-LAMP products in the current study. The test result of SARS-CoV-2-mRT-LAMP-LFB provided direct visualization by naked eyes and does not require special instruments. Due to the specificity and elimination of special instruments, the LFB-based LAMP assay could easily apply to various fields (Cheng et al., 2019; Wang et al., 2019). In particular, the LFB applied in this study can simultaneously and visually detect two target genes (*RdRp* and *N*) in a single test.

Compared with RT-PCR method, the mRT-LAMP-LFB technique is more sensitive, time-saving, and cost-saving. The newly developed mRT-LAMP-LFB method was able to detect 20 copies of genomic RNA, which was more sensitive than RT-PCR method (**Figure 5**). The entire detection process, including reaction preparation (approximately 10 min), template preparation (approximately 30 min), isothermal amplification (30 min), and LFB reading (approximately 2 min), could be accomplished within 80 min. The RT-PCR assay, however, requires 2~3 h during the whole process. The running cost of one test, including genomic RNA extraction (approximately $1 USD), LAMP reaction (approximately $3.5 USD), and LFB reading (approximately $2 USD), is estimated to be $6.5 USD, which is getting closer with RT-PCR testing (approximately $7.0 USD). In addition, the advanced technology can decrease labor costs because performing the mRT-LAMP-LFB assay does not require skilled technical personnel. More importantly, the mRT-LAMP-LFB technology has great potential to develop point-of-care (POC) testing in clinical practice. The detection results could be easily judged by the naked eye. The three crimson red bands (CL, TL1, and TL2) appeared indicating positive results, while the negative results only appeared as a crimson red line (CL) in the biosensor. The findings of this study have been applied for a patent from the State Intellectual Property Office of the People's Republic of China (Patent Application NO. 202010717954. X). The shortcoming of this detection is that the RT-LAMP amplification must be taken out from the reaction tube for LFB detection. There has a risk of contamination with the post-reaction processing of LAMP products. The strict control of the laboratory environment is critical for the reduction of the production of aerosols in experimental processes. Spraying timely 10~15% sodium hypochlorite solution and 70% ethanol after completion of detection is an effective way to overcome nucleic acid contamination in the laboratory. In the current study, the mRT-LAMP-LFB detection results were consistent with the RT-PCR methods in the evaluation of clinical samples. It is indicated that false-positive rates have been effective controlled in our laboratory.

The main limitation of this study is that with the widely spread of SARS-CoV-2 virus, the accuracy of the mRT-LAMP-LFB technology will be affected by the mutations occurring in the primers sequence region of the target genes. So, it is necessary to monitor the mutant sites of the virus genome by whole-genome sequencing. Besides, owning to laboratory biosafety, SARS-CoV and MERS-CoV viruses could not be tested for the specificity of the mRT-LAMP-LFB assay, we used pseudo-virus of SARS-CoV and MERS-CoV as alternatives.

In conclusion, a simple, rapid, and reliable mRT-LAMP-LFB technique based on the *RdRp* and *N* genes was successfully developed for assaying SARS-CoV-2 in the current study. This method could rapidly, reliably, specifically, and sensitively detect SARS-CoV-2. The amplification products were analyzed with LFB, which was objective, rapid, and easily interpretable. Hence, the mRT-LAMP-LFB assay could be considered as a useful method for the reliable and rapid detection of SARS-CoV-2 in clinical samples, especially in resource-constrained regions of the world.

DATA AVAILABILITY STATEMENT

The original contributions presented in the study are included in the article/**Supplementary Material**. Further inquiries can be directed to the corresponding author.

ETHICS STATEMENT

The study was approved by the Human Ethics Committee of the Second Affiliated Hospital of Guizhou University of Traditional Chinese Medicine (Approval No. TYH2020011) and the Human Ethics Committee of the Zhejiang Hospital (Approval No. 2020

Lin Shen Di (7K) Hao), and complied with the Declaration of Helsinki. All data/isolates were analyzed anonymously.

AUTHOR CONTRIBUTIONS

XC, QZ, and SD conceived and designed the study. XC and SD participated in primers design. XC, QZ, BC, YW, and HY contributed to all the laboratory works. BC and HY contributed to the data collection. XC, SL, and QZ performed the statistical analysis. XC wrote the initial draft of the manuscript, and SD revised the manuscript. All authors contributed to the article and approved the submitted version.

FUNDING

This work was supported by the Program of Scientific and Technological Project in Guizhou Province (Grant No. [2020] 4Y184, [2019]1186 and [2020]4Y197), the Scientific and Technological in Guiyang City (Grant No. Zhu Ke He [2020]-10-5 and [2020]-16-5), the Program of Scientific and Technological Innovation Team of Guizhou Province under Grant (Qian Ke He Platform talent [2018]5606), the Public Welfare Technology Application Research Program of Zhejiang Province (Grant No. LGF21H190001), and the National Natural Science Foundation of China under Grant (81801978).

ACKNOWLEDGMENTS

We thank all the medical workers in the second GZUTCM, GZCDC, ZJCDC, first ZJUSM, and ZJH for their cooperation in this study.

SUPPLEMENTARY MATERIAL

The Supplementary Material for this article can be found online at: https://www.frontiersin.org/articles/10.3389/fcimb.2021.581239/full#supplementary-material

REFERENCES

Bao, Y., Sun, Y., Meng, S., Shi, J., and Lu, L. (2020). 2019-Ncov Epidemic: Address Mental Health Care to Empower Society. *Lancet* 395, e37–e38. doi: 10.1016/S0140-6736(20)30309-3

Chen, J. (2020). Pathogenicity and Transmissibility of 2019-Ncov-A Quick Overview and Comparison With Other Emerging Viruses. *Microbes Infect.* 22, 69–71. doi: 10.1016/j.micinf.2020.01.004

Cheng, X., Yang, J., Wang, M., Wu, P., Du, Q., He, J., et al. (2019). Visual and Rapid Detection of *Acinetobacter Baumannii* by a Multiple Cross Displacement Amplification Combined With Nanoparticles-Based Biosensor Assay. *AMB Express.* 9, 30. doi: 10.1186/s13568-019-0754-0

Chen, L., Liu, W., Zhang, Q., Xu, K., Ye, G., Wu, W., et al. (2020). RNA Based mNGS Approach Identifies a Novel Human Coronavirus From Two Individual Pneumonia Cases in 2019 Wuhan Outbreak. *Emerg. Microbes Infect.* 9, 313–319. doi: 10.1080/22221751.2020.1725399

Chiappelli, F. (2020). 2019-Ncov-Towards a 4th Generation Vaccine. *Bioinformation* 16, 139–144. doi: 10.6026/97320630016139

Corman, V. M., Landt, O., Kaiser, M., Molenkamp, R., Meijer, A., Chu, D. K., et al. (2020). Detection of 2019 Novel Coronavirus-Ncov) by Real-Time RT-PCR. *Euro. Surveill.* 25, 2000045. doi: 10.2807/1560-7917.es.2020.25.3.2000045

Coronaviridae Study Group of the International Committee on Taxonomy of Viruses (2020). The Species Severe Acute Respiratory Syndrome-Related Coronavirus: Classifying 2019-Ncov and Naming It SARS-CoV-2. *Nat. Microbiol.* 5, 536–544. doi: 10.1038/s41564-020-0695-z

Gong, L., Liu, E., Che, J., Li, J., Liu, X., Xu, H., et al. (2019). Multiple Cross Displacement Amplification Coupled With Gold Nanoparticles-Based Lateral Flow Biosensor for Detection of the Mobilized Colistin Resistance Gene *Mcr-1*. *Front. Cell. Infect. Microbiol.* 9, 226. doi: 10.3389/fcimb.2019.00226

Huang, W. E., Lim, B., Hsu, C. C., Xiong, D., Wu, W., Yu, Y., et al. (2020). RT-LAMP for Rapid Diagnosis of Coronavirus SARS-CoV-2. *Microb. Biotechnol.* 13, 950–961. doi: 10.1111/1751-7915.13586

Huang, P., Wang, H., Cao, Z., Jin, H., Chi, H., Zhao, J., et al. (2018). A Rapid and Specific Assay for the Detection of MERS-CoV. *Front. Microbiol.* 9, 1101. doi: 10.3389/fmicb.2018.01101

Ji, J. S. (2020). Origins of MERS-CoV, and Lessons for 2019-Ncov. *Lancet Planet Health* 4, e93. doi: 10.1016/S2542-5196(20)30032-2

Jiang, S., Xia, S., Ying, T., and Lu, L. (2020). A Novel Coronavirus-Ncov) Causing Pneumonia-Associated Respiratory Syndrome. *Cell. Mol. Immunol.* 17, 554. doi: 10.1038/s41423-020-0372-4

Jiao, W., Wang, Y., Wang, G., Wang, Y., Xiao, J., Sun, L., et al. (2019). Development and Clinical Validation of Multiple Cross Displacement Amplification Combined With Nanoparticles-Based Biosensor for Detection of *Mycobacterium Tuberculosis*: Preliminary Results. *Front. Microbiol.* 10, 2135. doi: 10.3389/fmicb.2019.02135

Ki, M. (2020). Epidemiologic Characteristics of Early Cases With 2019 Novel Coronavirus-Ncov) Disease in Korea. *Epidemiol. Health* 42, e2020007. doi: 10.4178/epih.e2020007

Kim, J. H., Kang, M., Park, E., Chung, D. R., Kim, J., and Hwang, E. S. (2019). A Simple and Multiplex Loop-Mediated Isothermal Amplification (LAMP) Assay for Rapid Detection of SARS-CoV. *Biochip. J.* 13, 341–351. doi: 10.1007/s13206-019-3404-3

Li, S., Liu, C., Liu, Y., Ma, Q., Wang, Y., and Wang, Y. (2019). Development of a Multiple Cross Displacement Amplification Combined With Nanoparticles-Based Biosensor Assay to Detect *Neisseria Meningitidis*. *Infect. Drug Resist.* 12, 2077–2087. doi: 10.2147/IDR.S210735

Lu, R., Wu, X., Wan, Z., Li, Y., Jin, X., and Zhang, C. (2020). A Novel Reverse Transcription Loop-Mediated Isothermal Amplification Method for Rapid Detection of SARS-CoV-2. *Int. J. Mol. Sci.* 21, 2826. doi: 10.3390/ijms21082826

Notomi, T., Okayama, H., Masubuchi, H., Yonekawa, T., Watanabe, K., Amino, N., et al. (2000). Loop-Mediated Isothermal Amplification of DNA. *Nucleic Acids Res.* 28, E63. doi: 10.1093/nar/28.12.e63

Pang, J., Wang, M. X., Ang, I. Y. H., Tan, S. H. X., Lewis, R. F., Chen, J. I., et al. (2020). Potential Rapid Diagnostics, Vaccine and Therapeutics for 2019 Novel Coronavirus-Ncov): A Systematic Review. *J. Clin. Med.* 9, 623. doi: 10.3390/jcm9030623

Park, G. S., Ku, K., Baek, S. H., Kim, S. J., Kim, S. I., Kim, B. T., et al. (2020). Development of Reverse Transcription Loop-Mediated Isothermal Amplification Assays Targeting Severe Acute Respiratory Syndrome Coronavirus 2 (SARS-CoV-2). *J. Mol. Diagn.* 22, 729–735. doi: 10.1016/j.jmoldx.2020.03.006

Ravina,, Dalal, A., Mohan, H., Prasad, M., and Pundir, C. S. (2020). Detection Methods for Influenza A H1N1 Virus With Special Reference to Biosensors: A Review. *Biosci. Rep.* 40, BSR20193852. doi: 10.1042/bsr20193852

Rothe, C., Schunk, M., Sothmann, P., Bretzel, G., Froeschl, G., Wallrauch, C., et al. (2020). Transmission of 2019-Ncov Infection From an Asymptomatic Contact in Germany. *N. Engl. J. Med.* 382, 970–971. doi: 10.1056/NEJMc2001468

She, J., Jiang, J., Ye, L., Hu, L., Bai, C., and Song, Y. (2020). 2019 Novel Coronavirus of Pneumonia in Wuhan, China: Emerging Attack and Management Strategies. *Clin. Transl. Med.* 9, 19. doi: 10.1186/s40169-020-00271-z

Tahamtan, A., and Ardebili, A. (2020). Real-Time RT-PCR in COVID-19 Detection: Issues Affecting the Results. *Expert. Rev. Mol. Diagn.* 20, 453–454. doi: 10.1080/14737159.2020.1757437

Tu, Y. F., Chien, C. S., Yarmishyn, A. A., Lin, Y. Y., Luo, Y. H., Lin, Y. T., et al. (2020). A Review of SARS-CoV-2 and the Ongoing Clinical Trials. *Int. J. Mol. Sci.* 21, 2657. doi: 10.3390/ijms21072657

van Kasteren, P. B., van der Veer, B., van den Brink, S., Wijsman, L., de Jonge, J., van den Brandt, A., et al. (2020). Comparison of Seven Commercial RT-PCR Diagnostic Kits for COVID-19. *J. Clin. Virol.* 128, 104412. doi: 10.1016/j.jcv.2020.104412

Wang, C., Horby, P. W., Hayden, F. G., and Gao, G. F. (2020). A Novel Coronavirus Outbreak of Global Health Concern. *Lancet* 395, 470–473. doi: 10.1016/S0140-6736(20)30185-9

Wang, Y., Li, H., Wang, Y., Zhang, L., Xu, J., and Ye, C. (2017). Loop-Mediated Isothermal Amplification Label-Based Gold Nanoparticles Lateral Flow Biosensor for Detection of Enterococcus Faecalis and *Staphylococcus Aureus*. *Front. Microbiol.* 8, 192. doi: 10.3389/fmicb.2017.00192

Wang, Y., Wang, Y., Ma, A. J., Li, D. X., Luo, L. J., Liu, D. X., et al. (2015). Rapid and Sensitive Isothermal Detection of Nucleic-Acid Sequence by Multiple Cross Displacement Amplification. *Sci. Rep.* 5, 11902. doi: 10.1038/srep11902

Wang, Y., Wang, Y., Quan, S., Jiao, W., Li, J., Sun, L., et al. (2019). Establishment and Application of a Multiple Cross Displacement Amplification Coupled With Nanoparticle-Based Lateral Flow Biosensor Assay for Detection of *Mycoplasma Pneumoniae*. *Front. Cell. Infect. Microbiol.* 9, 325. doi: 10.3389/fcimb.2019.00325

Wilson, M. E., and Chen, L. H. (2020). Travellers Give Wings to Novel Coronavirus-Ncov). *J. Travel. Med.* 27, taaa015. doi: 10.1093/jtm/taaa015

Yan, C., Cui, J., Huang, L., Du, B., Chen, L., Xue, G., et al. (2020). Rapid and Visual Detection of 2019 Novel Coronavirus (SARS-CoV-2) by a Reverse Transcription Loop-Mediated Isothermal Amplification Assay. *Clin. Microbiol. Infect.* 26, 773–779. doi: 10.1016/j.cmi.2020.04.001

Younes, N., Al-Sadeq, D. W., AL-Jighefee, H., Younes, S., Al-Jamal, O., Daas, H. I., et al. (2020). Challenges in Laboratory Diagnosis of the Novel Coronavirus SARS-CoV-2. *Viruses* 12, 582. doi: 10.3390/v12060582

Zhang, H. (2020). Early Lessons From the Frontline of the 2019-Ncov Outbreak. *Lancet* 395, 687. doi: 10.1016/S0140-6736(20)30356-1

Zhen, W., Manji, R., Smith, E., and Berry, G. J. (2020). Comparison of Four Molecular *In Vitro* Diagnostic Assays for the Detection of SARS-CoV-2 in Nasopharyngeal Specimens. *J. Clin. Microbiol.* 58, e00743–20. doi: 10.1128/JCM.00743-20

Conflict of Interest: The authors declare that the research was conducted in the absence of any commercial or financial relationships that could be construed as a potential conflict of interest.

frontiers in Cellular and Infection Microbiology

ORIGINAL RESEARCH
published: 29 September 2021
doi: 10.3389/fcimb.2021.759965

Rapid Detection and Differentiating of the Predominant *Salmonella* Serovars in Chicken Farm by TaqMan Multiplex Real-Time PCR Assay

Suhua Xin†, *Hong Zhu*†, *Chenglin Tao*, *Beibei Zhang*, *Lan Yao*, *Yaodong Zhang*, *Dossêh Jean Apôtre Afayibo*, *Tao Li*, *Mingxing Tian*, *Jingjing Qi*, *Chan Ding*, *Shengqing Yu** *and Shaohui Wang**

Shanghai Veterinary Research Institute, Chinese Academy of Agricultural Sciences, Shanghai, China

OPEN ACCESS

Edited by:
Jianmin Zhang,
South China Agricultural University, China

Reviewed by:
Zhiming Pan,
Yangzhou University, China
Wenliang Li,
Jiangsu Academy of Agricultural Sciences (JAAS), China
Zhe Ma,
Nanjing Agricultural University, China

***Correspondence:**
Shaohui Wang
shwang0827@126.com
Shengqing Yu
yus@shvri.ac.cn

†*These authors have contributed equally to this work*

Specialty section:
This article was submitted to Clinical Microbiology, a section of the journal Frontiers in Cellular and Infection Microbiology

Received: *17 August 2021*
Accepted: *10 September 2021*
Published: *29 September 2021*

Citation:
Xin S, Zhu H, Tao C, Zhang B, Yao L, Zhang Y, Afayibo DJA, Li T, Tian M, Qi J, Ding C, Yu S and Wang S (2021) Rapid Detection and Differentiating of the Predominant Salmonella Serovars in Chicken Farm by TaqMan Multiplex Real-Time PCR Assay. Front. Cell. Infect. Microbiol. 11:759965. doi: 10.3389/fcimb.2021.759965

Salmonella has been known as an important zoonotic pathogen that can cause a variety of diseases in both animals and humans. Poultry are the main reservoir for the *Salmonella* serovars *Salmonella* Pullorum (*S*. Pullorum), *Salmonella* Gallinarum (*S*. Gallinarum), *Salmonella* Enteritidis (*S*. Enteritidis), and *Salmonella* Typhimurium (*S*. Typhimurium). The conventional serotyping methods for differentiating *Salmonella* serovars are complicated, time-consuming, laborious, and expensive; therefore, rapid and accurate molecular diagnostic methods are needed for effective detection and prevention of contamination. This study developed and evaluated a TaqMan multiplex real-time PCR assay for simultaneous detection and differentiation of the *S*. Pullorum, *S*. Gallinarum, *S*. Enteritidis, and *S*. Typhimurium. In results, the optimized multiplex real-time PCR assay was highly specific and reliable for all four target genes. The analytical sensitivity corresponded to three colony-forming units (CFUs) for these four *Salmonella* serovars, respectively. The detection limit for the multiplex real-time PCR assay in artificially contaminated samples was 500 CFU/g without enrichment, while 10 CFU/g after pre-enrichment. Moreover, the multiplex real-time PCR was applied to the poultry clinical samples, which achieved comparable results to the traditional bacteriological examination. Taken together, these results indicated that the optimized TaqMan multiplex real-time PCR assay will be a promising tool for clinical diagnostics and epidemiologic study of *Salmonella* in chicken farm and poultry products.

Keywords: multiplex real-time PCR, chicken, detection, differentiation, *Salmonella* serovars

INTRODUCTION

Salmonella is an important zoonotic pathogen that can cause a variety of diseases in both animals and humans (Majowicz et al., 2010). *Salmonella* is prevalent in domestic animals such as poultry, pigs, and cattle. Poultry are a main reservoir for *Salmonella*, including the most prevalent *Salmonella* serovars *Salmonella* Pullorum (*S*. Pullorum), *Salmonella* Gallinarum (*S*. Gallinarum), *Salmonella* Enteritidis (*S*. Enteritidis), and *Salmonella* Typhimurium (*S*. Typhimurium) (Medalla et al., 2016; Wang et al., 2020;

Xu et al., 2020; Zhao et al., 2020; Yu et al., 2021). These *Salmonella* serovars can lead to serious avian salmonellosis, which causes economic losses in the poultry industry. In addition, *Salmonella* can be transmitted to humans by contaminated poultry products and cause acute gastroenteritis or diarrhea, being a threat to public health (Balasubramanian et al., 2019). Currently, animals, in particular poultry, are considered to be the primary cause for salmonellosis and numerous other foodborne outbreaks (Keerthirathne et al., 2017; Biswas et al., 2019; Liu et al., 2021). Thus, detection and differentiation of these *Salmonella* serovars in poultry farms are required to prevent, control, and eliminate the spread of *Salmonella*.

Rapid and accurate diagnosis is curial for effective prevention and control of the disease. Currently, more than 2,600 *Salmonella* serovars have been identified based on the O, H, and Vi antigens (Issenhuth-Jeanjean et al., 2014). Although bacteriological culture and serum agglutination test were considered to be the gold standard for differentiating *Salmonella* serovars, there were many disadvantages for this routine diagnosis in practice. The conventional culture method tends to be complex, time-consuming, and laborious. Moreover, false-negative result for O and H antigens agglutination test occurs occasionally due to the loss of surface antigens in non-culturable state (Schrader et al., 2008). In efforts to avoid such disadvantages, several nucleic acid amplification methods have been developed to detect and differentiate the *Salmonella* serovars (Shi et al., 2015). Although there is extensive sequence conservation in *Salmonella* genome, comparative genomic analysis is effective to validate novel serovar-specific genes. The unique genes had been identified among the different *Salmonella* serovars (Liu et al., 2011; Zhang et al., 2019). The gene *lygD* in Sdf locus has been found specific in *S.* Enteritidis. Serovar-specific gene *STM4495* for identifying *S.* Typhimurium was obtained by comparative genomics (Agron et al., 2001; Akiba et al., 2011). In addition, comparative analysis of the *glgC* gene sequence identified an 11 bp (GATCGATCACG) deletion presented only in *S.* Gallinarum but not other *Salmonella* serovars (Kang et al., 2011). Based on these specific gene, PCR assays were applied for detecting different *Salmonella* serovars (Shah et al., 2005; Kim et al., 2006; Hong et al., 2008; Kang et al., 2011; Xu et al., 2018). Compared to conventional PCR, real-time PCR assay offers advantages in rapidity, quantitative measurement, and avoiding of cross-contamination. More importantly, real-time PCR assay enables to obtain both qualitative and quantitative measurement of the pathogen presented in samples. Thus, real-time PCR has been widely utilized to detect different pathogens (Ding et al., 2017; Liu et al., 2019). Recently, increasing studies developed single and multiplex real-time PCR for the specific detection of major *Salmonella* serovars in food products (Lee et al., 2009; Munoz et al., 2010; Prendergast et al., 2013; Kasturi and Drgon, 2017; Kim et al., 2017; Nair et al., 2019). The rapid detection and differentiation of *Salmonella* serovars are required for the epidemiologic investigation of *Salmonella* in chicken farms.

This study attempted to develop a rapid multiplex RT-PCR assay for the simultaneous detection and differentiation of the prevalent *S.* Pullorum, *S.* Gallinarum, *S.* Enteritidis, and *S.* Typhimurium. The specificity and sensitivity evaluations indicated that the developed multiplex real-time PCR assay appears to be a promising tool for clinical diagnostics and epidemiology studies for *Salmonella* in chicken farm and poultry products.

MATERIALS AND METHODS

Bacterial Strains and Growth Conditions

The *Salmonella* and non-*Salmonella* bacterial strains used to establish and verify the multiplex real-time PCR assay are listed in **Table 1**. The *Salmonella*, *Escherichia coli*, and *Pseudomonas aeruginosa* strains were cultured at 37°C in Luria-Bertani (LB) medium (BD, Detroit, MI, USA) with aeration. Other bacterial strains were grown in appropriate medium under recommended culture conditions.

DNA Extraction

Bacterial genomic DNA was extracted from fresh bacterial culture using TIANamp Bacteria DNA Kit (Tiangen Biotech, Beijing, China) following the manufacturer's instructions. Whereas, the total DNA from clinical samples was prepared using DNA Isolation Reagent for meat Products (Tiangen Biotech, Beijing, China). The concentration and purity of the DNA were measured with spectrophotometer.

Primers and Probes Designing

To design the suitable primers, the specific gene sequences of these *Salmonella* serovars were analyzed. By bioinformatics analysis, we found a specific gene segment (699 bp) SGP (GenBank No. CP012347.1 segment 2766328 to 2767027) was presented and generally conserved in *S.* Pullorum and *S.* Gallinarum. In addition, a previous study identified an 11 bp (GATCGATCACG) sequence deletion in *glgC* gene presented only in *S.* Gallinarum, but not other *Salmonella* serovars (Kang et al., 2011). Thus, the SGP gene segment and truncated sequence of *glgC* gene could be exploited to differentiate *S.* Pullorum and *S.* Gallinarum from other *Salmonella* serovars. The serovar-specific genes *lygD* and *STM4495* for specifically identifying and differentiating *S.* Enteritidis and *S.* Typhimurium were selected as targets according to previous studies (Agron et al., 2001; Akiba et al., 2011). Then, the specific primers and probes were designed based on the specific gene sequences (**Table 2** and **Figure 1**). Furthermore, the specificity of the primer sequences was tested by *in silico* analysis using BLAST at the National Center for Biotechnology Information (NCBI). All the primers and probes were synthesized by Sangon Biotech (Shanghai) Co., Ltd, China.

Optimization and Development of Multiplex Real-Time PCR Assay

The multiplex real-time PCR was carried out in a final volume of 20.0 μl, and the concentrations of primers, probes, and reaction condition were optimized using the purified DNA of *S.* Pullorum, *S.* Gallinarum, *S.* Enteritidis, and *S.* Typhimurium reference strains (**Table 1**). Sterile distilled water was used as negative control. The multiplex real-time PCR was performed on

TABLE 1 | Specificity of the multiplex real-time PCR for different bacterial strains.

Bacteria	No. of strains	Multiplex real-time PCR results			
		S. Pullorum	*S.* Gallinarum	*S.* Enteritidis	*S.* Typhimurium
***Salmonella* strains**					
S. Pullorum CVCC519	1	1	0	0	0
S. Gallinarum ATCC19945	1	0	1	0	0
S. Typhimurium 14028	1	0	0	0	1
S. Enteritidis CVCC1805	1	0	0	1	0
S. Typhimurium SL1344	1	0	0	0	1
S. Pullorum isolates	36	36	0	0	0
S. Gallinarum isolates	5	0	5	0	0
S. Typhimurium isolates	50	0	0	0	50
S. Enteritidis isolates	35	0	0	35	0
S. Anatum CAU0118	1	0	0	0	0
S. Agona BNCC192235	1	0	0	0	0
S. Anatis CMCC50774	1	0	0	0	0
S. Choleraesuis CVCC503	1	0	0	0	0
S. Newbort ATCC6962	1	0	0	0	0
S. Dublin CMCC50042	1	0	0	0	0
S. Heidelberg CMCC50111	1	0	0	0	0
S. Paratyphi B CMCC50094	1	0	0	0	0
S. Derby CMCC50112	1	0	0	0	0
S. Derby isolates	5	0	0	0	0
Non-*Salmonella* strains					
E. coli O157:H7 ATCC35150	1	0	0	0	0
E. coli O157:H7 ATCC43889	1	0	0	0	0
E. coli O38 CVCC1543	1	0	0	0	0
E. coli O73 CVCC1547	1	0	0	0	0
E. coli O78 CGMCC10602	1	0	0	0	0
E. coli isolates	50	0	0	0	0
Klebsiella pneumoniae isolates	10	0	0	0	0
Listeria monocytogenes 10403s	1	0	0	0	0
Listeria monocytogenes EGD	1	0	0	0	0
Listeria monocytogenes isolates	20	0	0	0	0
Pasteurella multocida isolates	10	0	0	0	0
Riemerella anatipestifer isolates	20	0	0	0	0
Staphylococcus aureus ATCC25923	1	0	0	0	0
Staphylococcus aureus isolates	15	0	0	0	0
Pseudomonas aeruginosa PAO1	1	0	0	0	0
Pseudomonas aeruginosa isolates	10	0	0	0	0
Proteus mirabilis isolates	6	0	0	0	0

the ABI 7500 Real-time PCR system (Applied Biosystems, CA, USA), and fluorescent signals were detected simultaneously during annealing/extension phase. All analyses were performed with ABI 7500 Software Version 1.4 (Applied Biosystems, CA, USA).

Specificity of the Multiplex Real-Time PCR Assay

A collection of bacterial strains, including various *Salmonella* serovars and non-*Salmonella* (**Table 1**), was used to evaluate the specificity of multiplex real-time PCR assay. All of the bacterial strains have been confirmed by biochemical identification, PCR, and serotyping with traditional agglutination assay. The bacterial genomic DNA was extracted and used as a template in the multiplex real-time PCR assay under optimized condition.

Standard Curve and Sensitivity Analysis

The standard curves and sensitivity of multiplex real-time PCR were determined using genomic DNA of various bacterial concentrations as described previously (Lee et al., 2009; Ding et al., 2017). The pure cultures of the *S.* Pullorum, *S.* Gallinarum, *S.* Enteritidis, and *S.* Typhimurium strains were 10-fold serially diluted to appropriate dilutions (ranging from 3 to 3×10^7 CFU/ml), which were counted by plating. The genomic DNA extracted from bacterial culture dilutions was used as templates for multiplex real-time PCR. Negative control includes sterile distilled water in place of DNA. The standard curves were calculated automatically based on the Cycle threshold (Ct) values using the ABI 7500 Software. The amplification efficiencies (E) were determined by using the slope of the standard curve and applying the equation: $E = (10^{-1/slope})-1$ (Kawasaki et al., 2010).

Evaluation of the Limit of Detection of Multiplex Real-Time PCR in Artificial Contamination Samples

The LOD of multiplex real-time PCR assay was evaluated for the artificial contamination samples with or without enrichment as

TABLE 2 | Primers and probes used for the multiplex real-time PCR.

Primers or probes	Sequence (5' to 3')	Optimal concentration	Target serovars/gene segments	*Salmonella* serovars			
				S. Pullorum	*S.* Gallinarum	*S.* Enteritidis	*S.* Typhimurium
SGP-F	GGATGTCCACGCTCATTTCTC	0.05 μM	*S.* Pullorum and *S.* Gallinarum/*SGP*	+	+	-	-
SGP-R	TGAAAGCTGGCGTTACGGTTA	0.05 μM	(CP012347.1, 2766328-2767027)				
SGP-Probe	FAM-CGTCAGGCCCACCGCCGACAG-BHQ1	0.05 μM					
SG-F	CAGGCGATCATATCTACAAGCAGG	0.1 μM	*S.* Pullorum and *S.* Gallinarum/*glgC*	-	+	-	-
SG-R	TCTTGTCGCTTTCATCGACCGC	0.1 μM	(11 bp deletion in *S.* Pullorum)				
SG- Probe	JOE-ACTCGCGTATGTTTTGAAAAGGGC-BHQ1	0.05 μM					
SE-F	TCTGGGACGCCAAAAAGC	0.1 μM	*S.* Enteritidis/*lygD*	-	-	+	-
SE -R	TGACGGTAGATTGTGTCTCAAAGC	0.1 μM					
SE- Probe	Cy5-TCAAACTTACTCAGGAGATCGCCGCTG-BHQ2	0.05 μM					
ST-F	GTTCAGCTCCGGTAAAGAGAA	0.2 μM	*S.* Typhimurium/*STM4495*	-	-	-	+
ST-R	AGCAGCGGCACTACATATTC	0.2 μM					
ST-Probe	Cy3-CGTTTGAGTGCCTGGTCTATCTGA-BHQ2	0.4 μM					

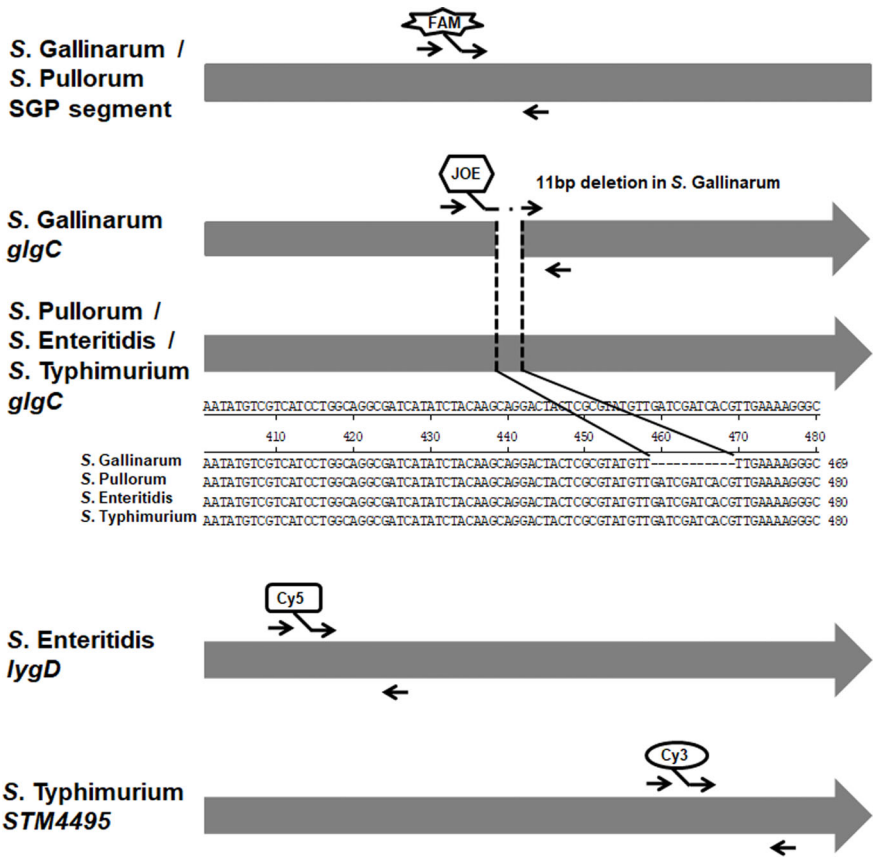

FIGURE 1 | Diagram of the primers and probes designing for the multiplex real-time PCR. The specific gene or segment of these four *Salmonella* serovars was analyzed and exploited to design the primers and probes. The primers and fluorophore-labeled probes were indicated. The arrows indicated the positions of the designed primers. In addition, the alignments of *glgC* genes in *S.* Gallinarum, *S.* Pullorum, *S.* Enteritidis, and *S.* Typhimurium were shown.

previously described (Lee et al., 2009), with some modifications. Briefly, 100 µl of each bacterial dilutions (1 to 10^8 CFU/ml) were individually added to 1 g of chicken meat samples. Then, these contaminated samples were thoroughly homogenized with 9 ml of buffered peptone water (BPW). The pre-enriched homogenized samples were used for DNA extraction using DNA Isolation Reagent for meat Products (Tiangen Biotech, Beijing, China). In addition, the homogenized samples were incubated at 37°C for 6 h. After primary enrichment, DNA extraction was performed. These DNA were used as templates for multiplex real-time PCR. Non-inoculated meat was subjected to the same procedure and used as a negative control.

Detection of Clinical Samples

The multiplex real-time PCR assay was applied to evaluate the presence of *Salmonella* in 60 sick or dead chicken with clinical signs collected from five farms. All animal experiments were conducted in strict accordance with the guidelines of the Humane Treatment of Laboratory Animals and were approved by the Animal Care and Use Committee at the Shanghai Veterinary Research Institute, China. The liver samples were collected aseptically from the chickens. The samples were homogenized for primary enrichment or DNA isolation as described above. The DNA extracted from these samples was analyzed by multiplex real-time PCR method. Meanwhile, each sample was also subjected to standard bacterial culture methods and traditional serum agglutination assay.

RESULTS

Development of the Multiplex Real-Time PCR Assay

Based on the bioinformatics analysis, the specific primers and probes were designed based on the target genes of these four *Salmonella* serovars (**Figure 1**). Then, multiplex real-time PCR was optimized by adjustment of different parameters. The optimal amplification reaction contained 10.0 µl Premix Ex Taq™ (Takara, Dalian, China), 0.2 µl ROX Reference Dye II (Takara, Dalian, China), each primer and probe at final concentrations of 0.05 to 0.4 µM (**Table 2**), 2.0 µl template and nuclease-free water. The reaction profile consisting of initial denaturation at 95°C for 30 s, followed by 40 cycles of denaturation at 95°C for 5 s and 40 s annealing/extension at 57°C. Accordingly, the reference strains of these four *Salmonella* serovars were specifically differentiated by the multiplex real-time PCR assay.

Analytical Specificity

The specificity of the multiplex real-time PCR was evaluated using the different bacterial templates listed in **Table 1**. All the *S.* Pullorum, *S.* Gallinarum, *S.* Enteritidis, and *S.* Typhimurium strains produced the corresponding amplified signals (**Figure 2**). Whereas, the non-target bacteria, including other *Salmonella* serovars and non-*Salmonella* strains, yielded negative results in the multiplex real-time PCR (**Table 1**). No false positive or negative results were found, indicating the multiplex real-time PCR was specific.

Standard Curve and Sensitivity of the Multiplex Real-Time PCR Assay

The standard curve of the multiplex real-time PCR assay was constructed using the mean Ct values for various *Salmonella* concentrations corresponding to the genomic DNA. As shown in **Figure 3**, the slopes of the standard curves for *S.* Pullorum, *S.* Gallinarum, *S.* Enteritidis, *S.* Typhimurium were −3.567, −3.464, −3.448, and −3.360, respectively. The correlation coefficients (R^2) were above 0.99, and the amplification efficiencies ranged from 90 to 110%, indicating high linearity for the multiplex real-time PCR assay. The sensitivity analysis showed that the bacterial DNA corresponding to 3 CFU of these four *Salmonella* serovars could be detected for the multiplex real-time PCR assay.

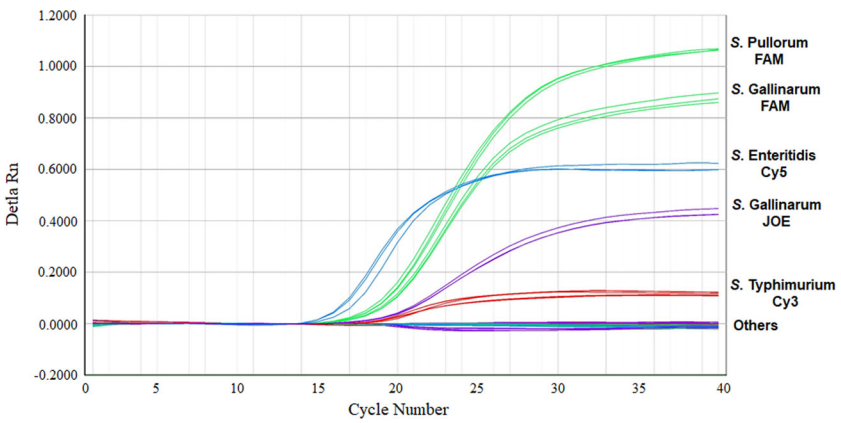

FIGURE 2 | Specificity of the multiplex real-time PCR for the detection and differentiation of *S.* Pullorum, *S.* Gallinarum, *S.* Enteritidis, and *S.* Typhimurium. Others: None of these four *Salmonella* serovars bacteria.

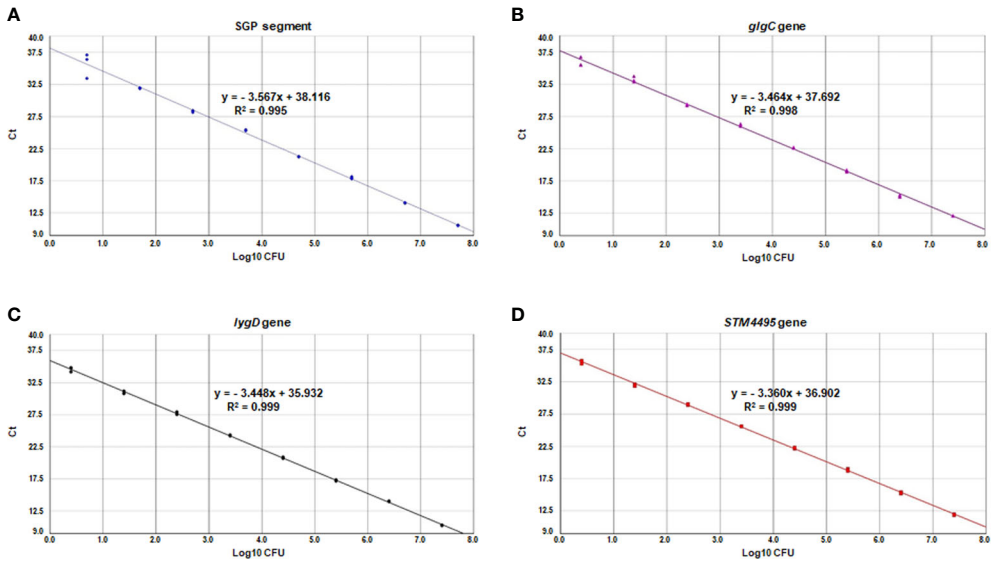

FIGURE 3 | Standard curves of the multiplex real-time PCR for SGP segment **(A)**, *glgC* gene **(B)**, *lygD* gene **(C)**, and *STM4495* gene **(D)** using serially diluted *S.* Pullorum **(A)**, *S.* Gallinarum **(B)**, *S.* Enteritidis **(C)**, and *S.* Typhimurium **(D)** bacterial DNA, respectively.

Limit of Detection in Artificially Contaminated Chicken Samples

The artificially contaminated samples with serial dilutions of each *Salmonella* were tested for the LOD of multiplex real-time PCR assay. For the samples without enrichment, each *Salmonella* of 500 CFU/g could be detected by the multiplex real-time PCR assay. However, when incubated for 6 h for the enrichment, the multiplex real-time PCR assay could successfully detect as low as 10 CFU of each *Salmonella* in 1 g chicken samples.

Clinical Samples Validation

To evaluate the discernibility and applicability of established method for clinical samples, a total of 60 suspected samples were collected and detected using our multiplex real-time PCR and conventional bacteriological tests. After enrichment, 35 of the 60 clinical samples were *Salmonella* positive by multiplex real-time PCR, whereas other samples had no *Salmonella*. Among these positive samples, 21 samples were identified as *S.* Pullorum, one for *S.* Gallinarum, nine for *S.* Enteritidis, and four for *S.* Typhimurium. Same samples were also examined by traditional bacteriological serotyping tests, which was in accordance with the multiplex real-time PCR results with enrichment. Whereas, two *Salmonella* positive samples gave negative results without the additional enrichment step (**Table 3**). This might be due to the limited bacterial amounts in the samples. Thus, the results indicated that the multiplex real-time PCR assay with enrichment is more sensitive than pre-enriched condition to detect the limited amounts of bacteria in samples.

DISCUSSION

It has been shown that *S.* Pullorum, *S.* Gallinarum, *S.* Enteritidis, and *S.* Typhimurium were the prevalent pathogens of salmonellosis in chicken farms (Medalla et al., 2016; Wang et al., 2020; Xu et al., 2020; Zhao et al., 2020; Yu et al., 2021). In addition, *S.* Enteritidis and *S.* Typhimurium could lead to serious zoonotic diseases *via* contaminated food, including poultry products (Coburn et al., 2007). Conventional, *Salmonella* serovars were identified according to the Kauffman-White scheme based on the specific cell-surface O and H antigens. Although serum agglutination assay offers a reliable method for differentiating *Salmonella* serovars, it is labor-intensive, complex, costly, and time-consuming (Schrader et al., 2008). Nowadays, reducing cost and time of experiment are critical for pathogen detection. Therefore, the rapid and accurate detection method has the potential to be of great significance for preventing the spread of salmonellosis. Several molecular methods, such as PCR and loop-mediated isothermal amplification, exist for

TABLE 3 | Consistency evaluation of the multiplex real-time PCR and conventional bacteriological method for the clinical samples.

	S. Pullorum	*S.* Gallinarum	*S.* Enteritidis	*S.* Typhimurium	Total
Multiplex real-time PCR with enrichment	21	1	9	4	35
Multiplex real-time PCR without enrichment	20	1	8	4	33
Bacteriological	21	1	9	4	35

identifying various *Salmonella* serovars with advantages in sensitivity, specificity, and speed (Shi et al., 2015; Yang et al., 2018). Among them, real-time PCR is more sensitive and suitable for high-throughput analysis (Kralik and Ricchi, 2017). Thus, this study developed a multiplex real-time PCR assay that simultaneously detected and differentiated the prevalent *S.* Pullorum, *S.* Gallinarum, *S.* Enteritidis, and *S.* Typhimurium, which exhibited efficiently identification in cultured bacteria and chicken samples.

Selection of specific target genes and design of compatible primers and probes are critical for the proper detection specificity of nucleic acid amplification. Although the homology of the genomes of various *Salmonella* serovars was very high, some genes were found to be related to specific serovars. Various genes, such as genes encoding the O, H, and Vi antigens (*rfb*, *fliC*, *fliB*, *viaB*, *ipaJ*), have been candidates suitable for the specific detection and serotyping of *Salmonella* in diverse clinical samples (Hirose et al., 2002; Hong et al., 2008; Xu et al., 2018). In the present study, analysis of genomic sequences identified a gene segment SGP (GenBank No. CP012347.1 segment 2766328 to 2767027) specifically existing in all *S.* Pullorum and *S.* Gallinarum. A previous study has revealed that the *glgC* gene is deemed to be the preferred target for differentiating *S.* Pullorum and *S.* Gallinarum from other *Salmonella* serovars (Kang et al., 2011). Based on literature (Agron et al., 2001; Akiba et al., 2011), the *S.* Enteritidis specific *lygD* gene and *STM4495* gene specific for *S.* Typhimurium were chosen as targets in this study. As a result, the primers and probes were designed and optimized targeting these specific genes. Furthermore, no mismatch in the primers and probes with the available bacterial genome in GenBank was found by *in silico* analysis. The developed multiplex real-time PCR showed excellent specificity and exclusivity by the detection of *Salmonella* strains as well as other bacterial species. No cross-reactivity, false positives, or false negatives were observed. Previously, real-time PCR assays targeting various specific genes had been applied for *Salmonella* (Lee et al., 2009; Kasturi and Drgon, 2017; Kim et al., 2017; Nair et al., 2019). This study incorporated these four target genes into a unified multiplex real-time PCR assay for the detection and differentiation of multiple *Salmonella* serovars in chicken samples.

In the analytical sensitivity evaluation, the developed multiplex real-time PCR assay was shown to detect as low as the bacterial DNA corresponding to 3 CFU/ml bacterial cultures. Although the LOD of this multiplex real-time PCR was 500 CFU/g in artificially contaminated chicken samples without enrichment, it had more improved detection limits and yielded positive results even at the lowest contamination levels tested (10 CFU/g chicken samples) for the enriched samples. There was some uncertainty, such as PCR inhibitors, competitor organisms, which might result in the lower LOD without enrichment step. Indeed, the pre-enrichment step was effective to increase the number of bacterial cells and to dilute inhibitory substances that exist in the sample. Thus, an additional enrichment step was actually applied to increase the sensitivity of the multiplex real-time PCR (Lee et al., 2009; Ding et al., 2017). The LOD of this multiplex real-time PCR assay was similar to previous studies (Munoz et al., 2010; Kasturi and Drgon, 2017; Liu et al., 2019), indicating its sensitivity for diagnostic purpose. Our multiplex real-time PCR was applied to detect these four *Salmonella* serovars in poultry clinical samples, which achieved same results comparable to the traditional bacteriological examination. However, two of the positive samples were tested as negative by multiplex real-time PCR lack of enrichment step. The possibility remains the amplification inhibition factors or low bacterial concentration in the samples (Lee et al., 2009; Ding et al., 2017). In terms of shortening time for multiple bacterial detection, the entire process of the multiplex real-time PCR assay from sample enrichment to data analysis can be completed in 12 h. The effectiveness of multiplex real-time PCR was significantly improved compared to the traditional culture method.

In summary, this study developed a TaqMan multiplex real-time PCR assay for simultaneous detection and differentiation of prevalent *S.* Pullorum, *S.* Gallinarum, *S.* Enteritidis, and *S.* Typhimurium. Considering the specificity, sensitivity, and effectiveness, the multiplex real-time PCR assay developed herein appears to be a promising tool for clinical diagnostics and epidemiologic study of *Salmonella* in chicken farm and poultry products.

DATA AVAILABILITY STATEMENT

The original contributions presented in the study are included in the article/supplementary material. Further inquiries can be directed to the corresponding authors.

ETHICS STATEMENT

The animal study was reviewed and approved by the Animal Care and Use Committee at the Shanghai Veterinary Research Institute, China.

AUTHOR CONTRIBUTIONS

SW conceived the project. SX and HZ developed the TaqMan multiplex real-time PCR assay and wrote the original manuscript draft. CT, BZ, LY, YZ, and DA were responsible for sampling and sample test. TL, MT, JQ, CD, SY, and SW analyzed and discussed the experimental results. SW and SY directed the experiments, funded the research, and edited the manuscript. All authors contributed to the article and approved the submitted version.

FUNDING

This work was supported by the National Key Research and Development Program of China (2016YFD0500800, 2018YFD0500500), the National Natural Science Foundation of China (31972654), Shanghai Pujiang Program (2019PJD057), Scientific and Technical Innovation Project of the Chinese Academy of Agricultural Sciences, China (SHVRI-ASTIP-2014-8), and the National Basic Fund for Research Institutes, which is supported by the Shanghai Veterinary Research Institute, Chinese Academy of Agricultural Sciences (2021JB07).

REFERENCES

Agron, P. G., Walker, R. L., Kinde, H., Sawyer, S. J., Hayes, D. C., Wollard, J., et al. (2001). Identification by Subtractive Hybridization of Sequences Specific for *Salmonella* Enterica Serovar Enteritidis. *Appl. Environ. Microbiol.* 67, 4984–4991. doi: 10.1128/AEM.67.11.4984-4991.2001

Akiba, M., Kusumoto, M., and Iwata, T. (2011). Rapid Identification of *Salmonella* Enterica Serovars, Typhimurium, Choleraesuis, Infantis, Hadar, Enteritidis, Dublin and Gallinarum, by Multiplex PCR. *J. Microbiol. Methods* 85, 9–15. doi: 10.1016/j.mimet.2011.02.002

Balasubramanian, R., Im, J., Lee, J. S., Jeon, H. J., Mogeni, O. D., Kim, J. H., et al. (2019). The Global Burden and Epidemiology of Invasive non-Typhoidal *Salmonella* Infections. *Hum. Vaccines Immunotherapeut.* 15, 1421–1426. doi: 10.1080/21645515.2018.1504717

Biswas, S., Li, Y., Elbediwi, M., and Yue, M. (2019). Emergence and Dissemination of *Mcr*-Carrying Clinically Relevant *Salmonella* Typhimurium Monophasic Clone St34. *Microorganisms* 7, 298. doi: 10.3390/microorganisms7090298

Coburn, B., Grassl, G. A., and Finlay, B. B. (2007). *Salmonella*, the Host and Disease: A Brief Review. *Immunol. Cell Biol.* 85, 112–118. doi: 10.1038/sj.icb.7100007

Ding, T., Suo, Y., Zhang, Z., Liu, D., Ye, X., Chen, S., et al. (2017). A Multiplex RT-PCR Assay for *S. Aureus*, L. *Monocytogenes*, and *Salmonella Spp.* Detection in Raw Milk With Pre-Enrichment. *Front. Microbiol.* 8, 989. eCollection 2017. doi: 10.3389/fmicb.2017.00989.eCollection2017

Hirose, K., Itoh, K., Nakajima, H., Kurazono, T., Yamaguchi, M., Moriya, K., et al. (2002). Selective Amplification of Tyv (*Rfbe*), *Prt* (*Rfbs*), Viab, and *fliC* Genes by Multiplex PCR for Identification of Salmonella *Enterica* Serovars Typhi and Paratyphi A. *J. Clin. Microbiol.* 40, 633–636. doi: 10.1128/JCM.40.02.633-636.2002

Hong, Y., Liu, T., Lee, M. D., Hofacre, C. L., Maier, M., White, D. G., et al. (2008). Rapid Screening of *Salmonella* Enterica Serovars Enteritidis, Hadar, Heidelberg and Typhimurium Using a Serologically-Correlative Allelotyping PCR Targeting the O and H Antigen Alleles. *BMC Microbiol.* 8:178. doi: 10.1186/1471-2180-8-178

Issenhuth-Jeanjean, S., Roggentin, P., Mikoleit, M., Guibourdenche, M., De Pinna, E., Nair, S., et al. (2014). Supplement 2008-2010 (No. 48) to the White-Kauffmann-Le Minor Scheme. *Res. Microbiol.* 165, 526–530. doi: 10.1016/j.resmic.2014.07.004

Kang, M. S., Kwon, Y. K., Jung, B. Y., Kim, A., Lee, K. M., An, B. K., et al. (2011). Differential Identification of *Salmonella* Enterica Subsp. Enterica Serovar Gallinarum Biovars Gallinarum and Pullorum Based on Polymorphic Regions of *glgC* and *speC* Genes. *Vet. Microbiol.* 147, 181–185. doi: 10.1016/j.vetmic.2010.05.039

Kasturi, K. N., and Drgon, T. (2017). Real-Time PCR Method for Detection of *Salmonella* Spp. In Environmental Samples. *Appl. Environ. Microbiol.* 83, e00644–17. doi: 10.1128/AEM.00644-17

Kawasaki, S., Fratamico, P. M., Horikoshi, N., Okada, Y., Takeshita, K., Sameshima, T., et al. (2010). Multiplex Real-Time Polymerase Chain Reaction Assay for Simultaneous Detection and Quantification of *Salmonella* Species, Listeria Monocytogenes, and *Escherichia Coli* O157:H7 in Ground Pork Samples. *Foodborne. Pathog. Dis.* 7, 549–554. doi: 10.1089/fpd.2009.0465

Keerthirathne, T. P., Ross, K., Fallowfield, H., and Whiley, H. (2017). Reducing Risk of Salmonellosis Through Egg Decontamination Processes. *Int. J. Environ. Res. Public Health* 14, 335. doi: 10.3390/ijerph14030335

Kim, T. H., Hwang, H. J., and Kim, J. H. (2017). Development of a Novel, Rapid Multiplex Polymerase Chain Reaction Assay for the Detection and Differentiation of *Salmonella* Enterica Serovars Enteritidis and Typhimurium Using Ultra-Fast Convection Polymerase Chain Reaction. *Foodborne. Pathog. Dis.* 14, 580–586. doi: 10.1089/fpd.2017.2290

Kim, H. J., Park, S. H., and Kim, H. Y. (2006). Comparison of *Salmonella* Enterica Serovar Typhimurium LT2 and non-LT2 *Salmonella* Genomic Sequences, and Genotyping of *Salmonellae* by Using PCR. *Appl. Environ. Microbiol.* 72, 6142–6151. doi: 10.1128/AEM.00138-06

Kralik, P., and Ricchi, M. (2017). A Basic Guide to Real Time PCR in Microbial Diagnostics: Definitions, Parameters, and Everything. *Front. Microbiol.* 8, 108. doi: 10.3389/fmicb.2017.00108

Lee, S. H., Jung, B. Y., Rayamahji, N., Lee, H. S., Jeon, W. J., Choi, K. S., et al. (2009). A Multiplex Real-Time PCR for Differential Detection and Quantification of *Salmonella* Spp., *Salmonella* Enterica Serovar Typhimurium and Enteritidis in Meats. *J. Vet. Sci.* 10, 43–51. doi: 10.4142/jvs.2009.10.1.43

Liu, Y., Cao, Y., Wang, T., Dong, Q., Li, J., and Niu, C. (2019). Detection of 12 Common Food-Borne Bacterial Pathogens by TaqMan Real-Time PCR Using a Single Set of Reaction Conditions. *Front. Microbiol.* 10, 222. doi: 10.3389/fmicb.2019.00222

Liu, Y., Jiang, J., Ed-Dra, A., Li, X., Peng, X., Xia, L., et al. (2021). Prevalence and Genomic Investigation of *Salmonella* Isolates Recovered From Animal Food-Chain in Xinjiang, China. *Food Res. Int.* 142, 110198. doi: 10.1016/j.foodres.2021.110198

Liu, B., Zhang, L., Zhu, X., Shi, C., Chen, J., Liu, W., et al. (2011). PCR Identification of *Salmonella* Serogroups Based on Specific Targets Obtained by Comparative Genomics. *Int. J. Food Microbiol.* 144, 511–518. doi: 10.1016/j.ijfoodmicro.2010.11.010

Majowicz, S. E., Musto, J., Scallan, E., Angulo, F. J., Kirk, M., O'brien, S. J., et al. (2010). The Global Burden of Nontyphoidal *Salmonella* Gastroenteritis. *Clin. Infect. Dis.* 50, 882–889. doi: 10.1086/650733

Medalla, F., Gu, W., Mahon, B. E., Judd, M., Folster, J., Griffin, P. M., et al. (2016). Estimated Incidence of Antimicrobial Drug-Resistant Nontyphoidal *Salmonella* Infections, United States 2004-2012. *Emerging. Infect. Dis.* 23, 29–37. doi: 10.3201/eid2301.160771

Munoz, N., Diaz-Osorio, M., Moreno, J., Sanchez-Jimenez, M., and Cardona-Castro, N. (2010). Development and Evaluation of a Multiplex Real-Time Polymerase Chain Reaction Procedure to Clinically Type Prevalent *Salmonella* Enterica Serovars. *J. Mol. Diagn.* 12, 220–225. doi: 10.2353/jmoldx.2010.090036

Nair, S., Patel, V., Hickey, T., Maguire, C., Greig, D. R., Lee, W., et al. (2019). Real-Time PCR Assay for Differentiation of Typhoidal and Nontyphoidal *Salmonella*. *J. Clin. Microbiol.* 57, e00167–19. doi: 10.1128/JCM.00167-19

Prendergast, D. M., Hand, D., Niota Ghallchoir, E., Mccabe, E., Fanning, S., Griffin, M., et al. (2013). A Multiplex Real-Time PCR Assay for the Identification and Differentiation of *Salmonella* Enterica Serovar Typhimurium and Monophasic Serovar 4,[5],12:I. *Int. J. Food Microbiol.* 166, 48–53. doi: 10.1016/j.ijfoodmicro.2013.05.031

Schrader, K. N., Fernandez-Castro, A., Cheung, W. K., Crandall, C. M., and Abbott, S. L. (2008). Evaluation of Commercial Antisera for *Salmonella* Serotyping. *J. Clin. Microbiol.* 46, 685–688. doi: 10.1128/JCM.01808-07

Shah, D. H., Park, J. H., Cho, M. R., Kim, M. C., and Chae, J. S. (2005). Allele-Specific PCR Method Based on *rfbS* Sequence for Distinguishing *Salmonella* Gallinarum From *Salmonella* Pullorum: Serotype-Specific *rfbS* Sequence Polymorphism. *J. Microbiol. Methods* 60, 169–177. doi: 10.1016/j.mimet.2004.09.005

Shi, C., Singh, P., Ranieri, M. L., Wiedmann, M., and Moreno Switt, ,. A. I. (2015). Molecular Methods for Serovar Determination of *Salmonella*. *Crit. Rev. Microbiol.* 41, 309–325. doi: 10.3109/1040841X.2013.837862

Wang, J., Li, J., Liu, F., Cheng, Y., and Su, J. (2020). Characterization of *Salmonella* Enterica Isolates From Diseased Poultry in Northern China Between 2014 and 2018. *Pathogens* 9, 95. doi: 10.3390/pathogens9020095

Xu, L., Liu, Z., Li, Y., Yin, C., Hu, Y., Xie, X., et al. (2018). A Rapid Method to Identify *Salmonella* Enterica Serovar Gallinarum Biovar Pullorum Using a Specific Target Gene *ipaJ*. *Avian Pathol.* 47, 238–244. doi: 10.1080/03079457.2017.1412084

Xu, Y., Zhou, X., Jiang, Z., Qi, Y., Ed-Dra, A., and Yue, M. (2020). Epidemiological Investigation and Antimicrobial Resistance Profiles of *Salmonella* Isolated From Breeder Chicken Hatcheries in Henan, China. *Front. Cell. Infect. Microbiol.* 10, 497. doi: 10.3389/fcimb.2020.00497

Yang, Q., Domesle, K. J., and Ge, B. (2018). Loop-Mediated Isothermal Amplification for *Salmonella* Detection in Food and Feed: Current Applications and Future Directions. *Foodborne. Pathog. Dis.* 15, 309–331. doi: 10.1089/fpd.2018.2445

Yu, X., Zhu, H., Bo, Y., Li, Y., Zhang, Y., Liu, Y., et al. (2021). Prevalence and Antimicrobial Resistance of *Salmonella* Enterica Subspecies Enterica Serovar Enteritidis Isolated From Broiler Chickens in Shandong Province, China 2013-2018. *Poult. Sci.* 100, 1016–1023. doi: 10.1016/j.psj.2020.09.079

Zhang, X., Payne, M., and Lan, R. (2019). In Silico Identification of Serovar-Specific Genes for Salmonella Serotyping. *Front. Microbiol.* 10, 835. doi: 10.3389/fmicb.2019.00835

Zhao, X., Hu, M., Zhang, Q., Zhao, C., Zhang, Y., Li, L., et al. (2020). Characterization of Integrons and Antimicrobial Resistance in *Salmonella* From Broilers in Shandong, China. *Poult. Sci.* 99, 7046–7054. doi: 10.1016/j.psj.2020.09.071

Conflict of Interest: The authors declare that the research was conducted in the absence of any commercial or financial relationships that could be construed as a potential conflict of interest.

Publisher's Note: All claims expressed in this article are solely those of the authors and do not necessarily represent those of their affiliated organizations, or those of the publisher, the editors and the reviewers. Any product that may be evaluated in this article, or claim that may be made by its manufacturer, is not guaranteed or endorsed by the publisher.

frontiers in Cellular and Infection Microbiology

ORIGINAL RESEARCH
published: 03 January 2022
doi: 10.3389/fcimb.2021.784610

Clinical Performance of the Xpert® CT/NG Test for Detection of *Chlamydia trachomatis* and *Neisseria gonorrhoeae*: A Multicenter Evaluation in Chinese Urban Hospitals

Yan Han[1,2†], Mei-Qin Shi[1,2†], Qing-Ping Jiang[3], Wen-Jing Le[1], Xiao-Lin Qin[4], Han-Zhen Xiong[3], He-Ping Zheng[4], Fred C. Tenover[5], Yi-Wei Tang[6] and Yue-Ping Yin[1,2]*

[1] Institute of Dermatology, Chinese Academy of Medical Sciences & Peking Union Medical College, Nanjing, China, [2] National Center for STD Control, Chinese Center for Disease Control and Prevention, Nanjing, China, [3] Depatment of Pathology, Third Affiliated Hospital, Guangzhou Medical University, Guangzhou, China, [4] Dermatology Hospital, Southern Medical University, Guangzhou, China, [5] Department of Medical and Scientific Affairs, Cepheid, Sunnyvale, CA, United States, [6] Department of Medical and Scientific Affairs, Danaher Diagnostic Platform China/Cepheid, Shanghai, China

OPEN ACCESS

Edited by:
Hongchao Gou,
Guangdong Academy of Agricultural Sciences, China

Reviewed by:
Bryan Schmitt,
Children's MN, United States
Dania AlQasrawi,
Mayo Clinic Florida, United States

***Correspondence:**
Yue-Ping Yin
yinyp@ncstdlc.org

[†]These authors have contributed equally to this work

Specialty section:
This article was submitted to Clinical Microbiology, a section of the journal Frontiers in Cellular and Infection Microbiology

Received: 28 September 2021
Accepted: 25 November 2021
Published: 03 January 2022

Citation:
Han Y, Shi M-Q, Jiang Q-P, Le W-J, Qin X-L, Xiong H-Z, Zheng H-P, Tenover FC, Tang Y-W and Yin Y-P (2022) Clinical Performance of the Xpert® CT/NG Test for Detection of Chlamydia trachomatis and Neisseria gonorrhoeae: A Multicenter Evaluation in Chinese Urban Hospitals. Front. Cell. Infect. Microbiol. 11:784610. doi: 10.3389/fcimb.2021.784610

Background: We aimed to evaluate the clinical performance of the GeneXpert® (Xpert) CT/NG assay for the detection of *Chlamydia trachomatis* (CT) and *Neisseria gonorrhoeae* (NG) using urine and cervical swabs collected from patients in China.

Methods: This study was conducted from September 2016 to September 2018 in three Chinese urban hospitals. The results from the Xpert CT/NG test were compared to those from the Roche cobas® 4800 CT/NG test. Discordant results were confirmed by DNA sequence analysis.

Results: In this study, 619 first void urine (FVU) specimens and 1,042 cervical swab specimens were included in the final dataset. There were no statistical differences between the results of the two tests for the detection of CT/NG in urine samples ($p > 0.05$), while a statistical difference was found in cervical swabs ($p < 0.05$). For CT detection, the sensitivity and specificity of the Xpert test were 100.0% (95%CI = 96.8–99.9) and 98.3% (95%CI = 96.6–99.2) for urine samples and 99.4% (95%CI = 96.5–100.0) and 98.6% (95%CI 97.5–99.2) for cervical swabs, respectively. For NG detection, the sensitivity and specificity of the Xpert test were 99.2% (95%CI = 94.9–100.0) and 100.0% (95%CI = 99.0–100.0) for urine and 100% (95%CI = 92.8–100.0) and 99.7% (95%CI = 99.0–99.9) for cervical swabs, respectively.

Conclusion: The Xpert CT/NG test exhibited high sensitivity and specificity in the detection of CT and NG in both urine and cervical samples when compared to the

reference results. The 90-min turnaround time for CT and NG detection at the point of care using Xpert may enable patients to receive treatment promptly.

Keywords: *Chlamydia trachomatis*, *Neisseria gonorrhoeae*, molecular testing, urine, cervical swabs, point-of-care testing

INTRODUCTION

Chlamydia trachomatis (CT) and *Neisseria gonorrhoeae* (NG) are two of the most common sexually transmitted bacterial pathogens across the world and are the main contributors to sexually transmitted infections (STIs) in China. Both infections can have serious sequelae, especially in women, including pelvic inflammatory disease, which can lead to ectopic pregnancy and infertility (Baud et al., 2008; Ginocchio et al., 2012) and facilitate the risk of HIV transmission (Cohen et al., 1999; Bernstein et al., 2010). The World Health Organization (WHO) estimated that the incident cases for CT were 127.2 million and for NG were 86.9 million in 2016 (Rowley et al., 2019). The average duration of CT is 1.4 years (Price et al., 2013), and that of NG is about 6 months in the absence of antimicrobial treatment (Grad et al., 2016). Most CT or NG infections are asymptomatic. The slower the clearance occurs, the higher the prevalence of untreated infection and the more effective a screening intervention is needed to be.

Traditionally, culture was used as the gold standard for the diagnosis of CT and NG. With the development of science and technology, nucleic acid amplification tests (NAATs) are currently recommended as the diagnostic methods for CT and NG in most high-income countries due to their high specificity and sensitivity (Garrett et al., 2016). The traditional culture method for CT is time-consuming, tedious, and typically requires cell culture preparations, such as McCoy, Hela 229, or Buffalo green monkey kidney cells. The samples need to be centrifuged, incubated for 48–72 h, and examined by microscopy (Barnes, 1989; Centers for Disease Control and Prevention, 2014). In contrast, nucleic acid amplification tests amplify the unique target sequences in a microorganism in real-time rapidly, which means identifying microorganisms directly in clinical specimens. However, this can potentially also be a long process. For example, most of the commercially available NAATs for CT and NG registered in China with the National Medical Products Administration (NMPA) require multiple steps and expensive equipment and take 1 or 2 days to generate results. On the other hand, the Cepheid GeneXpert® (Xpert) CT/NG assay is a rapid NAAT assay that can be performed on the GeneXpert instrument platform in laboratories and is simple to operate. The Xpert test detects the DNA of CT and NG in specimens by nucleic acid amplification in approximately 90 min. Anywhere from 1 to 80 specimens can be processed simultaneously depending on the type of the instrument used and the number of samples processed per day. The easy-to-use modular cartridges minimize the processing steps and control contamination. The assay was approved by the United States Food and Drug Administration and was CE-IVD (European CE Marking for *In Vitro* Diagnostic devices) marked in 2012. In order to introduce this assay into China, we undertook this study to compare the Xpert CT/NG test to the Roche Cobas 4800CT/NG, which was approved by the China NMPA in 2014.

MATERIALS AND METHODS

Study Population

This evaluation was conducted from September 2016 to September 2018 in three sites: 1) Institute of Dermatology, Chinese Academy of Medical Sciences and Peking Union Medical College, 2) Dermatology Hospital of Southern Medical University, and 3) The Third Affiliated Hospital of Guangzhou Medical University. All sites obtained institutional review board approval for the clinical study in accordance with the Declaration of Helsinki. The approval numbers for the study in three sites were 2016-LS-009, GDDHLS-20171201, and YLSJ-2018-002 for the Institute of Dermatology, the Chinese Academy of Medical Sciences and Peking Union Medical College, Dermatology Hospital of Southern Medical University, and The Third Affiliated Hospital of Guangzhou Medical University, respectively. The patients were ≥18 years of age and sought healthcare in sexually transmitted disease clinics in two dermatology hospitals or the Obstetrics and Gynecology Clinic in the general hospital. They signed an informed consent form and confirmed their willingness to provide urine or cervical swabs for this study.

Specimen Collection

Female patients were encouraged to provide cervical swabs and first void urine (FVU), while male patients were asked to provide FVU. The FVU specimens were collected in a urine cup by the patients. Approximately 5–7 ml of urine was aliquoted into the urine collection device of each manufacturer, which contained a preservative. The remaining urine was transferred into a cryogenic vial and frozen at −20°C at the local hospitals. The healthcare technicians collected two cervical swabs, and the order of cervical specimen collection was randomized for transfer into the cobas® or Cepheid® PCR Media tube, such that swabs for each of the two test assays had equal opportunity to be collected first or second. All swab samples were collected and transported according to the package insert directions of each manufacturer. Leftover specimens were stored at 4°C refrigerators in the local hospitals.

Laboratory Testing

The Xpert test was performed according to the instructions of the manufacturer instructions at each study site. Of the prepared sample, 300 µl was transferred into the sample chamber in the

cartridge, and an elution reagent was pipetted into the cartridge. Then, the cartridge was inserted into the GeneXpert platform and the test was initiated. The test included a specimen adequacy control and an amplification control. The adequacy control is to ensure that there is sufficient human DNA in the sample, and the amplification control is to guarantee an effective amplification of nucleic acid in the specimen. Results included a specimen adequacy control result and an amplification control result. The results were reported in <2 h as positive or negative for chlamydia, positive or negative for gonorrhea, or indeterminate (reading invalid, error, or no result). When a test failed or the test was read as indeterminate, the specimen was retested one additional time using a new aliquot of the specimen, if available, and a new Xpert cartridge.

The cobas® 4800 CT/NG assay (Roche Molecular Systems, Branchburg, NJ, USA) was used as the reference test to detect CT and NG according to the manufacturer's instructions. The cobas® x 480 instrument was used to extract nucleic acid from the urine and cervical samples and distribute it into the PCR reaction mixture. The cobas® z 480 analyzer was used to fully automate PCR amplification and detection. The test results were automatically reported according to the preset computer algorithm. The results were reported as positive, negative, or invalid for CT; positive, negative, or invalid for NG; or failed. Repeated equivocal results were reported as invalid or failed.

Data Analysis

Samples yielding indeterminate results in the second run after failing the first run were not included in the final dataset (Bristow et al., 2017). Concordance, positive percent agreement, and negative percent agreement were calculated for CT and NG for the urine and cervical swab samples. McNemar's test was used to compare the performances of the Xpert and the Roche cobas CT/NG tests. Concordant results for specimens were defined as positive or negative if the Xpert and Roche cobas CT/NG assays gave the same results for CT or NG. For discordant results of CT or NG, the samples underwent DNA sequence analysis for CT or NG conducted by independent clinical laboratories in China (the Guangzhou and Nanjing central laboratories operated by KingMed Diagnostics). The sensitivity and specificity of the Xpert assay for CT and NG were calculated by comparing with the final results for urine and cervical swabs, respectively.

RESULTS

During the study period, 657 participants provided FVU and 1,107 participants provided cervical swabs; 38 FVU specimens and 65 cervical swab specimens did not meet the study criteria or gave indeterminate Xpert results and were excluded from the analysis. Ultimately, 619 FVU specimens and 1,042 cervical swab specimens were included in the final dataset (**Figure 1**). The average age of the participants who provided FVU was 34.0 years (SD ± 9.95 years, range = 18–68 years), and 47.7% (295/619) were women. Furthermore, 197 (31.8%) urine specimens were obtained from the Institute of Dermatology, Chinese Academy of Medical Sciences, and Peking Union Medical College. The average age of participants who provided cervical swabs was 32.8 years (SD ± 9.0 years, range = 18–64 years).

The Xpert CT/NG test was performed on 1,764 specimens collected at three sites, with 91.0% (1,605/1,764) producing a valid result in the first test. There were 144 samples reported as indeterminant in the first run by the Xpert test, and four of them were also reported as indeterminant by the Roche test. There were 84 and 62 indeterminate results in the urine (12.8%, 84/657) and cervical samples (5.6%, 62/1,107), respectively. The majority (128/144, 89.9%) of the samples yielded valid results after retesting. Among these were 11 specimens reported after retesting as positive for CT and 5 specimens reported as positive for NG. Additionally, positive CT and NG results were reported for 20 and 10 specimens, respectively. All were initially

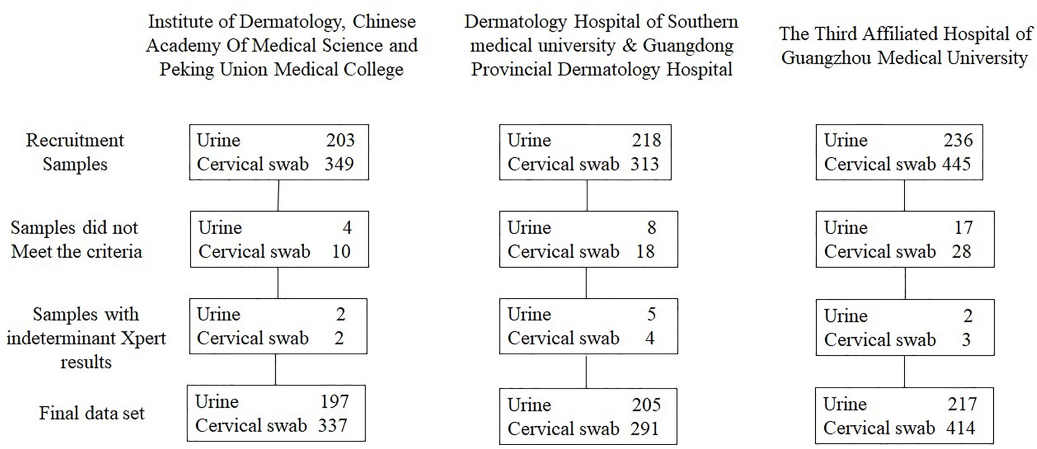

FIGURE 1 | The flowchart for the sample collection.

TABLE 1 | Indeterminate results yielded in the first run and retested in the second run using the Xpert assay.

Indeterminate		Urine retest results		Cervical swabs retest results	
		CT	NG	CT	NG
Invalid	Negative	32	33	12	17
	Positive	2	1	9	4
ERROR	Negative	15	18	20	27
	Positive	10	7	10	3
No result	Negative	5	2	2	1
	Positive	11	14	0	1
Total		75	75	53	53

reported as errors. Finally, among the specimens reported as "no result" in the first run, 11 were reported as positive CT, and 15 were reported as positive NG in the second run (**Table 1**). Among the 619 urine samples, 163 were CT positive and 121 were NG positive when using the Xpert assay, while 156 were CT positive and 125 were NG positive using the Roche test. Xpert reported 191 CT positive and 66 NG positive results among 1,042 cervical swabs. The Roche cobas® 4800 CT/NG assay gave 177 CT positive and 60 NG positive results. There were 617 urine samples that reported the same CT results using the two tests and 11 urine samples that yielded different results between Xpert and Roche cobas (McNemar and Fisher's exact test = 0.065). Similarly, there were 1,010 cervical swabs with the same results and 32 cervical samples with different results (McNemar's $\chi^2 = 6.125$, $p = 0.013$). Six hundred and thirteen urine samples gave concurrent NG results, but six urine samples reported different NG results by the Xpert and Roche cobas tests (McNemar and Fisher's exact test = 0.219). A total of 1,036 cervical swabs had the same NG results, while six cervical samples (McNemar's $\chi^2 = 6.000$, $p = 0.014$) had different NG results detected by the Xpert and Roche tests (**Table 2**).

Table 3 provides a summary of the concordance between the Xpert and Roche tests for the detection of urogenital CT and NG. For CT infection, the concordance was 98.2% (95%CI = 96.8–99.1) using the urine samples, with 98.6% (95%CI = 95.2–99.8) agreement among positive samples and 98.1% (95%CI = 96.4–99.1) agreement among negative samples. The concordance was 96.9% (95%CI = 95.7–97.9) for the cervical swabs, with 94.9% (95%CI = 90.6–97.7) agreement among positive samples and 97.3% (95%CI = 96.0–98.3) agreement among negative samples. For NG infection, the concordance was 99.0% (95%CI = 97.9–99.6) using the urine samples, with 96.0% (95%CI = 91.0–98.7) agreement among positive samples and 99.8% (95%CI = 98.9–100.0) agreement among negative samples. The concordance was 99.4% (95%CI = 98.8–99.8) for cervical swabs, with 100.0% (95% CI = 90.4–100.0) agreement among positive samples and 99.4% (95%CI = 98.7–99.8) agreement among negative samples.

The discordant results were resolved by DNA sequence analysis, shown in **Table 4**. Three urine samples (27.3%) were confirmed by the DNA sequence analysis as having the same results as those by Xpert for the detection of CT among 11 samples with discordant results produced by the Xpert and Roche assays, and 19 sequence results for the cervical samples (59.4%, 19/32) were the same as those of Xpert for the detection of CT. Five urine samples (83.3%, 5/6) and three cervical swabs (50%, 3/6) showing discordant results were verified by DNA

TABLE 2 | Comparison of Cepheid GeneXpert® and Roche cobas® 4800 CT/NG tests for the detection of urogenital *Chlamydia trachomatis* (CT) and *Neisseria gonorrhoeae* (NG).

			Xpert-CT				Xpert-NG	
			Negative	Positive			Negative	Positive
Urine	Roche-CT	Negative	463	9	Roche-NG	Negative	493	1
		Positive	2	154		Positive	5	120
Cervical swab	Roche-CT	Negative	842	23	Roche-NG	Negative	976	6
		Positive	9	168		Positive	0	60

TABLE 3 | Concordance between Cepheid GeneXpert® and Roche cobas® 4800 CT/NG tests for detection of urogenital *Chlamydia trachomatis* (CT) and *Neisseria gonorrhoeae* (NG).

			Xpert-CT				Xpert-NG	
			Negative	Positive			Negative	Positive
Urine	Roche-CT	Negative	463	9	Roche-NG	Negative	493	1
		Positive	2	154		Positive	5	120
Cervical swab	Roche-CT	Negative	842	23	Roche-NG	Negative	976	6
		Positive	9	168		Positive	0	60

TABLE 4 | Results of the validation for the discordant results detected by Cepheid GeneXpert® (Xpert) and Roche cobas® 4800 CT/NG tests for urogenital *Chlamydia trachomatis* (CT) and *Neisseria gonorrhoeae* (NG) .

Sequencing results		CT		Sequencing results		NG	
		Xpert positive and Roche negative	Xpert negative and Roche positive			Xpert positive and Roche negative	Xpert negative and Roche positive
CT-urine	Positive	1	0	NG-urine	Positive	1	1
	Negative	8	2		Negative	0	4
CT-swab	Positive	11	1	NG-swab	Positive	3	0
	Positive	12	8		Negative	3	0

sequencing as having the same results as those by Xpert for the detection of NG (**Table 4**). For CT infection after discrepant resolution, the sensitivity and specificity of the Xpert assay using urine estimates were 100.0% (95%CI = 96.8–99.9) and 98.3% (95%CI = 96.6–99.2), respectively. The sensitivity and specificity using cervical swab estimates were 99.4% (95%CI = 96.5–100.0) and 98.6% (95%CI = 97.5–99.2), respectively. For NG infection, the sensitivity and specificity of the Xpert assay using urine samples were 99.2% (95%CI = 94.9–100.0) and 100.0% (95% CI = 99.0–100.0), respectively. The sensitivity and specificity using cervical swab estimates were 100% (95%CI = 92.8–100.0) and 99.7% (95%CI = 99.0–99.9), respectively (**Table 5**).

DISCUSSION

This study is the first multicenter study in China to evaluate the performance of the Xpert CT/NG assay for the real-time simultaneous detection of chlamydia and gonorrhea using urine and cervical swab specimens. In this study, 8.3% of the specimens were initially reported either as "error", "invalid", or "no result" by the Xpert test, so the results could not be reported as either positive or negative. The reasons for indeterminate results include high sample viscosity, often due either to the presence of mucus, which interferes with amplification; or the presence of PCR inhibitors in the specimen, such as blood, which also gives an invalid result (Schrader et al., 2012; Parcell et al., 2015). After retesting, 89.9% of the samples with indeterminate results gave a valid result using the Xpert CT/NG test. This rate was comparable to that observed in a previous study with the cobas assay (i.e., ~80%) (Parcell et al., 2015). The results of the Xpert CT/NG test showed high concordance with the Roche cobas® 4800 CT/NG results for the detection of CT and NG using urine specimens. There were no statistical differences between these two assays (McNemar and Fisher's exact test = 0.065 and 0.219 for CT and NG, respectively), and the results demonstrated concordance for urine of 98.2% and 99.0% for CT and NG, respectively. The high concordance between the results of the Xpert and Roche cobas® 4800 CT/NG assays for the detection of CT and NG has previously been reported for urine samples (Causer et al., 2018; Speers et al., 2018) and rectal swabs (Badman et al., 2019). The Xpert CT/NG test results also showed high concordance with those of Roche cobas 4800 CT/NG for the detection of CT and NG using cervical swabs (CT: 96.9%, 95% CI = 95.7–97.9; NG: 99.4%, 95%CI = 98.8–99.8). These two assays showed statistical differences (CT: McNemar's $\chi^2 = 6.125$, $p = 0.013$: NG: McNemar's $\chi^2 = 6.000$, $p = 0.014$). For CT infection, the sensitivity for both urine samples and cervical swabs was near perfect and the specificity values were 98.3% and 98.6% for urine samples and cervical swabs, respectively. For NG infection, the sensitivity and the specificity for the urine samples and cervical swabs were both higher than 99.0%. These results were comparable to those of previous evaluation studies (Gaydos et al., 2013; Herbst-de-Cortina et al., 2016; Bristow et al., 2019; Xie et al., 2020).

The Xpert CT/NG assay was the first nucleic acid-based test for CT and NG available for point-of-care (POC) use. Generally, this assay can be completed in 90 min, reducing the delay in reporting the results and potentially enabling rapid effective treatment. It satisfies the REASSURED criteria for the design of STI diagnostic tests: real-time connectivity, ease of specimen collection, affordable, sensitive, specific, user-friendly, rapid and robust, equipment-free or requiring only simple epuipment, environment-friendly, and deliverable to end-users (Land et al., 2019). Prior unpublished data suggested that more than half (225/446, 50.4%) of patients preferred to pay higher expenses to obtain highly effective detection (high sensitivity and specificity with a reduced turnaround time). Nearly 62.8% (279/446) of patients would prefer to pay less than 60 Yuan Renminbi (US $9.4) for CT infection tests. This means that, if the cost of this assay was less than US $20, nearly more than half of patients would choose this assay for a reduced reporting time with high performance.

TABLE 5 | Sensitivity and specificity of the Cepheid GeneXpert® CT/NG test for the detection of urogenital *Chlamydia trachomatis* (CT) and *Neisseria gonorrhoeae* (NG).

		Sensitivity (95%CI)	Specificity (95%CI)
Urine	CT	100.0% (96.8–99.9)	98.3% (96.6–99.2)
	NG	99.2% (94.9–100.0)	100.0% (99.0–100.0)
Cervical swabs	CT	99.4% (96.5–100.0)	98.6% (97.5–99.2)
	NG	100% (92.8–100.0)	99.7% (99.0–99.9)

There are some limitations to this study. Firstly,we did not evaluate the vaginal swabs for female patients. Vaginal swabs tend to be preferable among female patients due to reduced pain and easy collection. Secondly, this assay was performed by trained technicians in urban hospitals which may not reflect the performance of this assay in remote settings with clinicians in the real world.

The Xpert CT/NG assay exhibited high sensitivity and specificity for the detection of CT and NG in urine samples and cervical swabs. The short turnaround time of this assay can be useful in reducing the reporting time and enable more patients to receive treatments quickly, thus potentially improving chlamydia and gonorrhea control efforts. The one drawback to the assay is the initial number of indeterminate results, which was approximately 8%, although most were resolved on retesting.

DATA AVAILABILITY STATEMENT

The original contributions presented in the study are included in the article/supplementary material. Further inquiries can be directed to the corresponding author.

ETHICS STATEMENT

The studies involving human participants were reviewed and approved by the Institute of Dermatology, the Chinese Academy of Medical Sciences and Peking Union Medical College, Dermatology Hospital of Southern Medical University, and The Third Affiliated Hospital of Guangzhou Medical University. The patients/participants provided written informed consent to participate in this study.

AUTHOR CONTRIBUTIONS

YH analyzed the data, interpreted the findings, and drafted the manuscript. MS and YY conceived the study and supervised all aspects of its implementation. QJ, HX, WL, and HZ recruited the subjects from the sites and examined the collected samples. WL recruited the subjects from the Nanjing site. MS examined the collected samples from the Nanjing site. FT and YT reviewed the drafts of the manuscripts. All authors contributed to the article and approved the submitted version.

FUNDING

This study was funded by Danaher Diagnostic Platform China/ Cepheid, Shanghai, China.

ACKNOWLEDGMENTS

We are grateful for the sites where this study took place and to the participants of this study for their cooperation.

REFERENCES

Badman, S. G., Willie, B., Narokobi, R., Gabuzzi, J., Pekon, S., Amos-Kuma, A., et al. (2019). A Diagnostic Evaluation of a Molecular Assay Used for Testing and Treating Anorectal Chlamydia and Gonorrhoea Infections at the Point-of-Care in Papua New Guinea. *Clin. Microbiol. Infect.* 25, 623–627. doi: 10.1016/j.cmi.2018.08.001

Barnes, R. C. (1989). Laboratory Diagnosis of Human Chlamydial Infections. *Clin. Microbiol. Rev.* 2, 119–136. doi: 10.1128/CMR.2.2.119

Baud, D., Regan, L., and Greub, G. (2008). Emerging Role of Chlamydia and Chlamydia-Like Organisms in Adverse Pregnancy Outcomes. *Curr. Opin. Infect. Dis.* 21, 70–76. doi: 10.1097/QCO.0b013e3282f3e6a5

Bernstein, K. T., Marcus, J. L., Nieri, G., Philip, S. S., and Klausner, J. D. (2010). Rectal Gonorrhea and Chlamydia Reinfection Is Associated With Increased Risk of HIV Seroconversion. *J. Acquir. Immune Defic. Syndr.* 53, 537–543. doi: 10.1097/QAI.0b013e3181c3ef29

Bristow, C. C., McGrath, M. R., Cohen, A. C., Anderson, L. J., Gordon, K. K., and Klausner, J. D. (2017). Comparative Evaluation of 2 Nucleic Acid Amplification Tests for the Detection of Chlamydia Trachomatis and Neisseria Gonorrhoeae at Extragenital Sites. *Sex. Transm. Dis.* 44 (7), 398–400. doi: 10.1097/OLQ.0000000000000627

Bristow, C. C., Morris, S. R., Little, S. J., Mehta, S. R., and Klausner, J. D. (2019). Meta-Analysis of the Cepheid Xpert® CT/NG Assay for Extragenital Detection of Chlamydia Trachomatis (CT) and Neisseria Gonorrhoeae (NG) Infections. *Sexual Health* 16, 314–319. doi: 10.1071/SH18079

Causer, L. M., Guy, R. J., Tabrizi, S. N., Whiley, D. M., Speers, D. J., Ward, J., et al. (2018). Molecular Test for Chlamydia and Gonorrhoea Used at Point of Care in Remote Primary Healthcare Settings: A Diagnostic Test Evaluation. *Sex Transm. Infect.* 94, 340–345. doi: 10.1136/sextrans-2017-053443

Centers for Disease Control and Prevention (2014). Recommendations for the Laboratory-Based Detection of Chlamydia Trachomatis and Neisseria Gonorrhoeae–2014. MMWR. Recommendations and Reports : Morbidity and Mortality Weekly Report. *Recommendations Rep.* 63, 1–19.

Cohen, C. R., Plummer, F. A., Mugo, N., Maclean, I., Shen, C., Bukusi, E. A., et al. (1999). Increased Interleukin-10 in the Endocervical Secretions of Women With Non-Ulcerative Sexually Transmitted Diseases: A Mechanism for Enhanced HIV-1 Transmission? *AIDS* 13, 327–332. doi: 10.1097/00002030-199902250-00004

Garrett, N., Mitchev, N., Osman, F., Naidoo, J., Dorward, J., Singh, R., et al. (2016). Diagnostic Accuracy of the Xpert CT/NG and OSOM Trichomonas Rapid Assays for Point-of-Care STI Testing Among Young Women in South Africa: A Cross-Sectional Study. *BMJ Open* 9, e026888. doi: 10.1136/bmjopen-2018-026888

Gaydos, C. A., Van-Der- Pol, B., Jett-Goheen, M., Barnes, M., Quinn, N., Clark, C., et al. (2013). Performance of the Cepheid CT/NG Xpert Rapid PCR Test for Detection of Chlamydia Trachomatis and Neisseria Gonorrhoeae. *J. Clin. Microbiol.* 51, 1666–1672. doi: 10.1128/JCM.03461-12

Ginocchio, C. C., Chapin, K., Smith, J. S., Aslanzadeh, J., Snook, J., Hill, C. S., et al. (2012). Prevalence of Trichomonas Vaginalis and Coinfection With Chlamydia Trachomatis and Neisseria Gonorrhoeae in the United States as Determined by the Aptima Trichomonas Vaginalis Nucleic Acid Amplification Assay. *J. Clin. Microbiol.* 50, 2601–2608. doi: 10.1128/JCM.00748-12

Grad, Y. H., Goldstein, E., Lipsitch, M., and White, P. J. (2016). Improving Control of Antibiotic-Resistant Gonorrhea by Integrating Research Agendas Across Disciplines: Key Questions Arising From Mathematical Modeling. *J. Infect. Dis.* 213, 883–890. doi: 10.1093/infdis/jiv517

Herbst-de-Cortina, S., Bristow, C. C., Joseph-Davey, D., and Klausner, J. D. (2016). A Systematic Review of Point of Care Testing for Chlamydia Trachomatis, Neisseria Gonorrhoeae, and Trichomonas Vaginalis. *Infect. Dis. Obstet. Gynecol.* 2016, 4386127. doi: 10.1155/2016/4386127

Land, K. J., Boeras, D. I., Chen, X. S., Ramsay, A. R., and Peeling, R. W. (2019). REASSURED Diagnostics to Inform Disease Control Strategies, Strengthen

Health Systems and Improve Patient Outcomes. *Nat. Microbiol.* 4, 46–54. doi: 10.1038/s41564-018-0295-3

Parcell, B. J., Ratnayake, L., Kaminski, G., Olver, W. J., and Yirrell, D. L. (2015). Value of Repeat Testing Using Cepheid GeneXpert CT/NG for Indeterminate PCR Results When Diagnosing Chlamydia Trachomatis and Neisseria Gonorrhoeae. *Int. J. STD AIDS* 26, 65–67. doi: 10.1177/0956462414531938

Price, M. J., Ades, A. E., Angelis, D. D., Welton, N. J., Macleod, J., Soldan, K., et al. (2013). Mixture-Of-Exponentials Models to Explain Heterogeneity in Studies of the Duration of Chlamydia Trachomatis Infection. *Stat. Med.* 32, 1547–1560. doi: 10.1002/sim.5603

Rowley, J., Vander Hoorn, S., Korenromp, E., Low, N., Unemo, M., Abu-Raddad, L. J., et al. (2019). Chlamydia, Gonorrhoea, Trichomoniasis and Syphilis: Global Prevalence and Incidence Estimate. *Bull. World Health Organ.* 97, 548–562P. doi: 10.2471/BLT.18.228486

Schrader, C., Schielke, A., Ellerbroek, L., and Johne, R. (2012). PCR Inhibitors - Occurrence, Properties and Removal. *J. Appl. Microbiol.* 113, 1014–1026. doi: 10.1111/j.1365-2672.2012.05384.x

Speers, D. J., Chua, I. J., Manuel, J., and Marshall, L. (2018). Detection of Neisseria Gonorrhoeae and *Chlamydia Trachomatis* From Pooled Rectal, Pharyngeal and Urine Specimens in Men Who Have Sex With Men. *Sex Transm. Infect.* 94, 293–297. doi: 10.1136/sextrans-2017-053303

Xie, T. A., Liu, Y. L., Meng, R. C., Liu, X. S., Fang, K. Y., Deng, S. T., et al. (2020). Evaluation of the Diagnostic Efficacy of Xpert CT/NG for Chlamydia Trachomatis and Neisseria Gonorrhoeae. *BioMed. Res. Int.* 2020, 2892734. doi: 10.1155/2020/2892734

Conflict of Interest: FT and YT are employees of Cepheid, the commercial manufacturer of the Xpert® CT/NG test.

The remaining authors declare that the research was conducted in the absence of any commercial or financial relationships that could be construed as a potential conflict of interest.

Publisher's Note: All claims expressed in this article are solely those of the authors and do not necessarily represent those of their affiliated organizations, or those of the publisher, the editors and the reviewers. Any product that may be evaluated in this article, or claim that may be made by its manufacturer, is not guaranteed or endorsed by the publisher.

frontiers in Cellular and Infection Microbiology

REVIEW
published: 10 February 2022
doi: 10.3389/fcimb.2022.807253

Advances in the Rapid Diagnostic of Viral Respiratory Tract Infections

Gratiela Gradisteanu Pircalabioru[1†], Florina Silvia Iliescu[2†], Grigore Mihaescu[3], Alina Irina Cucu[3], Octavian Narcis Ionescu[2,4], Melania Popescu[2], Monica Simion[2], Liliana Burlibasa[3], Mihaela Tica[5], Mariana Carmen Chifiriuc[1,3,6,7] and Ciprian Iliescu[2,6,8*]*

[1] Research Institute of the University of Bucharest, Bucharest, Romania, [2] National Institute for Research and Development in Microtechnologies—IMT, Bucharest, Romania, [3] Faculty of Biology, University of Bucharest, Bucharest, Romania, [4] Petroleum-Gas University of Ploiesti, Ploiesti, Romania, [5] Emergency University Hospital, Bucharest, Romania, [6] Academy of Romanian Scientists, Bucharest, Romania, [7] The Romanian Academy, Bucharest, Romania, [8] Faculty of Applied Chemistry and Materials Science, University "Politehnica" of Bucharest, Bucharest, Romania

OPEN ACCESS

Edited by:
Luc Bissonnette,
Université Laval, Canada

Reviewed by:
Yi-Wei Tang,
Cepheid, United States
Carlos Mastrangelo,
The University of Utah, United States

***Correspondence:**
Mariana Carmen Chifiriuc
carmen.chifiriuc@bio.unibuc.ro
Ciprian Iliescu
ciprian.iliescu@imt.ro

[†]These authors share first authorship

Specialty section:
This article was submitted to Clinical Microbiology, a section of the journal Frontiers in Cellular and Infection Microbiology

Received: 01 November 2021
Accepted: 04 January 2022
Published: 10 February 2022

Citation:
Gradisteanu Pircalabioru G, Iliescu FS, Mihaescu G, Cucu AI, Ionescu ON, Popescu M, Simion M, Burlibasa L, Tica M, Chifiriuc MC and Iliescu C (2022) Advances in the Rapid Diagnostic of Viral Respiratory Tract Infections. Front. Cell. Infect. Microbiol. 12:807253. doi: 10.3389/fcimb.2022.807253

Viral infections are a significant public health problem, primarily due to their high transmission rate, various pathological manifestations, ranging from mild to severe symptoms and subclinical onset. Laboratory diagnostic tests for infectious diseases, with a short enough turnaround time, are promising tools to improve patient care, antiviral therapeutic decisions, and infection prevention. Numerous microbiological molecular and serological diagnostic testing devices have been developed and authorised as benchtop systems, and only a few as rapid miniaturised, fully automated, portable digital platforms. Their successful implementation in virology relies on their performance and impact on patient management. This review describes the current progress and perspectives in developing micro- and nanotechnology-based solutions for rapidly detecting human viral respiratory infectious diseases. It provides a nonexhaustive overview of currently commercially available and under-study diagnostic testing methods and discusses the sampling and viral genetic trends as preanalytical components influencing the results. We describe the clinical performance of tests, focusing on alternatives such as microfluidics-, biosensors-, Internet-of-Things (IoT)-based devices for rapid and accurate viral loads and immunological responses detection. The conclusions highlight the potential impact of the newly developed devices on laboratory diagnostic and clinical outcomes.

Keywords: point-of-care, microfluidics, biosensors, viral respiratory infection, IoT - internet of things

INTRODUCTION

The increasing incidence of acute respiratory tract infections (RTI) leads to high mortality in children and adults worldwide. The RTI account for 56 million deaths in 2019 in all age groups representing the third worldwide leading cause of death after cardiovascular diseases and neoplasms (IHME, 2021). The current protocols used to confirm the diagnosis of viral infection rely on virologic laboratory methods that either isolate and identify the pathogens or monitor the levels of antibodies in the body fluids (Loeffelholz and Tang, 2020; Lu et al., 2021). These methods involve laboratory techniques that require specialised equipment and technical expertise. Also, the preanalytical components (e.g., samples collection, transportation,

preparation for batch testing, etc.) contributes to a slow turnaround time that further delays the results and related diagnostic and therapeutic decisions. Correctly identifying the viral aetiology of respiratory tract infectious diseases remains challenging despite the availability of multiplex nucleic acid amplification tests (NAATs) due to the problematic interpretation of the results. Moreover, essential deviations from the ideal scenario of acute infection progressing to pathogens' clearance, such as persistence, latency, reactivation, late disease, and drug resistance, influence the pattern for a particular virus, the immune competence of the host, and the decision about ordering tests and interpreting the results (Booss and Tselis, 2014).

Recently, microfluidics developed to be integrated into rapid and specific diagnostic tools. Lab-on-a-chip (LOC) technologies evolved from single-task-based analysis into advanced integrated systems for complex work (Schumacher et al., 2012). The complexity resides in the multiple interconnected elements such as microchannels, valves, mixers, pumps, chambers for reaction and detection assembled on the same platform where each microfluidic component performs distinct operations for specific and elaborated laboratory protocols. Benchtop protocols comprising tasks such as reagent storage, fluid transport, fluid mixing, product detection, and collection can be finalised directly on the self-operated microfluidic device, (Jung et al., 2015; Park et al., 2020) or near the patient bedside as point-of-care testing (POCT) (Wang et al., 2020). One of the clinical advantages resides in the ability of LOC-based techniques to be developed for viral detection (Aalberts et al., 2012). Previous work demonstrated the potential of microfluidic devices for single virus diagnoses platforms that included sample preparation and detection of Ebola (Coarsey et al., 2019), dengue fever -DENV (Darwish et al., 2018), hepatitis (Duchesne and Lacombe, 2018), human immunodeficiency virus -HIV- Mauk et al., 2017), highly pathogenic avian influenza viruses -HPAIVs- (Liu et al., 2018) or for testing the presence of multiple pathogens (Chen et al., 2021). The new strategies provide quick microbiological analysis for correct differential diagnosis, effective treatment, and disease clearance without complications. To reduce the risk of RTI complications, POCT can be a valuable instrument, especially in developing countries (WHO, 2020). These methods will decrease not only the empirical administration of antibiotics, the risk of selecting drug-resistant strains, or the rate of developing large-scale outbreaks, but eventually the healthcare costs.

Recent reviews approached the impact of microfluidics and biosensing on the rapid detection of RTI. For instance, an overview of available technologies used to detect SARS-CoV-2 in clinical laboratories was presented by Safiabadi and colleagues (Safiabadi et al., 2021). In 2014, Anema and colleagues suggested the potential use of digital surveillance for public health emergencies of international concern, such as the Ebola virus (Anema et al., 2014). Liu and colleagues approached the challenges of automated sample preparation, amplification and signal transduction for rapid diagnosis (Liu et al., 2021). Furthermore, the key advantages in the selection of smart material-based POCT platforms were reviewed by Sow and colleagues (Sow et al., 2020), while the "metal-organic frameworks" (metal clusters + organic linkers) involved in the viral detection (NAAT and immunological) were analysed by Wang and colleagues (Wang et al., 2020). Work focused on technology for virologic diagnostic and highlighted NAAT technologies for rapid molecular diagnostic (Lee et al., 2019) and the influence of micro- and nanotechnology on viral diagnostic (Nasrollahi et al., 2021). The present review covers the advances in microbiological diagnostic of viral RTI, focusing on miniaturised systems and evaluating the clinical perspectives for further use as POCT. We provide a nonexhaustive overview of conventional viral detection and infection monitoring methods and technological improvements. We discuss the potential of immunoassays and nucleic acid (NA) amplification and the new approaches such as microfluidics and biosensors-based techniques as rapid diagnostic platforms for viral respiratory infections detection methods and monitoring. Since viral infections impose stringent detection and spread monitoring, we present the emerging Internet-of-Things (IoT) and highlight their potential as a future solution in the virology diagnostic and respiratory infections prophylaxis.

TRENDS IN VIRAL RESPIRATORY INFECTIONS ETIOLOGY

Besides influenza and respiratory syncytial viruses (RSV) responsible for the highest mortality and hospitalisation rates, other viral pathogens such as parainfluenza, corona-, adeno-, boca-, and rhinoviruses are known for leading to high morbidity (severe diseases in addition to mild upper respiratory tract infections), mortality, and economic burden (Fendrick et al., 2003; Azar and Landry, 2018). Most respiratory infections are mainly caused by viruses and are often mild and self-limited. However, the zoonotic viruses with tropism for the human respiratory tract such as severe acute respiratory syndrome coronavirus (SARS-CoV, 2003), influenza A (H1N1, 2009), Middle East respiratory syndrome coronavirus (MERS-CoV, 2012), and severe acute respiratory syndrome coronavirus 2 (SARS-CoV-2, 2019) identified over the past decades affected the lower respiratory tract fast and infected millions of humans (Peeri et al., 2020). Since the natural progression of viral infections in humans depends on the virulence of viral strains, the general health, immune status and reaction of the hosts, the clinical manifestations range from mild to lethal acute or chronic debilitating complications (Basile et al., 2018; Jin et al., 2021). Moreover, it has been acknowledged that some respiratory infections viruses are drug-resistant strains, e.g., cytomegalovirus isolated from immunocompromised patients, human adenovirus 14p1, group C rhinovirus, human metapneumovirus (hMPV), polyomaviruses-KIPyV, WUPyV- (Ma et al., 2021). Furthermore, the zoonotic agents (avian influenza viruses and MERS-CoV- (Assiri et al., 2013) and severe acute respiratory syndrome -SARS coronaviruses- (Ksiazek et al., 2003) with extensive genetic modifications through recombinant mutations (coronaviruses), gene reassortment (avian influenza viruses), or cascade mutations, exceeded the species barrier and amplified the risk of

epidemic and pandemic emerging viral infections with the interhuman transmission (Dhama et al., 2020; Rodriguez-Morales et al., 2020).

Since the viral respiratory tract infections resemble other similar infections of bacterial origins, the differential diagnosis and adequate isolation and treatment measures are complex. For these reasons, the World Health Organization has included diagnosis and diagnostic tests for severe acute respiratory infections into a critical research agenda to develop effective laboratory techniques, from sampling to viral diagnosis and enable early and affordable detection and monitoring of the viruses that play critical roles in pandemics (WHO, 2020).

SAMPLE COLLECTION METHODS FOR RESPIRATORY VIRAL INFECTIONS

Non-invasive and invasive sampling methods have been used to isolate respiratory viruses in cell cultures and detect antigens in immunoassays. Currently, collecting respiratory ciliated epithelial cells or cell-free viruses is from swabs, aspirates, washes, brushes, lavages, or aspirates at various respiratory trach (RT) levels. The reference method is the nasopharyngeal swab collected by the healthcare personnel (Larios et al., 2011). The biological origin of clinical samples and time since recovery from patients significantly impact the accurate and early detection of viruses (Macfarlane et al., 2005; Lessler et al., 2009). The choice is based on the specificity and sensitivity of the diagnostic testing and the segment of the respiratory tract affected, either upper, (Su et al., 2016) or lower (Zaki et al., 2012), the viruses targeted (Hui et al., 2016) or the age group of patients (Doan et al., 2009). For instance, viruses accumulate at various locations within the respiratory tract during incubation times (Ahluwalia et al., 1987), and sputum may not be productive to be a valid sampling method indicating the aspirate collection (Lessler et al., 2009).

Furthermore, invasive respiratory samples collection such as nasopharyngeal aspirates or swabs are stressful, especially in children and if repeated testing is required. For these reasons, adequate virologic testing includes various sampling methods and sources. The clinical samples to diagnose respiratory infections are collected from various segments of the the respiratory tract or from the bloodstream. The methods are invasive from lavages swabs, aspirates from the anterior nasal, nasopharyngeal, oropharyngeal, bronchoalveolar samples, to phlebotomy for whole blood or serum. Since most of the techniques are invasive, anterior nare swabs or facial tissues were suggested as mitigators (Blaschke et al., 2011). SARS CoV-2 nucleic acid is generally detectable in saliva specimens during the acute phase of infection (Azzi et al., 2020).

Upper airway sampling is relatively simple, can be performed at the bedside, and is minimally invasive. Other specimens may be used instead of blood to detect different viral upper RTI, including SARS-CoV2 (Khan et al., 2017; Wyllie et al., 2020). In this sense, various respiratory samples such as oropharyngeal swabs/throat swabs (OPS/TS), nasopharyngeal swabs (NPS) or nasopharyngeal aspirates (NPA) are employed for the diagnosis of viral RTI (Loens et al., 2009; Corstjens et al., 2016; Charlton et al., 2019). The nasopharyngeal and nasal swabs (flocked, rayon, polyurethane) performed in conjunction with the present diagnostic assays equivalated the traditionally used nasal wash and aspirates specimens (Daley et al., 2006; Chan et al., 2008; Scansen et al., 2010). Furthermore, combined nose and throat specimens contributed to an excellent sensitivity of the polymerase chain reaction (PCR)-based test for influenza virus and RSV (Lambert et al., 2008). The collection protocols may also be altered to increase efficiency while maintaining sensitivity. For instance, parent-collected specimens could be used for PCR testing with equivalent sensitivity to swabs collected by the healthcare professionals in pediatrics (Lambert et al., 2008). The United States Centres for Disease Control and Prevention (CDC) currently offers and demonstrates the guidelines for each procedure while respecting the manufacturers' recommended specimen types. The CDC recommends collecting the upper respiratory NP swab. Collection of an OP specimen is a lower priority and, if collected, should be combined in the same tube as the NP swab. (CDC, 2021a) Food and Drug Administration (FDA)-cleared or validated laboratory tests (Centres for Disease Control and Prevention, Specimen collection, 2021). Recently, diagnostic testing from NPS and OPS have been approved by FDA to be used on commercial platforms and laboratory-developed tests (Thwe and Ren, 2021). The sampling methods give different detection sensitivities, depending on the respiratory virus. In this sense, Charlton et al. offer practical guidance about selecting specimen type, appropriate sampling time and detection technique concerning various factors, such as the clinical presentation, patient age, the nature of the potential pathogen (Charlton et al., 2019). Aside from the specimen mentioned above, salivary tests have been suggested as an alternative to OPS and NPS (Robinson et al., 2008). It has been demonstrated that human saliva contains specific antibodies for a wide range of viruses multiplying in the respiratory tract: SARS-CoV (Liu et al., 2011) SARS-CoV-2, CMV, Dengue, Ebola, enteroviruses, EBV, HSV 1, 2, influenza A, mumps, measles, poliovirus, rabies, rhino-, rubella, polyoma (BKV, JCV, WUV, KIV), and hepatitis (VHA, VHB, VHC) viruses (Corstjens et al., 2016; Baghizadeh, 2020). Therefore, self-collected specimens may become promising non-invasive diagnostic specimens (To et al., 2020). Newly developed methods based on viral agents in the exhaled breath to complement the existing sampling techniques and monitor the patients for airborne diseases (Rahmani et al., 2020; Soto et al., 2021). Moreover, wearable collectors have the potential to be integrated into a POCT system, like the one demonstrated by Rombach and colleagues (Rombach et al., 2020). For the most sensitive detection of viruses, the collection and testing of upper and lower respiratory samples such as sputum or bronchoalveolar lavage fluid (BAL) are recommended (Cheng et al., 2004). In contrast, lower airway sampling in patients with complex or severe disease (e.g., in intensive care, immune-compromised) or in children with chronic or recurrent respiratory tract symptoms, invasive, requiring a bronchoalveolar lavage (BAL) (De Blic et al., 2000). However, bronchoscopy increases the risk of healthcare

workers contamination through aerosol droplets created during the procedure. Therefore, donning proper personal protective equipment (PPE) is crucial. One meta-analysis provided evidence to support NPW, MTS and NPS from 16 sampling methods as the ones with higher diagnostic values for viral respiratory infections. The study also highlighted that each sampling method presents advantages and disadvantages. Therefore, selecting a particular sampling method is influenced by the pathophysiology and pathogenesis of each outbreak. For instance, positive rates, less comfort, and cost supported MTS, while sputum provided higher detection rate for coronaviruses, such as SARS-CoV-2 (Hou et al., 2020). Furthermore, the protocols consider that viral pneumonia cases do not produce purulent sputum and recommend bronchoscopy in the early stages or repeated NPS/NPW to increase the success rate. Interestingly, although generally less reliable than respiratory specimens, the stool, urine, and blood samples contain SARS-CoV and MERS-CoV RNA, and SARS-CoV RNA is consistently detected in faeces at about two weeks after symptom onset (Cheng et al., 2004; Xu et al., 2005).

ESTABLISHED DIAGNOSTIC METHODS OF VIRAL INFECTIONS

The virologic diagnostic of respiratory infections usually relies on hospital-based procedures to facilitate epidemiological surveillance (Doherty et al., 1998), implementation of timely antiviral therapy (Rocholl et al., 2004), control of nosocomial infections (Groothuis et al., 2008), and wise management of resources (Benito-Fernández et al., 2006) and antibiotics (Doan et al., 2009). Currently, monitoring the respiratory viral infections intends to:

1. measure the plasma levels of antibodies (IgG and IgM) in response to viruses, and
2. detect the viral load in the respiratory specimens.

The quantitative and qualitative analysis reflects the functionality of the host immune system and indicates viral replication in the primary infection site (Lu et al., 2021).

The classical methods to diagnose viral infections are represented by cell culture for the virus isolation (reference method) (Leland and Ginocchio, 2007) and the serological methods for identification (Loeffelholz and Chonmaitree, 2010). Virus isolation is generally performed on sensitive cell cultures inoculated with a sample of tissue or fluid collected from patients to allow the viral multiplication (Leland and Ginocchio, 2007). However, culture-based methods are time-consuming, expensive (depending on equipment and trained operators), and therefore performed mainly in specialised laboratories. The immunoassay testing measures the immunological responses to the virus to differentiate between exposed asymptomatic, acutely, or mildly sick, and recovered cases. The serological diagnosis is a systematic clinical approach to detect respiratory viruses and includes *serotyping* (detection of viral antigens in the patients' serum) and *serodiagnosis* (detection and quantification of specific antibodies in patients' bodily fluids). **Table 1** in **Supplementary Table 1** presents a brief comparison of these methods.

The immunoassays detect viral antigens or specific antibodies with high sensitivity and are routine methods for protein detection, especially at significantly low levels, as in influenza's case (Khanna et al., 2001). Compared to the rapid antibody detection tests, which are qualitative and do not discriminate between recent and old infections (Khalaf et al., 2020), the quantitative assays for specific antibodies (IgM, IgG and IgA) identify the viral agent and follow up the dynamics of the antiviral specific immune response, to establish the infection stages and discriminate between acute and chronic infections (Corstjens et al., 2016). In the case of SARS-CoV infection, the specific antibodies occur 10-20 days after symptoms appear, (Yeh et al., 2014) and the immunological profile shows false-negative results during the window between the viral infection and the start of antibody production (Loeffelholz and Tang, 2020). Since the window for rapid tests is narrow, testing will make with higher sensitivity methods such as PCR and reverse transcriptase (RT)-PCR, loop-mediated amplification (LAMP), and strand displacement amplification, which amplify a specific sequence of the viral genome. These methods, known as nucleic acid amplification techniques (NAAT), inactivate the virions during preliminary purification steps (Zhang et al., 2020) and can simultaneously detect multiple viruses (Lu et al., 2021). However, the presence of nucleic acid does not always mean active infection (Babiker et al., 2021), and significant issues stem during results interpretation: a weak signal explaining either the end of an infection or a recent evolving one and undetectable virus in the upper respiratory tract samples in the respiratory tract infections (Crozier et al., 2021). Furthermore, since respiratory viruses are prone to antigenic drift due to genetic point mutations and reassortment, it is fundamental to identify these changes within the viral genomes. The exciting advantage compared to conventional methods is diagnosing severe pneumonia, detecting coinfections in severe pneumonia patients or those with unknown origin infections. Furthermore, developing high-throughput whole-genome sequencing (WGS) portable platforms is crucial in identifying viral transmission better than subgenomic sequences (Zhang et al., 2020). Therefore, the evolving next-generation sequencing (NGS) technologies provide cost-effective rapid sequencing of exomes, transcriptomes, and genomes with increasing potential for diagnosing and identifying respiratory pathogens (Mercer and Salit, 2021). **Table 2 (Supplementary Table 2)** presents non-exhaustively the specific diagnostic testing for viral respiratory infections, either as single or multiplex diagnostic testing.

MICROFLUIDICS FOR VIROLOGIC TESTING

Since the first miniaturised microfluidic device was developed in 1970 at Stanford University, (Terry et al., 1979) the technologies in microfluidics and LOC (Weibel et al., 2007) advanced towards automation and the use of smaller volumes of clinical samples for a virus purification as efficient as the standard protocols.

Microfluidic systems were developed as portable point-of-care devices or "Doctor's office at home" to detect pathogens and diagnose infectious diseases (Nasseri et al., 2018). Zenhausern and colleagues reviewed microfluidic sample preparation methods such as bead-based, droplet-based, structure-based, fluid-properties-based and described the principles that allow these portable devices to extract, purify and concentrate the viral samples for biological analysis (Zenhausern et al., 2021). Microfluidic-based detection employs nucleic acids amplification, blood chemistry assays, flow cytometry and immunoassays (Li et al., 2021). The techniques differ in terms of turnaround time and cost-effectiveness (e.g., the quantity and number of reagents) the reproducibility. For instance, immunoassays use a simple strip, are rapid and simple diagnostic platforms, compared with blood chemistry testing, which is complex (e.g., measure tens of physiological parameters in one go), and time-consuming. Nucleic acid amplification techniques, however, require a limited copy number of nucleic acids for diagnosis. Furthermore, the micro-assays provide rapid, highly accurate results, as user-friendly and cheap devices (Whitesides, 2006) that perform specimen preparation, reagent manipulation, bioreaction and virus detection on the same miniaturised platform (at very low concentrations and in small sample volumes). The devices incorporate micro-channels and chambers (10-100 μm) designed to match the intended application based on the physical and biological properties of the targeted micro-organisms. The crucial steps are: (1) the design of the microchannels, (2) the manufacture of the integrated platform (soft lithography), and (3) the quantification of the chemicals and biomarkers involved in the process. LOC platforms have common elements with microarrays and biosensors (e.g., the substrates materials), and specific ones such as polymers (e.g., polytetrafluoroethylene, polymethylmethacrylate- (Becker and Gärtner, 2008) or biopolymers (e.g., calcium alginate, cross-linked gelatin) for the skeleton (Ertl et al., 2004). Detection chips on silicon substrates ensure the specificity of biological analysis (Morens et al., 2004). Furthermore, high detection ability of the devices (sensitivity and specificity) imposes a combination of several types of equipment for data acquisition, signal processing, amplification, and monitoring. However, attentive microenvironment control, mainly temperature and mechanical stress, is crucial for the desired functionality. The complexity of the device and the high sensitivity and specificity will ensure the real-time analysis specific to point-of-care-testing (POCT) (Lagally et al., 2000).

POINT-OF-CARE (POC) TESTING DEVICES

Generalities

The major problem of the RTI diagnosis is the lack of standardised, rapid, and accurate testing for a differential diagnosis: accurate identification of viruses, bacteria, and fungi, followed by their drug-sensitivity or -resistance profiling. Consequently, in the absence of appropriate and timely therapeutic and epidemiological measures, the detrimental impact of a viral infection increases exponentially (Burbelo et al., 2019). For instance, in influenza A virus infection, treatment with neuraminidase inhibitors (NAIs) should be started within 48 hours after the onset of symptoms. Therefore, it is imperative to create simple, cheap methodological alternatives as POCT. The POCT devices must meet the following criteria: accessibility, availability, sensitivity, specificity, user-friendliness, speed, no accessory equipment required (Drain et al., 2014; Iliescu et al., 2021). The purpose of using POCT is to get a quick diagnosis after analysis of bodily fluids (e.g., blood, serum, urine, or saliva) samples and to provide the clinicians with valuable and timely information for the optimal therapeutic decision (Nelson et al., 2020).

Types of POCT Used in the Diagnosis of Viral Infections

The use of POCT for viruses was hampered by the low sensitivity of antigen detection tests and the limited spectrum of detected viruses (Brendish et al., 2015), but this field of research has significantly advanced in the last years mainly due to the COVID-19 pandemic. POC tests, molecular or non-molecular, detect different biomarkers, including antibodies, whose concentration in the body fluids changes during the infectious process (O'Sullivan et al., 2019). POC tests, especially non-molecular tests, have several advantages. For instance, they do not require permanent dedicated space or expensive laboratory equipment, clinical laboratory facilities or surgical expertise; they provide real-time results; the infection can be detected in an early stage, and this facilitates rapid therapeutic interventions, eliminating unnecessary investigations.

The point of care diagnostics market is segmented into cardiometabolic testing, glucose monitoring, pregnancy and fertility testing, haematology testing, coagulation testing, infectious disease testing, tumour/cancer marker testing, cholesterol testing, urinalysis testing, and other POC products. The infectious diseases segment is divided into influenza testing, HIV testing, sexually transmitted disease testing, hepatitis C testing, tropical disease testing, respiratory infection testing, other infectious disease testing and healthcare-associated infection testing. Due to the COVID-19 pandemic, which leads to a growing demand for rapid test kits for faster diagnosis at public places, the POC diagnostics market has encountered substantial growth. The POC diagnostics market was US$ 36,000.4 million in 2021 and is expected to reach US$ 82,958.3 million by 2028 (Business Wire, 2021).

Molecular POCT methods for multiple detections of respiratory viruses are based on the identification of one or more nucleic acid sequences (RNA or DNA) specific for the pathogen after amplification using a PCR-based method. The PCR based techniques need between 20 and 100 minutes (involving reverse transcription for RNA detection) for achieving 30-40 amplification cycles at 72°C. The isothermal amplification of nucleic acids using LAMP (Zhang et al., 2019) is a new variant of DNA amplification, using a DNA-polymerase acting at a constant temperature of 60-65°C, thus eliminating the need for a thermocycler and being cheaper and easier to run) (Drancourt et al., 2016).

A new generation of molecular technologies for POC diagnosis is CRISPR (clustered regularly interspaced short palindromic repeats). The CRISPR - POC was implemented after discovering that certain enzymes of this system, namely Cas13 (CRISPR associated) have RNase activity related to various RNA molecules. The RNase activity of CRISPR enzymes is used for signal amplification and nucleic acids detection. The first step is described as the isothermal amplification of the DNA and RT-RNA in the sample to increase the amount of viral RNA as potential targets of RNase. Subsequently, the Cas13a enzyme with specific activity to the specific viral RNA sequence is added. If viral RNA is present, Cas13a binds to it and is activated to cleave a fluorescent-labelled reporter molecule, which produces a light signal measured on a fluorescent plate. Through these steps results, the presence of RNA is detected in a few hours (Burbelo et al., 2019; Li et al., 2019).

The CRISPR/Cas12a-based precision technique, called SARS-CoV-2 DNA endonuclease-targeted CRISPR trans reporter (DETECTR) described by Broughton et al. enables the rapid and straightforward diagnosis of SARS-CoV-2 RNA extracted from patient respiratory tract swab samples in less than 40 min. The diagnostic test combined CRISPR/Cas12a DETECTR system with RT-LAMP for purified RNA from nasopharyngeal or oropharyngeal swabs. Cas12a subsequently detects predetermined viral sequences followed by the cleavage of the reporter molecule, confirming the presence of the virus (Broughton et al., 2020).

The all-in-one dual CRISPR-Cas12a (AIOD-CRISPR) system designed by Ding and colleagues uses dual CRISPR RNAs (crRNAs) to efficiently detect the target genome sequence (both SARS-CoV-2 and HIV-1). The AIOD-CRISPR system combines all the components required for target nucleic acid amplification and CRISPR system-based detection into one reaction (Ding et al., 2020).

Yoshimi and colleagues developed an *in vitro* nucleic acid diagnostic tool based on Cas3, Cas3-operated nucleic acid detection N (CONAN). The CONAN tool was described as a fast, sensitive, and device-free diagnostic system for SARS-CoV-2 detection combined with isothermal amplification methods (Yoshimi et al., 2020).

The CRISPR/Cas12a-based system that allows reading with the naked eye (CRISPR/Cas12a-NER) described by Wang and colleagues was shown to detect at least ten copies of a viral gene in 40 min without the demand for specialized instruments. The designed system comprises Cas12 protein, SARS-COV-2-specific crRNAs, and a single-stranded DNA molecule as a reporter (labelled with a green fluorescent off–on molecule). When the coronavirus genome is present in the sample, it is detected by the designed diagnostic system - the reporter molecule is being cleaved by the Cas12 protein, triggering a green fluorescent light visible to the naked eye at 458 nm (Wang et al., 2020).

While a lot of research focus is targeted against the development of diagnostic systems based on SARS-CoV-2 nucleic acid detection rapidly and conveniently, only a few systems have addressed the issue of mutations and genomic rearrangements. Notably, RNA viruses frequently mutate to elude attacks from the host immune response. Multiple genomes of SARS-CoV-2 are continuously sequenced, and different mutations have been identified. For instance, mutations in the gRNA binding site can trigger mismatches that hinder the ability of CRISPR/Cas system's ability to recognize the target area. The variant nucleotide guard procedure has been developed to address this issue and identify mutated and altered nucleic acid regions of SARS-CoV-2 (Ooi et al., 2020). The DETECTR system and different forms of Cas12a enzymes were initially analyzed, and among the tested molecules, enAsCas12a harboured the greatest tolerance in the CRISPR target area for single mismatches (Ooi et al., 2020).

Non-molecular POCT methods

POCT devices for the selective detection of biomolecules using metallic or magnetic nanoparticles are an important direction of research in the field of diagnostic optimization, the nanodiagnostic platforms having the ability to quickly detect, in real-time, the target biomarkers in minimal sample volumes. By comparison, conventional blood biomarker tests have lower sensitivity and require high concentrations of biomarkers. At the same time, while nanoparticle sensors present very high sensitivity and can detect the same biomarkers at concentrations thousands of times lower, thus enabling an early diagnosis (Wang et al., 2017).

POCT non-molecular technologies have two targets, respectively antibodies or antigens. One non-molecular POCTs is immunochromatography testing (ICT), which diagnoses several bacterial, viral, parasitic, and fungal infections. *Lateral flow immunochromatography* for *antibodies* detection has the most extensive use, despite the low sensitivity and the impossibility of concomitant analysis of multiple samples (multiplex).

The immunoassay POCT (lateral flow immunochromatography) applied to detect the influenza virus has a lower sensitivity and specificity and a narrower target spectrum than the molecular POCT. However, the diagnosis time is significantly shorter (15 minutes *versus* 30-60 minutes) (Egilmezer et al., 2018).

In the specific conditions of the pandemic with type A influenza ($H1N1_{2009}$), detection of antibodies by lateral flow immunochromatography, although it did not have high sensitivity, was a valuable indicator for negative cases, thus, in the conditions of a high degree of contagiousness, decreasing the risk of contamination occurred in the analysis of suspected samples by NAAT. By extrapolation, this reasoning is also applicable to the SARS-CoV2 pandemic, with a very high degree of transmissibility.

Another category of the non-molecular POCTs are the immunofluorescence (IF) tests, providing the results in 15 minutes but with low sensitivity (~50%) for the influenza virus and even lower for the respiratory syncytial virus (RSV). The *Sophia Fluorescent Immunoassay Analyzer* works on the principle of lateral IF flow and consists of a kit for antigen detection and an optical sensor, providing the result in 10 minutes (Drancourt et al., 2016).

Other non-molecular POCTs are based on the detection of antibody using different *ELISA* (enzyme-linked immunosorbent assay) protocols, silver-coated microspheres, or the protein array technology. In the case of the two-photon excitation assay

technique and dry-chemistry reagents, the virus is sandwiched with polymer microspheres and fluorescently labelled antibodies. Immunocomplexes are formed on the surface of the microspheres, proportional to the concentration of the analyte in the sample. The fluorescent signal emitted by the microspheres is measured using two-photon-excited fluorescence detection (Koskinen et al., 2007).

In surface plasmon resonance (SPR), biomolecules bind to a metal surface and absorb a part of the incident light flux, leading to decreased reflection. Qiu and colleagues described a dual-functional plasmonic biosensor combining the plasmonic photothermal (PPT) effect and localized LSPR as a promising solution for diagnosing SARS-CoV-2 infection. The two-dimensional gold nanoislands functionalized with complementary DNA receptors performed a sensitive detection of the selected sequences from SARS-CoV-2 through nucleic acid hybridization (Qiu et al., 2020).

Biosensors-Based POCT

Recently, biosensors have gained significant interest due to their ability to provide rapid, portable, sensitive, miniaturised, and inexpensive alternative diagnostic platforms. Typically, a biosensor is made of three parts: a "bioreceptor" unit (DNA, enzyme, antibody) combined with ion conductive materials able to recognize the analyte, a physio-chemical signal transducer (optical, electrochemical or piezoelectric) and a reader device (Afroj et al., 2021). Biosensors can be designed to detect viral antigens, antibodies produced against a virus or the virus genome. Viral antigens are easier to detect since they are displayed on the outer surface of the virus and can strongly bind to the biosensor receptors or antibodies. Notably, the efficient liquid mixing in biosensors favours the interaction between assay reagents and the target biomarkers, shortening the assay duration and providing a fast readout (Rasmi et al., 2021). Until recently, most biosensors developed focused on detecting Influenza due to the many subtypes of this virus and increased mortality and morbidity (Dziąbowska et al., 2018). However, the emergence of the SARS-CoV-2 pandemic has significantly moved the focus on this new virus. Indeed, many biosensors have been designed in the last two years for the diagnostics of COVID-19. For instance, chip-, paper-, and graphene-based biosensors have been developed as complementary diagnostic modalities. Furthermore, connecting the devices to smartphone could become an easy and rapid analysis method for remote diagnosis, data collection, and disease monitoring. An overview of the entire process, from sample collection and detection to distant communication and disease management with possible POCT application is described in **Figure 1**.

The development of diagnostic systems to customize the assessment of the pathophysiological condition is the next stage in the development of POC systems. POC biosensors are made of poly-dimethyl-siloxane (PDMS), paper and other flexible materials such as textiles, film and carbon nanosheets (Choi, 2020). The analytical performance of POC systems can be evaluated by electrochemical biosensors, which are components of POC devices. The biosensor estimates the quantitative level of biomarkers based on a specific chemical reaction and generates a quantifiable signal: the signal strength is proportional to the concentration of the analyte in the sample. Thus, the condition can be diagnosed based on the signal of body fluid markers) (Noah and Ndangili, 2019).

The electronic circuit, transducer element and the recognition section are the three main components of a biosensor. There are different types of biosensors: electrochemical, optical, electrical, thermometric, and piezoelectric. In the case of electrochemical biosensors, there have been multiple transistors used, including conductometric, potentiometric, amperometric, voltametric and impedimetric. The types of electrodes vary as well, and they can be solid (gold, platinum, diamond, or carbon) or composite electrodes. There are three types of electrodes for conducting

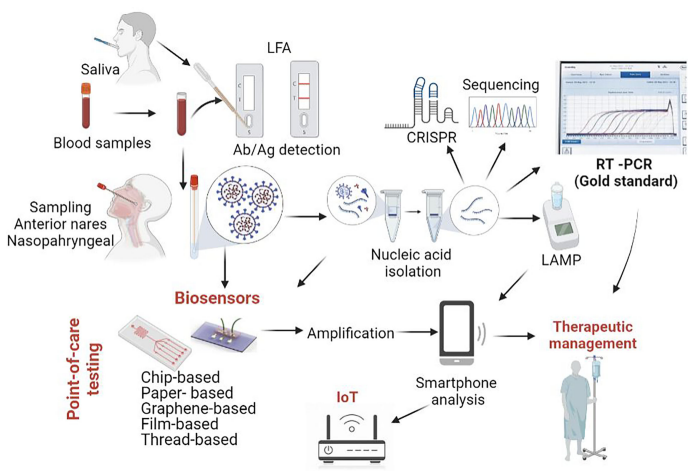

FIGURE 1 | SARS-CoV-2 diagnostic tools. While Real Time PCR from nasopharyngeal swabs represents the gold standard from COVID-19 diagnostic, other approaches are currently being employed or developed. Among these, research is focused on various types of biosensors (chip based, paper based, graphene-based biosensors), some of them coupled with smartphone analysis. Original figure, created using biorender.com.

these techniques: reference, working and auxiliary. These electrodes can use various biological elements that they can recognize, such as tissue, antibodies, nucleic acids, enzymes, organelles, cell receptors. Electrochemical biosensors are investigated for their use in POC technology, with conductometric biosensors being seen as the best candidate for this (Anik, 2017; Tepeli and Ülkü, 2018; Qazi and Raza, 2020).

Electrochemical biosensors have high sensitivity and accuracy, low detection limits and high real-time analysis potential. These biosensors offer many electrode materials and target detection molecules with multiple modification methods. Importantly, these sensors can successfully be exploited to detect different viruses by changing the probe immobilized on the electrode surface. The gold-coated array of carbon electrodes was the method of identifying the S protein of MERS-CoV in 20 min. In the case of SARS-CoV infections, the specific antibodies competitively bind the viral particles present in the sample, or the viral antigen immobilized on the electrode bind the serum antibodies. A peak current through the chip measures the antibody or antigen bound on the electrode (Nelson et al., 2020). A chip-based electrochemical biosensor made of ion-sensitive field-effect transistors (ISFETs) using complementary metal-oxide-semiconductor (CMOS) technology was developed for SARS-CoV-2 detection. The platform was reported to harbour a detection limit of 10 copies of SARS-CoV-2 RNA per reaction with 90.55% sensitivity and 100% specificity (Rodriguez-Manzano et al., 2020). The sample preparation (nucleic acid isolation and LAMP amplification) was done off-chip, and the amplicons were added into the developed biosensor for nucleic acid detection. The voltage change triggered by the pH variations was recorded and analysed with the help of a custom smartphone Android OS application. Even though this biosensor has clear advantages related to costs and portability and provides quantitative data, it could be further improved by eliminating the sample preparation step. An electrochemical biosensor made of a three-electrode system including platinum reference electrodes, a counter electrode and a titanium substrate functionalized with gold nanoparticles was developed for COVID-19 diagnostic. The sensor contained a single-stranded probe with a thiol end immobilised on the gold surface, which was complementary to target viral nucleotides. The main disadvantage of this assay was again related to the need for sample preparation -isolation of target DNA/RNA- (Tripathy et al., 2020). From this perspective, simplified techniques were approached for ready-to-use small volumes of biological samples. Fabiani and colleagues developed an electrochemical sensor for saliva testing using screen-printed electrodes and magnetic beads with selectivity for SARS-CoV-2 spike protein (19 ng/mL) or nucleocapsid protein -8 ng/mL- (Fabiani et al., 2021), while Ahmadivand and colleagues described a toroidal plasmonic immunosensor to detect SARS-CoV-2 spike protein at femtomolar level with POCT potential (Ahmadivand et al., 2021). Dalal and colleagues employed immobilised HA gene-specific oligoprobe and developed a genosensor to detect sensitive POC H1N1 (swine flu) in human nasal swabs (Dalal et al., 2020). The complementary ssDNA probe immobilized on a cysteine-functionalised screen-printed gold electrode generated an electrochemical differential pulse voltammetry signal upon hybridisation to the target viral genome in the presence of a redox indicator -methylene blue- (Dalal et al., 2020).

Another type of technology that offers a variety of advantages is *microfluidic sensors*. Paper-based microfluidic POC sensors are based on colorimetric and electrochemical assays, and they present the great advantage of having a widespread application, from the environment to food and human health. Since biosensors present various advantages, such as their high sensitivity, specificity, and user-friendliness, the biosensor-based devices can be integrated with different types of material, including paper, silicon, and magnetic beads. Nanomaterials are combined to give these electrodes more power (Li et al., 2017; Zhang et al., 2017). *Nanotechnology* is the field that uses the atomic and molecular levels to create systems with physical, chemical and biological applications, with nanoparticles (nanomaterials) achieving dimensions of 1-100 nm. *Nanodiagnostics* is defined as the use of nanotechnology in diagnostic applications, including biosensors (e.g., magnetic, silver and gold metallic nanoparticles) for the diagnosis of infectious diseases. Nanostructures have a very high surface/volume ratio and are very suitable for binding many target molecules to immobilised probes, which increases the sensitivity of the detection results (Brazaca et al., 2017; Younis et al., 2020). Biosensors based on metallic nanoparticles are often used due to their unique optical properties. Gold is generally used for biosensor development due to its biocompatibility and surface chemistry. Colorimetric detection based on gold nanoparticles (AuNPs) takes advantage of the colour change from red to blue due to localized surface plasmon resonance (LSPR) coupling among the nanoparticles (Li et al., 2015). However, researchers claim that nanomaterials can be problematic due to their inconsistent signal amplification and metallic impurities (Kuila et al., 2011).

Fluorescence chip-based biosensors are also promising diagnostic tools. For instance, Sun and colleagues developed a fluorescence-based biosensor that allowed the detection of Equine herpesvirus 1 (EHV1) from horse nasal swabs in 30 min with a detection limit of 18 copies per reaction. In this paper, EHV1 served as a model system for diagnosing SARS-CoV-2: the amplification primers were injected into the microfluidic channels and dried, the sample was introduced to the channel, followed by LAMP amplification at 65°C. After LAMP, fluorescence images were captured by a smartphone. The display was based on the emission of the DNA-intercalating dye EvaGreen to obtain an average pixel intensity value for detecting target nucleic acids (Sun et al., 2020).

Ganguli and colleagues elaborated a fluorescence chip-based biosensor based on LAMP for real-time detection of SARS-Cov-2 (with a detection limit of 5000 RNA copies/μL in nasal samples). The chip was made from 3D-printed microfluidic polymer cartridges consisting of a heater and optics *via* syringes and used EvaGreen, a double-stranded DNA-intercalating dye. The fluorescence signal generated by the amplicons was recorded *via* a smartphone, followed by analysis using ImageJ software (Ganguli et al., 2020).

Liu and colleagues developed a biosensor based on a fluorescent immunoassay to detect IgM, IgG, and SARS-CoV-2 antigen simultaneously. Each analyte is selectively detected on an individual microfluidic chip while they are simultaneously read in a portable device combining liquid handling and signal readout for POC diagnostics (Liu et al., 2020). Importantly, simultaneous detection of viral antigen and corresponding antibodies gives a specific and accurate diagnosis of SARS-CoV-2, overcoming barriers such as the transient expression of IgM in the blood (Lee et al., 2020) and the cross-reaction of antibodies targeting various coronavirus strains (Yuan et al., 2020). Chen and colleagues designed a lateral flow immunoassay to test for the presence of anti-SARS-CoV-2 IgG antibodies in serum samples. The test comprised lanthanide-doped polystyrene nanoparticles (L-NPs) acting as fluorescence reporters functionalized with either mouse anti-human IgG (M-HIgG) or rabbit IgG (rIgG) antibodies. As human serum was loaded onto the flow assay, human anti-SARS-CoV-2 IgG antibodies conjugated with M-HIgG@L-NPs and attached to the test line material leading to a change in the fluorescent signal at the test line (Chen et al., 2020).

Paper-based biosensors such as lateral flow test strips are versatile, cost-effective, and widely used in the clinical setup. Indeed, paper-based sensors have been used for the detection of cancer biomarkers as well as for the diagnostic of viral infections such as Ebola (Brangel et al., 2018), influenza A H1N1 (Lei et al., 2015) and recently, SARS-CoV-2 (Li et al., 2019). Paper-based biosensors can be classified into dipstick assay, lateral flow assay (LFA) and microfluidic paper-based analytical devices (μPADs). Generally, LFA is frequently used for pathogen detection due to their user-friendliness, low cost, and relatively high sensitivity. The paper substrates routinely used are cellulose (dipstick, μPADs) and nitrocellulose (LFA) membranes (Hu et al., 2014).

Wu and colleagues (Wu et al., 2017) developed an automated and portable paper-based microfluidic system for Influenza diagnosis, which consisted of a storage module with reagent chambers and a reaction module with the absorbent pad and nitrocellulose membrane functionalized with specific monoclonal antibodies. A smartphone was used to capture the image from the membrane and process the image with a Java algorithm.

Photonic biosensors have a high signal-to-noise ratio, and they can convert the molecular binding events to optical signals, easing the integration into mobile phones. For example, Su and colleagues developed a portable module that can detect clinically relevant levels of a secretory leukocyte protease inhibitor, an established biomarker for a lung infection in cystic fibrosis patients. Moreover, the results can be interpreted instantly and transmitted to the medical personnel (Sun et al., 2016).

Graphene-based biosensors have a higher electron transfer rate and a larger electrochemical surface area exhibiting advantages such as low cost and high production rate. A graphene-based FET biosensor was developed for SARS-CoV-2 diagnostics, using spike protein antibodies as the detection probe. Sensor performance was tested on a cultured virus, antigen protein and clinical nasopharyngeal samples and showed detection of SARS-CoV-2 spike protein at concentrations of 100 fg/mL in clinical transport medium and 1 fg/mL in phosphate-buffered saline (Seo et al., 2020). Mojsoska and colleagues reported the first optimization steps of a label-free electrochemical immunosensor using a graphene-modified working electrode to detect the SARS-CoV-2 spike protein. The biosensor detected subunit 1 (S1) of recombinant spike S protein at 260 nM (20 μg/mL) of subunit 1 of recombinant spike protein and SARS-CoV-2 (5.5×10^5 PFU/mL) (Mojsoska et al., 2021).

Integrated Systems With Potential for POC Use

Future devices will need to be ultra-sensitive and accessible for POCT detection of respiratory viruses (Noah and Ndangili, 2019). In this regard, the use of multiplex, integrated LOC systems will allow the simultaneous identification of several pathogens in a sample, although coinfection is not common in the case of viral RTI. Integrated systems should operate on a 'sample in and answer out' principle. During the early stages of infection, the biomarkers of viral infection have very low concentrations, and in conditions of the low sensitivity of POCT, the result will be negative. Enriching the biomarkers or the virus in the sample before detection is necessary (Yeh et al., 2014). Examples of integrated systems with potential POC use include the Alere BinaxNOW® (formerly Alere i) Influenza A&B platform (Abbott, United States; uses a fluorescent molecular signal) and the FILMARRAY Respiratory Panel (bioMérieux, France). The FILMARRAY Respiratory Panel employs nested real-time PCR to detect twenty respiratory pathogens. Seventeen viruses (AH1, AH1 2009, AH3, influenza B, adenovirus, the four common coronaviruses that produce the common cold, human metapneumovirus, human Rhinovirus/Enterovirus, parainfluenza 1, 2, 3, 4 and RSV) and three bacteria (*Bordetella pertussis*, *Chlamydophila pneumoniae*, and *Mycoplasma pneumoniae*) are detected. The specimens are from buccopharyngeal swabs, nasopharyngeal aspirates, and lower respiratory tract samples. The FILMARRAY Respiratory Panel platform has the precision of PCR diagnosis, it can be used as a POCT, it does not require laboratory specialists, and the results are available in one hour. MariPOC system (produced in Turku-Finland) is a multianalyte detection system that can simultaneously detect nine respiratory viruses (influenza A and B, RSV, parainfluenza 1, 2, 3, metapneumovirus, HboV - a parvovirus, adenovirus) and *Streptococcus pneumoniae*. (Bruning et al., 2017) Compared to RT-PCR, it presents moderate sensitivity for influenza and RSV and low sensitivity for adenovirus (Ivaska et al., 2013).

The GeneXpert systems automate and integrate sample preparation, nucleic acid extraction and amplification, and detection of the target sequences using real-time PCR and RT-PCR assays (Cepheid, a Danaher company, United States). The system runs on disposable (Xpert) cartridges that contain the RT-PCR reagents and allow the RT-PCR process. The GeneXpert panel Xpert Xpress SARS-CoV-2/Flu/RSV test is a rapid, multiplexed real-time RT-PCR test designed for the simultaneous qualitative detection and differentiation of influenza A, influenza B, SARS-CoV-2, and respiratory

syncytial virus (RSV) viral RNA in a nasopharyngeal swab, nasal swab or nasal wash/aspirate (Mostafa et al., 2021).

POCT Performance and Unmet Needs

Only a rapid, sensitive, and specific identification of pathogens will allow effective antiviral therapy and enable infection control measures. Even though POCT are simple to operate, correct sample collection, conditioning and/or preparation is essential to improve test performance. Moreover, multiple factors hindered the performance of POCT, such as the quality and handling of the specimen and the respiratory specimen type. Respiratory viruses are more likely to be detected when patient samples are collected soon after symptom onset because viral loads are generally higher early in the illness, with viral shedding peaking in the first 2-3 days of illness in adults (Foo and Dwyer, 2009). However, in children, viral shedding can take longer (Hazelton et al., 2015).

Because POCT can be performed outside the laboratory setting, they are not subject to quality assurance requirements. These rapid tests are approved by governing bodies (i.e., FDA), but their manufacturers are not obliged to monitor and improve their diagnostic tests. (Gill and Shepard, 2010) Hence, the performance of POCT may diminish once antigenic and genetic variants emerge. Continuous monitoring of POCT is of paramount importance to provide clinically relevant results.

While POC biosensors are widely available, there are still some unmet needs. For instance, commercial diagnostic kits involving IgG/IgM test strips need improved sensitivity and specificity. In addition, the multiplexing capability is essential for improved diagnosis and subsequent therapeutic management. For instance, the combination of both IgG/IgM and nucleic acid tests would detect both early and late stages of infection (such as COVID-19), thus yielding more accurate and reliable results.

Currently available POCT can be improved by incorporating antiviral susceptibility testing and identifying coinfections. For example, Hwang and colleagues described a lateral flow assay capable of detecting Tamiflu-resistant influenza virus using oseltamivir hexylthiol AuNPs with binding selectivity to Tamiflu-resistant virus. The test comprised detection and a control line marked with anti-influenza A virus nucleoprotein antibody and Tamiflu resistant neuraminidase protein (Hwang et al., 2018). This type of approach could potentially be developed for SARS-CoV-2 infection as well.

Another point for POCT improvement would be using alternative samples for diagnostic. For instance, respiratory droplets and aerosols are the main transmission vessel for respiratory infectious diseases but they are rarely used for diagnostic means (Tromberg et al., 2020). An interesting recent study by Nguyen and colleagues (Nguyen et al., 2020) described the use of wearable materials with embedded synthetic sensors for biomolecule detection, including SARS-CoV-2 (Nguyen et al., 2020). The research group developed a face mask sensor because viral particles accumulate inside masks because of respiration, sneezing, talking and coughing. The biosensor was made of four modular components, including a large surface collection sample pad, a reservoir for hydration, a lateral flow assay strip and a wax-patterned μPAD. All collected fluid and viral particles from the sample were shown to migrate from the sample collection pad to the μPAD, carrying an arrangement of freeze-dried lysis and detection components (Nguyen et al., 2020).

It is essential to highlight that POCT provides test results with a faster turnaround time in most instances compared to traditional approaches informing the clinical personnel before the patient reaches the hospital. Although detection of a virus does not exclude the possibility of a bacterial infection or a benefit from antibiotic treatment, a positive POCT result might also permit the premature discontinuation of precautionary antibiotics in patients with exacerbation of airways disease. If negative, a POCT result can shorten unnecessary quarantine measures and the use of antiviral treatments. Even though they are important tools in diagnosis, rapid tests do not necessarily guarantee improved clinical outcomes for all patients (Crozier et al., 2021).

INTERNET-OF-THINGS IN DETECTION OF RESPIRATORY VIRAL INFECTIONS' DETECTION

IoT is an application-specific, low power, effective, and easy to use tool to provide solutions to any real-time problems. Since IoT means are approached from various points of view, billions of connected things are already in use in 2015, and that number will reach 25 billion in just a few short years (Middleton et al., 2013). In the IoT world, sensors provide inputs from the physical world, which are transferred over a network, and actuators allow devices/things to act or react according to the received inputs. Gil and colleagues reviewed the surveys related to IoT, their general purpose and provided a well-integrated perspective for IoT, including a state-of-the-art of IoT to integrate IoT and social networks in the emerging Social Internet-of-Things (SIoT) term (Gil et al., 2016). Meanwhile, Internet-of-Medical-Things (IoMT) (Gatouillat et al., 2018) generates and aggregates abundant data in various ways. For instance, medical devices track the physiological parameters of patients (Bharadwaj et al., 2021) from home and the remote healthcare providers receive information about the mobility, slipping dynamics, heart rate, allergic reactions, blood pressure, blood glucose, body temperature, and oxygen saturation of the patients (Patel and Wang, 2010; Fortino et al., 2014; Jayanth et al., 2017), and decide on an accurate diagnosis (Panesar, 2019), build therapeutic plans, improve the security of patients, simplify caregiving, and continuously monitor critically ill patients (Gómez et al., 2016). Online consultations with doctors *via* Telehealth (Craig and Petterson, 2005) and imaging investigations (Huang et al., 2020) are more examples of IoT in healthcare, which contribute significantly to the quality of medical care and wellbeing of patients whose health status prevents them from going to hospitals. Additional modalities of remote healthcare *via* IoT medical devices facilitate personal emergency response systems (PERS). The solutions can make automatic calls for help in case of sudden changes in the medical status of the patients that make them appear at risk of being unable to call the ambulance on their own. Furthermore, in the case of infectious diseases such as

COVID-19 remote assistance and testing can significantly reduce hospital occupancy rates during the pandemic (Tuli et al., 2020). Currently, several IoT devices and applications are being employed in COVID-19 management, including smartphone applications, wearables, drones, IoT buttons and robots. Their characteristics are summarised in **Supplementary Table 3**.

A real-time response should follow a rapid diagnostic of viral RTI. Current advances in information technology exploit IoT related equipment and offer a large capacity for pandemic monitoring. For instance, smartphones are equipped with "lab-in-a-phone" IoT devices and an instant global positioning system (GPS) for rapid contact tracing (Xu et al., 2018; MD-Bio, 2021). There is an excellent opportunity to integrate IoT-POC connected devices by using cloud-based connectivity, and thus the results of the immediate analysis will be delivered to control centres for disease monitoring. Newly developed swarm technologies will develop real-time maps of the spread of infectious at the global level.

The first step in this direction was a hand-held IoT PCR used for dengue fever detection and its spread monitoring reported by Zhu and colleagues (Zhu et al., 2020). Such an IoT system is illustrated in **Figure 2** -adapted and improved from (Zhu et al., 2020). The sample tested for dengue fever can be processed anywhere, and the results and GPS location are submitted wireless using the patient's handphone to a control centre. A network can collect all results as cloud data to map a disease outbreak, show the respective area and continuously monitor. Surely, the solution can raise the question about the cybersecurity.

The IoT based biosensor 'RapidPlex' was grafted for ultra-rapid assessment of COVID-19 biomarkers (Torrente-Rodríguez et al., 2020). RapidPlex is a multiplex electrochemical platform that quantifies four COVID-19 markers: nucleocapsid protein, IgM, IgG antibodies and inflammatory C-reactive protein.

Recently, Mukhtar and colleagues described a device for measuring patients' critical status of the effects of SARS-CoV-2 infection or its symptoms using cough, temperature, heartbeat, and oxygen concentration. The device comprises wearable medical sensors integrated using the Arduino hardware interfacing, a smartphone application and an IoT framework (Mukhtar et al., 2021).

Kumar and colleagues presented a list of IoT sensors and their application areas and proposed an IoT architecture to avoid the spreading of COVID-19 (Kumar et al., 2020). Sensors in crowded places such as airports, malls, transport, public toilets, hospitals, and offices communicate data through a gateway device to cloud gateway and the big data used by machine learning (ML) will create models of the system based on requirements and received data. The configuration includes one thermo-sensor, one NodeMCU or Arduino board with sensors, the Internet, and possibly one mobile application at a smaller scale. Several open sources can be used to implement the protocol. Furthermore, Peeri and colleagues presented the role of big data in understanding the epidemiology and clinical factors that characterise the MERS, SARS and COVID-19. (Peeri et al., 2020) In terms of SARS-CoV-2 infection diagnostics, Lopez-Rincon and colleagues (Lopez-Rincon et al., 2020) proposed a deep convoluted neural network (CNN) to create features from genome sequencing automatically. The accuracy of identification and classification into different coronaviruses were 98% and 98.75%, respectively, despite the limited data set and limited genome sequences being considered. A model that demonstrated the superiority of a Support Vector Machine (SVM) classifier in identifying influenza-like illnesses -i.e., acute respiratory infections- (Ginantra et al., 2020) used neural networks, level 2 models with better results than a single level model. The design stemmed from the rapid antigenic shift as the source of virus variants makes the understanding of effects of specific mutations on pathogenicity difficult to understand. The results for a confusion matrix showed 97.4% sensitivity, 90% specificity, and for the K-Nearest Neighbours (KNN) classifier, 94.7% accuracy. Pineda and colleagues studied seven ML classifiers for influenza detection, compared their diagnostic capabilities against an expert-built influenza Bayesian classifier, and evaluated different ways of handling missing clinical

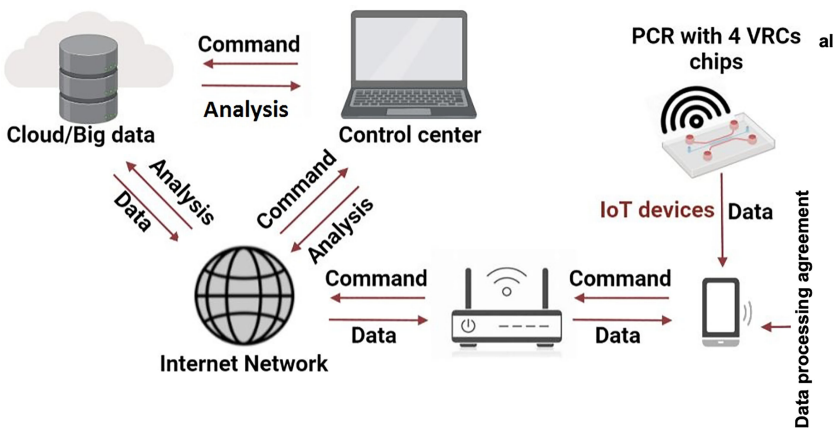

FIGURE 2 | Working principle of an IoT PCR for RTI detection and spread monitoring. Adapted with permission from (Zhu et al., 2020).

information from the free-text reports in four hospitals emergency departments (Pineda et al., 2015). The study, despite its limitations, showed that ML classifiers had a better performance than expert constructed classifiers are given a particular natural language processing (NLP) extraction system and that analysing information from the electronic health records using machine learning classifiers can achieve significant accuracies in the presence of abundant clinical reports. Since large data is crucial to the early identification of acute upper RTI during early stages, it minimizes adverse effects on infants and prevents mortality. Therefore, studies addressed disease prediction of cases. For instance, Yin and colleagues established a stacking model to predict on antigenic variants of the H1N1 influenza virus (Yin et al., 2018). The study first classified past cases as pandemic-based and epidemic-based and concluded that ML classifiers showed superior performance to expert Bayesian classifiers for the given use case. Sato and colleagues built an epidemic spread model using IoT technologies to monitor human mobility and contact data (Sato et al., 2016). They introduced the agent-based infections diffusion simulation using real human mobility data as a metapopulation network to control the spread of outbreaks. A study by Chen and colleagues used mobile phone data to build a model to track dynamic changes in a network as an epidemic spread network (Chen et al., 2016). The control of epidemics was also addressed by Miller and colleagues who proposed methods to generate accurate forecast data for influenza outbreaks using smart thermometers connected to a mobile application (Miller et al., 2018). The data aggregated and stored onto a cloud-based platform, analysed in conjunction with the Centre for Disease Communication and users' location, developed a model for forecasting ILI up to three weeks in advance and helped track fever duration to identify biphasic patterns. Referring to influenza outbreaks, Tapak and colleagues investigated different ML methods for building models on illness frequencies (Tapak et al., 2019). However, not including factors of climatic parameters, weather conditions, and sentinel data from ILI limited the and asked for careful evaluation before implementing the algorithm for predicting the outbreaks of the disease. Since the limitations of these studies needed to be addressed, significant effort concentrated on solutions such as remote labs to complement the control engineering laboratories and include industrial revolution relevant methods. For instance, an open-source feature with LINX and Arduino board was incorporated to assist in the data acquisition with cost-effective platforms that interact with the actual labs *via* mobile devices (Ferrari et al., 2017; Andreini et al., 2018; França et al., 2021; Hairuddin et al., 2021). Furthermore, IoT enables further development of remote medicine for the on-body monitoring *via* either consumer wearables (track the health conditions of patients and healthy people) or clinical devices -track and transmit some highly specialised health metrics directly to healthcare organisations and doctors- (Atzori et al., 2010). Notably, these devices can be customised for other viral agents. Hence they harbour tremendous potential in the management of infectious diseases. Despite their considerable advantages, IoT devices raise concerns regarding the privacy issues occurring when patients are asked to share their information. Clearly, defining secure channels for communications or different encryption techniques before sharing private information is essential for the successful implementation of IoT devices. Therefore, optimising nano-enabled viral biosensing, IoT, and artificial intelligence (AI) could open avenues for various integrated low cost highly performant detection technology for error-free, smart controlling at a personalised level. In conclusion, IoT technology coupled with POCT platforms would be instrumental in offering diagnostic platforms and therapeutic approaches for future global health challenges (Konwarh and Cho, 2021, Swayamsiddha et al., 2021).

NEXT STEP IN THE DETECTION OF RESPIRATORY VIRAL INFECTIONS - AI

Internet-connected POC testing devices, coupled with predictive models and artificial intelligence (AI), would be a great asset in disease evolution monitoring and provide a valuable tool to stop their spreading (Sim and Cho, 2021). AI programs developed to diagnose a disease would be trained on data-like symptoms, lab results, and scans and images of confirmed and susceptible cases. AI-based detection techniques can be successfully employed for diagnosis. For instance, end-to-end portable systems can record data from symptomatic patients (*i.e.* coughs) and further translate them into health data for diagnosis. Subsequently, with ML symptoms can be linked to different respiratory illnesses, including COVID-19.

CONCLUSIONS

Recently, significant improvements in respiratory virus diagnostics, from novel specimen collection instruments to highly sensitive and multiplexed nucleic acid amplification tests, demonstrated the potential of the expanding list of antigen and molecular-based tests for comprehensive laboratory testing of respiratory viruses without even virus isolation. However, cell culture remains the reference method with excellent sensitivity and specificity (detects a broad spectrum of viruses as little as 1 infectious unit). Compared with cell-culture-based viral load quantification, immunofluorescent staining provides results within several hours, but the sensitivity and availability of antisera can be limiting factors. Furthermore, PCR assays with superior sensitivity to culture or immunofluorescent staining have been transformed into an essential viral diagnostic tool. Also, the main challenge NAAT technology faces is to achieve inexpensive, high-throughput, and automatic NA detection from raw samples (e.g., whole blood). Therefore, most diagnostic virology laboratories use a combination of viral culture, immunofluorescent staining, and PCR assays to detect respiratory viruses. The continuous advances of technology to improve turnaround time (combined shell vial cultures and immunostaining) and sensitivity (nucleic acid amplification

technologies such as PCR and LAMP) has paved the future of additional commercial test kits for molecular detection of respiratory viruses, including multiplexed assays.

Moreover, further research is required to elucidate the clinical significance of persistent positive PCR results in a patient and viral coinfection. Ultimately, the utilisation of molecular testing, particularly highly multiplexed tests in routine patient management, will depend on the cost/benefit ratio. The solution might be the fully integrated microfluidics devices easily manufactured and used (Li et al., 2020, Nelson et al., 2020). Therefore, cost-effective LOC platforms (microfluidics- and biosensors-based) as future technology developments in respiratory virus diagnostics should accurately and rapidly detect a spectrum of clinically significant viruses to influence the patient and epidemiologic management at higher standards for systematic implementation of standardised infection control measures not achievable with laboratory-developed tests. The current COVID-19 pandemic highlights again the stringent need for tools and technology for fast, accurate, non-molecular and molecular POCT cum IoT devices for efficient diagnosis. Other studies revealed the applicability of digital PCR (Chen et al., 2021), surface-enhanced Raman scattering -SERS- (Chen et al., 2021), plasmonic- (Li et al., 2019) and nanophotonic label free-based biosensors (Soler et al., 2020) in nucleic acid rapid testing and respiratory viral disease diagnosis in the future.

Additionally, their large-scale implementation will require laboratory validation and quality assurance protocols as the performance will vary with each generation of assays and clinical environment (Bouzid et al., 2021). It is also crucial that specialists understand the characteristics and limitations of commercial kits provided to keep the costs affordable. Since novel viral outbreaks are foreseeable, it is imperative to have portable, fast, and accurate virus sensing technology for timely diagnosis. Virus identification can be used to (1) determine treatment strategies (antiviral medications), (2) predict disease course and expected outcome, (3) predict the potential for virus spread, (4) allow identification and vaccination of susceptible individuals, and (5) trace the movement of a virus through a community or worldwide. The efforts invested into this rapidly developing domain should continue and materialise.

AUTHOR CONTRIBUTIONS

GP, FI, MP, MS, GM, AC, OI, LB, and MT wrote the manuscript. MC and CI revised and edited the manuscript. All authors contributed to the article and approved the submitted version.

FUNDING

This research was funded by the grant PN-III-P2-2.1-SOL-2020-0090-Contract 13Sol/15.06.2020, project "Advanced techniques for early SARS-CoV2 detection" and PN-III-P4-ID-PCE-2020-1886 Contract PCE 180/17/02/2021 awarded to CI and by CNFIS-FDI-2021-0405, awarded to MC.

SUPPLEMENTARY MATERIAL

The Supplementary Material for this article can be found online at: https://www.frontiersin.org/articles/10.3389/fcimb.2022.807253/full#supplementary-material

REFERENCES

Aalberts, M., van Dissel-Emiliani, F. M. F., van Adrichem, N. P., van Wijnen, H. M., Wauben, M. H., Stout, T. A., et al. (2012). Identification of Distinct Populations of Prostasomes That Differentially Express Prostate Stem Cell Antigen, Annexin A1, and GLIPR2 in Humans. *Biol. Reprod.* 86, 1–8. doi: 10.1095/biolreprod.111.095760

Afroj, S., Britnell, L., Hasan, T., Andreeva, D. V., Novoselov, K. S., and Karim, N. (2021). Graphene-Based Technologies for Tackling COVID-19 and Future Pandemics. *Adv. Funct. Mater.* 31, 2107407. doi: 10.1002/adfm.202107407

Ahluwalia, G., Embree, J., McNicol, P., Law, B., and Hammond, G. (1987). Comparison of Nasopharyngeal Aspirate and Nasopharyngeal Swab Specimens for Respiratory Syncytial Virus Diagnosis by Cell Culture, Indirect Immunofluorescence Assay, and Enzyme-Linked Immunosorbent Assay. *J. Clin. Microbiol.* 25, 763–767. doi: 10.1128/jcm.25.5.763-767.1987

Ahmadivand, A., Gerislioglu, B., Ramezani, Z., Kaushik, A., Manickam, P., and Ghoreishi, S. A. (2021). Functionalized Terahertz Plasmonic Metasensors: Femtomolar-Level Detection of SARS-CoV-2 Spike Proteins. *Biosens. Bioelectron.* 177, 112971. doi: 10.1016/j.bios.2021.112971

Andreini, P., Bonechi, S., Bianchini, M., Mecocci, A., and Scarselli, F. (2018). "A Deep Learning Approach to Bacterial Colony Segmentation", in *International Conference on Artificial Neural Networks* (Rhodes, Greece: Springer).

Anema, A., Kluberg, S., Wilson, K., Hogg, R. S., Khan, K., Hay, S. I., et al. (2014). Digital Surveillance for Enhanced Detection and Response to Outbreaks. *Lancet Infect. Dis.* 14 (11), 1035–1037. doi: 10.1016/S1473-3099(14)70953-3

Anik, Ü. (2017). "Electrochemical Medical Biosensors for POC Applications", in *Medical Biosensors for Point of Care (POC) Applications* (Sawston, United Kingdom: Woodhead Publishing), 275–292. doi: 10.1016/B978-0-08-100072-4.00012-5

Assiri, A., Al-Tawfiq, J. A., Al-Rabeeah, A. A., Al-Rabiah, F. A., Al-Hajjar, S., Al-Barrak, A., et al. (2013). Epidemiological, Demographic, and Clinical Characteristics of 47 Cases of Middle East Respiratory Syndrome Coronavirus Disease From Saudi Arabia: A Descriptive Study. *Lancet Infect. Dis.* 13 (9), 752–761. doi: 10.1016/S1473-3099(13)70204-4

Atzori, L., Iera, A., and Morabito, G. (2010). The Internet of Things: A Survey. *Comput. Netw.* 54 (15), 2787–2805. doi: 10.1016/j.comnet.2010.05.010

Azar, M. M., and Landry, M. L. (2018). Detection of Influenza A and B Viruses and Respiratory Syncytial Virus by Use of Clinical Laboratory Improvement Amendments of 1988 (CLIA)-Waived Point-of-Care Assays: A Paradigm Shift to Molecular Tests. *J Clin. Microbiol.* 56 (7), e00367–e00318. doi: 10.1128/JCM.00367-18

Azzi, L., Carcano, G., Gianfagna, F., Grossi, P., Dalla Gasperina, D., Genoni, A., et al. (2020). Saliva is a Reliable Tool to Detect SARS-CoV-2. *J. Infect.* 81 (1), e45–e50. doi: 10.1016/j.jinf.2020.04.005

Babiker, A., Immergluck, S. K., Stampfer, D., Rao, A., Bassit, L., Su, M., et al. (2021). Single-Amplicon, Multiplex Real-Time RT-PCR With Tiled Probes to Detect SARS-CoV-2 Spike Mutations Associated With Variants of Concern. *J. Clin. Microbiol.* 59 (12), 01446–01421. doi: 10.1128/jcm.01446-21

Baghizadeh Fini, M. (2020). Oral Saliva and COVID-19. *Oral. Oncol.* 108, 104821–104821. doi: 10.1016/j.oraloncology.2020.104821

Basile, K., Kok, J., and Dwyer, D. E. (2018). Point-Of-Care Diagnostics for Respiratory Viral Infections. *Expert Rev. Mol. Diagn.* 18 (1), 75–83. doi: 10.1080/14737159.2018.1419065

Becker, H., and Gärtner, C. (2008). Polymer Microfabrication Technologies for Microfluidic Systems. *Anal. Bioanal. Chem.* 390 (1), 89–111. doi: 10.1007/s00216-007-1692-2

Benito-Fernández, J., Vázquez-Ronco, M. A., Morteruel-Aizkuren, E., Mintegui-Raso, S., Sánchez-Etxaniz, J., and Fernández-Landaluce, A. (2006). Impact of Rapid Viral Testing for Influenza A and B Viruses on Management of Febrile Infants Without Signs of Focal Infection. *Pediatr. Infect. Dis. J.* 25 (12), 1153–1157. doi: 10.1097/01.inf.0000246826.93142.b0

Bharadwaj, H. K., Agarwal, A., Chamola, V., Lakkaniga, N. R., Hassija, V., and Guizani, M. (2021). Sikdar (B.2021). A Review on the Role of Machine Learning in Enabling IoT Based Healthcare Applications. *IEEE Access* 9, 38859–38890. doi: 10.1109/ACCESS.2021.3059858

Blaschke, A. J., Allison, M. A., Meyers, L., Rogatcheva, M., Heyrend, C., Mallin, B., et al. (2011). Non-Invasive Sample Collection for Respiratory Virus Testing by Multiplex PCR. *J. Clin. Virol.* 52 (3), 210–214. doi: 10.1016/j.jcv.2011.07.015

Booss, J., and Tselis, A. C. (2014). "A History of Viral Infections of the Central Nervous System: Foundations, Milestones, and Patterns," in *Handbook of Clinical Neurology*. Amsterdam, Netherlands: Elsevier, vol. 123., 3–44. doi: 10.1016/B978-0-444-53488-0.00001-8

Bouzid, D., Zanella, M.-C., Kerneis, S., Visseaux, B., May, L., Schrenzel, J., et al. (2021). Rapid Diagnostic Tests for Infectious Diseases in the Emergency Department. *Clin. Microbiol. Infect.* 27 (2), 182–191. doi: 10.1016/j.cmi.2020.02.024

Brangel, P., Sobarzo, A., Parolo, C., Miller, B. S., Howes, P. D., Gelkop, S., et al. (2018). A Serological Point-of-Care Test for the Detection of IgG Antibodies Against Ebola Virus in Human Survivors. *ACS Nano* 12 (1), 63–73. doi: 10.1021/acsnano.7b07021

Brazaca, L., Ribovski, L., Janegitz, B., and Zucolotto, V. (2017). "Nanostructured Materials and Nanoparticles for Point of Care (POC) Medical Biosensors," in *Medical Biosensors for Point of Care (POC) Applications* (Sawston, United Kingdom: Woodhead Publishing), 229–254. doi: 10.1016/B978-0-08-100072-4.00010-1

Brendish, N. J., Schiff, H. F., and Clark, T. W. (2015). Point-Of-Care Testing for Respiratory Viruses in Adults: The Current Landscape and Future Potential. *J. Infect.* 71 (5), 501–510. doi: 10.1016/j.jinf.2015.07.008

Broughton, J. P., Deng, X., Yu, G., Fasching, C. L., Servellita, V., Singh, J., et al. (2020). CRISPR–Cas12-Based Detection of SARS-CoV-2. *Nat. Biotechnol.* 38 (7), 870–874. doi: 10.1038/s41587-020-0513-4

Bruning, A. H., Leeflang, M. M., Vos, J. M., Spijker, R., de Jong, M. D., Wolthers, K. C., et al. (2017). Rapid Tests for Influenza, Respiratory Syncytial Virus, and Other Respiratory Viruses: A Systematic Review and Meta-Analysis. *Clin. Inf. Dis.* 65 (6), 1026–1032. doi: 10.1093/cid/cix461

Burbelo, P. D., Iadarola, M. J., and Chaturvedi, A. (2019). Emerging Technologies for the Detection of Viral Infections. *Future Virol.* 14 (1), 39–49. doi: 10.1021/acsomega.0c05850

Business Wire. (2021). *Global Point of Care Diagnostics Marke to 2028) - COVID-19 Impact and Analysis ResearchAndMarkets.Com*. Available at: https://www.businesswire.com/news/home/20211209005712/en/Global-Point-of-Care-Diagnostics-Market-2021-to-2028—COVID-19-Impact-and-Analysis—ResearchAndMarkets.com.

CDC (Centers for Disease Control and Prevention). (2021a). *Interim Guidelines for Collecting and Handling of Clinical Specimens for COVID-19 Testing*. Available at: https://www.cdc.gov/coronavirus/2019-ncov/lab/guidelines-clinical-specimens.html (Accessed December 20, 2021).

CDC (Centers for Disease Control and Prevention). (2021b). *How to Collect an Anterior Nasal Swab Specimen for COVID-19 Testing*. Available at: https://www.cdc.gov/coronavirus/2019-ncov/testing/How-To-Collect-Anterior-Nasal-Specimen-for-COVID-19.pdf (Accessed December 20, 2021).

Centres for Disease Control and Prevention. (2021). *Specimen Collection*. Available at: https://stacks.cdc.gov/view/cdc/105541 (Accessed December 20, 2021).

Chan, K., Peiris, J., Lim, W., Nicholls, J., and Chiu, S. (2008). Comparison of Nasopharyngeal Flocked Swabs and Aspirates for Rapid Diagnosis of Respiratory Viruses in Children. *J. Clin. Virol.* 42 (1), 65–69. doi: 10.1016/j.jcv.2007.12.003

Charlton, C. L., Babady, E., Ginocchio, C. C., Hatchette, T. F., Jerris, R. C., Li, Y., et al. (2019). Practical Guidance for Clinical Microbiology Laboratories: Viruses Causing Acute Respiratory Tract Infections. *Clin. Microbiol. Rev.* 32 (1), e00042–e00018. doi: 10.1128/CMR.00042-18

Chen, P., Chen, C., Su, H., Zhou, M., Li, S., Du, W., et al. (2021). Integrated and Finger-Actuated Microfluidic Chip for Point-of-Care Testing of Multiple Pathogens. *Talanta* 224, 121844. doi: 10.1016/j.talanta.2020.121844

Cheng, P. K., Wong, D. A., Tong, L. K., Ip, S.-M., Lo, A. C., Lau, C.-S., et al. (2004). Viral Shedding Patterns of Coronavirus in Patients With Probable Severe Acute Respiratory Syndrome. *Lancet* 363 (9422), 1699–1700. doi: 10.1016/S0140-6736(04)16255-7

Chen, Y., Shu, L., Crespi, N., Lee, G. M., and Guizani, M. (2016). "Understanding the Impact of Network Structure on Propagation Dynamics Based on Mobile Big Data," in *2016 International Wireless Communications and Mobile Computing Conference (IWCMC)* (Paphos, Cyprus: IEEE). doi: 10.1109/IWCMC.2016.7577198

Chen, L., Yadav, V., Zhang, C., Huo, X., Wang, C., Senapati, S., et al. (2021). E Elliptical Pipette Generated Large Microdroplets for POC Visual ddPCR Quantification of Low Viral Load. *Anal. Chem.* 93 (16), 6456–6462. doi: 10.1021/acs.analchem.1c00192

Chen, Z., Zhang, Z., Zhai, X., Li, Y., Lin, L., Zhao, H., et al. (2020). Rapid and Sensitive Detection of Anti-SARS-CoV-2 IgG, Using Lanthanide-Doped Nanoparticles-Based Lateral Flow Immunoassay. *Anal. Chem.* 92 (10), 7226–7231. doi: 10.1021/acs.analchem.0c00784

Choi, J. R. (2020). Development of Point-of-Care Biosensors for COVID-19. *Front. Chem.* 8, 517. doi: 10.3389/fchem.2020.00517

Coarsey, C., Coleman, B., Kabir, M. A., Sher, M., and Asghar, W. (2019). Development of a Flow-Free Magnetic Actuation Platform for an Automated Microfluidic ELISA. *RSC Adv.* 9 (15), 8159–8168. doi: 10.1039/C8RA07607C

Corstjens, P. L., Abrams, W. R., and Malamud, D. (2016). Saliva and Viral Infections. *Periodontol. 2000* 70 (1), 93–110. doi: 10.1111/prd.12112

Craig, J., and Petterson, V. (2005). Introduction to the Practice of Telemedicine. *J. Telemed. Telecare* 11 (1), 3–9. doi: 10.1177/1357633X0501100102

Crozier, A., Rajan, S., Buchan, I., and McKee, M. (2021). Put to the Test: Use of Rapid Testing Technologies for Covid-19. *BMJ* 372:208. doi: 10.1136/bmj.n208

Dalal, A., Gill, P. S., Narang, J., Prasad, M., and Mohan, H. (2020). Genosensor for Rapid, Sensitive, Specific Point-of-Care Detection of H1N1 Influenza (Swine Flu). *Process Biochem.* 98, 262–268. doi: 10.1016/j.procbio.2020.09.016

Daley, P., Castriciano, S., Chernesky, M., and Smieja, M. (2006). Comparison of Flocked and Rayon Swabs for Collection of Respiratory Epithelial Cells From Uninfected Volunteers and Symptomatic Patients. *J. Clin. Microbiol.* 44 (6), 2265–2267. doi: 10.1128/JCM.02055-05

Darwish, N. T., Sekaran, S. D., and Khor, S. M. (2018). Point-Of-Care Tests: A Review of Advances in the Emerging Diagnostic Tools for Dengue Virus Infection. *Sens. Actuators B Chem.* 255, 3316–3331. doi: 10.1016/j.snb.2017.09.159

De Blic, J., Midulla, F., Barbato, A., Clement, A., Dab, I., Eber, E., et al. (2000). Bronchoalveolar Lavage in Children. ERS Task Force on Bronchoalveolar Lavage in Children. *Eur. Respir. J.* 15 (1), 217–231. doi: 10.1183/09031936.00.15121700

Dhama, K., Patel, S. K., Sharun, K., Pathak, M. R., Tiwari, M. I., Yatoo, Y., et al. (2020). SARS-CoV-2 Jumping the Species Barrier: Zoonotic Lessons From SARS, MERS and Recent Advances to Combat This Pandemic Virus. *Travel Med. Infect. Dis.* 37, 101830. doi: 10.1016/j.tmaid.2020.101830

Ding, X., Yin, K., Li, Z., and Liu, C. (2020). All-In-One Dual CRISPR-Cas12a (AIOD-CRISPR) Assay: A Case for Rapid, Ultrasensitive and Visual Detection of Novel Coronavirus SARS-CoV-2 and HIV Virus. *BioRxiv* 11 (1), 4711. doi: 10.1101/2020.03.19.998724

Doan, Q. H., Kissoon, N., Dobson, S., Whitehouse, S., Cochrane, D., Schmidt, B., et al. (2009). A Randomized, Controlled Trial of the Impact of Early and Rapid Diagnosis of Viral Infections in Children Brought to an Emergency Department With Febrile Respiratory Tract Illnesses. *J. Pediatr.* 154 (1), 91–95. doi: 10.1016/j.jpeds.2008.07.043

Doherty, J., Brookfield, D., Gray, J., and McEwan, R. (1998). Cohorting of Infants With Respiratory Syncytial Virus. *J. Hosp. Infect.* 38 (3), 203–206. doi: 10.1016/S0195-6701(98)90275-4

Drain, P. K., Hyle, E. P., Noubary, F., Freedberg, K. A., Wilson, D., Bishai, W. R., et al. (2014). Diagnostic Point-of-Care Tests in Resource-Limited Settings. *Lancet Infect. Dis.* 14 (3), 239–249. doi: 10.1016/S1473-3099(13)70250-0

Drancourt, M., Michel-Lepage, A., Boyer, S., and Raoult, D. (2016). The Point-of-Care Laboratory in Clinical Microbiology. *Clin. Microbiol. Rev.* 29 (3), 429–447. doi: 10.1128/CMR.00090-15

Duchesne, L., and Lacombe, K. (2018). Innovative Technologies for Point-of-Care Testing of Viral Hepatitis in Low-Resource and Decentralized Settings. *J. Viral Hep.* 25 (2), 108–117. doi: 10.1111/jvh.12827

Dziąbowska, K., Czaczyk, E., and Nidzworski, D. (2018). Detection Methods of Human and Animal Influenza Virus—Current Trends. *Biosensors* 8 (4), 94. doi: 10.3390/bios8040094

Egilmezer, E., Walker, G. J., Bakthavathsalam, P., Peterson, J. R., Gooding, J. J., Rawlinson, W., et al. (2018). Systematic Review of the Impact of Point-of-Care Testing for Influenza on the Outcomes of Patients With Acute Respiratory Tract Infection. *Rev. Med. Virol.* 28 (5), e1995. doi: 10.1002/rmv.1995

Ertl, P., Emrich, C. A., Singhal, P., and Mathies, R. A. (2004). Capillary Electrophoresis Chips With a Sheath-Flow Supported Electrochemical Detection System. *Anal. Chem.* 76 (13), 3749–3755. doi: 10.1021/ac035282a

Fendrick, A. M., Monto, A. S., Nightengale, B., and Sarnes, M. (2003). The Economic Burden of Non–Influenza-Related Viral Respiratory Tract Infection in the United States. *Arch. Intern. Med.* 163 (4), 487–494. doi: 10.1001/archinte.163.4.487

Ferrari, A., Lombardi, S., and Signoroni, A. (2017). Bacterial Colony Counting With Convolutional Neural Networks in Digital Microbiology Imaging. *Pattern Recognit.* 61, 629–640. doi: 10.1016/j.patcog.2016.07.016

Fabiani, L., Saroglia, M., Galatà, G., et al (2021). Magnetic Beads Combined With Carbon Black-Based Screen-Printed Electrodes for COVID-19: A Reliable and Miniaturized Electrochemical Immunosensor for SARS-CoV-2 Detection in Saliva. *Biosens Bioelectron* 171, 112686. doi: 10.1016/j.bios.2020.112686

Foo, H., and Dwyer, D. E. (2009). Rapid Tests for the Diagnosis of Influenza. *Aust. Prescr.* 32, 64–67. doi: 10.18773/austprescr.2009.034

Fortino, G., Parisi, D., Pirrone, V., and Di Fatta, G. (2014). BodyCloud: A SaaS Approach for Community Body Sensor Networks. *Future Gener. Comput. Syst.* 35, 62–79. doi: 10.1016/j.future.2013.12.015

França, R. P., Iano, Y., Monteiro, A. C. B., and Arthur, R. (2021). "A Methodology for Improving Efficiency in Data Transmission in Healthcare Systems," in *Internet of Things for Healthcare Technologies* (Singapore: Springer), 49–70. doi: 10.1007/978-981-15-4112-4_3

Ganguli, A., Mostafa, A., Berger, J., Aydin, M. Y., Sun, F., de Ramirez, S. A. S., et al. (2020). Rapid Isothermal Amplification and Portable Detection System for SARS-CoV-2. *Proc. Natl. Acad. Sci. U. S. A.* 117 (37), 22727–22735. doi: 10.1073/pnas.2014739117

Gatouillat, A., Badr, Y., Massot, B., and Sejdić, E. (2018). Internet of Medical Things: A Review of Recent Contributions Dealing With Cyber-Physical Systems in Medicine. *IEEE Internet Things J.* 5 (5), 3810–3822. doi: 10.1109/JIOT.2018.2849014

Gil, D., Ferrández, A., Mora-Mora, H., and Peral, J. (2016). Internet of Things: A Review of Surveys Based on Context Aware Intelligent Services. *Sensors* 16 (7), 1069. doi: 10.3390/s16071069

Gill, J. P., and Shephard, M. D. (2010). The Conduct of Quality Control and Quality Assurance Testing for PoCT Outside the Laboratory. *Clin. Biochemist. Rev.* 31 (3), 85.

Ginantra, N., Indradewi, I., and Hartono, E. (2020). Machine Learning Approach for Acute Respiratory Infections (ISPA) Prediction: Case Study Indonesia. *J. Phys. Conf. Ser.* 1469, 12044. doi: 10.1088/1742-6596/1469/1/012044

Gómez, J., Oviedo, B., and Zhuma, E. (2016). Patient Monitoring System Based on Internet of Things. *Proc. Comput. Sci.* 83, 90–97. doi: 10.1016/j.procs.2016.04.103

Groothuis, J., Bauman, J., Malinoski, F., and Eggleston, M. (2008). Strategies for Prevention of RSV Nosocomial Infection. *J. Perinatol.* 28 (5), 319–323. doi: 10.1038/jp.2008.37

Hairuddin, M. A., Ashar, N. D. K. A., Abidin, F. Z., and Tahir, N. M. (2021). *Cost-Effective Interfaces With Arduino-LabVIEW for an IOT-Based Remote Monitoring Application* (London, UK: IntechOpen). doi: 10.5772/intechopen.97784

Hazelton, B., Gray, T., Ho, J., Ratnamohan, V. M., Dwyer, D. E., and Kok, J. (2015). Detection of Influenza A and B With the Alere™ I Influenza A & B: A Novel Isothermal Nucleic Acid Amplification Assay. *Influenza Other Respir. Viruses* 9 (3), 151–154. doi: 10.1111/irv.12303

Hou, N., Wang, K., Zhang, H., Bai, M., Chen, H., Song, W., et al. (2020). Comparison of Detection Rate of 16 Sampling Methods for Respiratory Viruses: A Bayesian Network Meta-Analysis of Clinical Data and Systematic Review. *BMJ Glob. Health* 5 (11), e003053. doi: 10.1136/bmjgh-2020-003053

Huang, L., Han, R., Ai, T., Yu, P., Kang, H., Tao, Q., et al. (2020). Serial Quantitative Chest CT Assessment of COVID-19: A Deep Learning Approach. *Radiol.: Cardiothor. Imaging* 2 (2), e200075. doi: 10.1148/ryct.2020200075

Hui, D. S., Rossi, G. A., and Johnston, S. L. (2016). *SARS, MERS and Other Viral Lung Infections: ERS Monograph* (Sheffield (UK): European Respiratory Society). doi: 10.1183/2312508X.10008516

Hu, J., Wang, S., Wang, L., Li, F., Pingguan-Murphy, B., Lu, T. J., et al. (2014). Advances in Paper-Based Point-of-Care Diagnostics. *Biosens. Bioelectron.* 54, 585–597. doi: 10.1016/j.bios.2013.10.075

Hwang, S. G., Ha, K., Guk, K., Lee, D. K., Eom, G., Song, S., et al. (2018). Rapid and Simple Detection of Tamiflu-Resistant Influenza Virus: Development of Oseltamivir Derivative-Based Lateral Flow Biosensor for Point-of-Care (POC) Diagnostics. *Sci. Rep.* 8 (1), 12999. doi: 10.1038/s41598-018-31311-x

IHME IHME. (2021). *Global, Regional, and National Burden of Respiratory Tract Cancers and Associated Risk Factors From 1990 to 2019: A Systematic Analysis for the Global Burden of Disease Study 2019*. Available at: https://www.healthdata.org/research-article/global-regional-and-national-burden-respiratory-tract-cancers-and-associated-risk (Accessed December 20, 2021).

Iliescu, F. S., Ionescu, A. M., Gogianu, L., Simion, M., Dediu, V., Chifiriuc, M. C., et al. (2021). Point-of-Care Testing-The Key in the Battle Against SARS-CoV-2 Pandemic. *Micromachines* 12 (12), 1464. doi: 10.3390/mi12121464

Influenza Specimen Collection. Available at: https://www.cdc.gov/flu/pdf/1126freeresources/healthcare/flu1127specimen-collection-guide.pdf (Accessed December 20, 2021).

Ivaska, L., Niemelä, J., Heikkinen, T., Vuorinen, T., and Peltola, V. (2013). Identification of Respiratory Viruses With a Novel Point-of-Care Multianalyte Antigen Detection Test in Children With Acute Respiratory Tract Infection. *J. Clin. Virol.* 57 (2), 136–140. doi: 10.1016/j.jcv.2013.02.011

Jayanth, S., Poorvi, M., Shreyas, R., Padmaja, B., and Sunil, M. (2017). "Wearable Device to Measure Heart Beat Using IoT," in *2017 International Conference on Inventive Systems and Control (ICISC)* (Coimbatore, India: IEEE). doi: 10.1109/ICISC.2017.8068704

Jin, X., Ren, J., Li, R., Gao, Y., Zhang, H., Li, J., et al. (2021). Global Burden of Upper Respiratory Infections in 204 Countries and Territories, From 1990 to 2019. *EClinicalMedicine* 37, 100986. doi: 10.1016/j.eclinm.2021.100986

Jung, W., Han, J., Choi, J.-W., and Ahn, C. H. (2015). Point-Of-Care Testing (POCT) Diagnostic Systems Using Microfluidic Lab-on-a-Chip Technologies. *Microelectron. Eng.* 132, 46–57. doi: 10.1016/j.mee.2014.09.024

Khalaf, K., Papp, N., Chou, J. T.-T., Hana, D., Mackiewicz, A., and Kaczmarek, M. (2020). SARS-CoV-2: Pathogenesis, and Advancements in Diagnostics and Treatment. *Front. Immun.* 11, 570927. doi: 10.3389/fimmu.2020.570927

Khan, R. S., Khurshid, Z., and Yahya, F. (2017). Advancing Point-of-Care (PoC) Testing Using Human Saliva as Liquid Biopsy. *Diagnostics* 7 (3), 39. doi: 10.3390/diagnostics7030039

Khanna, M., Kumar, P., Chugh, L., Prasad, A., and Chhabra, S. (2001). Evaluation of Influenza Virus Detection by Direct Enzyme Immunoassay (EIA) and Conventional Methods in Asthmatic Patients. *J. Commun. Dis.* 33 (3), 163–169.

Konwarh, R., and Cho, W. C. (2021). Fortifying the Diagnostic-Frontiers With Nanoscale Technology Amidst the COVID-19 Catastrophe. *Expert Rev. Mol. Diagn.* 21 (2), 131–135. doi: 10.1080/14737159.2021.1878879

Koskinen, J. O., Vainionpää, R., Meltola, N. J., Soukka, J., Hänninen, P. E., and Soini, A. E. (2007). Rapid Method for Detection of Influenza A and B Virus Antigens by Use of a Two-Photon Excitation Assay Technique and Dry-Chemistry Reagents. *J. Clin. Microbiol.* 45 (11), 3581–3588. doi: 10.1128/JCM.00128-07

Ksiazek, T. G., Erdman, D., Goldsmith, C. S., Zaki, S. R., Peret, T., Emery, S., et al. (2003). A Novel Coronavirus Associated With Severe Acute Respiratory Syndrome. *N. Engl. J. Med.* 348 (20), 1953–1966. doi: 10.1056/NEJMoa030781

Kuila, T., Bose, S., Khanra, P., Mishra, A. K., Kim, N. H., and Lee, J. H. (2011). Recent Advances in Graphene-Based Biosensors. *Biosens. Bioelectron.* 26 (12), 4637–4648. doi: 10.1016/j.bios.2011.05.039

Kumar, K., Kumar, N., and Shah, R. (2020). Role of IoT to Avoid Spreading of COVID-19. *Int. J. Intell. Net.* 1, 32–35. doi: 10.1016/j.ijin.2020.05.002

Lagally, E. T., Simpson, P. C., and Mathies, R. A. (2000). Monolithic Integrated Microfluidic DNA Amplification and Capillary Electrophoresis Analysis System. *Sens. Actuators B Chem.* 63 (3), 138–146. doi: 10.1016/S0925-4005(00)00350-6

Lambert, S. B., Allen, K. M., and Nolan, T. M. (2008). Parent-Collected Respiratory Specimens—A Novel Method for Respiratory Virus and Vaccine Efficacy Research. *Vaccine* 26 (15), 1826–1831. doi: 10.1016/j.vaccine.2008.01.055

Lambert, S. B., Whiley, D. M., O'Neill, N. T., Andrews, E. C., Canavan, F. M., Bletchly, C., et al. (2008). Comparing Nose-Throat Swabs and Nasopharyngeal Aspirates Collected From Children With Symptoms for Respiratory Virus Identification Using Real-Time Polymerase Chain Reaction. *Pediatrics* 122 (3), e615–e620. doi: 10.1542/peds.2008-0691

Larios, O. E., Coleman, B. L., Drews, S. J., Mazzulli, T., Borgundvaag, B., Green, K., et al. (2011). Self-Collected Mid-Turbinate Swabs for the Detection of Respiratory Viruses in Adults With Acute Respiratory Illnesses. *PloS One* 6 (6), e21335. doi: 10.1371/journal.pone.0021335

Lee, C. Y.-P., Lin, R. T., Renia, L., and Ng, L. F. (2020). Serological Approaches for COVID-19: Epidemiologic Perspective on Surveillance and Control. *Front. Immun.* 11, 879. doi: 10.3389/fimmu.2020.00879

Lee, S. H., Park, S.-M., Kim, B. N., Kwon, O. S., Rho, W.-Y., and Jun, B.-H. (2019). Emerging Ultrafast Nucleic Acid Amplification Technologies for Next-Generation Molecular Diagnostics. *Biosens. Bioelectron.* 141, 111448. doi: 10.1016/j.bios.2019.111448

Lei, K. F., Huang, C.-H., Kuo, R.-L., Chang, C.-K., Chen, K.-F., Tsao, K.-C., et al. (2015). Based Enzyme-Free Immunoassay for Rapid Detection and Subtyping of Influenza A H1N1 and H3N2 Viruses. *Anal. Chim. Acta* 883, 37–44. doi: 10.1016/j.aca.2015.02.071

Leland, D. S., and Ginocchio, C. C. (2007). Role of Cell Culture for Virus Detection in the Age of Technology. *Clin. Microbiol. Rev.* 20 (1), 49–78. doi: 10.1128/CMR.00002-06

Lessler, J., Reich, N. G., Brookmeyer, R., Perl, T. M., Nelson, K. E., and Cummings, D. A. (2009). Incubation Periods of Acute Respiratory Viral Infections: A Systematic Review. *Lancet Inf. Dis.* 9 (5), 291–300. doi: 10.1016/S1473-3099(09)70069-6

Li, Z., Bai, Y., You, M., Hu, J., Yao, C., Cao, L., et al. (2021). Fully Integrated Microfluidic Devices for Qualitative, Quantitative and Digital Nucleic Acids Testing at Point of Care. *Biosens. Bioelectron.* 177, 112952. doi: 10.1016/j.bios.2020.112952

Li, M., Cushing, S. K., and Wu, N. (2015). Plasmon-Enhanced Optical Sensors: A Review. *Analyst* 140 (2), 386–406. doi: 10.1039/C4AN01079E

Li, Z., Leustean, L., Inci, F., Zheng, M., Demirci, U., and Wang, S. (2019). Plasmonic-Based Platforms for Diagnosis of Infectious Diseases at the Point-of-Care. *Biotech. Adv.* 37 (8):107440. doi: 10.1016/j.biotechadv.2019.107440

Li, Z., Li, F., Xing, Y., Liu, Z., You, M., Li, Y., et al. (2017). Pen-On-Paper Strategy for Point-of-Care Testing: Rapid Prototyping of Fully Written Microfluidic Biosensor. *Biosens. Bioelectron.* 98, 478–485. doi: 10.1016/j.biotechadv.2019.107440

Liu, L., Wei, Q., Alvarez, X., Wang, H., Du, Y., Zhu, H., et al. (2011). Epithelial Cells Lining Salivary Gland Ducts are Early Target Cells of Severe Acute Respiratory Syndrome Coronavirus Infection in the Upper Respiratory Tracts of Rhesus Macaques. *J. Virol.* 85 (8), 4025–4030. doi: 10.1128/JVI.02292-10

Liu, W., Yue, F., and Lee, L. P. (2021). Integrated Point-Of-Care Molecular Diagnostic Devices for Infectious Diseases. *Acc. Chem. Res.* 54 (22), 4107–4119. doi: 10.1021/acs.accounts.1c00385

Liu, Q., Zhang, X., Chen, L., Yao, Y., Ke, S., Zhao, W., et al. (2018). A Sample-to-Answer Labdisc Platform Integrated Novel Membrane-Resistance Valves for Detection of Highly Pathogenic Avian Influenza Viruses. *Sens. Actuators B Chem.* 270, 371–381. doi: 10.1016/j.snb.2018.05.044

Liu, Q., Zhou, X., Wu, H., and Zheng, B. (2020). Blocking-Free and Self-Contained Immunoassay Platform for One-Step Point-of-Care Testing. *Biosens. Bioelectron.* 165, 112394. doi: 10.1016/j.bios.2020.112394

Li, Y., Wang, J., and Liu, G. (2019). CRISPR/Cas Systems Towards Next-Generation Biosensing. *Trends Biotechnol.* 37 (7), 730–743. doi: 10.1016/j.tibtech.2018.12.005

Loeffelholz, M., and Chonmaitree, T. (2010). Advances in Diagnosis of Respiratory Virus Infections. *Int. J. Microbiol.* 2010, 126049. doi: 10.1155/2010/126049

Loeffelholz, M. J., and Tang, Y.-W. (2020). Laboratory Diagnosis of Emerging Human Coronavirus Infections–The State of the Art. *Emerg. Microbes Infect.* 9 (1), 747–756. doi: 10.1080/22221751.2020.1745095

Loens, K., Van Heirstraeten, L., Malhotra-Kumar, S., Goossens, H., and Ieven, M. (2009). Optimal Sampling Sites and Methods for Detection of Pathogens Possibly Causing Community-Acquired Lower Respiratory Tract Infections. *J. Clin. Microbiol.* 47 (1), 21–31. doi: 10.1128/JCM.02037-08

Lopez-Rincon, A., Tonda, A., Mendoza-Maldonado, L., Claassen, E., Garssen, J., and Kraneveld, A. D. (2020). Accurate Identification of Sars-Cov-2 From Viral Genome Sequences Using Deep Learning. *bioRxiv* 11 (1), 947. doi: 10.1101/2020.03.13.990242

Lu, S., Lin, S., Zhang, H., Liang, L., and Shen, S. (2021). Methods of Respiratory Virus Detection: Advances Towards Point-Of-Care for Early Intervention. *Micromachines* 12 (6), 697. doi: 10.3390/mi12060697

Macfarlane, P., Denham, J., Assous, J., and Hughes, C. (2005). RSV Testing in Bronchiolitis: Which Nasal Sampling Method is Best? *Arch. Dis. Child.* 90 (6), 634–635. doi: 10.1136/adc.2004.065144

Ma, Y., Frutos-Beltrán, E., Kang, D., Pannecouque, C., De Clercq, E., Menéndez-Arias, L., et al. (2021). Medicinal Chemistry Strategies for Discovering Antivirals Effective Against Drug-Resistant Viruses. *Chem. Soc Rev.* 50, 4514–4540. doi: 10.1039/D0CS01084G

Mauk, M., Song, J., Bau, H. H., Gross, R., Bushman, F. D., Collman, R. G., et al. (2017). Miniaturized Devices for Point of Care Molecular Detection of HIV. *Lab. Chip* 17 (3), 382–394. doi: 10.1039/C6LC01239F

MD-Bio (2021). Available at: https://mdbio.com/ (Accessed December 20, 2021).

Mercer, T. R., and Salit, M. (2021). Testing at Scale During the COVID-19 Pandemic. *Nat. Rev. Gen.* 22 (7), 415–426. doi: 10.1038/s41576-021-00360-w

Middleton, P., Kjeldsen, P., and Tully, J. (2013). Forecast: The Internet of Things, Worldwid. *Gartner Res.* 2013, 1258.

Miller, A. C., Singh, I., Koehler, E., and Polgreen, P. M. (2018). A Smartphone-Driven Thermometer Application for Real-Time Population-and Individual-Level Influenza Surveillance. *Clin. Infect. Dis.* 67 (3), 388–397. doi: 10.1093/cid/ciy073

Mojsoska, B., Larsen, S., Olsen, D. A., Madsen, J. S., Brandslund, I., and Alatraktchi, F. A. (2021). Rapid SARS-CoV-2 Detection Using Electrochemical Immunosensor. *Sensors* 21 (2):390. doi: 10.3390/s21020390

Morens, D. M., Folkers, G. K., and Fauci, A. S. (2004). The Challenge of Emerging and Re-Emerging Infectious Diseases. *Nature* 430 (6996), 242–249. doi: 10.1038/nature02759

Mostafa, H. H., Carroll, K. C., Hicken, R., Berry, G. J., Manji, R., Smith, E., et al. (2021). Multicenter Evaluation of the Cepheid Xpert Xpress SARS-CoV-2/Flu/RSV Test. *J. Clin. Microbiol.* 59 (3), e02955–e02920. doi: 10.1128/JCM.02955-20

Mukhtar, H., Rubaiee, S., Krichen, M., and Alroobaea, R. (2021). An IoT Framework for Screening of COVID-19 Using Real-Time Data From Wearable Sensors. *Int. J. Env. Res. Pub. Health* 18 (8):4022. doi: 10.3390/ijerph18084022

Nasrollahi, F., Haghniaz, R., Hosseini, V., Davoodi, E., Mahmoodi, M., Karamikamkar, S., et al. (2021). Micro and Nanoscale Technologies for Diagnosis of Viral Infections. *Small* 17 (45), 2100692. doi: 10.1002/smll.202100692

Nasseri, B., Soleimani, N., Rabiee, N., Kalbasi, A., Karimi, M., and Hamblin, M. R. (2018). Point-Of-Care Microfluidic Devices for Pathogen Detection. *Biosens. Bioelectron.* 117, 112–128. doi: 10.1016/j.bios.2018.05.050

Nelson, P. P., Rath, B. A., Fragkou, P. C., Antalis, E., Tsiodras, S., and Skevaki, C. (2020). Current and Future Point-of-Care Tests for Emerging and New Respiratory Viruses and Future Perspectives. *Front. Cell. Infect. Microbiol.* 10, 181. doi: 10.3389/fcimb.2020.00181

Nguyen, T., Duong Bang, D., and Wolff, A. (2020). 2019 Novel Coronavirus Disease (COVID-19): Paving the Road for Rapid Detection and Point-of-Care Diagnostics. *Micromachines* 11 (3), 306. doi: 10.3390/mi11030306

Noah, N. M., and Ndangili, P. M. (2019). Current Trends of Nanobiosensors for Point-of-Care Diagnostics. *J. Anal. Method. Chem.* 2019, 2179718. doi: 10.1155/2019/2179718

Ooi, K. H., Tay, J. W. D., Teo, S. Y., Liu, M. M., Kaewsapsak, P., Jin, S., et al. (2020). A CRISPR-Based SARS-CoV-2 Diagnostic Assay That is Robust Against Viral Evolution and RNA Editing. *bioRxiv* 12 (1), 1739. doi: 10.1101/2020.07.03.185850

O'Sullivan, S., Ali, Z., Jiang, X., Abdolvand, R., Ünlü, M. S., Plácido da Silva, H., et al. (2019). Developments in Transduction, Connectivity and AI/machine Learning for Point-of-Care Testing. *Sensors* 19 (8), 1917. doi: 10.3390/s19081917

Panesar, A. (2019). *Future of Healthcare. Machine Learning and AI for Healthcare* (Berkeley, CA: Apress), 255–304. doi: 10.1007/978-1-4842-6537-6_1

Park, J., Han, D. H., and Park, J.-K. (2020). Towards Practical Sample Preparation in Point-of-Care Testing: User-Friendly Microfluidic Devices. *Lab. Chip* 20 (7), 1191–1203. doi: 10.1039/D0LC00047G

Patel, M., and Wang, J. (2010). Applications, Challenges, and Prospective in Emerging Body Area Networking Technologies. *IEEE Wireless Commun.* 17 (1), 80–88. doi: 10.1109/MWC.2010.5416354

Peeri, N. C., Shrestha, N., Rahman, M. S., Zaki, R., Tan, Z., Bibi, S., et al. (2020). The SARS, MERS and Novel Coronavirus (COVID-19) Epidemics, the Newest and Biggest Global Health Threats: What Lessons Have We Learned? *Int. J. Epidemiol.* 49 (3), 717–726. doi: 10.1093/ije/dyaa033

Pineda, A. L., Ye, Y., Visweswaran, S., Cooper, G. F., Wagner, M. M., and Tsui, F. R. (2015). Comparison of Machine Learning Classifiers for Influenza Detection From Emergency Department Free-Text Reports. *J. Biomed. Inf.* 58, 60–69. doi: 10.1016/j.jbi.2015.08.019

Qazi, S., and Raza, K. (2020). *Smart Biosensors for an Efficient Point of Care (PoC) Health Management. Smart Biosensors in Medical Care* (Amsterdam, Netherlands: Elsevier), 65–85. doi: 10.1016/B978-0-12-820781-9.00004-8

Qiu, G., Gai, Z., Tao, Y., Schmitt, J., Kullak-Ublick, G. A., and Wang, J. (2020). Dual-Functional Plasmonic Photothermal Biosensors for Highly Accurate Severe Acute Respiratory Syndrome Coronavirus 2 Detection. *ACS Nano* 14 (5), 5268–5277. doi: 10.1021/acsnano.0c02439

Rahmani, A. R., Leili, M., Azarian, G., and Poormohammadi, A. (2020). Sampling and Detection of Corona Viruses in Air: A Mini Review. *Sci. Total Environ.* 740, 140207. doi: 10.1016/j.scitotenv.2020.140207

Rasmi, Y., Li, X., Khan, J., Ozer, T., and Choi, J. R. (2021). Emerging Point-of-Care Biosensors for Rapid Diagnosis of COVID-19: Current Progress, Challenges, and Future Prospects. *Anal. Bioanal. Chem.* 413 (16), 4137–4159. doi: 10.1007/s00216-021-03377-6

Robinson, J. L., Lee, B. E., Kothapalli, S., Craig, W. R., and Fox, J. D. (2008). Use of Throat Swab or Saliva Specimens for Detection of Respiratory Viruses in Children. *Clin. Infect. Dis.* 46 (7), e61–e64. doi: 10.1086/529386

Rocholl, C., Gerber, K., Daly, J., Pavia, A. T., and Byington, C. L. (2004). Adenoviral Infections in Children: The Impact of Rapid Diagnosis. *Pediatrics* 113 (1), e51–e56. doi: 10.1542/peds.113.1.e51

Rodriguez-Manzano, J., Moser, N., Malpartida-Cardenas, K., Moniri, A., Fisarova, L., Pennisi, I., et al. (2020). Rapid Detection of Mobilized Colistin Resistance Using a Nucleic Acid Based Lab-on-a-Chip Diagnostic System. *Sci. Rep.* 10 (1), 1–9. doi: 10.1038/s41598-020-64612-1

Rodriguez-Morales, A. J., Bonilla-Aldana, D. K., Balbin-Ramon, G. J., Rabaan, A. A., Sah, R., Paniz-Mondolfi, A., et al. (2020). History is Repeating Itself: Probable Zoonotic Spillover as the Cause of the 2019 Novel Coronavirus Epidemic. *Infez. Med.* 28 (1), 3–5.

Rombach, M., Hin, S., Specht, M., Johannsen, B., Lüddecke, J., Paust, N., et al. (2020). RespiDisk: A Point-of-Care Platform for Fully Automated Detection of Respiratory Tract Infection Pathogens in Clinical Samples. *Analyst* 145 (21), 7040–7047. doi: 10.1039/D0AN01226B

Safiabadi Tali, S. H., LeBlanc, J. J., Sadiq, Z., Oyewunmi, O. D., Camargo, C., Nikpour, B., et al. (2021). Tools and Techniques for Severe Acute Respiratory Syndrome Coronavirus 2 (SARS-CoV-2)/COVID-19 Detection. *Clin. Microbiol. Rev.* 34 (3), e00228–e00220. doi: 10.1128/CMR.00228-20

Sato, H., Ide, K., and Namatame, A. (2016). "Agent-Based Infectious Diffusion Simulation Using Japanese Domestic Human Mobility Data as Metapopulation Network", in *2016 Second Asian Conference on Defence Technology (ACDT)* (Chiang Mai, Thailand: IEEE). doi: 10.1109/ACDT.2016.7437650

Scansen, K. A., Bonsu, B. K., Stoner, E., Mack, K., Salamon, D., Leber, A., et al. (2010). Comparison of Polyurethane Foam to Nylon Flocked Swabs for Collection of Secretions From the Anterior Nares in Performance of a Rapid Influenza Virus Antigen Test in a Pediatric Emergency Department. *J. Clin. Microbiol.* 48 (3), 852–856. doi: 10.1128/JCM.01897-09

Schumacher, S., Nestler, J., Otto, T., Wegener, M., Ehrentreich-Förster, E., Michel, D., et al. (2012). Highly-Integrated Lab-on-Chip System for Point-of-Care Multiparameter Analysis. *Lab. Chip* 12 (3), 464–473. doi: 10.1039/C1LC20693A

Seo, G., Lee, G., Kim, M. J., Baek, S.-H., Choi, M., Ku, K. B., et al. (2020). Rapid Detection of COVID-19 Causative Virus (SARS-CoV-2) in Human Nasopharyngeal Swab Specimens Using Field-Effect Transistor-Based Biosensor. *ACS Nano* 14 (4), 5135–5142. doi: 10.1021/acsnano.0c02823

Sim, S., and Cho, M. (2021). Convergence Model of AI and IoT for Virus Disease Control System. *Pers. Ubiquitous Comput.* 7, 1–11. doi: 10.1007/s00779-021-01577-6

Soler, M., Estevez, M. C., Cardenosa-Rubio, M., Astua, A., and Lechuga, L. M. (2020). How Nanophotonic Label-Free Biosensors can Contribute to Rapid and Massive Diagnostics of Respiratory Virus Infections: COVID-19 Case. *ACS Sens.* 5 (9), 2663–2678. doi: 10.1021/acssensors.0c01180

Soto, F., Ozen, M. O., Guimarães, C. F., Wang, J., Hokanson, K., Ahmed, R., et al. (2021). Wearable Collector for Noninvasive Sampling of SARS-CoV-2 From Exhaled Breath for Rapid Detection. *ACS Appl. Mater. Interfaces* 13 (35), 41445–41453. doi: 10.1021/acsami.1c09309

Sow, W. T., Ye, F., Zhang, C., and Li, H. (2020). Smart Materials for Point-of-Care Testing: From Sample Extraction to Analyte Sensing and Readout Signal Generator. *Biosens. Bioelectron.* 170, 112682. doi: 10.1016/j.bios.2020.112682

Sun, Y., Koh, V., Marimuthu, K., Ng, O. T., Young, B., Vasoo, S., et al. (2020). Epidemiological and Clinical Predictors of COVID-19. *Clin. Infect. Dis.* 71 (15), 786–792. doi: 10.1093/cid/ciaa322

Sun, A. C., Yao, C., Venkatesh, A., and Hall, D. A. (2016). An Efficient Power Harvesting Mobile Phone-Based Electrochemical Biosensor for Point-of-Care Health Monitoring. *Sens. Actuators B Chem.* 235, 126–135. doi: 10.1016/j.snb.2016.05.010

Su, S., Wong, G., Shi, W., Liu, J., Lai, A. C., Zhou, J., et al. (2016). Epidemiology, Genetic Recombination, and Pathogenesis of Coronaviruses. *Trends Microbiol.* 24 (6), 490–502. doi: 10.1016/j.tim.2016.03.003

Swayamsiddha, S., and Mohanty, C. (2020). Application of Cognitive Internet of Medical Things for COVID-19 Pandemic. *Diabetes Metab. Syndr.* 14 (5), 911–915. doi: 10.1016/j.dsx.2020.06.014

Tapak, L., Hamidi, O., Fathian, M., and Karami, M. (2019). Comparative Evaluation of Time Series Models for Predicting Influenza Outbreaks: Application of Influenza-Like Illness Data From Sentinel Sites of Healthcare Centers in Iran. *BMC Res. Notes* 12 (1), 1–6. doi: 10.1186/s13104-019-4393-y

Tepeli, Y., and Ülkü, A. (2018). Electrochemical Biosensors for Influenza Virus a Detection: The Potential of Adaptation of These Devices to POC Systems. *Sens. Actuators B Chem.* 254, 377–384. doi: 10.1016/j.snb.2017.07.126

Terry, S. C., Jerman, J. H., and Angell, J. B. (1979). A Gas Chromatographic Air Analyzer Fabricated on a Silicon Wafer. *IEEE Trans. Electron Devices* 26 (12), 1880–1886. doi: 10.1109/T-ED.1979.19791

Thwe, P. M., and Ren, P. (2021). Analysis of Sputum/Tracheal Aspirate and Nasopharyngeal Samples for SARS-CoV-2 Detection by Laboratory-Developed Test and Panther Fusion System. *Diagn. Microbiol. Infect. Dis.* 99 (1), 115228. doi: 10.1016/j.diagmicrobio.2020.115228

Torrente-Rodríguez, R. M., Lukas, H., Tu, J., Min, J., Yang, Y., Xu, C., et al. (2020). SARS-CoV-2 RapidPlex: A Graphene-Based Multiplexed Telemedicine Platform for Rapid and Low-Cost COVID-19 Diagnosis and Monitoring. *Matter* 3 (6), 1981–1998. doi: 10.1016/j.matt.2020.09.027

To, K. K.-W., Tsang, O. T.-Y., Yip, C. C.-Y., Chan, K.-H., Wu, T.-C., Chan, J. M.-C., et al. (2020). Consistent Detection of 2019 Novel Coronavirus in Saliva. *Clin. Inf. Dis.* 71 (15), 841–843. doi: 10.1093/cid/ciaa149

Tripathy, S., Dassarma, B., Roy, S., Chabalala, H., and Matsabisa, M. G. (2020). A Review on Possible Modes of Action of Chloroquine/Hydroxychloroquine: Repurposing Against SAR-CoV-2 (COVID-19) Pandemic. *Int. J. Antimicrob. Agents* 56 (2), 106028. doi: 10.1016/j.ijantimicag.2020.106028

Tromberg, B. J., Schwetz, T. A., Pérez-Stable, E. J., Hodes, R. J., Woychik, R. P., Bright, R. A., et al. (2020). Rapid Scaling Up of Covid-19 Diagnostic Testing in the United States—the NIH RADx Initiative. *N. Engl. J. Med.* 383 (11), 1071–1077. doi: 10.1056/NEJMsr2022263

Tuli, S., Tuli, S., Tuli, R., and Gill, S. S. (2020). Predicting the Growth and Trend of COVID-19 Pandemic Using Machine Learning and Cloud Computing. *Internet Things* 11, 100222. doi: 10.1016/j.iot.2020.100222

Wang, D., Chan, H. N., Liu, Z., Micheal, S., Li, L., Baniani, D. B., et al. (2020). "Recent Developments in Microfluidic-Based Point-of-Care Testing (POCT) Diagnoses", in *Nanotechnology and Microfluidics (Book)*, 239–280. doi: 10.1002/9783527818341.ch8

Wang, Y., Hu, Y., He, Q., Yan, J., Xiong, H., Wen, N., et al. (2020). Metal-Organic Frameworks for Virus Detection. *Biosens. Bioelectron.* 169, 112604. doi: 10.1016/j.bios.2020.112604

Wang, Y., Yu, L., Kong, X., and Sun, L. (2017). Application of Nanodiagnostics in Point-of-Care Tests for Infectious Diseases. *Int. J. Nanomed.* 12, 4789. doi: 10.2147/IJN.S137338

Wang, X., Zhong, M., Liu, Y., Ma, P., Dang, L., Meng, Q., et al. (2020). Rapid and Sensitive Detection of COVID-19 Using CRISPR/Cas12a-Based Detection With Naked Eye Readout, CRISPR/Cas12a-NER. *Sci. Bull.* 65 (17), 1436. doi: 10.1016/j.scib.2020.04.041

Weibel, D. B., DiLuzio, W. R., and Whitesides, G. M. (2007). Microfabrication Meets Microbiology. *Nat. Rev. Microbiol.* 5 (3), 209–218. doi: 10.1038/nrmicro1616

Whitesides, G. M. (2006). The Origins and the Future of Microfluidics. *Nature* 442 (7101), 368–373. doi: 10.1038/nature05058

WHO. (2020). Available at: https://www.who.int/news-room/commentaries/detail/advice-on-the-use-of-point-of-care-immunodiagnostic-tests-for-covid-19 (Accessed December 20, 2021).

World Health Organization. (2015). *Improving the Quality of HIV-Related Point-of-Care Testing: Ensuring the Reliability and Accuracy of Test Results*. Available at: https://www.who.int/publications/i/item/97892415081791414 (Accessed December 20, 2021).

Wu, D., Zhang, J., Xu, F., Wen, X., Li, P., Zhang, X., et al. (2017). A Paper-Based Microfluidic Dot-ELISA System With Smartphone for the Detection of Influenza A. *Microfluid Nanofluidics* 21 (3), 43. doi: 10.1007/s10404-017-1879-6

Wyllie, A. L., Fournier, J., Casanovas-Massana, A., Campbell, M., Tokuyama, M., Vijayakumar, P., et al. (2020). Saliva or Nasopharyngeal Swab Specimens for Detection of SARS-CoV-2. *N. Engl. J. Med.* 383 (13), 1283–1286. doi: 10.1056/NEJMc2016359

Xu, D., Huang, X., Guo, J., and Ma, X. (2018). Automatic Smartphone-Based Microfluidic Biosensor System at the Point of Care. *Biosens. Bioelectron.* 110, 78–88. doi: 10.1016/j.bios.2018.03.018

Xu, D., Zhang, Z., Jin, L., Chu, F., Mao, Y., Wang, H., et al. (2005). Persistent Shedding of Viable SARS-CoV in Urine and Stool of SARS Patients During the Convalescent Phase. *Eur. J. Clin. Microbiol. Infect. Dis.* 24 (3), 165–171. doi: 10.1007/s10096-005-1299-5

Yeh, Y.-T., Nisic, M., Yu, X., Xia, Y., and Zheng, S.-Y. (2014). Point-Of-Care Microdevices for Blood Plasma Analysis in Viral Infectious Diseases. *Ann. Biomed. Eng.* 2 (11), 2333–2343. doi: 10.1007/s10439-014-1044-2

Yin, R., Tran, V. H., Zhou, X., Zheng, J., and Kwoh, C. K. (2018). Predicting Antigenic Variants of H1N1 Influenza Virus Based on Epidemics and Pandemics Using a Stacking Model. *PloS One* 13 (12), e0207777. doi: 10.1371/journal.pone.0207777

Yoshimi, K., Takeshita, K., Yamayoshi, S., Shibumura, S., Yamauchi, Y., Yamamoto, M., et al. (2020) *Rapid and Accurate Detection of Novel Coronavirus SARS-CoV-2 Using CRISPR-Cas3*. Available at: https://ssrn.com/abstract=3640844.

Younis, S., Taj, A., Zia, R., Hayat, H., Shaheen, A., Awan, F. R., et al. (2020). "Nanosensors for the Detection of Viruses," in *Nanosensors for Smart Cities* (Amsterdam, Netherlands: Elsevier), 327–338. doi: 10.1016/B978-0-12-819870-4.00018-9

Yuan, M., Wu, N. C., Zhu, X., Lee, C.-C. D., So, R. T., Lv, H., et al. (2020). A Highly Conserved Cryptic Epitope in the Receptor Binding Domains of SARS-CoV-2 and SARS-CoV. *Science* 368 (6491), 630–633. doi: 10.1126/science.abb7269

Zaki, A. M., Van Boheemen, S., Bestebroer, T. M., Osterhaus, A. D., and Fouchier, R. A. (2012). Isolation of a Novel Coronavirus From a Man With Pneumonia in Saudi Arabia. *N. Engl. J. Med.* 367 (19), 1814–1820. doi: 10.1056/NEJMoa1211721

Zenhausern, R., Chen, C.-H., and Yoon, J.-Y. (2021). Microfluidic Sample Preparation for Respiratory Virus Detection: A Review. *Biomicrofluidics* 15 (1), 011503. doi: 10.1063/5.0041089

Zhang, L., Ding, B., Chen, Q., Feng, Q., Lin, L., and Sun, J. (2017). Point-Of-Care-Testing of Nucleic Acids by Microfluidics. *Trends Anal. Chem.* 94, 106–116. doi: 10.1016/j.trac.2017.07.013

Zhang, N., Wang, L., Deng, X., Liang, R., Su, M., He, C., et al. (2020). Recent Advances in the Detection of Respiratory Virus Infection in Humans. *J. Med. Virol.* 92 (4), 408–417. doi: 10.1002/jmv.25674

Zhang, H., Xu, Y., Fohlerova, Z., Chang, H., Iliescu, C., and Neuzil, P. (2019). LAMP-On-a-Chip: Revising Microfluidic Platforms for Loop-Mediated DNA Amplification. *Trends Anal. Chem.* 113, 44–53. doi: 10.1016/j.trac.2019.01.015

Zhang, M., Ye, J., He, J.-S., Zhang, F., Ping, J., Qian, C., et al. (2020). Visual Detection for Nucleic Acid-Based Techniques as Potential on-Site Detection Methods. A Review. *Anal. Chim. Acta* 1099, 1–15. doi: 10.1016/j.aca.2019.11.056

Zhu, H., Podesva, P., Liu, X., Zhang, H., Teply, T., Xu, Y., et al. (2020). IoT PCR for Pandemic Disease Detection and its Spread Monitoring. *Sens. Actuators B Chem.* 303, 127098. doi: 10.1016/j.snb.2019.127098

Conflict of Interest: The authors declare that the research was conducted in the absence of any commercial or financial relationships that could be construed as a potential conflict of interest.

frontiers in Cellular and Infection Microbiology

ORIGINAL RESEARCH
published: 17 February 2022
doi: 10.3389/fcimb.2022.816238

Rapid Visual Detection of Hepatitis C Virus Using Reverse Transcription Recombinase-Aided Amplification–Lateral Flow Dipstick

Haili Wang[1], Yuhang Zhang[2], Jingming Zhou[1], Ming Li[3], Yumei Chen[1], Yankai Liu[1], Hongliang Liu[1], Peiyang Ding[1], Chao Liang[1], Xifang Zhu[1], Ying Zhang[1], Cheng Xin[1], Gaiping Zhang[1,2] and Aiping Wang[1]**

[1] School of Life Sciences, Zhengzhou University, Zhengzhou, China, [2] College of Veterinary Medicine, Henan Agricultural University, Zhengzhou, China, [3] Henan Key Laboratory of Population Defects Prevention, National Health Commission Key Laboratory of Birth Defects Prevention, Henan Institute of Reproduction Health Science and Technology, Zhengzhou, China

OPEN ACCESS

Edited by:
Ciprian Iliescu, National Institute for Research and Development in Microtechnologies, Romania

Reviewed by:
Gratiela Gradisteanu Pircalabioru, University of Bucharest, Romania
Sabri Saeed Sanabani, Universidade de São Paulo, Brazil

***Correspondence:**
Gaiping Zhang
zhanggaip@126.com
Aiping Wang
pingaw@126.com

Specialty section:
This article was submitted to Clinical Microbiology, a section of the journal Frontiers in Cellular and Infection Microbiology

Received: *16 November 2021*
Accepted: *17 January 2022*
Published: *17 February 2022*

Citation:
Wang H, Zhang Y, Zhou J, Li M, Chen Y, Liu Y, Liu H, Ding P, Liang C, Zhu X, Zhang Y, Xin C, Zhang G and Wang A (2022) Rapid Visual Detection of Hepatitis C Virus Using Reverse Transcription Recombinase-Aided Amplification–Lateral Flow Dipstick. Front. Cell. Infect. Microbiol. 12:816238. doi: 10.3389/fcimb.2022.816238

Hepatitis C virus (HCV) infection is a global public health threat. Reaching the World Health Organization's objective for eliminating viral hepatitis by 2030 will require a precise disease diagnosis. While immunoassays and qPCR play a significant role in detecting HCV, rapid and accurate point-of-care testing is important for pathogen identification. This study establishes a reverse transcription recombinase-aided amplification–lateral flow dipstick (RT-RAA-LFD) assay to detect HCV. The intact workflow was completed within 30 min, and the detection limit for synthesized C/E1 plasmid gene-containing plasmid was 10 copies/μl. In addition, the test showed good specificity, with no cross-reactivity observed for hepatitis A virus, hepatitis B virus, HIV, syphilis, and human papillomavirus virus. Using extracted RNAs from 46 anti-HCV antibody-positive samples, RT-RAA-LFD showed 100% positive and negative concordance rates with qPCR. In summary, the RT-RAA-LFD assay established in this study is suitable for the rapid clinical detection of HCV at the community level and in remote areas.

Keywords: hepatitis C virus, nucleic acid detection, point-of-care testing, recombinase-aided amplification, lateral flow dipstick

INTRODUCTION

Infectious diseases pose a critical global threat that has caused significant morbidity and mortality as well as great economic losses (Houghton, 2009; Massimo and Vincenzo, 2018). Hepatitis C virus (HCV) infection is a major cause of severe liver diseases, including chronic hepatitis, cirrhosis, and hepatocellular carcinoma. According to the World Health Organization (WHO, 2017), approximately 71 million people worldwide are infected with HCV, and at least 400,000 people die annually from HCV-related liver disease (WHO, 2017; Spearman et al., 2019; Roger et al., 2021). HCV transmission primarily occurs through accidental needle sticks in medical settings, using injectable drugs, and receiving a blood transfusion before 1992, which was when blood screening became routine (Pietschmann and Brown, 2019; Hollande et al., 2020). Acute HCV cases account for about 15–20% of total cases, and post-acute HCV-infected patients have a 50–80% chance of

developing a chronic infection (Narayanamurthy et al., 2021). If untreated, patients have a 20% risk of developing cirrhosis, of whom a small percentage may also develop hepatocellular carcinoma (Roger et al., 2021).

The WHO created a guide for the elimination of HCV by 2030, along with quantifiable targets (Warkad et al., 2018). The main factors required to eliminate HCV include increasing and strengthening outreach screening, improving prevention, and increasing access to treatment. Achieving HCV elimination requires scaling up rapid and accurate testing of populations worldwide, which inevitably places a heavy burden on developing countries (Foster et al., 2019; Dash et al., 2020). As a result, micro-elimination and cure have not been achieved because high-risk groups, including migrants from HCV-endemic countries, injecting drug users, prisoners, and men who have sex with men, and target groups, including hemophiliacs and those with a concurrent HIV infection (Hollande et al., 2020), require the development of rapid diagnostic testing methods and new therapeutic drugs. During the COVID-19 pandemic, less attention has focused on improving HCV testing. The timely detection of HCV, along with appropriate intervention measures, information dissemination, and outreach, is critical for an effective public health response to this virus (Javier et al., 2021).

HCV is a single-stranded, positive-stranded RNA virus belonging to the genus *Flaviviridae* (Houghton, 2009), which is composed of about 9,600 nucleotides. Due to its high degree of variation, vaccines and specific antiviral drugs are difficult to develop. Thus, an early diagnosis of HCV is critically important (Marcus et al., 2018). The gene encoding the capsid protein is comparatively conserved among different HCV genotypes, maintaining approximately 80% sequence identity (Adams et al., 2018). Current methods for detecting HCV include immunological and molecular biological tests. The immunological methods are generally utilized because of their simplicity and the convenience of automating batch operations. However, due to the long window of antigen and antibody detection, false negatives occur with some frequency (Kun et al., 2016; Llibre et al., 2019). Polymerase chain reaction (PCR)-based temperature-variable amplification technology is the most reliable HCV-RNA detection method and is considered the gold standard for HCV diagnosis (Fitzpatrick et al., 2018; Wang et al., 2021). While PCR-based tests are highly sensitive, they are expensive, are time-consuming, and require complex equipment, so they cannot be used for rapid point-of-care-testing (POCT) in low-resource areas with high HCV infection rates. Furthermore, the application of these tests may be restricted as a result of their detection potential.

In recent years, isothermal amplification methods have been studied and used for the detection of foodborne pathogens. Recombinase-aided amplification (RAA) is a novel isothermal amplification technology in which rapid amplification of DNA or RNA is achieved at constant temperatures. The entire RAA reaction is simple, rapid, accurate, power-saving, and convenient (Ivan and Ciara, 2017; Chen et al., 2018; Azmi et al., 2021). Other common isothermal amplification approaches include loop-mediated isothermal amplification (Notomi et al., 2000), rolling circle amplification (Blanco et al., 1989), recombinase polymerase amplification (Piepenburg et al., 2006), nucleic acid sequence-based amplification (Compton, 1991), and helicase-dependent amplification (Vincent et al., 2004). Isothermal amplification is commonly combined with a downstream portable result reading strategy to develop fast and convenient diagnostic testing methods, which are expected for use in remote areas and by developed countries that are performing mass screenings (Jia et al., 2018; Zhang et al., 2021). Of the isothermal amplification techniques, the RAA detection method is completed within 30 min at a constant temperature of 37 to 42°C. Thus, the technology is widely used for the rapid detection of viruses, bacteria, parasites, and other pathogens (Yan et al., 2014; Daher et al., 2016). RAA technology can also be combined with other novel detection methods, making pathogen detection more efficient and convenient. Its portable detection equipment also provides the possibility of POCT.

In this study, a rapid RT-RAA-LFD diagnostic platform was established for the detection of HCV, and its sensitivity, specificity, and stability were evaluated, providing a rapid, convenient, and accurate POCT strategy for HCV detection. A schematic figure representing the major steps of sample preparation for HCV detection using the RT-RAA-LFD method is shown in **Figure 1**. This method has great application potential because of its convenience, short detection time, and POCT application.

MATERIALS AND METHODS

Clinical Samples

Two thousand clinical samples were collected at random from patients presenting to the outpatient clinic or physical examination center of the Henan Institute of Reproduction Health Science and Technology between January 2020 and January 2021. Each patient was given a health interview and asked to sign an informed consent. Of the 2,000 samples, 46 were found to be HCV-antibody-positive using automated chemiluminescence immunoassay. The blood pressure and serum indexes of the participant, the liver and kidney function as well as the results of B-ultrasound imaging examinations were normal. After fasting, 2 ml of blood was obtained from each patient and stored in a vacuum coagulation booster tube. Serum was then separated by centrifugation for 10 min at 3,500 *g*. The collected samples were deactivated by heating at 56°C for 30 min and immediately tested or stored at -20°C until use.

Nucleic Acid Extraction

Nucleic acids were extracted from each clinical sample using TaKaRa MiniBEST Viral RNA/DNA Extraction Kit version 5.0 (Takara, Dalian, China) according to the manufacturer's instructions. In brief, 200-µl serum samples were used for extraction. Total viral genomic RNA was eluted with 50 µl nuclease-free water and stored at -80°C until use. Based on the extracted HCV RNA genome, cDNAs were prepared with a PrimeScript™ RT reagent Kit (Takara, Dalian, China). The reaction conditions were 15 min at 37°C for reverse transcription and 5 s at 85°C for denaturation. The cDNAs were then stored at -80°C for later use.

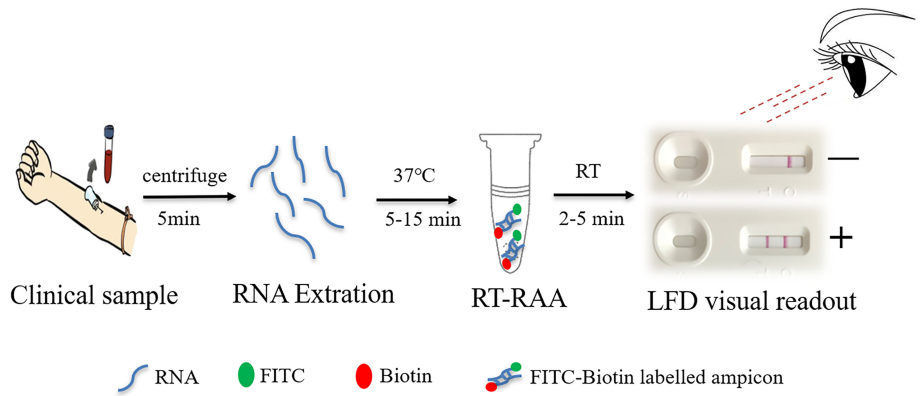

FIGURE 1 | Schematic representation of the reverse transcription recombinase-aided amplification–lateral flow dipstick (RT-RAA-LFD) workflow for hepatitis C virus. RNA extraction for 15 min, RT-RAA reaction for 5 min, and LFD visual readout for 5 to 10 min. All work was performed within 30 min with minimal equipment requirements.

Primers and Plasmids

RAA primers targeting the HCV C/E1 genes were designed as described in the Twist-Dx (Maidenhead, UK) protocol. The RAA primers and the standard plasmid pUC57-pC/E1 (GenBank: AJ238799.1) used in this study were all synthesized by Sangon Biotech (Shanghai, China) (**Table 1**).

Basic PCR for HCV C/E1 Gene Detection

A 473-bp fragment in the C/E1 region of the HCV gene was amplified using conventional PCR methods and primers (PCR-F and PCR-R; **Table 1**). The region position of the three sets of primers targeted the C/E1 gene of the HCV 1b genome (GenBank: AJ238799.1). The 25-μl PCR reaction contained 1 μl of DNA template (10^8 copies/μl to 1 copy/μl), 1 μl each of 10 μmol/L upstream and downstream primer, and 22 μl of Golden Star T6 Super PCR Mix (Beijing Tsingke Biotechnology Co., Ltd., China). The PCR program was conducted as follows: 95°C for 5 min, then 40 cycles at 95°C for 1 min, 47°C for 30 s, 72°C for 1 min, and a final extension at 72°C for 2 min. Amplicons were tested using 1% agarose gel electrophoresis.

Quantitative Real-Time PCR

A commercial diagnostic kit for HCV RNA (PCR-fluorescence probing) (Daan Gene, Guangzhou, China) and an ABI 7500 fluorescence quantitative PCR system (Life Technologies, Foster City, CA, USA) were used for qPCR detection. The 25-μl qPCR reaction contained 20 μl of fluorescent PCR reaction mix and 5 μl of RNA template. qPCR was conducted as follows: 15 min at 37°C for reverse transcription and 5 s at 85°C for denaturation, followed by 45 cycles of 45 s at 93°C and 20 s at 55°C. The results were considered positive if the Ct value was <40, with an "S" type amplification curve, and considered negative if the Ct value was reported as undetermined, with fluorescent signal maintaining a background level.

RT-RAA Assay

RT-RAA was performed using a basic RT-RAA nucleic acid amplification kit (nfo) (Zhongce, Jiangsu, China). The 50-μl RT-RAA reaction contained one RT-RAA lyophilized powder, 41.5 μl buffer A, 2 μl of 10 μM forward primer, and 2 μl of 10 μM reverse primer that was mixed and centrifuged. The mixture was added to the RT-RAA reaction tube containing lyophilized powder, and either 2 μl of RNA template or 2 μl of RNase-free water (negative control) was added next. The reaction was incubated in a 37°C water bath for 5 to 15 min. The amplified product was either purified with QIAquick PCR purification kit (Qiagen, USA) for agarose gel electrophoresis or diluted with PBST (1× phosphate-buffered saline with 0.1% Tween-20) for LFD readout.

Preparation of Colloidal Gold and Dipstick

The dipstick was predominantly composed of the following parts: sample pad, backing card, conjugate pad, absorbent pad, and

TABLE 1 | Primer sequences used in this study.

Primer	Sequence (5′-3′)	Position (nt)
PCR-F	AAYYTDCCCGGTTGCTCTTTYTCTAT	842–867
PCR-R	TTCATCATCATRTCCCANGCCAT	1,309–1,331
RAA-F1	AGTACAGGACTGCAATTGCTCAATATATCC	1,241–1,270
RAA-R1	GCAAAGATAGCATCACAATCAGAACCTTAG	1,477–1,447
RAA-F2	CTTGGGATATGATGATGAACTGGTCACCTAC	1,297–1,327
RAA-R2	AAGAGTAGCATCACAATCAGAACCTTAGCC	1,474–1,445
LFA-F2	5′-FITC-CTTGGGATATGATGATGAACTGGTCACCTAC	
LFA-R2	5′-Biotin-AAGAGTAGCATCACAATCAGAACCTTAGCC	

nitrocellulose membrane. The test strip test line (T line) and the quality control line (C line) were sprayed with BioDot XYZ3050 Dispense Platform (Irvin, CA, USA). The distance between these lines was about 5 mm. Streptavidin was fixed on the T line for specific binding with biotin groups. The antibody against rabbit/mouse antibody Fc fragment was fixed on the C line to intercept excess colloidal gold-labeled anti-FITC antibodies. If a target detection substance was present in the sample to be tested, it formed a colloidal gold marker–target detection substance–antibody complex, which gathered on the corresponding detection line, forming a colored precipitation line.

RT-RAA Visual Readout With LFD

The RT-RAA-LFD primers (**Table 1**) included a 5′-FITC-labeled forward primer (LFD-F) and a 5′-biotin-labeled reverse primer (LFD-R). The 50-μl amplification system was configured according to the supplier's instructions. The optimal reaction temperature and time for RT-RAA-LFD were achieved by individually performing a group of RT-RAA reactions at room temperature and at 35, 37, or 40°C in a water bath for 5, 10, or 15 min. After amplification, 20 μl RT-RAA reaction mix was then immediately diluted with 80 μl PBST for LFD readout. The result was read after the reaction was left to stand for 5 to 15 min. When the C line appeared in red, it indicated that the test results were valid. When the quality C line and T line were red at the same time, the result was interpreted as a positive result. When only the C line is red but the T line does not respond, it was interpreted as a negative result.

Analytical Sensitivity and Specificity

RT-RAA-LFA sensitivity was evaluated using optimal reaction conditions. Tenfold serial dilutions of pUC57-pC/E1 were measured from 10^8 copies to 1 copy/μl by RT-RAA-LFA and compared with PCR. RT-RAA-LFA specificity was estimated using serum samples from common infectious diseases, including hepatitis A virus (HAV), hepatitis B virus (HBV), HIV, syphilis, and human papillomavirus virus (HPV).

RESULTS

Establishment of HCV RT-RAA-LFD and Optimization of Reaction Conditions

To determine the best primer combination, RAA amplification was conducted as described above. The four pairs of primer combinations produced brighter bands and a single band by agarose gel electrophoresis (**Figure 2**). Since a smaller amplification product increases the efficiency of amplification, the primer pair with the smallest product, RAA-F2 and RAA-R2, was selected for subsequent experiments.

Next, the temperature of the RT-RAA amplification system was optimized. The amplification and incubation were developed at 35 to 40°C for 10 min, and the results indicated that, when the amplification temperature was 37°C, the detection line color of the positive control was observed (**Figures 3A**). At 35°C, the color of the T line was weak, which was not significant, and a temperature of 40°C was considered too high for on-site experiments. Thus, 37°C was selected as the amplification temperature.

The amplification incubation time was also optimized. The amplification system was incubated in a 37°C water bath for 5, 10, and 15 min. After 5 min of incubation, the color of the T line started to turn red (**Figure 3B**). Thus, the final RT-RAA-LFD conditions used in this study included amplification at 37°C for 5 min and incubation at room temperature for 10 to 15 min to ensure that the results could be read.

Sensitivity and Specificity of the RT-RAA-LFD Assay

The HCV standard plasmid was diluted into different concentration gradients (10^8 copies/μl–1 copy/μl) for RT-RAA-LFD detection. While the detection limit of conventional

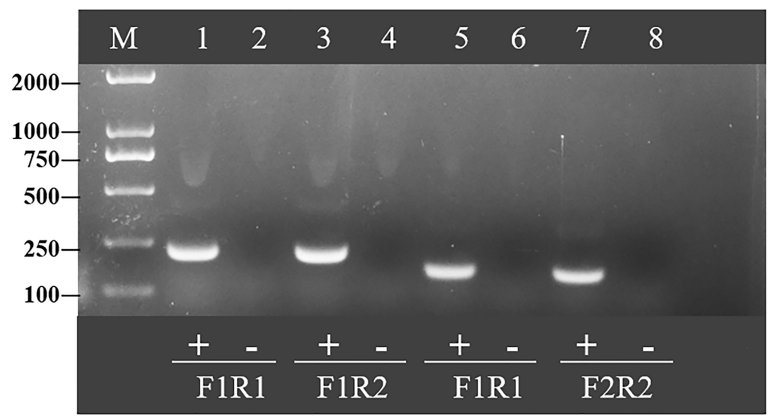

FIGURE 2 | Optimal primer selection. Products amplified by different reverse transcription recombinase-aided amplification primers were analyzed by 1.5% agarose gel electrophoresis to select the optimal primer pairs. M is a 2,000-bp DNA marker. The primers and templates used in lanes 1–8 are as follows: 1, HCV-RAA-F1/R1 + HCV; 2, HCV-RAA-F1/R1 + ddH_2O; 3, HCV-RAA-F1/R2 + HCV; 4, HCV-RAA-F1/R2 + ddH_2O; 5, HCV-RAA-F2/R1 + HCV; 6, HCV-RAA-F2/R1 + ddH_2O; 7, HCV-RAA-F2/R2 + HCV; 8, HCV-RAA-F2/R2 + ddH_2O.

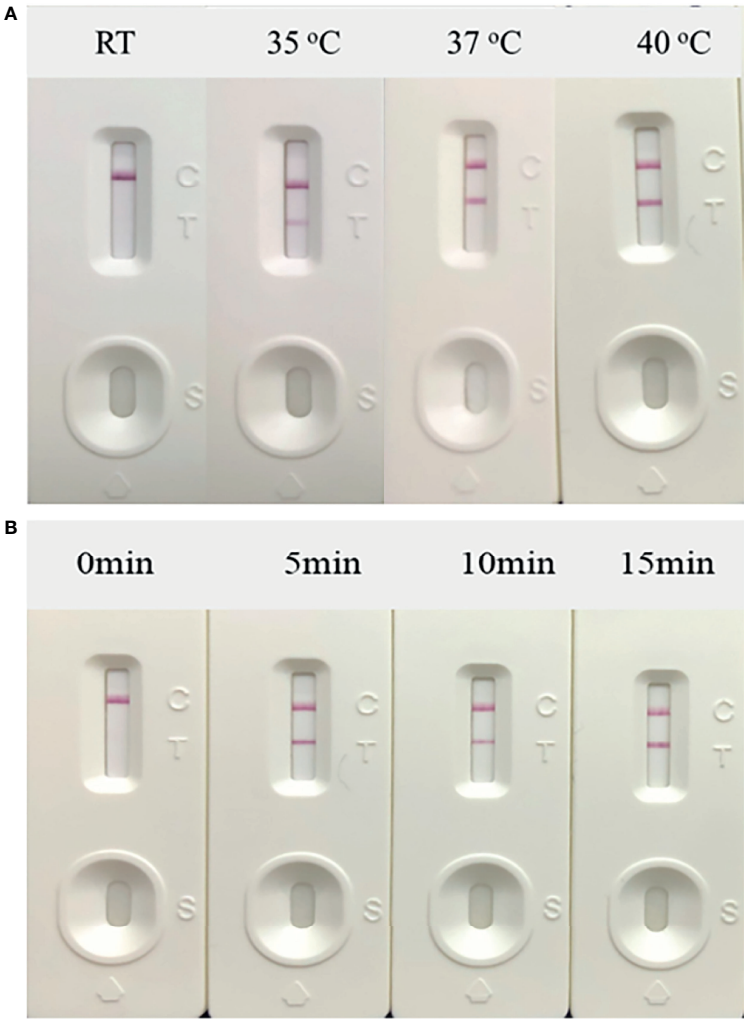

FIGURE 3 | Optimization of reaction conditions. Using the recombinant plasmid PUC57-pC/E1 as a template to optimize the temperature conditions of hepatitis C virus (HCV) reverse transcription recombinase-aided amplification (RAA) strip. C is the control line, T is the test line, and N is negative control. **(A)** Determination of the optimal reaction temperature range of the HCV RAA strip. **(B)** Detection of the optimized amplification time.

PCR was 10^4 copies/μl (**Figure 4C**), the detection limit of RAA was 10^2 copies/μl (**Figure 4A**). The sensitivity and detection limit of RT-RAA-LFD were 100 and 10 times higher (reaching 10 copies/μl), respectively, than those of basic RAA (**Figure 4B**). Each assay was repeated three times.

In the specificity tests, the other four of the five inspections for infectious diseases, HAV, HBV, HIV, and syphilis, and the HPV standard plasmid were used as specific test samples. These samples only developed color at the quality control line and were defined as negative. RT-RAA-LFD showed adequate specificity and no cross-reactivity with other viruses (**Figures 5A, B**).

Stability Assay of RT-RAA-LFD

The RT-RAA-LFD stability assay was performed at 0, 4, 8, and 12 months after the sensitivity assay by testing in triplicate strong positive samples (10^5 copies/μl; +++) and weak positive samples (10 copies/μl; +) of standard plasmid pUC57-pC/E1 and negative samples (double-distilled water; -) at three times each (**Figure 6**). LFD was stored at room temperature and in dry conditions. The relative optical density value of the LFD T line was recorded using the TSR3000 filmstrip reader (BioDot). As shown in **Table 2**, the coefficient of variance (Cv) values for strong positive, weak positive, and negative samples at the four time points were 4.43, 3.51, and 9.67%, respectively, which were all lower than 10%. This indicated that the RT-RAA-LFD method had adequate detection stability within 1 year.

Clinical Sample Analysis Using Quantitative Real-Time PCR

Following positive serology, the gold standard confirmation test of HCV infection was the detection of HCV RNA by qPCR. HCV-RNA >1.0×10^3 IU/ml was considered positive, HCV-RNA quantification <1.0×10^6 IU/ml was considered a low viral load, and HCV-RNA quantification ≥1.0×10^6 IU/ml was

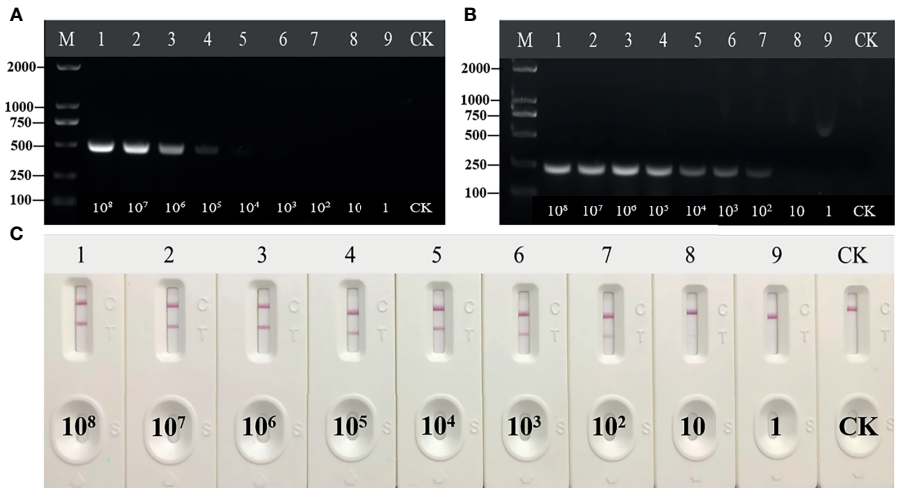

FIGURE 4 | Sensitivity of reverse transcription recombinase-aided amplification (RT-RAA), RT-RAA-lateral flow dipstick, and PCR for plasmid pUC57-pC/E1. **(A)** Agarose gel electrophoresis of PCR. M, DL2000DNA marker; 1 to 9, decimal dilutions of plasmid pUC57-pC/E1 from 10^8 copies/ml to 1 copy/ml. **(B)** Agarose gel electrophoresis of basic RAA. **(C)** RAA-LFA visual readout. CK, negative control with double-distilled water.

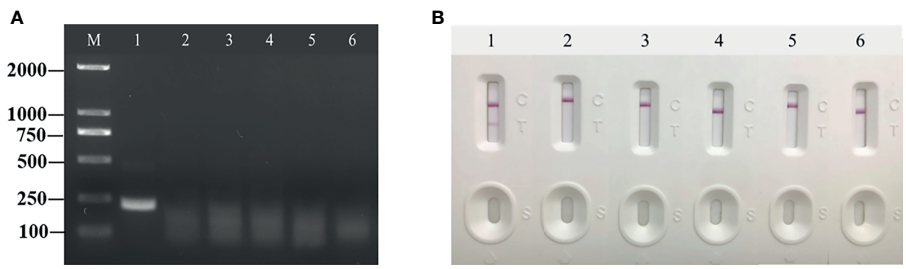

FIGURE 5 | Specificity of reverse transcription recombinase-aided amplification (RT-RAA) and RT-RAA-lateral flow dipstick for common porcine diseases. **(A)** Agarose gel electrophoresis of RT-RAA. M, DL 2000 DNA marker; 1, HCV; 2, HAV; 3, HBV; 4, HIV; 5, syphilis; and 6, HPV. **(B)** RT-RAA-LFA visual readout. 1, HCV; 2, HAV; 3, HBV; 4, HIV; 5, syphilis; and 6, HPV.

considered a high viral load. The RNA extracted from 46 clinical samples were tested using the commercially available qPCR kit. The qPCR results showed that nine of the 46 clinical samples were positive, with a viral load ranging from 2.81×10^8 IU/ml to 8.4×10 IU/ml. HCV RNA-positive patients accounted for 19.56% (9/46), while HCV RNA-negative patients accounted for 80.44% (37/46) (**Table 3**).

Performance of the RT-RAA-LFD Assay on Clinical Samples

Forty-six cases of anti-HCV antibody-positive clinical samples were used to evaluate the performance of RT-RAA-LFD. The clinical samples were detected by RT-RAA, RT-RAA-LFD. The results of RT-RAA, RT-RAA-LFD on nine clinical serum samples were consistent with the results of the traditional qPCR, indicating that this method has the potential for clinical application (**Figures 7A, B** and **Table 4**). In addition, the positive samples containing a high viral load showed color very quickly (2 to 3 min) at the T lines.

DISCUSSION

Infectious diseases caused by viruses, bacteria, fungi, and other pathogens are an inevitable challenge to global health and food security (Chevaliez, 2019). During the COVID-19 pandemic, most secondary and above-detection institutions were equipped with real-time quantitative PCR machines. However, PCR detection technology is expensive and has strict requirements for the detection, collection, and storage of samples so that it is not suitable for widespread use. The disruption to the existing medical service system by COVID-19 led to a reduction in routine HCV antibody screening and a delay in clinical care and treatment (Wan et al., 2020; Yoo et al., 2021). The later

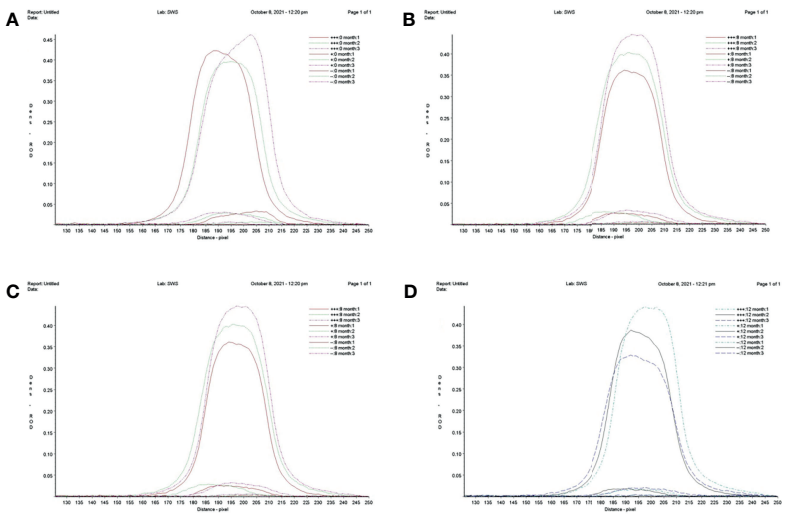

FIGURE 6 | Repeatability and stability of reverse transcription recombinase-aided amplification–lateral flow dipstick. **(A)** Screening of lateral flow dipstick's test lines at 0 month. **(B)** Screening of lateral flow dipstick's test lines at 4 months. **(C)** Screening of lateral flow dipstick's test lines at 8 months. **(D)** Screening of lateral flow dipstick's test lines at 12 months. +++, strong positive sample, 10^5 copies/ml; +, weak positive sample 10 copies/ml; -, negative sample, double-distilled water.

TABLE 2 | Readability and stability assay of RT-RAA-LFA.

Time point (month) sample	0	4	8	12	Cv value
	Average relative optical density of three repeat tests + SD				
10^5 copies/μl, +++	960.3892 ± 169.97	871.9121 ± 71.21	897.6027 ± 240.09	880.2978 ± 188.98	4.43%
10 copies/μl, +	61.8697 ± 5.81	58.3425 ± 19.23	57.3541 ± 13.68	57.7576 ± 7.69	3.51%
Double-distilled water, -	7.4354 ± 2.4073	6.2999 ± 1.0155	7.8315 ± 0.51	7.7612 ± 0.95	9.67%

detection of HCV infections that have occurred during the COVID-19 pandemic has resulted in higher morbidity and mortality. To prevent the spread of disease and protect human populations, rapid POCT for human diseases has played an increasingly important role. Rapid pathogenic diagnosis methods are critical to animal disease control and prevention, public health safety, and other issues (Patchsung et al., 2020; Zhao et al., 2021).

In this study, a novel and complete POCT method for HCV detection, combined with RT-RAA and LFD, was described to have demonstrated good sensitivity and specificity. The detection limit for detecting synthesized plasmids reached 10 copies/μl, and no cross-reactivity was seen with HAV, HBV, HIV, syphilis, and HPV, showing adequate specificity. With RNA extracted from clinical samples, the RT-RAA-LFD method showed 100% concordance with qPCR. However, RT-RAA-LFD could be completed with 5-min amplification and 5–15-min LFD readout times (clinical samples with high RNA concentrations only required 2 to 3 min), indicating that this method was simpler and more efficient than qPCR. Thus, RT-RAA-LFD is a new method of HCV diagnosis that shows good results using exploratory tests. One limitation of this study is the small number of HCV-positive samples used for the evaluation. A field evaluation of this assay with a larger sample size is necessary. Clinical trial protocols will need to be developed and institutions selected for large-scale testing. In addition, the feasibility and accuracy of the RT-RAA-LFD method will need to be evaluated in remote areas.

The RT-RAA experimental method established in this study is based on the use of commercial nucleic acid extraction kits to extract viral genomic RNA, which requires significant preparation costs and expensive instruments like centrifuges and automated RNA extractors. While the traditional qPCR method costs about $5 dollars per test, the cost of an RT-RAA-LFD reaction is about $3 dollars, A significant limitation of this method is that the enzymes must be purchased in a commercial kit. Future studies will focus on independent production from recombinant enzymes, which should reduce the cost and make the test more accessible for POCT. One of the main obstacles for COVID-19 testing is also the extraction of viral RNA, which slows the detection (Min et al., 2021). In recent years, a number of simple RNA extraction-free methods have been used for clinical testing, which play an important role in disease detection and promote the development of rapid-detection reagents (Azmi et al., 2021). However, these methods have their own limitations and shortcomings. In future research, diagnostics may be simplified by preparing microfluidic samples on a chip and implementing an aqueous two-phase-system-based sample preparation and/or paper-based filtration. Efforts must be made to reduce the limitations of the current isothermal

TABLE 3 | Analysis of quantitative detection results of HCV-RNA in 46 patients.

Quantification of HCV-RNA (IU/ml)	Number of samples	Proportion (%)
(-) $<1.0 \times 10^3$	37	80.44
(+) 10^3–$<1.0 \times 10^6$	6	13.04
(+) $\geq 1.0 \times 10^6$	3	6.52
Total	46	100%

amplification methods, like non-specific binding and false positives. With the rapid development of this technology, traditional RAA technology may be combined with other novel technologies, such as real-time fluorescent RAA, quantum dots, CRISPR techniques, electrochemical sensors, and other auxiliary methods, to determine results more conveniently and intuitively. If quantitative detection is required, fluorescent strips may be used for the semi-quantitative rapid detection of diseases. At the same time, the application prospect of this technology for the detection of pathogenic microorganisms has greatly expanded.

In conclusion, this study has shown that RT-RAA-LFD is a highly sensitive and specific method for HCV detection. This method is fast, convenient, and instrument-free, so it may also be performed in remote areas.

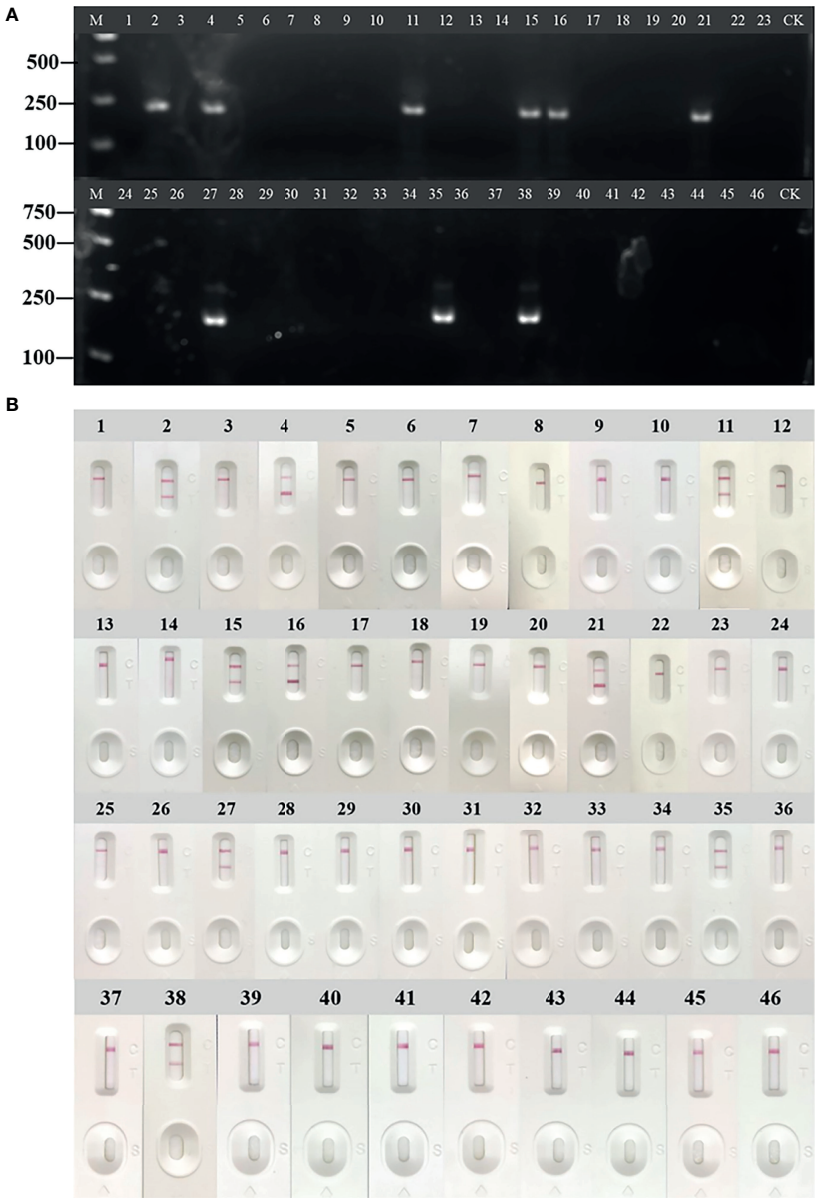

FIGURE 7 | Evaluation of reverse transcription recombinase-aided amplification (RT-RAA) and RT-RAA-lateral flow dipstick (LFD) in RNA extracted from clinical samples. **(A)** Agarose gel electrophoresis of RT-RAA. **(B)** RT-RAA-LFD visual readout. M, DL2000 DNA marker; 1 to 46, blood sample number; CK, negative control with double-distilled water.

TABLE 4 | Detection in clinical samples by RT-RAA, RT-RAA-LFA and qPCR.

Assay	Number of samples	
	Positive	Negative
RT-RAA	9	37
RT-RAA-LFA	9	37
qPCR	9	37

DATA AVAILABILITY STATEMENT

The original contributions presented in the study are included in the article/supplementary material. Further inquiries can be directed to the corresponding authors.

ETHICS STATEMENT

Ethics committee approval was obtained from the Institutional Ethics Committee of Henan Institute of Reproduction Health Science prior to the commencement of the study (approval number EC-258 20200713-1012).

AUTHOR CONTRIBUTIONS

All the authors involved played an important role and contributed to the article. All authors approved the submitted version. HW, YuZ, GZ, and AW contributed to the research design. CL and XZ analyzed the data. HW, ML, JZ, and YC provided clinical samples and conducted the molecular biology experiments. YuZ, HL, CL, XZ, YiZ, and CX performed the experiments and provided study supervision. HW and YuZ wrote the manuscript.

FUNDING

This work was supported by grants from the Science and Technology Project of Henan Province (no. 212102310180), the Open Project of National Health Commission Key Laboratory of Birth Defects Prevention (no. ZD202106), and the Scientific and Technological Innovation Team Plan of Henan Province (19IRTSTHN006).

REFERENCES

Adams, L. M., Balderson, B., and Packett, B. N. (2018a). Meeting the Challenge: Hepatitis C Virus and HIV Care Experiences Among HIV Specialty Providers. *AIDS Patient Care STDS* 32 (8), 314–320. doi: 10.1089/apc.2018.0006

Azmi, I., Faizan, M. I., Kumar, R., Raj Yadav, S., Chaudhary, N., Kumar Singh, D., et al. (2021). A Saliva-Based RNA Extraction-Free Workflow Integrated With Cas13a for SARS-CoV-2 Detection. *Front. Cell. Infection Microbiol.* 11. doi: 10.3389/fcimb.2021.632646

Blanco, L., Bernad, A., Lázaro, J. M., Martín, G., Garmendia, C., and Salas, M. (1989). Highly Efficient DNA Synthesis by the Phage Φ 29 DNA Polymerase: Symmetrical Mode of DNA Replication. *J. Biol. Chem.* 264 (15), 8935–8940. doi: 10.1016/S0021-9258(18)81883-X

Chen, J. S., Ma, E., Harrington, L. B., Da, C. M., Tian, X., Palefsky, J. M., et al. (2018). CRISPR-Cas12a Target Binding Unleashes Indiscriminate Single-Stranded DNase Activity. *Science* 360 (6387), 436–439. doi: 10.1126/science.aar6245

Chevaliez, S. (2019). Strategies for the Improvement of HCV Testing and Diagnosis. *Expert Rev. Anti Infect. Ther.* 17 (5), 341–347. doi: 10.1080/14787210.2019.1604221

Compton, J. (1991). Nucleic Acid Sequence-Based Amplification. *Nature* 350 (6313), 91–92. doi: 10.1038/350091a0

Daher, R. K., Stewart, G., Boissinot, M., and Bergeron, M. G. (2016). Recombinase Polymerase Amplification for Diagnostic Applications. *Clin. Chem.* 62 (7), 947–958. doi: 10.1373/clinchem.2015.245829

Dash, S., Aydin, Y., Widmer, K. E., and Nayak, L. (2020). Hepatocellular Carcinoma Mechanisms Associated With Chronic HCV Infection and the Impact of Direct-Acting Antiviral Treatment. *J. Hepatocell Carcinoma* 7, 45–76. doi: 10.2147/JHC.S221187

Fitzpatrick, T., Pan, S. W., Tang, W., Guo, W., and Tucker, J. D. (2018). HBV and HCV Test Uptake and Correlates Among Men Who Have Sex With Men in China: A Nationwide Cross-Sectional Online Survey. *Sex Transm Infect.* 94 (7), 502–507. doi: 10.1136/sextrans-2018-053549

Foster, G. R., Dore, G. J., Wang, S., Grebely, J., Sherman, K. E., Baumgarten, A., et al. (2019). Glecaprevir/pibrentasvir in Patients With Chronic HCV and Recent Drug Use: An Integrated Analysis of 7 Phase III Studies. *Drug Alcohol Depend* 194, 487–494. doi: 10.1016/j.drugalcdep.2018.11.007

Hollande, C., Parlati, L., and Pol, S. (2020). Micro-Elimination of Hepatitis C Virus. *Liver Int.* 40 Suppl 1, 67–71. doi: 10.1111/liv.14363

Houghton, M. (2009). Discovery of the Hepatitis C Virus. *Liver Int.* 29 (Suppl 1), 82–88. doi: 10.1111/j.1478-3231.2008.01925.x

Ivan, M. L., and Ciara, K. O. (2017). Recombinase Polymerase Amplification: Basics, Applications and Recent Advances. *Trends Analyt Chem.* 98, 19–35. doi: 10.1016/j.trac.2017.10.015

Javier, C., Álvaro, D., and Joaquín, C. (2021). HCV Detection is Possible During SARS CoV-2 Testing; and Throughout COVID-19 Vaccination? *J. Hepatol.* 75 (2), 486–487. doi: 10.1016/j.jhep.2021.04.043

Jia, L., Joanne, M., and Felix, V. S. (2018). Review: A Comprehensive Summary of a Decade Development of the Recombinase Polymerase Amplification. *Analyst.* 144 (1), 31–67. doi: 10.1039/c8an01621f

Kun, W., Daoqing, F., Yaqing, L., and Shaojun, D. (2016). Cascaded Multiple Amplification Strategy for Ultrasensitive Detection of HIV/HCV Virus DNA. *Biosens. Bioelectron.* 87, 116–121. doi: 10.1016/j.bios.2016.08.017

Llibre, A., Shimakawa, Y., and Duffy, D. (2019). Potential Utility of the Genedrive Point-of-Care Test for HCV RNA Detection. *Gut.* 68 (10), 1903–1904. doi: 10.1136/gutjnl-2018-317218

Marcus, J. L., Hurley, L. B., Chamberland, S., Champsi, J. H., Gittleman, L. C., Korn, D. G., et al. (2018). No Difference in Effectiveness of 8 vs 12 Weeks of Ledipasvir and Sofosbuvir for Treatment of Hepatitis C in Black Patients. *Clin. Gastroenterol. Hepatol.* 16 (6), 927–935. doi: 10.1016/j.cgh.2018.03.003

Massimo, C., and Vincenzo, B. (2018). HCV Therapy and Risk of Liver Cancer Recurrence: Who to Treat? *Nat. Rev. Gastroenterol. Hepatol.* 15 (7), 392–393. doi: 10.1038/s41575-018-0018-5

Min, L., Fangfei, Y., Lu, S., Xiuhai, M., Fan, L., Chunhai, F., et al. (2021). Nucleic Acid Tests for Clinical Translation. *Chem. Rev.* 121 (17), 10469–10558. doi: 10.1021/acs.chemrev.1c00241

Narayanamurthy, V., Jeroish, Z. E., Bhuvaneshwari, K. S., and Samsuri, F. (2021). Hepatitis C Virus (HCV) Diagnosis via Microfluidics. *Analytical Methods* 13 (6), 74–763. doi: 10.1039/d0ay02045a

Notomi, T., Okayama, H., Masubuchi, H., Yonekawa, T., Watanabe, K., Amino, N., et al. (2000). Loop-Mediated Isothermal Amplification of DNA. *Nucleic Acids Res.* 28 (12), E63. doi: 10.1093/nar/28.12.e63

Patchsung, M., Jantarug, K., Pattama, A., Aphicho, K., Suraritdechachai, S., Meesawat, P., et al. (2020). Clinical Validation of a Cas13-Based Assay for the Detection of SARS-CoV-2 RNA. *Nat. Biomed. Eng.* 4 (12), 1140–1149. doi: 10.1038/s41551-020-00603-x

Piepenburg, O., Williams, C. H., Stemple, D. L., and Armes, N. A. (2006). DNA Detection Using Recombination Proteins. *PloS Biol.* 4 (7), e204. doi: 10.1371/journal.pbio.0040204

Pietschmann, T., and Brown, R. J. P. (2019). Hepatitis C Virus. *Trends Microbiol.* 27 (4), 379–380. doi: 10.1016/j.tim.2019.01.001

Roger, S., Ducancelle, A., Le Guillou-Guillemette, H., Gaudy, C., and Lunel, F. (2021). HCV Virology and Diagnosis. *Clinics Res. Hepatol. Gastroenterol.* 45 (3), 101626. doi: 10.1016/j.clinre.2021.101626

Spearman, C. W., Dusheiko, G. M., Hellard, M., and Sonderup, M. (2019). Hepatitis C. *Lancet* 394 (10207), 1451–1466. doi: 10.1016/S0140-6736(19)32320-7

Vincent, M., Xu, Y., and Kong, H. (2004). Helicase-Dependent Isothermal DNA Amplification. *EMBO Rep.* 5 (8), 795–800. doi: 10.1038/sj.embor.7400200

Wang, Y., Jie, W., Ling, J., and Yuanshuai, H. (2021). HCV Core Antigen Plays an Important Role in the Fight Against HCV as an Alternative to HCV-RNA Detection. *J. Clin. Lab. Anal.* 35 (6), e23755. doi: 10.1002/jcla.23755

Wan, D. Y., Luo, X. Y., Dong, W., and Zhang, Z. W. (2020). Current Practice and Potential Strategy in Diagnosing COVID-19. *Eur. Rev. Med. Pharmacol. Sci.* 24 (8), 4548–4553. doi: 10.26355/eurrev_202004_21039

Warkad, S. D., Nimse, S. B., Song, K. S., and Kim, T. (2018). HCV Detection, Discrimination, and Genotyping Technologies. *Sensors (Basel)* 18 (10), 3423. doi: 10.3390/s18103423

World Health Organization. (2017). Guidelines on Hepatitis B and C Testing. Geneva: World Health Organization.

Yan, L., Zhou, J., Zheng, Y., Gamson, A. S., Roembke, B. T., Nakayama, S., et al. (2014). Isothermal Amplified Detection of DNA and RNA. *Mol. Biosyst.* 10 (5), 970–1003. doi: 10.1039/c3mb70304e

Yoo, H. M., Kim, I., and Kim, S. (2021). Nucleic Acid Testing of SARS-CoV-2. *Int. J. Mol. Sci.* 22 (11), 6150. doi: 10.3390/ijms22116150

Zhang, Y., Li, Q., Guo, J., Li, D., Wang, L., Wang, X., et al. (2021). An Isothermal Molecular Point of Care Testing for African Swine Fever Virus Using Recombinase-Aided Amplification and Lateral Flow Assay Without the Need to Extract Nucleic Acids in Blood. *Front. Cell. Infection Microbiol.* 11. doi: 10.3389/fcimb.2021.633763

Zhao, L., Wang, J., Sun, X. X., Wang, J., Chen, Z., Xu, X., et al. (2021). Development and Evaluation of the Rapid and Sensitive RPA Assays for Specific Detection of Salmonella Spp. In Food Samples. *Front. Cell. Infection Microbiol.* 11. doi: 10.3389/fcimb.2021.631921

Conflict of Interest: The authors declare that the research was conducted in the absence of any commercial or financial relationships that could be construed as a potential conflict of interest.

Publisher's Note: All claims expressed in this article are solely those of the authors and do not necessarily represent those of their affiliated organizations, or those of the publisher, the editors and the reviewers. Any product that may be evaluated in this article, or claim that may be made by its manufacturer, is not guaranteed or endorsed by the publisher.

frontiers in Cellular and Infection Microbiology

ORIGINAL RESEARCH
published: 31 March 2022
doi: 10.3389/fcimb.2022.863435

Visual Identification and Serotyping of Toxigenic *Vibrio cholerae* Serogroups O1 and O139 With CARID

*Pan Lu, Jialiang Chen, Zhenpeng Li, Zhe Li, Jingyun Zhang, Biao Kan and Bo Pang**

State Key Laboratory of Infectious Disease Prevention and Control, National Institute for Communicable Disease Control and Prevention, Chinese Center for Disease Control and Prevention, Beijing, China

There is a growing demand for rapid, sensitive, field-deployable nucleic acid tests for cholera, which usually occurs in rural areas. In this study, we developed a Cas12a-assisted rapid isothermal detection (CARID) system for the detection of toxigenic *V. cholerae* serogroups O1 and O139 by combining recombinase-aided amplification and CRISPR-Cas (clustered regularly interspaced short palindromic repeats and CRISPR-associated proteins). The results can be determined by fluorescence signal and visualized by lateral flow dipstick. We identified 154 *V. cholerae* strains and 129 strains of other intestinal diarrheagenic bacteria with a 100% coincidence rate. The limit of detection of CARID was 20 copies/reaction of *V. cholerae* genomic DNA, which is comparable to that of polymerase chain reaction (PCR) and qPCR. Multiple-CARID was also established for efficiency and economic considerations with an acceptable decrease in sensitivity. Simulated sample tests showed that CARID is suitable for complex samples. In conclusion, CARID is a rapid, sensitive, economically efficient, and portable method for the detection of *V. cholerae*, which makes it suitable for field responses to cholera.

Keywords: CARID, CRISPR-Cas, RAA, detection, *Vibrio cholerae*, cholera

OPEN ACCESS

Edited by:
Ciprian Iliescu, National Institute for Research and Development in Microtechnologies, Romania

Reviewed by:
Md Nur Hossain, Bangladesh Council of Scientific and Industrial Research, Bangladesh
Hengyi Xu, Nanchang University, China

***Correspondence:**
Bo Pang
pangbo@icdc.cn

Specialty section:
This article was submitted to Clinical Microbiology, a section of the journal Frontiers in Cellular and Infection Microbiology

Received: *27 January 2022*
Accepted: *07 March 2022*
Published: *31 March 2022*

Citation:
Lu P, Chen J, Li Z, Li Z, Zhang J, Kan B and Pang B (2022) Visual Identification and Serotyping of Toxigenic Vibrio cholerae Serogroups O1 and O139 With CARID. Front. Cell. Infect. Microbiol. 12:863435. doi: 10.3389/fcimb.2022.863435

INTRODUCTION

Cholera remains a threat to public health in many countries with poor sanitation or that are short of safe water (Deen et al., 2020). It has been estimated that there are roughly 1.3 to 4.0 million cases of cholera annually, with 21,000 to 143,000 deaths worldwide (Ali et al., 2015). *Vibrio cholerae*, the causative agent of cholera, can be transmitted through contaminated water and/or food (Sack et al., 2004). Cholera toxin (CT), an important pathogenic factor of *V. cholerae*, is encoded by *ctxA* and *ctxB*, and *V. cholerae* that carry *ctxA* and *ctxB* are referred to as toxigenic strains (Bharati and Ganguly, 2011). To date, only the toxigenic serogroups O1 and O139 are known to have caused epidemics and pandemics of cholera, even though there are more than 200 serogroups of *V. cholerae* (Harris et al., 2012; Chowdhury et al., 2017).

Early detection and confirmation of cholera cases are critical for rapid implementation of interventions. However, traditional culture methods for isolation and identification of *V. cholerae* can take three days or more and require extensive laboratory infrastructure and experienced staff (Ramamurthy et al., 2020). While molecular methods such as polymerase chain reaction (PCR) and quantitative real-time PCR (qPCR) have accelerated the diagnosis process, they rely heavily on

expensive instruments and require elaborate experimental conditions, which are often difficult to obtain in rural areas. Therefore, rapid and point-of-care testing methods are essential for timely cholera detection and control.

CRISPR-Cas (clustered regularly interspaced short palindromic repeats and CRISPR-associated proteins) systems are adaptive immune systems consisting of Cas effector proteins and CRISPR RNAs (crRNAs) that are widely distributed in archaea and bacteria (Li and Du, 2011; Terns and Terns, 2011). CRISPR-Cas relies on crRNAs for sequence-specific detection and silencing of foreign nucleic acids, thereby protecting organisms from viruses and phages (Barrangou et al., 2007; Al-Attar et al., 2011; Bhaya et al., 2011; Wiedenheft et al., 2012). CRISPR-Cas12a systems can cleave single-stranded DNA (ssDNA) indiscriminately when bound to target sequences under the guidance of crRNA *in vitro* (Chen et al., 2018); therefore, this principle has been used in the specific detection of pathogens (Chen et al., 2018; Gootenberg et al., 2018; Li et al., 2018). For double-stranded target DNA activators, the prerequisite for Cas12a to effectively cleave non-target DNA is identification of a short T-rich (5 '-TTTN-3') protospacer-adjacent motif (PAM) in the target strand (Zetsche et al., 2015; Chen et al., 2018), which provides theoretical guidance for the design of crRNA.

Because the detection ability of CRISPR-Cas systems relies on the template provided, it is usually combined with several amplification methods, such as recombinase polymerase amplification (RPA) (Chen et al., 2018), PCR (Li et al., 2018) and recombinase-aided amplification (RAA) (Xiao et al., 2021). RAA is a sensitive, rapid, low-cost isothermal amplification technique that can be completed within 15–30 min at 37 to 42°C without using large, expensive instruments (Shen et al., 2019; Wang et al., 2020).

Based on the detection principles of CRISPR-Cas12a and RAA, we developed CARID (Cas12a-assisted rapid isothermal detection) for the rapid visual detection of toxigenic *V. cholerae* serogroups O1 and O139 (**Figure 1**). Using simulated samples, we demonstrated that CARID could be completed within an hour, and that the results could be visualized through fluorescent signals or lateral flow dipstick (LFD). The method established in this study can detect the *ctxA* gene and identify the O1 and O139 serogroups with a specificity of 100%. The minimum detectable genomic concentration is 20 copies/reaction, and the sensitivity is comparable to that of PCR and qPCR.

MATERIALS AND METHODS

Bacterial Strains

A total of 154 strains of *V. cholerae* were included in this study, namely, 112 strains of *V. cholerae* carrying cholera toxin (22 strains of serogroup O1 and 90 strains of serogroup O139) and 42 strains of *V. cholerae* without CT (22 strains of serogroup O1 and 20 strains of serogroup O139). These strains were isolated from cholera patients and environmental samples. Oral consent was obtained from each eligible patient (or the legal guardian of the patient, if the patient is <18 years of age). Other intestinal diarrheagenic bacteria, namely, 20 strains of *Vibrio parahaemolyticus*, 14 strains of *Vibrio alginolyticus*, 13 strains of *Vibrio mimicus*, 14 strains of *Vibrio furnis*, 10 strains of *Vibrio fluvialis*, 14 strains of *Escherichia coli*, 15 strains of *Salmonella enteritidis*, 14 strains of *Shigella*, and 15 strains of *Yersinia enterocolitica* were also evaluated in this study.

Purification of LbCas12a Protein

To prepare recombinant LbCas12a proteins (Zetsche et al., 2015), protein sequences were codon-optimized for *E. coli* expression. Synthetic oligonucleotide fragments were then cloned into bacterial protein expression vector pET-28a and transfected into *E. coli* BL21. *E. coli* cells were first grown with 50 μg/ml Kanamycin at 37°C until OD_{600} reached 0.5–0.6, followed by incubation with 0.5 mM IPTG at 21°C for 16 h to induce LbCas12a expression. The cultures were then lysed by sonication, filtered through 0.22-μm filters, and applied to a nickel column (Ni-NTA agarose, Qiagen, Germany) for protein purification. The eluted protein was stored in a storage solution (500 mM NaCl, 20 mM Sodium Acetate, 0.1 mM EDTA, 0.1 mM DTT, 50% Glycerol). Purified LbCas12a proteins were examined by SDS-PAGE and protein concentrations were determined using a Pierce™ BCA Protein Assay Kit (Thermo Scientific, Shanghai, China).

Specificity Determination of CARID

DNA was extracted from bacterial colonies cultured overnight using the boiling method, after which the extracted nucleic acid was dissolved in 50 μl ddH_2O. Target DNA was amplified using an RAA isothermal amplification kit (Qitian, Jiangsu, China) followed by Cas12a detection. Briefly, 50 μl RAA reactions contained 2 μl template, 0.4 μM forward and reverse primer, 1× reaction buffer,

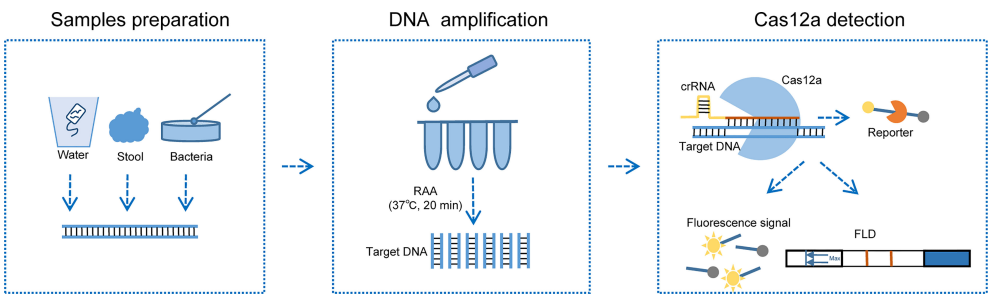

FIGURE 1 | Schematic diagram of CARID detecting *V. cholerae*. Nucleic acid can be extracted from *V. cholerae* contaminated river water samples, stool, and clones cultured on LB agar plates. RAA amplifies the template at 37°C for 20 min, after which it is added to the Cas12a reaction mixture and incubated at 37°C for 30 min. The fluorescent signal and lateral flow dipstick can be used to determine the results.

nuclease-free water, lyophilized powder reaction unit, and 2.5 μl of 280 mM magnesium acetate. The RAA mix was incubated at 37°C for 20 min. For the fluorescence assay, the amplification product was added to CRISPR reaction mix consisting of 1× CRISPR reaction buffer (10 mM Tris–HCl, 10 mM $MgCl_2$, pH = 8.0), 100 nM crRNA, 100 nM Cas12a, and 200 nM ssDNA reporter (5'-6FAM-TTATT-BHQI-3'). This final reaction was incubated at 37°C and monitored for fluorescence for 30 min using a Gentier 96E qPCR machine (TIANLONG, Xian, China). Samples that produced fluorescence at levels 2.0-fold or greater above the NC were considered positive. For the LFD detection reactions, the ssDNA reporter was replaced with 5'-6FAM-TTATT-Biotin-3'. The final reaction system was incubated at 37°C for 30 min, after which the reaction products were diluted with ddH_2O and then inserted into the LFD (Tiosbio, Beijing, China) to read the results. A band on the T test line can be judged as positive.

Sensitivity of CARID

To evaluate the sensitivity of CARID, *V. cholerae* genomic DNA was extracted using a Wizard Genomic DNA Purification Kit (Promega, Madison, WI, USA) and diluted with ddH_2O to concentrations of 10^7 to 1 copies/μl (DNA copies number were determined using following formula: $(6.02 \times 10^{23}) \times (ng/\mu l \times 10^{-9})/(DNA\ length \times 660) = copies/\mu l$). Diluted samples were then used as templates for CARID detection, PCR, and qPCR. PCR was conducted using TaKaRa Premix Taq™ (TaKaRa, Dalian, China) and a 50-μL reaction system that contained 1×Premix Taq, 0.4 μM forward primer, 0.4 μM reverse primer, and 2 μl of template. The reaction conditions were 95°C for 5 min, followed by 40 cycles of 95°C for 10 s, 50°C for 30 s, and 72°C for 30 s, and then 72°C for 10 min. A qPCR assay was performed in a 50-μl volume using Premix Ex TaqTM (TaKaRa, Dalian, China). The reaction system contained 1× Premix Ex Taq (Probe qPCR), 0.4 μM forward primer, 0.4 μM reverse primer, 0.4 μM probe, and 2 μl of template. The reaction conditions for qPCR were 95°C for 30 s, followed by 40 cycles of 95°C for 10 s and 60°C for 30 s. The amplification process was conducted using a Gentier 96E qPCR machine (Tianlong, Xian, China).

Verification of CARID With Simulated Samples

Verification of CARID With Simulated Environmental Water Samples

One toxigenic serogroup O1 and one toxigenic serogroup O139 of *V. cholerae* was cultured on nutrient agar overnight. Individual colonies were then selected and incubated in Luria–Bertani (LB) broth (Oxoid, Basingstoke, UK) at 37°C with shaking (200 rpm) to a concentration of OD_{600} = 1.0 (approximately 1×10^9 colony forming units (CFU)/ml), after which the bacteria were gradient-diluted into a bacterial suspension in PBS with a concentration of 10^9–10 CFU/ml. Simulated water samples with bacterial concentrations of 10^7–10^{-1} CFU/ml were prepared by adding 50 μl of bacterial suspension to 5 ml of pre-mixed and sterilized river water (4.5 ml of river water and 0.5 ml of 10× 1% sodium chloride alkaline peptone water). The simulated water samples were then shaken at 200 rpm and 37°C for 4 h, and 1 ml of bacterial suspension was taken every hour for nucleic acid extraction and CARID detection as described above. Fluorescent signal detection and LFD were then used to visualize the results.

Verification of CARID With Simulated Stool Samples

The bacterial deposits of 10^9–10 CFU were mixed with 250-mg stool samples of healthy adults, after which nucleic acid was extracted using a QIAamp® Power Fecal® Pro DNA Kit (Qiagen, Germany) according to the manufacturer instructions. The extracted nucleic acid was then dissolved in 50 μl ddH_2O, after which 2-μl aliquots were used as templates for detection of the *ctxA* and O-PS specific genes. Fluorescent signal detection and LFD were used to visualize the results.

Identification of *V. cholerae* With Multiple CARID

The multiple RAA system included 1× reaction buffer, 0.4 μM forward and reverse primers for *V. cholerae ctxA*, serogroups O1 and O139 O-PS specific genes, and the RAA reagent. After preparing the system, 2 μl of DNA template and 2.5 μl of 280 mM magnesium acetate solution were added and samples were then incubated at 37°C for 30 min. CrRNA was then used to detect *ctxA*, O1, and O139 O-PS specific genes in the product. Fluorescent signal detection and LFD were used to visualize the results.

Statistical Analysis

The GraphPad Prism 9 software was used for statistical analyses and preparation of figures. Analyses were based on three replicate values. Unpaired t-tests were used to identify differences between two groups.

RESULTS

Design of Primers and crRNA

Primers and crRNA were designed according to the conserved regions of *ctxA*, rfb-O1, and rfb-O139 genes of *V. cholerae*. Conserved fragments containing the PAM sequence (5'-TTTN-3') were selected as the target to design primers and guide sequences. CrRNA contains a conserved stem-loop structure that is necessary for forming the Cas12a–crRNA complex, and the adaptive crRNA stem-loop sequence of Cas12a is different for each Cas12a type (Zetsche et al., 2015). After the guide sequence was designed, a stem-loop sequence homologous to LbCas12a was added to its 5' end to ensure that the protein had strong cleavage ability. The primers and RNA sequences are not published herein because they are currently being patented.

Validation of LbCas12a Protein Activity and crRNA Adaptation

The LbCas12a protein is composed of 1,228 amino acids with a molecular weight of 143,035 g/mol. The results of SDS-PAGE analysis of purified LbCas12a protein were consistent with the expected size of the target protein (**Figure 2**). To verify the protein activity of LbCas12a, the target DNA (*ctxA*: 691bp, O1: 1033bp, O139: 965bp) was amplified by PCR and then added

into the CRISPR reaction system to detect its fluorescent signal. The CRISPR reaction could detect fluorescent signals in the absence of buffer, but the fluorescence value was much lower than when the buffer is included (**Figure 3A**). This indicates that buffer significantly enhanced the accessory cleavage ability of the protein. The LbCas12a protein, crRNA, reporter, and target DNA were obligate for successful detection by the fluorescence method or the LFD method (**Figures 3A, B**). The CRISPR reaction products were detected by electrophoresis. The LbCas12a protein cleaved the target DNA successfully under the guidance of crRNA. Taken together, these findings indicated that *ctxA*-crRNA, O1-crRNA, and O139-crRNA were suitable for detection of the target DNA (**Figure 3C**).

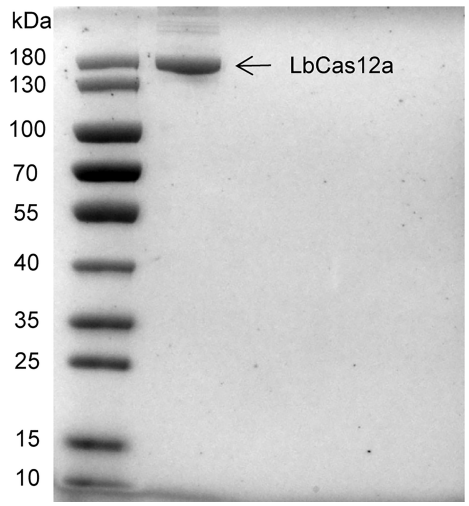

FIGURE 2 | Purification of Cas12 proteins. SDS-PAGE gel of LbCas12 proteins was used in this study.

Specificity of CARID for Detection of *V. cholerae*

A total of 154 strains of *V. cholerae* were used to evaluate the specificity of CARID, and 112 toxigenic *V. cholerae* and 42 nontoxigenic strains were successfully identified. Forty-four serogroup O1 strains and 110 serogroup O139 strains were also successfully identified. The identification rate was 100%, which was consistent with whole-genome sequencing data. The RAA primers and crRNA of *ctxA*, O1, and O139 were used to detect other diarrheagenic bacteria, namely, *E. coli*, *Salmonella enteritidis*, *Shigella*, *Y. enterocolitica* and other Vibrios to confirm the specificity of the method. There were no positive results for these bacteria, and the coincidence rate was 100% (**Table 1**). The results of the fluorescence assay were consistent with those of the LFD.

Sensitivity of CARID for Detection of *V. cholerae*

A series of samples containing *V. cholerae* genomic DNA that had been diluted from 10^7 to 1 copies/μl were analyzed by CARID, PCR, and qPCR. Furthermore, the primers of RAA

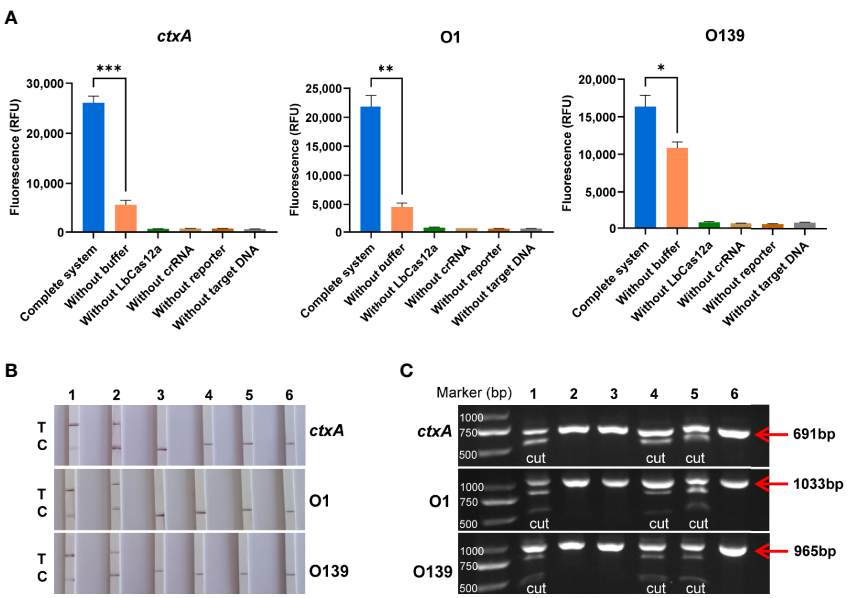

FIGURE 3 | Validation of LbCas12a protein activity and crRNA adaptation. **(A)** Fluorescence value of the complete Cas12a system, and the absence of buffer, Cas12a, crRNA, reporter or target DNA (n = 3 technical replicates; two-tailed Student's t-test; *p < 0.05; **p < 0.01; ***p < 0.001; bars represent the mean ± SEM). **(B)** LFD results of the complete Cas12a system and the absence of buffer, Cas12a, crRNA, reporter, or target DNA (T is the test band and C is the control band). 1 is the complete system, 2, is the system without buffer, and 3–6 are systems without LbCas12a protein, crRNA, reporter, and target DNA, respectively. **(C)** Cas12a cutting target DNA was detected by agarose gel electrophoresis. 1 is the complete system, 2–5 are systems without Cas12a, crRNA, buffer, and reporter, respectively, and 6 is the target DNA alone.

TABLE 1 | Specificity of CARID for detection of *V. cholerae* and other intestinal diarrheagenic bacteria.

Pathogens	Number	Positive rate		
		ctxA	O1	O139
Toxigenic serogroup O1 *V. cholerae*	22	22/22 (100%)	22/22 (100%)	0
Toxigenic serogroup O139 *V. cholerae*	90	90/90 (100%)	0	90/90 (100%)
Nontoxigenic serogroup O1 *V. cholerae*	22	0	22/22 (100%)	0
Nontoxigenic serogroup O139 *V. cholerae*	20	0	0	20/20 (100%)
V. parahaemolyticus	20	0	0	0
V. alginolyticus	14	0	0	0
V. mimicus	13	0	0	0
V. furnis	14	0	0	0
V. fluvialis	10	0	0	0
E. coli	14	0	0	0
Salmonella enteritidis	15	0	0	0
Shigella	14	0	0	0
Y. enterocolitica	15	0	0	0

were used in the PCR experiment. The results showed that CARID could detect 20 copies/reaction (**Figure 4A**). However, only weakly positive or negative results were observed when samples containing 20 copies/reaction of genome DNA were tested by LFD (**Figure 4B**). When the genome concentration was 20 copies/reaction, the CT values of *ctxA*, O1, and O139 O-PS specific genes were 34.15 ± 0.92, 32.63 ± 0.40, and 34.19 ± 1.08 (mean ± SD), respectively, for qPCR (**Figure 4C**). Moreover, only weak bands were amplified by PCR at a genomic concentration of 200 copies/reaction (**Figure 4D**).

Verification of CARID With Simulated Samples

A series of simulated river water samples containing 10^{7}–10^{-1} CFU/ml toxigenic *V. cholerae* was used to evaluate the limit of detection (LOD) of CARID. For the toxigenic serogroup O1, positive results for *ctxA* and O1 O-PS specific genes were obtained in samples containing 10^{4} CFU/ml of *V. cholerae*. Samples containing 10^{3} CFU/ml could be detected after 1 h of culture, while 10 CFU/ml could be detected after 2 h of culture,

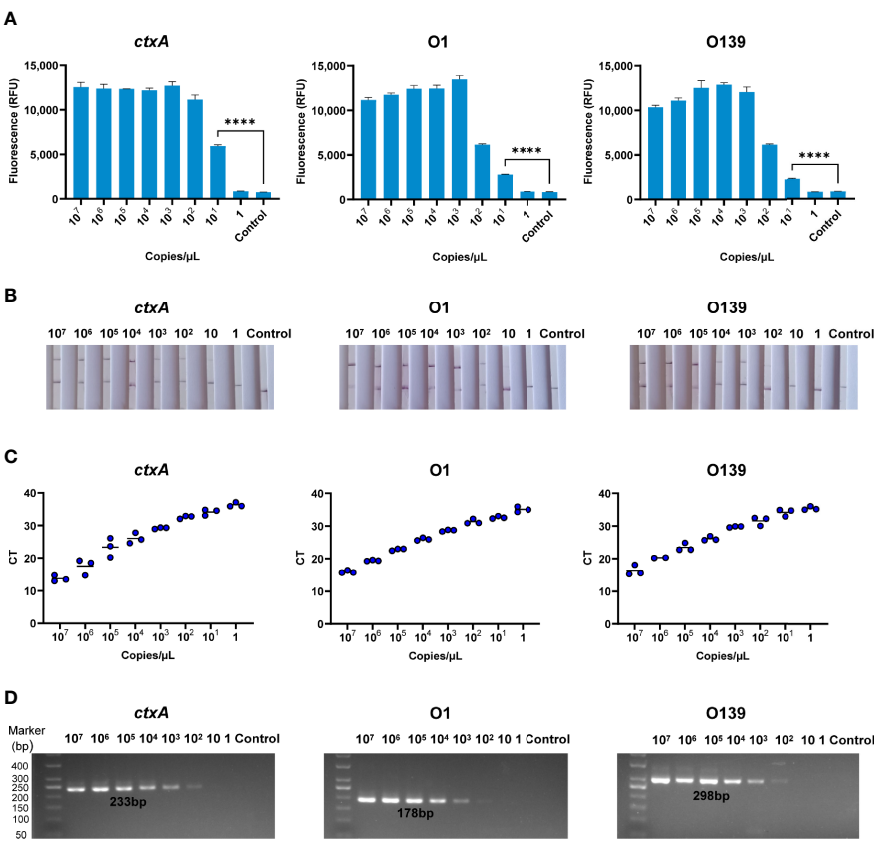

FIGURE 4 | Sensitivity of CARID for detection of *V. cholerae*. **(A)** The 10^{7}–1 copies/μl *V. cholerae* templates were detected by fluorescence method of CARID (n = 3 technical replicates; two-tailed Student's t-test; ****p <0.0001; bars represent the mean ± SEM). **(B)** The 10^{7}–1 copies/μl *V. cholerae* templates were detected by LFD. **(C)** QPCR detected *ctxA*, O1, and O139 genes from 10^{7}–1 copies/μl *V. cholerae* templates. **(D)** PCR detected *ctxA*, O1, and O139 genes from 10^{7}–1 copies/μl *V. cholerae* templates.

and 1 CFU/ml could be detected after 4 h. In contrast to *ctxA* and O1, O139 O-PS specific genes could be detected in river water containing 10^5 CFU/ml before culture and 10^2 CFU/ml after 2 h of culture (**Figure 5**). Overall, river water samples containing 1 CFU/ml of *V. cholerae* could be successfully detected by CARID after culture for 4 h with alkaline peptone water.

Application of CARID to stool samples containing 10^9–10 CFU/250 mg bacteria revealed the *ctxA* gene could be detected at 10^3 CFU/250 mg bacteria (equivalent to 4×10^3 CFU/g). In addition, the O1 and O139 genes could be detected from simulated stool samples at 4×10^4 CFU/g bacteria (**Figure 6**).

Identification and Serotyping of *V. cholerae* With Multiple-CARID

Owing to efficiency and economic considerations, we set up multiple-CARID for simultaneous detection of *ctxA* and O-PS specific genes. Using the protocol described in the *Materials and Methods* section, a nucleic acid mixture of toxigenic *V. cholerae* serogroups O1 and O139 was analyzed, and positive results were obtained using all three CRISPR reactions (**Figures 7A, B**). To evaluate the LOD of multiple-CARID, 10^3–10 copies/μl of *V. cholerae* genomic DNA was examined, and 10 repeats were performed for each dose. The lowest dose point with a 100% detection rate was taken as the LOD. For the fluorescence assay, *ctxA* and O1 O-PS specific genes showed higher sensitivity than O139, with 200 copies/reaction of *V. cholerae* DNA consistently detected in 10 out of 10 tests, and 20 copies/reaction detected in 7 out of 10 tests. However, an O139 O-PS specific gene was detected in 9 out of 10 tests of samples containing 200 copies/reaction of *V. cholerae* DNA (**Figure 7C**). When LFD analysis was conducted, *ctxA* and O1 O-PS specific genes were detected from samples containing 200 copies/reaction of *V. cholerae* DNA with clear bands in all 10 replicates. In comparison, O139 O-PS specific genes were detected in samples containing 2,000 copies/reaction of *V. cholerae* DNA with 100% detection rates **Figure 7D**.

DISCUSSION

Cholera often occurs in areas with poor sanitation, limited resources, and low testing capabilities, and *V. cholerae* serogroups O1 and O139 are the predominant agents of cholera epidemics

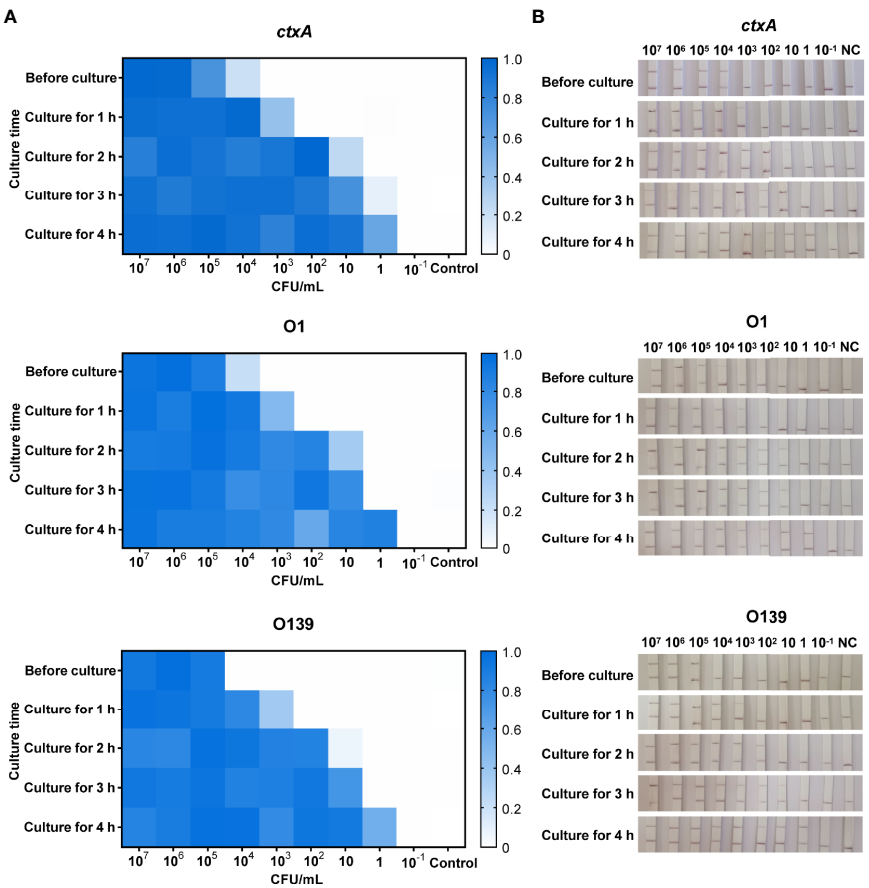

FIGURE 5 | CARID detection of simulated river water samples. **(A)** Simulated water samples were tested by fluorescent CARID before culture and after culture for 1–4 h. The fluorescent signal of each sample was normalized against the negative control of the same batch. The heatmap represents normalized mean fluorescence values (n = 3 technical replicates). **(B)** Simulated water samples were tested by the LFD method of CARID before culture and after culture for 1–4 h.

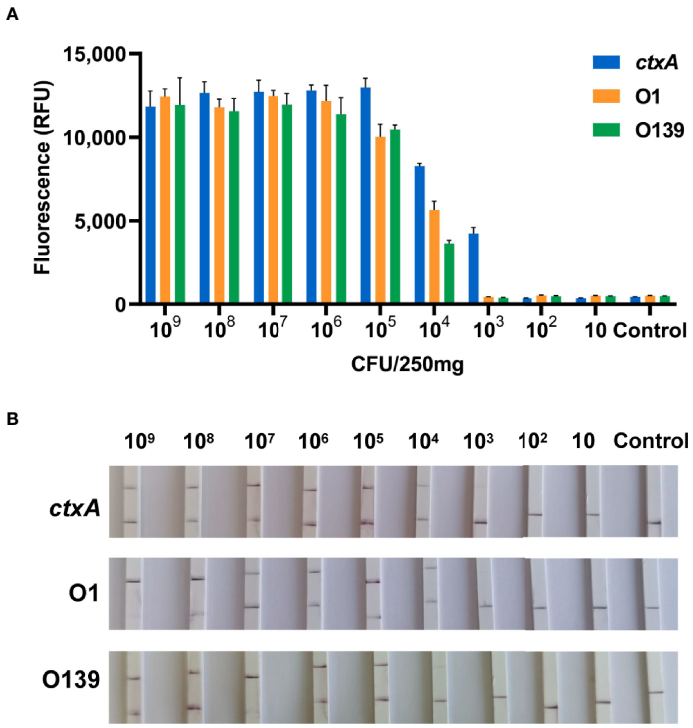

FIGURE 6 | CARID detection of simulated stool samples. **(A)** Templates extracted from stool containing 10^9–10 CFU/250 mg *V. cholerae* were analyzed by fluorescent CARID (n = 3 technical replicates; bars represent the mean ± SEM). **(B)** Templates extracted from stool containing 10^9–10 CFU/250 mg *V. cholerae* were analyzed by the LFD method.

(Deen et al., 2020). Accordingly, rapid field detection and pathogen identification are critical to controlling cholera. In the present study, we developed a visual detection method for toxigenic *V. cholerae* under isothermal conditions based on the principle of CRISPR-Cas12a. The developed method successfully detected toxigenic *V. cholerae* and identified serogroups O1 and O139 in less than 1 h, which is ideal for rapid responses in cholera control. The buffer can significantly improve the fluorescence value, which supported that the addition of a buffer with Mg^{2+} significantly improved the reaction efficiency of Cas12a (Wu et al., 2020). To confirm that the system works effectively, we set the detection time of the Cas12a reaction to 30 min; however, 10 min was found to be sufficient to produce robust results. Nevertheless, our findings indicate that the efficiency of the test could be improved in the future.

The specificity of CARID for detection of *V. cholerae* and other intestinal diarrheagenic bacteria was comparable to those of other methods. The detection limits were 20 copies/reaction and 200 copies/reaction, respectively, for fluorescent signal and LFD detection, which are comparable to the detection limits of PCR and qPCR. In areas of cholera outbreaks, polluted water is the main infectious medium (Rafique et al., 2016). In the present study, CARID could detect the target pathogens from simulated river water samples with the concentration of 10^4–10^5 CFU/ml *V. cholerae*, while the infection dose of *Vibrio cholerae* in humans is 10^8–10^{11} cells (Nelson et al., 2009). Our results showed that, after 4 h of enrichment, *V. cholerae* at an initial concentration of 1 CFU/ml could reach the detection limit of CARID. Therefore, for water samples, we recommend an enrichment step, which can improve the detection rate. Patients with symptoms of cholera usually shed 10^7–10^9 cells of *Vibrio cholerae* per gram of stool (Nelson et al., 2009), and the detection limit of CARID is 4×10^3 CFU/g of stool. Therefore, these findings indicate that CARID is sensitive enough for application in cholera control and for analysis of surveillance samples. The LOD of simultaneous detection of *ctxA*, O1, and O139 serogroup-specific genes in a single amplification was 200–2,000 copies/reaction, which was comparable to single amplifications. Hence, the multiplex protocol is both time-saving and economically efficient.

A major concern of the CRISPR-Cas-mediated detection protocol is that cross-contamination transfer of amplicons can lead to aerosol contamination; therefore, we recommend that the configuration system, addition of templates, and transfer of amplification products be conducted in different experimental areas. For example, in SARS-COV-2 detection with CRISPR-Cas12a, Chen et al. (2020) effectively avoided aerosol contamination of the amplicon by covering the isothermal amplification reaction solution with mineral oil and pre-adding CRISPR reagents to the tube lid, which avoided opening of the tube cap during the entire process Chen et al. (2020). In addition, lab-on-a-chip and microfluidics can also be used to develop portable, sensitive, and cost-effective biosensing systems for Cas12a-mediated detection (Khizar et al., 2020; Ramachandran et al., 2020). In such systems, the RAA and CRISPR reagents can

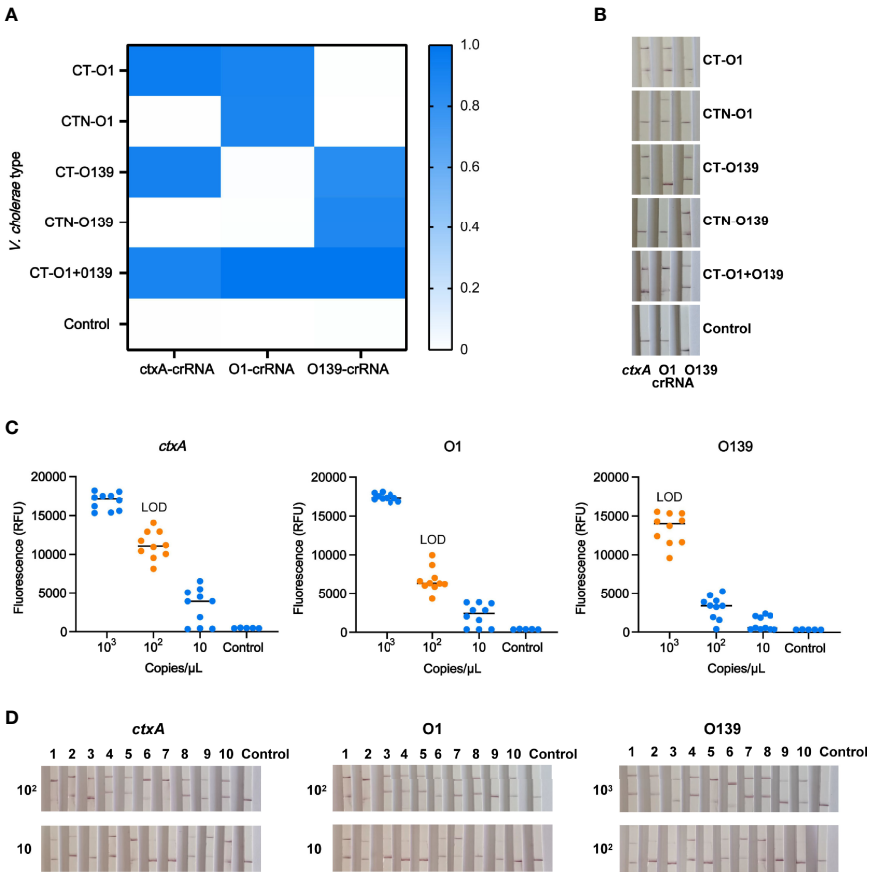

FIGURE 7 | Identification and typing of *V. cholerae* with multiple-CARID. **(A)** Fluorescent CARID for detection of *ctxA* and identification of serogroups O1 and O139. The heatmap represents normalized mean fluorescence values (n = 3 technical replicates). CT-O1 refers to *V. cholerae* serogroup O1 containing cholera toxin; CTN-O1 refers to *V. cholerae* serogroup O1 without cholera toxin. CT-O139 refers to O139 containing cholera toxin; CTN-O139 refers to O139 without cholera toxin. CT-O1 + O139 refers to mixed *V. cholerae* serogroups O1 and O139 CT. **(B)** LFD method of CARID for detection of *ctxA* and identification of serogroups O1 and O139. **(C)** LOD of the fluorescent method of multiple-CARID. Ten repetitions were performed. **(D)** LOD of the LFD method of multiple-CARID.

be integrated onto a chip in advance, which enables the application of CRISPR-Cas-mediated steps in various settings, namely, clinics, mobile testing stations, and rural areas.

DATA AVAILABILITY STATEMENT

The original contributions presented in the study are included in the article/supplementary material. Further inquiries can be directed to the corresponding author.

AUTHOR CONTRIBUTIONS

BP conceived and designed the study. PL and JC contributed to the experiment. ZhenL contributed to the analysis of bioinformatics. PL and BP contributed to writing the manuscript. JZ, ZheL, and BK contributed to the design of the experiment. All authors listed have made a substantial, direct, and intellectual contribution to the work and approved it for publication.

FUNDING

This work was supported by the National Science and Technology Major Project (2018ZX10714-002).

ACKNOWLEDGMENTS

We thank Professor Weili Liang and Meiying Yan for their helpful discussion.

SUPPLEMENTARY MATERIAL

The Supplementary Material for this article can be found online at: https://www.frontiersin.org/articles/10.3389/fcimb.2022.863435/full#supplementary-material

REFERENCES

Al-Attar, S., Westra, E. R., van der Oost, J., and Brouns, S. J. J. (2011). Clustered Regularly Interspaced Short Palindromic Repeats (CRISPRs): The Hallmark of an Ingenious Antiviral Defense Mechanism in Prokaryotes. *Biol. Chem.* 392 (4), 277–289. doi: 10.1515/bc.2011.042

Ali, M., Nelson, A. R., Lopez, A. L., and Sack, D. A. (2015). Updated Global Burden of Cholera in Endemic Countries. *PloS Negl. Trop. Dis.* 9, e0003832. doi: 10.1371/journal.pntd.0003832

Barrangou, R., Fremaux, C., Deveau, H., Richards, M., Boyaval, P., Moineau, S., et al. (2007). CRISPR Provides Acquired Resistance Against Viruses in Prokaryotes. *Science* 315, 1709–1712. doi: 10.1126/science.1138140

Bharati, K., and Ganguly, N. K. (2011). Cholera Toxin: A Paradigm of a Multifunctional Protein. *Indian J. Med. Res.* 133, 179–187.

Bhaya, D., Davison, M., and Barrangou, R. (2011). CRISPR-Cas Systems in Bacteria and Archaea: Versatile Small RNAs for Adaptive Defense and Regulation. *Annu. Rev. Genet.* 45, 273–297. doi: 10.1146/annurev-genet-110410-132430

Chen, J. S., Ma, E., Harrington, L. B., Da Costa, M., Tian, X., Palefsky, J. M., et al. (2018). CRISPR-Cas12a Target Binding Unleashes Indiscriminate Single-Stranded DNase Activity. *Science* 360, 436–439. doi: 10.1126/science.aar6245

Chen, Y, Shi, Y, Chen, Y, Yang, Z, Wu, H, Zhou, Z, et al (2020). Contamination-Free Visual Detection of SARS-CoV-2 With CRISPR/Cas12a: A Promising Method in the Point-of-Care Detection. *Biosens. Bioelectron.* 169, 112642 doi: 10.1016/j.bios.2020.112642

Chowdhury, F. R., Nur, Z., Hassan, N., von Seidlein, L., and Dunachie, S. (2017). Pandemics, Pathogenicity and Changing Molecular Epidemiology of Cholera in the Era of Global Warming. *Ann. Clin. Microbiol. Antimicrob.* 16, 10. doi: 10.1186/s12941-017-0185-1

Deen, J., Mengel, M. A., and Clemens, J. D. (2020). Epidemiology of Cholera. *Vaccine* 38, A31–A40. doi: 10.1016/j.vaccine.2019.07.078

Gootenberg, J. S., Abudayyeh, O. O., Kellner, M. J., Joung, J., Collins, J. J., and Zhang, F. (2018). Multiplexed and Portable Nucleic Acid Detection Platform With Cas13, Cas12a, and Csm6. *Science* 360, 439–444. doi: 10.1126/science.aaq0179

Harris, J. B., LaRocque, R. C., Qadri, F., Ryan, E. T., and Calderwood, S. B. (2012). Cholera. *Lancet* 379, 2466–2476. doi: 10.1016/S0140-6736(12)60436-X

Khizar, S., Ben Halima, H., Ahmad, N. M., Zine, N., Errachid, A., and Elaissari, A. (2020). Magnetic Nanoparticles in Microfluidic and Sensing: From Transport to Detection. *Electrophoresis* 41, 1206–1224. doi: 10.1002/elps.201900377

Li, S.-Y., Cheng, Q.-X., Wang, J.-M., Li, X.-Y., Zhang, Z.-L., Gao, S., et al. (2018). CRISPR-Cas12a-Assisted Nucleic Acid Detection. *Cell Discov.* 4, 20. doi: 10.1038/s41421-018-0028-z

Li, T.-M., and Du, B. (2011). CRISPR-Cas System and Coevolution of Bacteria and Phages: CRISPR-Cas System and Coevolution of Bacteria and Phages. *Hereditas (Beijing)* 33, 213–218. doi: 10.3724/SP.J.1005.2011.00213

Nelson, E. J., Harris, J. B., Glenn Morris, J., Calderwood, S. B., and Camilli, A. (2009). Cholera Transmission: The Host, Pathogen and Bacteriophage Dynamic. *Nat. Rev. Microbiol.* 7, 693–702. doi: 10.1038/nrmicro2204

Rafique, R., Rashid, M., Monira, S., Rahman, Z., Mahmud, T., Mustafiz, M., et al. (2016). Transmission of Infectious Vibrio Cholerae Through Drinking Water Among the Household Contacts of Cholera Patients (CHoBI7 Trial). *Front. Microbiol.* 7. doi: 10.3389/fmicb.2016.01635

Ramachandran, A., Huyke, D. A., Sharma, E., Sahoo, M. K., Huang, C., Banaei, N., et al. (2020). Electric Field-Driven Microfluidics for Rapid CRISPR-Based Diagnostics and its Application to Detection of SARS-CoV-2. *Proc. Natl. Acad. Sci. U. S. A.* 117, 29518–29525. doi: 10.1073/pnas.2010254117

Ramamurthy, T., Das, B., Chakraborty, S., Mukhopadhyay, A. K., and Sack, D. A. (2020). Diagnostic Techniques for Rapid Detection of Vibrio Cholerae O1/O139. *Vaccine* 38, A73–A82. doi: 10.1016/j.vaccine.2019.07.099

Sack, D. A., Sack, R. B., Nair, G. B., and Siddique, A. (2004). Cholera. *Lancet* 363, 223–233. doi: 10.1016/S0140-6736(03)15328-7

Shen, X., Qiu, F., Shen, L.-P., Yan, T., Zhao, M., Qi, J.-J., et al. (2019). A Rapid and Sensitive Recombinase Aided Amplification Assay to Detect Hepatitis B Virus Without DNA Extraction. *BMC Infect. Dis.* 19, 229. doi: 10.1186/s12879-019-3814-9

Terns, M. P., and Terns, R. M. (2011). CRISPR-Based Adaptive Immune Systems. *Curr. Opin. Microbiol.* 14, 321–327. doi: 10.1016/j.mib.2011.03.005

Wang, J., Cai, K., He, X., Shen, X., Wang, J., Liu, J., et al. (2020). Multiple-Centre Clinical Evaluation of an Ultrafast Single-Tube Assay for SARS-CoV-2 RNA. *Clin. Microbiol. Infect.* 26, 1076–1081. doi: 10.1016/j.cmi.2020.05.007

Wiedenheft, B., Sternberg, S. H., and Doudna, J. A. (2012). RNA-Guided Genetic Silencing Systems in Bacteria and Archaea. *Nature* 482, 331–338. doi: 10.1038/nature10886

Wu, H., He, J., Zhang, F., Ping, J., and Wu, J. (2020). Contamination-Free Visual Detection of CaMV35S Promoter Amplicon Using CRISPR/Cas12a Coupled With a Designed Reaction Vessel: Rapid, Specific and Sensitive. *Anal. Chim Acta* 1096, 130–137. doi: 10.1016/j.aca.2019.10.042

Xiao, X., Lin, Z., Huang, X., Lu, J., Zhou, Y., Zheng, L., et al. (2021). Rapid and Sensitive Detection of Vibrio Vulnificus Using CRISPR/Cas12a Combined With a Recombinase-Aided Amplification Assay. *Front. Microbiol.* 12. doi: 10.3389/fmicb.2021.767315

Zetsche, B., Gootenberg, J. S., Abudayyeh, O. O., Slaymaker, I. M., Makarova, K. S., Essletzbichler, P., et al. (2015). Cpf1 Is a Single RNA-Guided Endonuclease of a Class 2 CRISPR-Cas System. *Cell* 163, 759–771. doi: 10.1016/j.cell.2015.09.038

Conflict of Interest: The authors declare that the research was conducted in the absence of any commercial or financial relationships that could be construed as a potential conflict of interest.

frontiers | Frontiers in Bioengineering and Biotechnology

ORIGINAL RESEARCH
published: 12 April 2022
doi: 10.3389/fbioe.2022.831332

Highly Sensitive Detection Method for HV69-70del in SARS-CoV-2 Alpha and Omicron Variants Based on CRISPR/Cas13a

Mengwei Niu[1,2†], Yao Han[1†], Xue Dong[1†], Lan Yang[1], Fan Li[1], Youcui Zhang[1], Qiang Hu[1], Xueshan Xia[2], Hao Li[1]* and Yansong Sun[1]**

[1]State Key Laboratory of Pathogen and Biosecurity, Beijing Institute of Microbiology and Epidemiology, Beijing, China, [2]Faculty of Life Science and Technology, Kunming University of Science and Technology, Kunming, China

OPEN ACCESS

Edited by:
Jianmin Zhang,
South China Agricultural University, China

Reviewed by:
Yong Shin,
Yonsei University, South Korea
Sumit Ghosh,
The Research Institute at Nationwide Children's Hospital, United States

***Correspondence:**
Yansong Sun
sunys1964@outlook.com
Hao Li
lihao88663239@126.com
Xueshan Xia
oliverxia2000@yahoo.con.cn

†These authors have contributed equally to this work

Specialty section:
This article was submitted to Biosafety and Biosecurity, a section of the journal Frontiers in Bioengineering and Biotechnology

Received: 08 December 2021
Accepted: 21 March 2022
Published: 12 April 2022

Citation:
Niu M, Han Y, Dong X, Yang L, Li F, Zhang Y, Hu Q, Xia X, Li H and Sun Y (2022) Highly Sensitive Detection Method for HV69-70del in SARS-CoV-2 Alpha and Omicron Variants Based on CRISPR/Cas13a. Front. Bioeng. Biotechnol. 10:831332. doi: 10.3389/fbioe.2022.831332

As SARS-CoV-2 variants continue to evolve, identifying variants with adaptive diagnostic tool is critical to containing the ongoing COVID-19 pandemic. Herein, we establish a highly sensitive and portable on-site detection method for the HV69-70del which exist in SARS-CoV-2 Alpha and Omicron variants using a PCR-based CRISPR/Cas13a detection system (PCR-CRISPR). The specific crRNA (CRISPR RNA) targeting the HV69-70del is screened using the fluorescence-based CRISPR assay, and the sensitivity and specificity of this method are evaluated using diluted nucleic acids of SARS-CoV-2 variants and other pathogens. The results show that the PCR-CRISPR detection method can detect 1 copies/μL SARS-CoV-2 HV69-70del mutant RNA and identify 0.1% of mutant RNA in mixed samples, which is more sensitive than the RT-qPCR based commercial SARS-CoV-2 variants detection kits and sanger sequencing. And it has no cross reactivity with ten other pathogens nucleic acids. Additionally, by combined with our previously developed ERASE (Easy-Readout and Sensitive Enhanced) lateral flow strip suitable for CRISPR detection, we provide a novel diagnosis tool to identify SARS-CoV-2 variants in primary and resource-limited medical institutions without professional and expensive fluorescent detector.

Keywords: variants, SARS-CoV-2, CRISPR/Cas13a, nucleic acid detection, lateral flow strip

INTRODUCTION

Some of SARS-CoV-2 variants have demonstrated possible immune escape and increased transmissibility, such as the Alpha variant (B.1.1.7) and Omicron variant (B.1.1.529), which have caused worldwide concern (Kirby, 2021). The Alpha variant, firstly identified in southern England, has enhanced binding affinity with human ACE2 receptor and increased viral infectivity (Meng et al., 2021; Ramírez et al., 2021; Yaniv et al., 2021). The Omicron variant, firstly identified in South Africa, has enhanced viral replication and infection ability, making it quickly became the current dominant pandemic strain globally (Karim and Karim, 2021; Dächert et al., 2022). Both of Alpha and Omicron variants contain HV69-70del mutant, which has been shown to have potential biological implications and associated with human immune response evasion (Andrés et al., 2020; Ho et al., 2021). Hence, as global SARS-CoV-2 outbreaks continue, early identification of SARS-CoV-2 variants is critical. To date, two mainly methods have been used to detect SARS-CoV-2 variants. The most commonly used is gene sequencing technology, including Sanger sequencing and next-generation sequencing, and the other detection method commonly employed is based on reverse

transcription quantitative PCR (RT-qPCR). While, both of them are time-consuming, depending on professional equipment and gene database, which is not suitable for those resource-limited regions (Khan et al., 2020; Perchetti et al., 2021). Therefore, an urgent need exists for the development of a sensitive, specific and on-site detection method to accurately identify SARS-CoV-2 variants on time.

The nucleic acid detection technology based on clustered regularly interspaced short palindromic repeats (CRISPR)/CRISPR-associated (Cas) system provided the opportunity for researchers to achieve accurate and on-site test (Harrington et al., 2018). Up to now, there are various CRISPR/Cas-systems had been developed for COVID-19 diagnosis such as Cas9, Cas12a/b and Cas13a. Shortly after the COVID-19 pandemic started, Doudna's group developed a LbuCas13a-based method for the quantitative detection of SARS-CoV-2 RNA without a pre-amplification (Ackerman et al., 2020; Fozouni et al., 2021). Lately, Rauch and colleagues also developed an on-site SARS-CoV-2 diagnosis tool based on CRISPR/Cas13a system and minimal LED infrastructure (Rauch et al., 2021). Additionally, researchers also showed the practicability of CRISPR detection system for identifying SARS-CoV-2 variants (Broughton et al., 2020; Wang R. et al., 2021), including D614G and N501Y variants (Huang et al., 2021; Kumar et al., 2021; Zhang et al., 2021a). For instance, Wang and colleagues developed a light-up RNA aptamer signaling-CRISPR-Cas13 amplification method for SARS-CoV-2 variants D614G identification (Wang Y. et al., 2021). While, the limits of detection (LOD) and specificity of exist detection strategies are still need to improve for SARS-CoV-2 variants identification (Patchsung et al., 2020). In this study, by combining our previously developed PCR-CRISPR genotypic detection (Wang S. et al., 2021) and the easy-readout and sensitive enhanced (ERASE) lateral flow strip (Li H. et al., 2021), we demonstrated a highly sensitive, and specific detection method for the SARS-CoV-2 HV69-70del. And this method facilitated us to identify SARS-CoV-2 variants in primary and resource limited medical institutions without professional and expensive fluorescent detector.

METHODS

Materials

The SARS-CoV-2 sequence (NC_045512.2) was obtained from the NCBI database. The spike gene of the SARS-CoV-2 RNA reference material was obtained from the China National Institute Metrology (NIM-RM5208). The primers and probes were purchased from Sangon Biotech Co., Ltd. (Shanghai, China). Plasmids containing 144del, 243del, 3675del, L452R, N501Y, P681H, D614G, and other SARS-CoV-2 mutation sites were synthesized by Tianyi Huiyuan Biotech Co., Ltd. In addition, the ten pathogens nucleic acids for be preserved by Academy of Military Medical Sciences.

Reagents and Instruments

NTP mix (art. No. N0466S), and T7 transcription kit (art. No. E2050S) and T7 RNA polymerase (art. No. E2050S), and RNase inhibitors (art. No. E2050S) were purchased from the New England Biological Laboratory (NEB) of the United States, Cas13a (art. No. db005) protein was purchased from Nanjing Genscript Biotechnology Co., Ltd. The RNaseAlert™ QC System v2; art. No. 4479769 was purchased from Thermo Fisher company of the United States. In addition, a One-step TB Green PrimeScript RT-PCR Kit (art. No. RR066A) was purchased from Takara, Japan, and 2× Super Pfx MasterMix (art. No. CW2965M) was purchased from Jiangsu Cowin Biotechnology Co., Ltd. SARS-CoV-2 (strain B.1.1.7) S gene N501Y and HV69-70del mutation detection kits (art. No. JC10226N) were purchased from Jiangsu BioPerfectus Technologies Co., Ltd. The PCR Instrument Applied Biosystems, Thermo Scientific, USA; fluorescence quantitative PCR instrument of Mastercycler-realplex4 was produced by Eppendorf (Germany).

Design and Preparation of Primers and crRNAs

RT-PCR primers (**Supplementary Table S1**) targeting SARS-CoV-2 HV69-70del and N501Y mutations were designed using the Primer-BLAST tool from the NCBI website. To design the specific crRNAs of the SARS-CoV-2 variant, the genome sequence was downloaded and compared from GISAID; crRNAs were designed to nucleic acid fragments of 28 bp. The crRNA transcripts were prepared by annealing with T7-crRNA-F and crRNA-R. crRNAs were prepared by first synthesizing DNA with a T7 promoter sequence. The crRNA DNA was then annealed to a short T7 sequence with the HiScribe T7 Fast High Yield RNA Synthesis Kit (NEB) and incubated overnight with T7 polymerases at 37°C. Finally, the RNA clean XP volume (Beckman Coulter) was used for crRNA purification at a ratio of 1:1.8. All crRNA sequences used in this study are available in **Supplementary Table S2**.

RT-PCR Condition of Synthesized RNA Template

RT-PCR was performed using a One-step TB Green PrimeScript RT-PCR Kit, using a standard manufacturer protocol (RR066A, TAKARA, Japan). The reaction system contained 12.5 μL of 2× One-Step TB Green RT-PCR Buffer, 0.5 μL of PrimeScript RT enzyme mix, 2 μL of diluted RNA template, 2.5 U Takara Ex Taq HS, 0.2 μM F and R primer, and DNase/RNase-free water up to 25 μL. The thermal cycling procedure was 42°C for 5 min and 85°C for 10 min, followed by 40 cycles at 95°C for 5 s, 55°C for 30 s, and 72°C for 30 s. After amplification, 5 μL of the RT-PCR product was analyzed using the PCR-CRISPR fluorescence method for 60 min.

RT-qPCR Quantitative Detection and Mutation Detection of RNA Template

Different SARS-CoV-2 mutation sites were executed using SARS-CoV-2 (strain B.1.1.7) S gene N501Y and HV69-70del mutation detection kits, according to the manufacturer's protocol (JC10226N, bioPerfectus, Jiangsu). The thermal cycling procedure was 50°C for 10 min and 97°C for 1 min, followed by 45 cycles at 97°C for 5 s, and 58°C for 30 s. All RT-qPCR

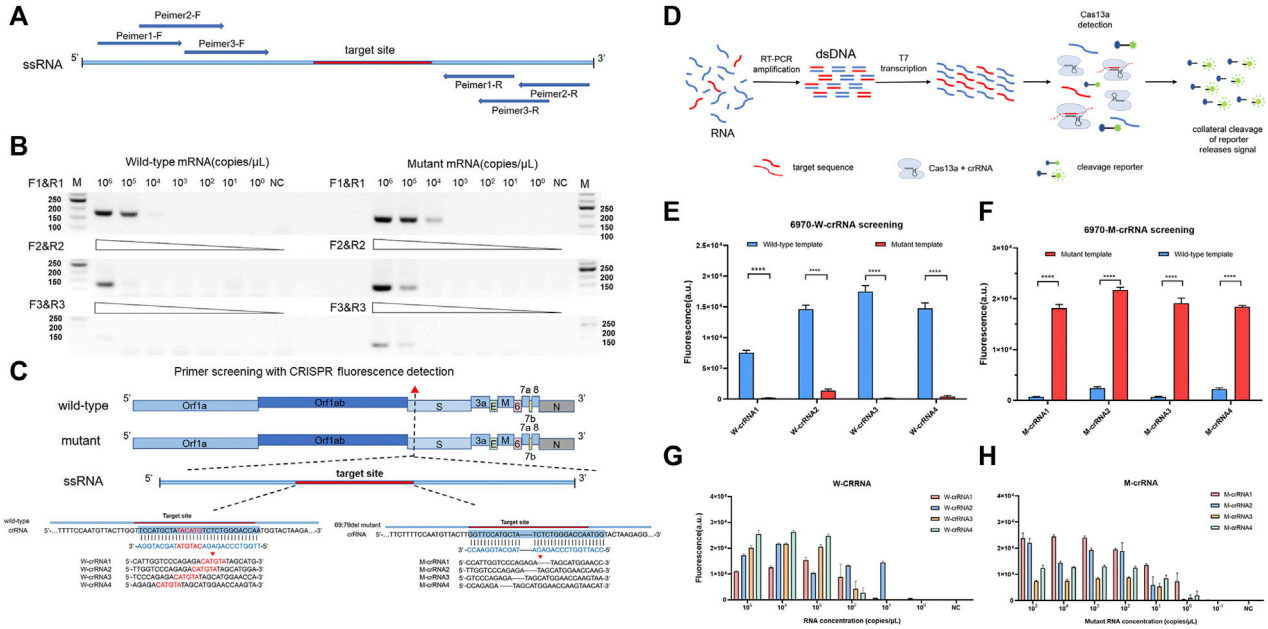

FIGURE 1 | Identifying the sensitivity and specificity of different crRNA and primer sets with RT-PCR followed by Cas13a detection. **(A)** Schematic of the primer design. **(B)** Agarose gel electrophoresis confirms the amplification efficiency of RT-PCR 69-70 primers. **(C)** Schematic of SARS-CoV-2 mutant target regions and the crRNA sequences used for detection. The target site is blue, and the mutant site is red. **(D)** Schematic of RT-PCR + CRISPR detection. **(E)** Highly specificity detection of wild-type and mutant template for the differentiation of SARS-CoV-2 wild-type crRNA targets using Cas13a. **(F)** Highly specificity detection of wild-type and mutant template for the differentiation of SARS-CoV-2 mutant crRNA targets using Cas13a. **(G)** Sensitivity detection of four different wild-type crRNAs carried out using PCR-CRISPR and wild-type templates. **(H)** Sensitivity detection of four different mutant crRNAs carried out using PCR-CRISPR and mutant templates. (n = 3 technical replicates, two-tailed Student t-test; **, $p < 0.01$; ****, $p < 0.0001$; ns, no significant difference; bars represent mean ± s.e.m.).

experiments included quality controls, comprising DNase/RNase-free water instead of RNA template (non-template control, NC), in each run.

Cas13a-Mediated crRNA/Cas13a Collateral Cleavage

Cas13a-mediated RNA cleavage contain 1.6 IU/μL RNase inhibitor (NEB), 20 mM N-2-hydroxyethylpiperazine-N-2-ethane sulfonic acid (HEPES), 25 nM Cas13a, 2 μM crRNA, 2.5 mM ribonucleoside triphosphates (rNTP) (NEB), 2 nM reporter RNA, 1 IU/μL T7 RNA polymerase (NEB), 10 mM $MgCl_2$, and 5 μL of the RT-PCR amplified product. The reaction is carried out at 37°C for 60 min using a fluorescence quantitative PCR system. Alternatively, the reaction system is incubated for 30 min at 37°C, and the reaction mixture is added to the ERASE strip subsequently.

ERASE Lateral Flow Strip Detection

This experiment used test notes called ERASE lateral flow strips (Li H. et al., 2021) that were previously developed by our research team. The ERASE strip was visualized and analyzed according to the "band-cutting method;" if, on the lateral flow strip, the C-band was visible, while the T-band was absent, a positive result was recorded, whereas if both the T-band and C-band were visible, the result was recorded as negative. If the C-band was not visible on the ERASE strip, the test was deemed to have failed and the lateral flow strip was replaced prior to retesting.

Statistical Analysis

Statistical significance was determined by unpaired two-tailed Student's t-tests using GraphPad Prism 8.0.2 software. Data are represented as mean ± SEM (ns, no significant difference, $^{*}p < 0.05$, $^{**}p < 0.01$, $^{***}p < 0.001$, $^{****}p < 0.0001$).

RESULTS

Identification of Efficient Primers and crRNA for SARS-CoV-2 HV69-70del Detection

The RT-PCR amplified efficiency is determined by the reverse and forward primer regions, so we designed the corresponding amplification primers in different regions (**Figure 1A** and **Supplementary Table S1**) and screened them by agarose gel electrophoresis. The results showed that primer 1 had an obvious amplification band compared to primers 2 and 3, which had an obvious band in the template of 10^4 copies/μL, while primers 2 and 3 had obvious bands when amplifying the template of 10^5 copies/μL (**Figure 1B**). To establish a highly sensitive and specific detection method, we selected four candidate crRNAs targeting the wild-type (W-6970-1, 2, 3, 4) and four candidate crRNAs targeting the mutant-type (M-6970-1, 2, 3, 4) (**Figure 1C** and **Supplementary Table S2**) in the HV69-70del region of SARS-CoV-2 genome. Then we used fluorescence-based PCR-CRISPR

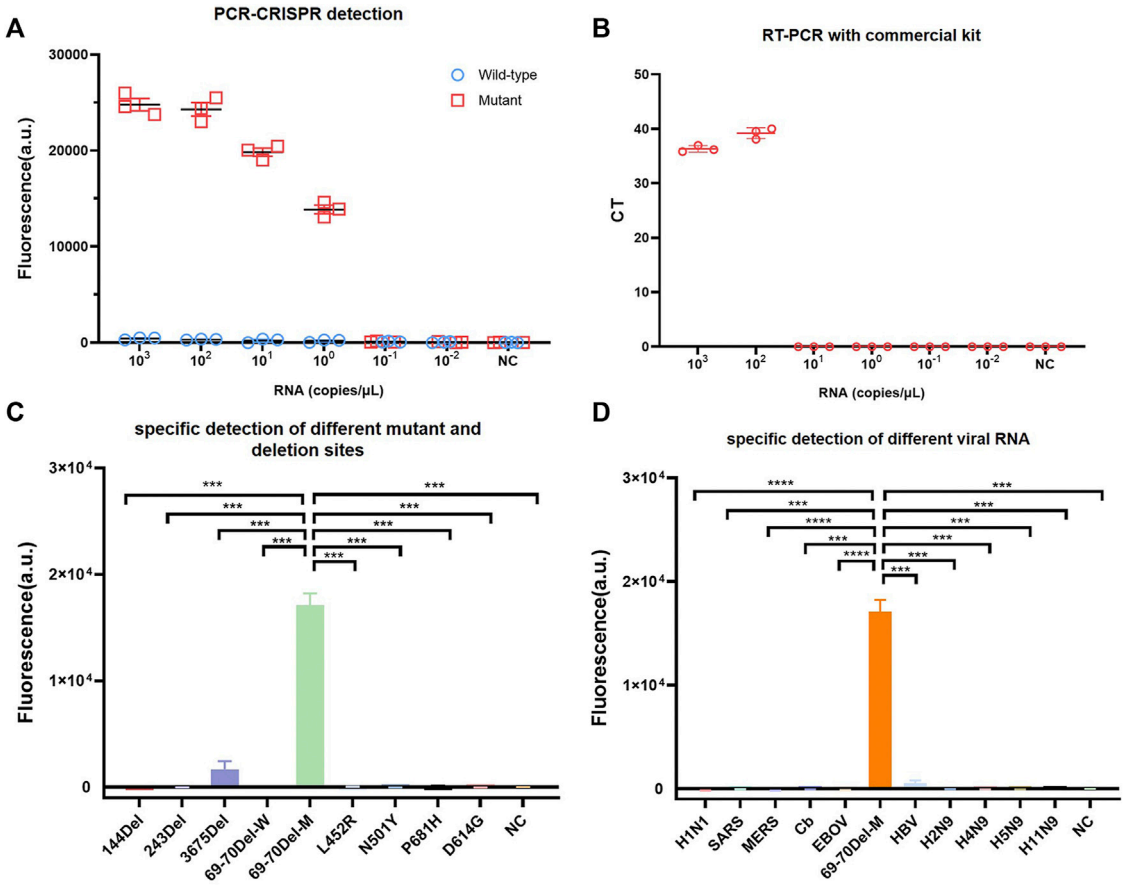

FIGURE 2 | Identifying the sensitivity and specificity of PCR-CRISPR detection and comparing sensitivity with other nucleic acid detection tools. **(A)** Sensitivity detection of wild and mutant templates carried out using PCR-CRISPR and M-crRNA-1. **(B)** Detection analysis of mutant RNA dilution series with RT-qPCR with a commercial kit. **(C)** PCR-CRISPR can discriminate different viral mutant or deletion sites. **(D)** PCR-CRISPR achieves specific detection of different viral RNA. (n = 3 technical replicates, two-tailed Student t-test; ***, $p < 0.001$; ****, $p < 0.0001$; bars represent mean ± s.e.m.).

detection method to screening these crRNA (**Figure 1D**). The results show that all crRNAs in different locations could distinguish between wild-type RNA templates and HV69-70del templates (**Figures 1E,F**). To determine the sensitivity of different crRNAs, synthetic RNA templates were prepared using a serial dilution that ranged from 1×10^5 to 1×10^{-1} copies/μL in each reaction. The results show that W-crRNA-2 detection sensitivity is higher for detecting wild RNA templates and the detection limit is 10^1 copies/μL. M-crRNA-1 detection sensitivity is higher for detecting HV69-70del RNA templates and the detection limit is 10^0 copies/μL (**Figures 1G,H**). Therefore, W-crRNA-2 and M-crRNA-1 were selected for further studies.

Sensitivity and Specificity Evaluation of PCR-CRISPR in SARS-CoV-2 HV69-70del Detection

To compare PCR-CRISPR detection with the existing TaqMan probe RT-qPCR, we purchased SARS-CoV-2 (strain B.1.1.7) S gene N501Y and HV69-70del mutation detection kits (BioPerfectus). The results showed that PCR-CRISPR was more sensitive than SARS-CoV-2 (strain B.1.1.7) S gene N501Y and HV69-70del mutation detection kits and can detect 1×10^0 copies/μL template RNA. In contrast, SARS-CoV-2 (strain B.1.1.7) S gene N501Y and HV69-70del mutation detection kits detected only 1×10^2 copies/μL template RNA (**Figures 2A,B**). In addition, fluorescence signals were observed to increase over time and become stabilized after 30 min (**Supplementary Figure S1**). Therefore, in all subsequent studies involving combined Cas13a and lateral flow strip, 30 min was set as the Cas13a detection time.

To evaluate the specificity of PCR-CRISPR detection of SARS-CoV-2 HV69-70del, we synthesized a plasmid that contained 144del, 243del, 3675del, L452R, N501Y, P681H, and D614G. We evaluated the specificity of SARS-CoV-2 HV69-70del in different pathogens for nucleic acid detection, and extracted H1N1, SARS, MERS, Cb, EBOV, HBV, H2N9, H4N9, H5N9, and H11N9 nucleic acids for PCR-CRISPR fluorescence detection. The results show that the PCR-CRISPR fluorescence detection method has high specificity for detecting different SARS-CoV-2 mutation sites (**Figure 2C**) and nucleic acids of different pathogens (**Figure 2D**).

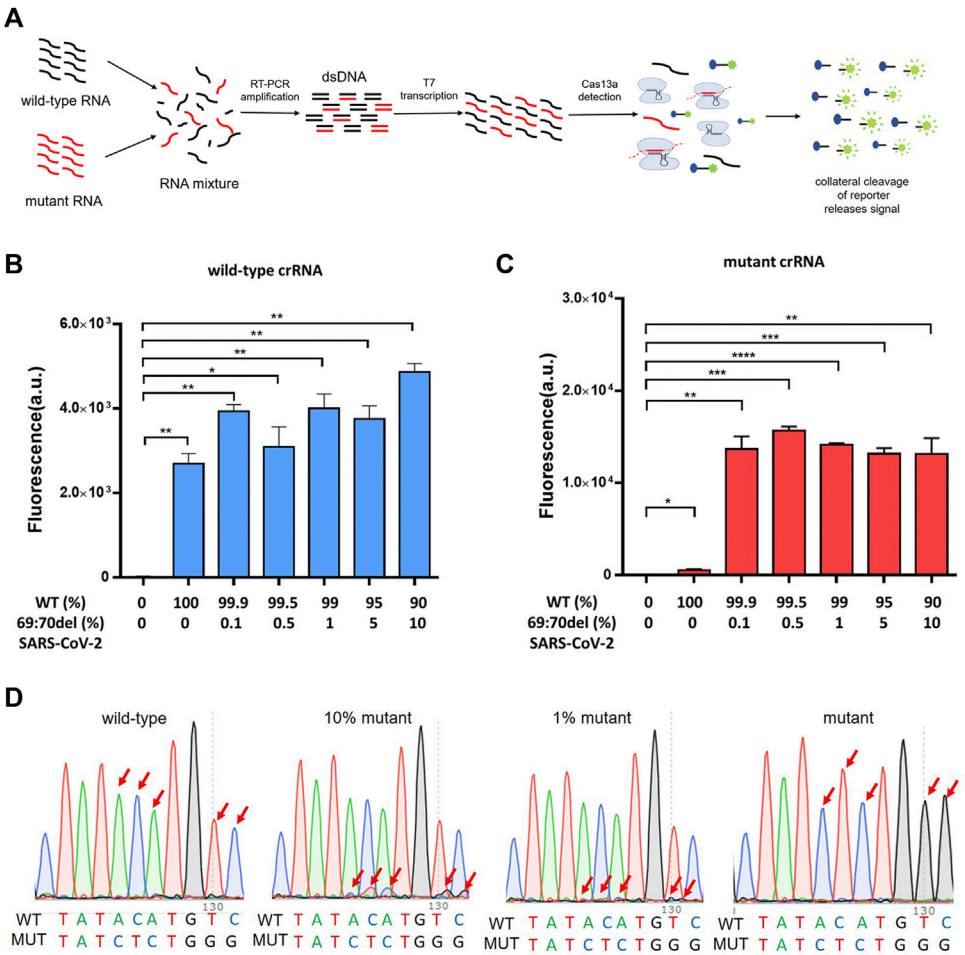

FIGURE 3 | The PCR-CRISPR method detects mixed mutant genes of low proportion. **(A)** Schematic of PCR-CRISPR detection of mutant RNA on a background of wild-type RNA. **(B)** PCR-CRISPR detects mixed wild-type RNA of different proportions on a background of RNA mixture. **(C)** PCR-CRISPR detects mixed mutant RNA of different proportions on a background of RNA mixture. **(D)** Sequencing peak of Sanger sequencing for RNA mixtures of different proportions. (n = 3 technical replicates, two-tailed Student t-test; **, $p < 0.01$; ***, $p < 0.001$; ****, $p < 0.0001$; ns, no significant difference; bars represent mean ± s.e.m.).

The PCR-CRISPR Method Detects the Low-Proportion Mutant Genes in Mixed Samples

To verify that the PCR-CRISPR method was capable of efficiently detecting low-proportion mutant genes in mixed samples, we tested different proportions of mixed samples (10%, 5%, 1%, 0.5%, and 0.1%) and compared the results with those of Sanger sequencing (**Figure 3A**). The results showed that PCR-CRISPR testing could detect mixed samples as low as 0.1% (**Figures 3B,C**), while the gene sequencing technology results showed that it could only distinguish between ≥10% of mixed mutant genes (**Figure 3D**). Thus, it indicates that PCR-CRISPR method could detect a low proportion of target nucleic acids in complex nucleic acid samples.

Combination of PCR-CRISPR With ERASE Strip to Detect SARS-CoV-2 Variants

To achieve on-site testing of the SARS-CoV-2 variants, we combined PCR-CRISPR detection with lateral flow strip—ERASE. After the CRISPR reaction completed, the reaction products are fully added onto ERASE strip and the test results could be judged by naked eyes. To determine the sensitivity of this assay, RNA templates were prepared using a 10-fold gradient dilution and then detected using strip-based PCR-CRISPR (**Figure 4A**). As shown in **Figures 4B,C**, the sensitivity detection results are consistent with the fluorescence detection results and can reach 1–10 copies/μL. To evaluate the specificity of ERASE strip detection, we used nucleic acids from ten pathogens and different mutant site nucleic acids for the strip-based PCR-CRISPR test. It shows that as the same with the fluorescence-based PCR-CRISPR assay, the strip-based PCR-CRISPR assay could specifically distinguish the SARS-CoV-2 containing HV69-70del mutation with other pathogens (**Figures 4D,E**). Simultaneously, to show its practicability for identifying SARS-CoV-2 variants, we had also detected other common variants, such as N501Y, D614G, and P681H using this strip-based PCR-CRISPR assay (**Supplementary Figure S3**).

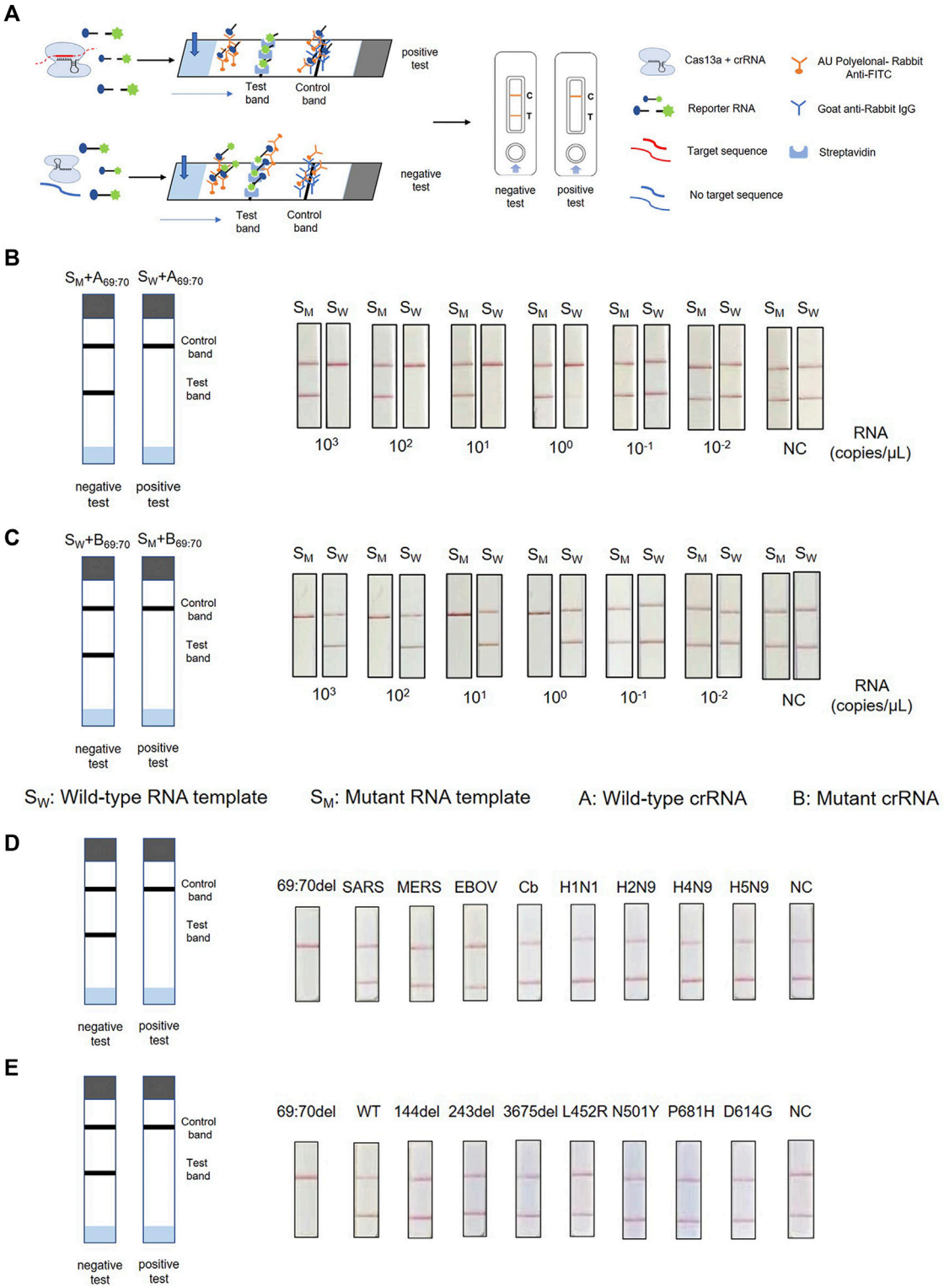

FIGURE 4 | Combination of PCR-CRISPR detection with ERASE strip for lateral flow readout. **(A)** Schematic of PCR-CRISPR detection with lateral flow strip. **(B,C)** Sensitivity of PCR-CRISPR detection with lateral flow strip. **(B)** Detection of wild-type target RNA by PCR-CRISPR and wild-type crRNA followed by application to the lateral flow strip. **(C)** Detection of mutant target RNA by PCR-CRISPR and mutant crRNA followed by application to the lateral flow strip. **(D,E)** Specificity of PCR-CRISPR detection with the lateral flow strip. **(D)** PCR-CRISPR with lateral flow strip can discriminate other viral RNA. **(E)** PCR-CRISPR with lateral flow strip achieves specific detection of other viral mutant or deletion sites.

DISCUSSION

Continued efforts are being made toward global COVID-19 pandemic prevention and control, however, SARS-CoV-2 variants continue to emerge with mutations at different sites (Yaniv et al., 2021). As defined by the World Health Organization, five variants of concern (VOC) and six variants of interest (VOI) have emerged since the beginning of the SARS-CoV-2 pandemic (Duchene et al., 2020). The increased transmissibility of certain SARS-CoV-2 variants poses serious challenges to the prevention and control of the pandemic. Amino acid mutation sites, such as N501Y, E484K, and HV69-70del cross-appear or appear simultaneously in multiple VOC and VOI variants, indicating that SARS-CoV-2 has undergone adaptive changes and evolution during the COVID-19 pandemic in the process of continuous adaptation to the host (Li Q. et al., 2021; Kemp et al., 2021; Lubinski et al., 2022). In this study, we chose HV69-70del mutation site as the detect target to identify the Alpha and Omicron variants. Besides, based on PCR-CRISPR method, we continually developed the detection method for N501Y, D614G, and P681H mutant sites of SARS-CoV-2. It indicates its practicability of PCR-CRISPR method in identifying various SARS-CoV-2 variants.

Currently, main national health authorities are employing gene sequencing of patients' samples to identify SARS-CoV-2 variants, however, this method is expensive and time-consuming (McNamara et al., 2020; Meredith et al., 2020; Bhoyar et al., 2021). Furthermore, when outbreaks occur locally and spread quickly, gene sequencing will not meet the needs of large-scale rapid screening. Presently, several countries and regions have carried out mixed testing of unknown SARS-CoV-2 samples to achieve the goal of rapid screening of positive cases (Bogere et al., 2021; Heaney et al., 2021; Hofman et al., 2021), which requires a higher sensitivity of testing methods. Our experiments showed that the PCR-CRISPR method could detect 0.1% of target nucleic acids in mixed samples (Wen et al., 2021), providing new insights for large-scale rapid screening of variants (**Figure 3C**). Certainly, this method cannot replace gene sequencing, but it has the ability to quickly detect clusters and help guide gene sequencing, making it an invaluable tool in the SARS-CoV-2 testing toolbelt. Furthermore, the method described in this study can be extended to the rapid detection of other pathogen variants (Kumar et al., 2021).

By combining the inherent high sensitivity and specificity of the PCR-CRISPR system with the simplicity of the ERASE lateral flow strip, we could read the results by naked eyes without fluorescence equipment. Compared with previously reported CRISPR-based SARS-CoV-2 variant detection methods (Zhang W. S. et al., 2021), ours provides a practical on-site test method to detect SARS-CoV-2 HV69-70del with obvious advantages. For example, strip-based PCR-CRISPR assay could eliminate the need for expensive fluorescence detectors, and improve the ability to diagnose SARS-CoV-2 variant on-site, particularly in under-developed and resource-limited regions (Myers et al., 2013; Li H. et al., 2021). Besides, by combined with smartphone-assisted visualization tools (Wen et al., 2021) or more accurate isothermal amplification, CRISPR detection system is expected to become a robust, rapid, quantitative and field-deployable POCT method for SARS-CoV-2 variants.

CONCLUSION

As SARS-CoV-2 variants continue to evolve, identifying variants and rapidly adapting diagnostics to track variants will be critical to containing the ongoing COVID-19 pandemic (de Puig et al., 2021). In this study, we report a PCR-CRISPR method for SARS-CoV-2 HV69-70del mutant site detection with high specificality and sensitivity. By combined with the ERASE strip, it could enable rapid detection in resource-limited regions without fluorescence equipment, which provide a powerful tool for SARS-CoV-2 variants early identification.

DATA AVAILABILITY STATEMENT

The original contributions presented in the study are included in the article/**Supplementary Material**, further inquiries can be directed to the corresponding authors.

AUTHOR CONTRIBUTIONS

HL, YS, MN and XX conceived the experiments; MN, XD, LY and FL performed the experiments; MN, QH, and YH conducted statistical analysis; MN, YH, HL and XD prepared the tables and figures; XD, MN and YZ extracted viral nucleic acid; MN and HL prepared the manuscript. All authors have reviewed approved the final manuscript.

FUNDING

This work was supported by the National Key Research and Development Program of China (2021YFC2301102, 2020YFC0841200); National Natural Science Foundation of China (grant number 31901051); and National Science and Technology Major Project of China (grant number 2018ZX10301407).

SUPPLEMENTARY MATERIAL

The Supplementary Material for this article can be found online at: https://www.frontiersin.org/articles/10.3389/fbioe.2022.831332/full#supplementary-material

REFERENCES

Ackerman, C. M., Myhrvold, C., Thakku, S. G., Freije, C. A., Metsky, H. C., Yang, D. K., et al. (2020). Massively Multiplexed Nucleic Acid Detection with Cas13. *Nature* 582 (7811), 277–282. doi:10.1038/s41586-020-2279-8

Andrés, C., Garcia-Cehic, D., Gregori, J., Piñana, M., Rodriguez-Frias, F., Guerrero-Murillo, M., et al. (2020). Naturally Occurring SARS-CoV-2 Gene Deletions Close to the Spike S1/S2 Cleavage Site in the Viral Quasispecies of COVID19 Patients. *Emerging Microbes & Infections* 9 (1), 1900–1911. doi:10.1080/22221751.2020.1806735

Bhoyar, R. C., Jain, A., Sehgal, P., Divakar, M. K., Sharma, D., Imran, M., et al. (2021). High Throughput Detection and Genetic Epidemiology of SARS-CoV-2 Using COVIDSeq Next-Generation Sequencing. *PLoS One* 16 (2), e0247115. doi:10.1371/journal.pone.0247115

Bogere, N., Bongomin, F., Katende, A., Ssebambulidde, K., Ssengooba, W., Ssenfuka, H., et al. (2021). Performance and Cost-Effectiveness of a Pooled Testing Strategy for SARS-CoV-2 Using Real-Time Polymerase Chain Reaction in Uganda. *Int. J. Infect. Dis.* 113, 355–358. doi:10.1016/j.ijid.2021.10.038

Broughton, J. P., Deng, X., Yu, G., Fasching, C. L., Singh, J., Streithorst, J., et al. (2020). Rapid Detection of 2019 Novel Coronavirus SARS-CoV-2 Using a CRISPR-Based DETECTR Lateral Flow Assay. *medRxiv*. doi:10.1101/2020.03.06.20032334

Dächert, C., Muenchhoff, M., Graf, A., Autenrieth, H., Bender, S., Mairhofer, H., et al. (2022). Rapid and Sensitive Identification of Omicron by Variant-specific PCR and Nanopore Sequencing: Paradigm for Diagnostics of Emerging SARS-CoV-2 Variants. *Med. Microbiol. Immunol.* 211 (1), 71–77. doi:10.1007/s00430-022-00728-7

de Puig, H., Lee, R. A., Najjar, D., Tan, X., Soenksen, L. R., Angenent-Mari, N. M., et al. (2021). Minimally Instrumented SHERLOCK (miSHERLOCK) for CRISPR-Based point-of-care Diagnosis of SARS-CoV-2 and Emerging Variants. *Sci. Adv.* 7 (32), eabh2944. doi:10.1126/sciadv.abh2944

Duchene, S., Featherstone, L., Haritopoulou-Sinanidou, M., Rambaut, A., Lemey, P., and Baele, G. (2020). Temporal Signal and the Phylodynamic Threshold of SARS-CoV-2. *Virus. Evol.* 6 (2), veaa061. doi:10.1093/ve/veaa061

Fozouni, P., Son, S., Díaz de León Derby, M., Knott, G. J., Gray, C. N., D'Ambrosio, M. V., et al. (2021). Amplification-free Detection of SARS-CoV-2 with CRISPR-Cas13a and mobile Phone Microscopy. *Cell* 184 (2), 323–333. doi:10.1016/j.cell.2020.12.001

Harrington, L. B., Burstein, D., Chen, J. S., Paez-Espino, D., Ma, E., Witte, I. P., et al. (2018). Programmed DNA Destruction by Miniature CRISPR-Cas14 Enzymes. *Science* 362 (6416), 839–842. doi:10.1126/science.aav4294

Heaney, K., Ritchie, A. V., Henry, R., Harvey, A. J., Curran, M. D., Allain, J.-P., et al. (2022). Evaluation of Sample Pooling Using the SAMBA II SARS-CoV-2 Test. *J. Virol. Methods* 299, 114340. doi:10.1016/j.jviromet.2021.114340

Ho, D., Wang, P., Liu, L., Iketani, S., Luo, Y., Guo, Y., et al. (2021). Increased Resistance of SARS-CoV-2 Variants B.1.351 and B.1.1.7 to Antibody Neutralization. *Res. Sq.* doi:10.21203/rs.3.rs-155394/v1

Hofman, P., Allegra, M., Salah, M., Benzaquen, J., Tanga, V., Bordone, O., et al. (2021). Evaluation of Sample Pooling for SARS-CoV-2 Detection in Nasopharyngeal Swab and Saliva Samples with the Idylla SARS-CoV-2 Test. *Microbiol. Spectr.* 9, e0099621. doi:10.1128/Spectrum.00996-21

Huang, X., Zhang, F., Zhu, K., Lin, W., and Ma, W. (2021). dsmCRISPR: Dual Synthetic Mismatches CRISPR/Cas12a-based Detection of SARS-CoV-2 D614G Mutation. *Virus. Res.* 304, 198530. doi:10.1016/j.virusres.2021.198530

Karim, S. S. A., and Karim, Q. A. (2021). Omicron SARS-CoV-2 Variant: a New Chapter in the COVID-19 Pandemic. *The Lancet* 398 (10317), 2126–2128. doi:10.1016/s0140-6736(21)02758-6

Kemp, S. A., Collier, D. A., Collier, D. A., Datir, R. P., Ferreira, I. A. T. M., Gayed, S., et al. (2021). SARS-CoV-2 Evolution during Treatment of Chronic Infection. *Nature* 592 (7853), 277–282. doi:10.1038/s41586-021-03291-y

Kemp, S., Datir, R., Collier, D., Ferreira, I., Carabelli, A., Harvey, W., et al. (2020). *Recurrent Emergence and Transmission of a SARS-CoV-2 Spike Deletion △H69/V70.*

Khan, M. I., Khan, Z. A., Baig, M. H., Ahmad, I., Farouk, A.-E., Song, Y. G., et al. (2020). Comparative Genome Analysis of Novel Coronavirus (SARS-CoV-2) from Different Geographical Locations and the Effect of Mutations on Major Target Proteins: An In Silico Insight. *PLoS One* 15 (9), e0238344. doi:10.1371/journal.pone.0238344

Kirby, T. (2021). New Variant of SARS-CoV-2 in UK Causes Surge of COVID-19. *Lancet Respir. Med.* 9 (2), e20–e21. doi:10.1016/s2213-2600(21)00005-9

Kumar, M., Gulati, S., Ansari, A. H., Phutela, R., Acharya, S., Azhar, M., et al. (2021). FnCas9-based CRISPR Diagnostic for Rapid and Accurate Detection of Major SARS-CoV-2 Variants on a Paper Strip. *Elife* 10, e67130. doi:10.7554/eLife.67130

Li, H., Dong, X., Wang, Y., Yang, L., Cai, K., Zhang, X., et al. (2021a). Sensitive and Easy-Read CRISPR Strip for COVID-19 Rapid Point-of-Care Testing. *CRISPR J.* 4 (3), 392–399. doi:10.1089/crispr.2020.0138

Li, Q., Nie, J., Wu, J., Zhang, L., Ding, R., Wang, H., et al. (2021b). SARS-CoV-2 501Y.V2 Variants Lack Higher Infectivity but Do Have Immune Escape. *Cell* 184 (9), 2362–2371. doi:10.1016/j.cell.2021.02.042

Lubinski, B., Fernandes, M. H. V., Frazier, L., Tang, T., Daniel, S., Diel, D. G., et al. (2022). Functional Evaluation of the P681H Mutation on the Proteolytic Activation the SARS-CoV-2 Variant B.1.1.7 (Alpha) Spike. *iScience* 25 (1), 103589. doi:10.1016/j.isci.2021.103589

McNamara, R. P., Caro-Vegas, C., Landis, J. T., Moorad, R., Pluta, L. J., Eason, A. B., et al. (2020). High-Density Amplicon Sequencing Identifies Community Spread and Ongoing Evolution of SARS-CoV-2 in the Southern United States. *Cel Rep.* 33 (5), 108352. doi:10.1016/j.celrep.2020.108352

Meng, B., Kemp, S. A., Papa, G., Datir, R., Ferreira, I., Marelli, S., et al. (2021). Recurrent emergence of SARS-CoV-2 spike deletion H69/V70 and its role in th Alpha variant B.1.1.7. *Cell Rep.* 35 (13), 109292. doi:10.1016/j.celrep.2021.109292

Meredith, L. W., Hamilton, W. L., Warne, B., Houldcroft, C. J., Hosmillo, M., Jahun, A. S., et al. (2020). Rapid Implementation of SARS-CoV-2 Sequencing to Investigate Cases of Health-Care Associated COVID-19: a Prospective Genomic Surveillance Study. *Lancet Infect. Dis.* 20 (11), 1263–1271. doi:10.1016/s1473-3099(20)30562-4

Myers, F. B., Henrikson, R. H., Bone, J., and Lee, L. P. (2013). A Handheld point-of-care Genomic Diagnostic System. *PLoS One* 8 (8), e70266. doi:10.1371/journal.pone.0070266

Patchsung, M., Jantarug, K., Pattama, A., Aphicho, K., Suraritdechachai, S., Meesawat, P., et al. (2020). Clinical Validation of a Cas13-Based Assay for the Detection of SARS-CoV-2 RNA. *Nat. Biomed. Eng.* 4 (12), 1140–1149. doi:10.1038/s41551-020-00603-x

Perchetti, G. A., Zhu, H., Mills, M. G., Shrestha, L., Wagner, C., Bakhash, S. M., et al. (2021). Specific Allelic Discrimination of N501Y and Other SARS-CoV-2 Mutations by ddPCR Detects B.1.1.7 Lineage in Washington State. *J. Med. Virol.* 93 (10), 5931–5941. doi:10.1002/jmv.27155

Ramírez, J. D., Muñoz, M., Patiño, L. H., Ballesteros, N., and Paniz-Mondolfi, A. (2021). Will the Emergent SARS-CoV2 B.1.1.7 Lineage Affect Molecular Diagnosis of COVID-19? *J. Med. Virol.* 93 (5), 2566–2568. doi:10.1002/jmv.26823

Rauch, J. N., Valois, E., Solley, S. C., Braig, F., Lach, R. S., Audouard, M., et al. (2021). A Scalable, Easy-To-Deploy Protocol for Cas13-Based Detection of SARS-CoV-2 Genetic Material. *J. Clin. Microbiol.* 59 (4), e02402. doi:10.1128/jcm.02402-20

Wang, R., Qian, C., Pang, Y., Li, M., Yang, Y., Ma, H., et al. (2021a). opvCRISPR: One-Pot Visual RT-LAMP-CRISPR Platform for SARS-Cov-2 Detection. *Biosens. Bioelectron.* 172, 112766. doi:10.1016/j.bios.2020.112766

Wang, S., Li, H., Kou, Z., Ren, F., Jin, Y., Yang, L., et al. (2021b). Highly Sensitive and Specific Detection of Hepatitis B Virus DNA and Drug Resistance Mutations Utilizing the PCR-Based CRISPR-Cas13a System. *Clin. Microbiol. Infect.* 27 (3), 443–450. doi:10.1016/j.cmi.2020.04.018

Wang, Y., Zhang, Y., Chen, J., Wang, M., Zhang, T., Luo, W., et al. (2021c). Detection of SARS-CoV-2 and its Mutated Variants via CRISPR-Cas13-Based Transcription Amplification. *Anal. Chem.* 93 (7), 3393–3402. doi:10.1021/acs.analchem.0c04303

Wen, J., Gou, H., Wang, S., Lin, Q., Chen, K., Wu, Y., et al. (2021). Competitive Activation Cross Amplification Combined with Smartphone-Based Quantification for point-of-care Detection of Single Nucleotide

Polymorphism. *Biosens. Bioelectron.* 183, 113200. doi:10.1016/j.bios.2021.113200

Yaniv, K., Ozer, E., Shagan, M., Lakkakula, S., Plotkin, N., Bhandarkar, N. S., et al. (2021). Direct RT-qPCR Assay for SARS-CoV-2 Variants of Concern (Alpha, B.1.1.7 and Beta, B.1.351) Detection and Quantification in Wastewater. *Environ. Res.* 201, 111653. doi:10.1016/j.envres.2021.111653

Zhang, T., Zhao, W., Zhao, W., Si, Y., Chen, N., Chen, X., et al. (2021a). Universally Stable and Precise CRISPR-LAMP Detection Platform for Precise Multiple Respiratory Tract Virus Diagnosis Including Mutant SARS-CoV-2 Spike N501Y. *Anal. Chem.* 93 (48), 16184–16193. doi:10.1021/acs.analchem.1c04065

Zhang, W. S., Pan, J., Li, F., Zhu, M., Xu, M., Zhu, H., et al. (2021b). Reverse Transcription Recombinase Polymerase Amplification Coupled with CRISPR-Cas12a for Facile and Highly Sensitive Colorimetric SARS-CoV-2 Detection. *Anal. Chem.* 93 (8), 4126–4133. doi:10.1021/acs.analchem.1c00013

Conflict of Interest: The authors declare that the research was conducted in the absence of any commercial or financial relationships that could be construed as a potential conflict of interest.

frontiers | Frontiers in Cellular and Infection Microbiology

ORIGINAL RESEARCH
published: 11 May 2022
doi: 10.3389/fcimb.2022.879887

Rapid and Visual Detection of Porcine Parvovirus Using an ERA-CRISPR/Cas12a System Combined With Lateral Flow Dipstick Assay

Jing Wei[1,2†], *Yanan Li*[1,2†], *Yingli Cao*[1,2], *Qi Liu*[1,2], *Kankan Yang*[1,2], *Xiangjun Song*[1,2], *Ying Shao*[1,2], *Kezong Qi*[1,2] *and Jian Tu*[1,2*]

[1] *Anhui Province Engineering Laboratory for Animal Food Quality and Bio-safety, College of Animal Science and Technology, Anhui Agricultural University, Hefei, China,* [2] *Anhui Province Key Laboratory of Veterinary Pathobiology and Disease Control, Anhui Agricultural University, Hefei, China*

OPEN ACCESS

Edited by:
Hongchao Gou, Guangdong Academy of Agricultural Sciences, China

Reviewed by:
Yani Sun, Northwest A&F University, China
Chengming Wang, Auburn University, United States

***Correspondence:**
Jian Tu
tujian1980@126.com

[†]*These authors have contributed equally to this work*

Specialty section:
This article was submitted to Clinical Microbiology, a section of the journal Frontiers in Cellular and Infection Microbiology

Received: *20 February 2022*
Accepted: *11 April 2022*
Published: *11 May 2022*

Citation:
Wei J, Li Y, Cao Y, Liu Q, Yang K, Song X, Shao Y, Qi K and Tu J (2022) Rapid and Visual Detection of Porcine Parvovirus Using an ERA-CRISPR/Cas12a System Combined With Lateral Flow Dipstick Assay. Front. Cell. Infect. Microbiol. 12:879887. doi: 10.3389/fcimb.2022.879887

Porcine parvovirus (PPV) is one of the important causes of pig reproductive diseases. The most prevalent methods for PPV authentication are the polymerase chain reaction (PCR), enzyme-linked immunosorbent assay, and quantitative real-time PCR. However, these procedures have downsides, such as the fact that they take a long time and require expensive equipment. As a result, a rapid, visible, and economical clinical diagnostic strategy to detect PPV is necessary. In this study, three pairs of crRNA primers were designed to recognize the VP2 gene, and an ERA-CRISPR/Cas12a system for PPV detection was successfully developed. The approach involved isothermal detection at 37°C, and the method can be used for visual inspection. The detection limit of the ERA-CRISPR/Cas12a system was 3.75×10^2 copies/μL, and no cross reactions with other porcine viruses were found. In view of the preceding, a rapid, visible, and low-cost nucleic acid testing approach for PPV has been developed using the ERA-CRISPR/Cas12a system.

Keywords: CRISPR-Cas12a, enzymatic recombinase amplification, porcine parvovirus, lateral flow dipstick, rapid detection

INTRODUCTION

Porcine parvovirus belongs to the *Parvoviridae family*, which consists of two subfamilies *Parvovirinae* and *Densovirinae*. It is a leading cause of reproductive failure in pigs, which is a serious issue in the pig breeding industry. Amto Mayr and colleagues in Munich, Germany, used primary pig cells to propagate the classical swine fever virus in 1965, and discovered and isolated compromised porcine parvovirus (PPV), proving the presence of the virus. Seven parvovirus species, PPV1–7, have been discovered in pigs so far. PPV1 is the dominant causal agent in swine herds, and it was initially found in Germany in 1965 (Streck and Truyen, 2020). The incidence of infections with PPV2–7 is low and the clinical signs are not obvious. PPV1 infection gives rise to embryonic mortality, infertility, stillbirths and other signs; involvement of the other porcine parvovirus serotypes in reproductive failure is still to be determined (Ellis et al., 2000; Kennedy et al., 2000).

PPV1 is a hexagonal, circular or symmetrical icosahedral DNA virus with a diameter between 22 and 23 nm and has no capsule. The genome of PPV1 mainly consists of two open reading frames (ORFs), ORF1 encoding non-structural proteins NS1, NS2 and NS3; and ORF2 encoding structural proteins VP1 and VP2. VP2 accounts for more than 90% of the capsid components of the virus, and the VP2 gene is the most important structural protein and immunogenic protein of PPV. The sequence homology of VP2 genes of different genotypes ranges from 26.5% to 40.0%. It not only stimulates the immune response of the host but also plays an important role in the replication process of the virus (Kamstrup et al., 1998; Streck et al., 2011; Xu et al., 2013). PPV1 can occur in different seasons, and pigs of different varieties, sexes, purposes and ages, as well as wild boar, can be infected. The virus mainly causes signs in pregnant sows, especially primiparous sows, resulting in sick pigs, abortion, stillbirth, fetal deformities, and mummies. Repeated infections are associated with conditions such as infertility, which affects the sow's farrowing rate, and thus affects the economic benefits of pig breeding farms, causing serious economic losses (Meszaros et al., 2017).

At present, the clinical detection of PPV is based mainly on polymerase chain reaction (PCR), enzyme-linked immunosorbent assay (ELISA), real-time PCR, etc. PCR is the main method used to detect parvovirus (Huang et al., 2004; Caprioli et al., 2006; Jiang et al., 2010), but it is insufficiently sensitive and the amplification efficiency may be compromised by many factors (Green and Sambrook, 2018). ELISA is also commonly used to detect parvovirus (Deng et al., 2018), but its sample processing procedures are relatively complex and time-consuming, and easily produce false positive (Terato et al., 2016). Both real-time PCR and loop-mediated isothermal amplification (LAMP) are also used for detection of PPV and, although they are highly sensitive, they require expensive equipment and are time-consuming, limiting their use in daily testing and rapid field detection (H.-Y. Chen et al., 2009; H.-t. Chen et al., 2010).

Therefore, a convenient and simple approach for identifying PPV was essential. Enzymatic recombinase amplification (ERA) is an upgrade of recombinase polymerase amplification (RPA) and can be operated at constant temperature without thermal cycling. ERA achieves rapid amplification of nucleic acid by the simultaneous action of multiple functional proteins at constant temperature, with strong specificity, high sensitivity and easy operation (Yu et al., 2015; Mukama et al., 2020). With the continuous updating of rapid molecular diagnostic technology, nucleic acid detection technology has been developed and applied that is based on the CRISPR-Cas system, a short palindrome repeat sequence with regular aggregation in the prokaryotic immune system. Studies have shown that several endonucleases in the CRISPR-Cas system (Cas12a/b, Cas13a/b and Cas14) are characterized by lateral cleavage activity, and Cas12a is capable of nonspecifically cleaving single-stranded DNA and binding to the corresponding target site. The CRISPR-Cas system, a nucleic acid detection tool, shows great potential in establishing novel molecular diagnostic methods, owing to its reliability, high specificity, and sensitivity (Guk et al., 2017; S.-Y. Li et al., 2018; L. Li et al., 2019; B. Wang et al., 2019).

In this study, we established a molecular detection system aimed at the VP2 gene for PPV detection that combined ERA-CRISPR/Cas12a technology and lateral flow dipstick approaches. The method had the advantages of rapidity and high specificity, it was easy to read and had no professional operation requirement.

MATERIALS AND METHODS

Sample Source and Nucleic Acid Extraction

PPV2, porcine circovirus type 3 (PCV3) and PPV were stored in the Anhui Province Key Laboratory of Veterinary Pathobiology and Disease Control. Porcine pseudorabies live vaccine (PRV, HB-98 strain), porcine epidemic diarrhea live vaccine (PEDV, ZJ08 strain), swine fever live vaccine (CSFV, AV1412 strain), and porcine reproductive and respiratory syndrome live vaccine (PRRSV, R98 strain) were purchased from China Animal Husbandry Industry Co., LTD. Clinical materials, including the liver, spleen and kidney, were collected from pig farms suspected to be infected with PPV in Anhui Province, and donated by the Anhui Animal Disease Prevention and Control Center. Viral DNA was extracted from diseased tissues using a commercial viral genome DNA/RNA extraction kit, the TIANamp Virus DNA/RNA Kit (TIANGEN, Beijing, China), for immediate use or storage at −20°C. Plasmids were extracted according to the instructions for the SanPrep Column Plasmid Mini-Preps Kit (Sangon Biotech, Shanghai, China). Agarose gel electrophoresis was performed on the extracted plasmids, as shown in **Figure 1**.

Design of Primers and Probes

The primers used for ERA-CRISPR/Cas12a detection were designed to be within the conserved region of PPV, encoding structural protein VP2, according to the crRNA primer principle of CRISPR/Cas12a, as shown in **Figure 2**. According to the design principles for crRNA primers, three pairs of crRNA primers were designed using the online CRISPR primer design websites of Liang Cpf1 (http://bioinfolab.miamioh.edu/CRISPR-DT/). According to the principles of ERA primer design, three upstream and three downstream primers were designed using Primer Premier 5 for the conserved sequence of the VP2 gene. Primers and probes were synthesized by Anhui General Co., LTD. (Anhui, China). Oligonucleotide sequences of the CRISPR/Cas12a primers and probes used in this study are shown in **Table 1**.

The ERA-CRISPR/Cas12a/LFD Assay

Lateral flow dipsticks were purchased from Tiosbio (Beijing, China), and EnGenVR Lba Cas12a (Cpf1) (M0653T) and NEBuffer 2.1 (B7203S) were purchased from New England Biolabs (NEB). Mouse RNase inhibitors were purchased from Vazyme Biotech Co., Ltd. (R301-01). The total reaction system of CRISPR/Cas12a/LFD was made up to 20 μL, and consisted of 2 μL NEBuffer 2.1, 1 μL RNase inhibitor, 1 μL 500 nM crRNA, 0.5 μL Cas12a, 0.6 μL probe, 6 μL plasmid template and 8.9 μL ddH_2O. The reaction system was added to the Eppendorf, gently blown

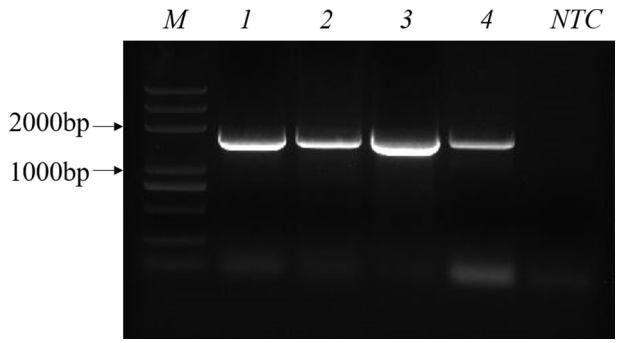

FIGURE 1 | Results of PCR agarose gel electrophoresis. M: Marker; 1–4: PPV-VP2 plasmid; NTC: negative control with ddH_2O.

and mixed, oscillated and centrifuged for 1 s. The reaction mixture was incubated in a water bath for 30 min at 39°C. After the reaction, the reaction tube was opened and the system replenished with ultra-pure water to 50 μL, blown and mixed well. The binding pad end of the test strip was inserted into the reaction tube, with the liquid level not above the top of the binding pad **(Figure 3)**. After the Absorbent Pad was fully infiltrated and the quality control line (C line) was colored, the strip was removed. Red strips on both the test line and the quality control line indicated a positive result, while only the quality control line being red indicated a negative result. Only one test line showed suspicious results and needed to be retested **(Figure 4)**.

Sensitivity and Specificity of the Assay

The recombinant plasmid pMD-19T-VP2 was constructed by ligating the pMD-19T Vector (TaKaRa) with the conserved sequence of the VP2 gene for 30 min at 16°C, and was transformed into DH5α receptor cells (Tsingke, Nanjing, China). The recombinant plasmid was sequenced by Nanjing Tsingke Biotechnology Co., LTD. The plasmid concentration was determined with an ND-2000c spectrophotometer (NanoDrop, Wilmington, DE, USA), and the plasmid copy number was calculated according to the formula: number of copies = (amount × 6.02 × 10^{23})/(length × 10^9 × 660). The plasmid was diluted to 10^6–10^1 copies/μL and stored at −20°C.

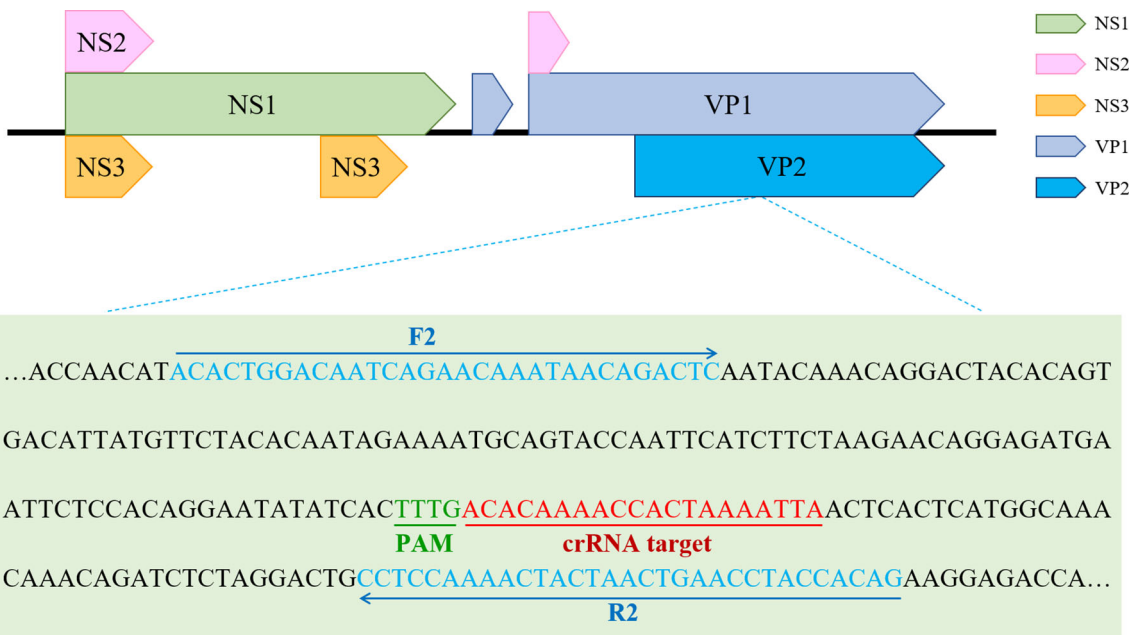

FIGURE 2 | The optimal primer pairs for ERA and crRNA binding sites in the target VP2 gene sequence of PPV.

TABLE 1 | Sequences of the primers and LFD probe used in this work.

Primers	Sequences (5'-3')	Size/bp
VP2-F	GTCTGCAACAGGAAATGAATC	1658
VP2-R	ATTCTGGAAACATTCTTATGC	
qPCR-F	GGGGAGGGCTTGGTTAGAAT	319
qPCR-R	TTGGTGGTGAGGTTGCTGAT	
ERA-1-F	ACACTGGACAATCAGAACAAATAACAGACTC	227
ERA-1-R	CTGTGGTAGGTTCAGTTAGTAGTTTTGGAGG	
ERA-2-F	ACCAACATACACTGGACAATCAGAACAAATA	225
ERA-2-R	GGTAGGTTCAGTTAGTAGTTTTGGAGGCAGT	
ERA-3-F	ATGCAGTACCAATTCATCTTCTAAGAACAGGA	147
ERA-3-R	TGGTAGGTTCAGTTAGTAGTTTTGGAGGCAGT	
crRNA-1-F	GAAATTAATACGACTCACTATAGGGTAATTTCTACTAAGTGTAGATTAAAAATAGCACCAAACCTA	66
crRNA-1-R	TAGGTTTGGTGCTATTTTTAATCTACACTTAGTAGAAATTACCCTATAGTGAGTCGTATTAATTTC	
crRNA-2-F	GAAATTAATACGACTCACTATAGGGTAATTTCTACTAAGTGTAGATACACAAAACCACTAAAATTA	66
crRNA-2-R	TAATTTTAGTGGTTTTGTGTATCTACACTTAGTAGAAATTACCCTATAGTGAGTCGTATTAATTTC	
crRNA-3-F	GAAATTAATACGACTCACTATAGGGTAATTTCTACTAAGTGTAGATTAAAAACAATCCACCAGGAC	66
crRNA-3-R	GTCCTGGTGGATTGTTTTTAATCTACACTTAGTAGAAATTACCCTATAGTGAGTCGTATTAATTTC	
Probe	6-FAM-TTTTTT-BHQ1	
	6-FAM-TTTTTTTATTTTTTT-Biotin	

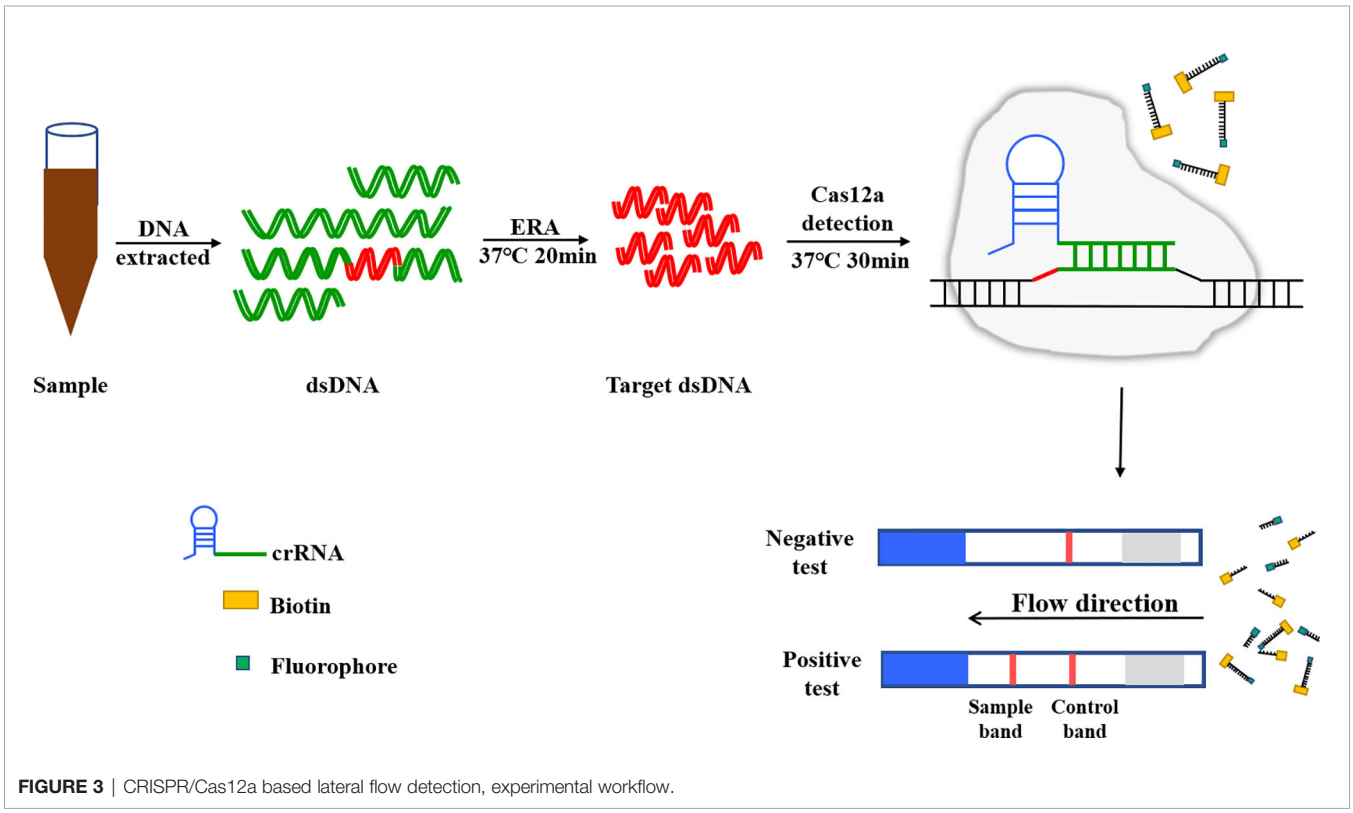

FIGURE 3 | CRISPR/Cas12a based lateral flow detection, experimental workflow.

PPV2, PCV3, PRV (HB-98 strain), CSFV (AV1412 strain), PEDV (ZJ08 strain) and PRRSV (R98 strain) specific tests were performed.

Evaluation of the ERA-CRISPR/Cas12a/LFD Assay Using Clinical Samples

The ERA-CRISPR/Cas12a/LFD was performed on 15 tissue samples to evaluate the specificity of the assay. Nucleic acids in clinical samples were amplified by the ERA method: the reaction system (50 μL) contained Lytic Agent, 20 μL; forward primer (10 μM), 2.5 μL; reverse primer (10 μM), 2.5 μL; template and water, 23 μL. The mixture was placed in the tube, mixed thoroughly and centrifuged briefly after which 2 μL activator was added to the reaction cap, the tube cap was closed, and centrifuge briefly. The amplified samples were tested by CRISPR/Cas12a combined with the lateral flow dipstick, and the reaction results were compared with qPCR.

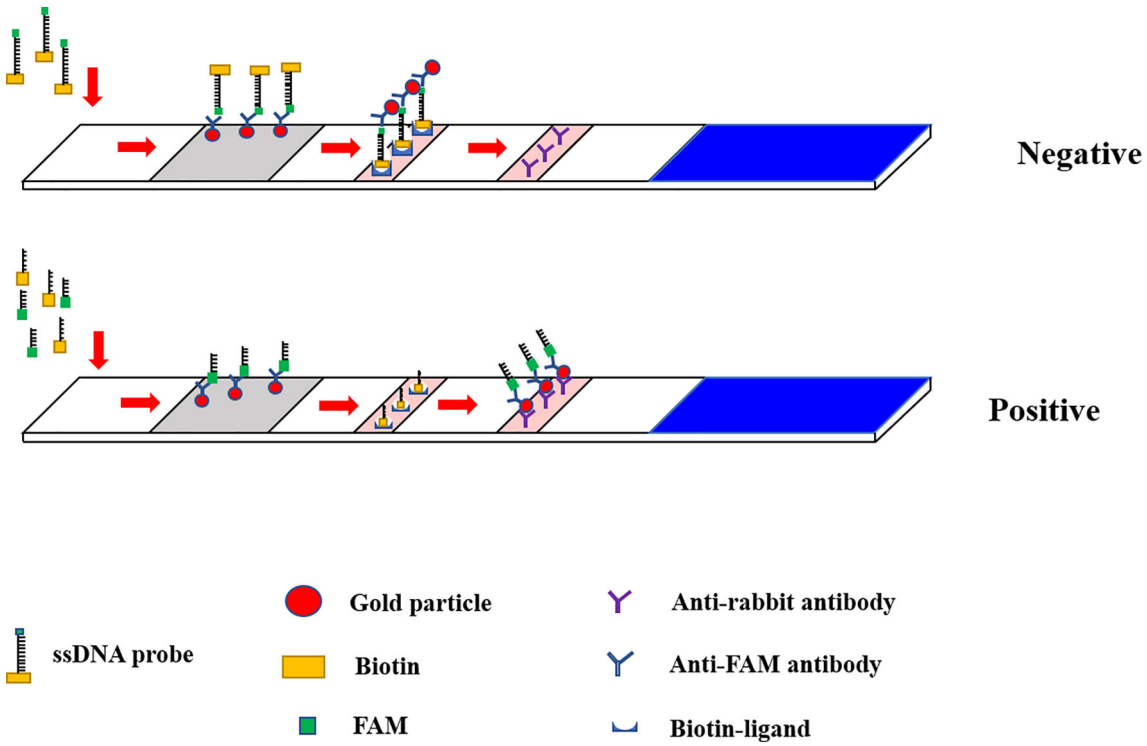

FIGURE 4 | Schematic diagram of Lateral flow dipstick detection.

RESULTS

Design and Screening of the ERA Primers

Three pairs of ERA upstream primers were paired with three pairs of downstream primers, and the upstream primers were utilized to screen the downstream primers, while the upstream primers were screened by the chosen downstream primers. To evaluate the nine primer pairs for ERA, the ERA reaction was carried out for 20 min at 39°C, and the resultant products were evaluated on an electrophoresis gel. After the nucleic acid of clinical samples was amplified by these nine pairs of primers and agarose nucleic acid gel electrophoresis was performed, the results revealed that the second pair of primers had the best efficiency. The primers and probes detected by ERA-CRISPR/Cas12a were created artificially, as shown in **Figure 5A**.

Optimization of the crRNA Primers

The CRISPR/Cas12a visualization test was performed after three pairs of crRNA primers were purified. The reaction was carried out in a water bath at 39°C for 30 minutes, the fluorescence values were measured on ABI StepOnePlusTM (Applied Biosystems) equipment after the reaction. All three pairs of primers were able to amplify the target band, as shown in **Figures 5B, C**, but the second pair was the brightest and had the highest fluorescence value under UV light. The second pair had the greatest effect on crRNA primers, therefore it was utilized in the following tests.

Comparing the Sensitivity of ERA-CRISPR/Cas12a/LFD and PCR Amplification

To evaluate the detection sensitivity of ERA-CRISPR/Cas12a/LFD, the plasmid pMD-19T-VP2 was diluted from 3.75×10^6 to 3.75×10^0 copies/μL, and was used as a template. The detection sensitivity of the PCR and ERA-CRISPR/Cas12a/LFD assays was compared. We found that the limit of detection for the general PCR assay for the PPV VP2 gene was only 3.75×10^4 copies (data not shown). As shown in **Figure 6**, the detection sensitivity of ERA-CRISPR/Cas12a/LFD for the PPV VP2 gene was 3.75×10^2 copies. The experimental results showed that the ERA-CRISPR/Cas12a/LFD assay was more sensitive than the conventional PCR assay in detecting PPV.

Specificity Assessment of ERA-CRISPR/Cas12a/LFD Assay

To appraise the detection specificity of ERA-CRISPR/Cas12a/LFD, the genomic DNA or cDNA from PPV2, PCV3, PRV, CAFV, PEDV, and PRRSV was used. As shown in **Figure 7**, we discovered that only the PPV1 sample was positive, with bands at both the detection and quality control lines, while the other virus samples and negative control were negative (only the quality control line had bands). These results suggested that ERA-CRISPR/Cas12a/LFD could effectively distinguish PPV from other viruses. The ERA-CRISPR/Cas12a/LFD showed high specificity for PPV detection (100%).

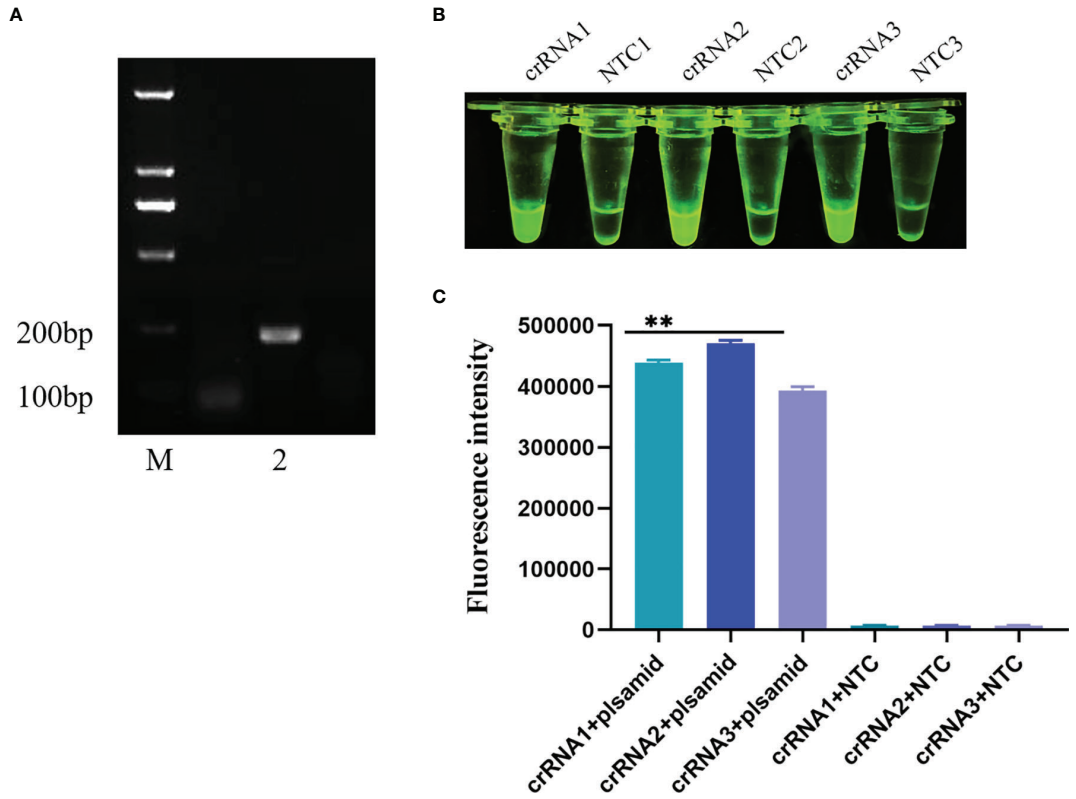

FIGURE 5 | Screening of crRNA primers. **(A)** ERA primer was applied to agarose gel electrophoresis after nucleic acid amplification. M: Marker; 2: The second upstream primer and the second downstream primer constitute the ERA primers for nucleic acid amplification results. **(B, C)** Three pairs of crRNA primers visualized for CRISPR/Cas12a. Comparison of results and fluorescence values under UV light. All data are presented as the statistical significance of differences were **p < 0.01.

Performance of ERA-CRISPR/Cas12a/LFD on Clinical Samples Tested for PPV

The ERA-CRISPR/Cas12a/LFD and qPCR were utilized to identify PPV in clinical samples to assess the clinical effectiveness of ERA-CRISPR/Cas12a/LFD for detection of PPV. ERA-CRISPR/Cas12a/LFD detection was performed on 15 tissue samples, as shown in **Table 2**. The qPCR analyses revealed that four samples tested positive for PPV. The ERA-CRISPR/Cas12a/LFD results were equivalent to the qPCR results, with a positive rate of 26.7%. These findings demonstrated that ERA-CRISPR/Cas12a/LFD was effective in detecting clinical PPV, and the coincidence rate was 100% when compared with qPCR data. The clinical PPV detection results for the ERA-CRISPR/Cas12a/LFD are shown in **Figure 8**.

DISCUSSION

PPV can cause reproductive disorders in pigs, most notably infection and death of embryos and fetuses, particularly stillbirth, malformed and mummified fetuses in sows at first farrowing, but sows show no obvious clinical signs. PPV is very insensitive to acid, alkali and heat, and can survive for a long time in the external environment, which seriously affects the litter rate of sows and causes losses to the pig industry (Wu et al., 2014; Streck et al., 2015). As a result, early detection of PPV is critical in clinical practice. The existing PPV detection approach requires specialized equipment and is not suitable for on-the-spot detection. As a consequence, we require a method that does not rely on sophisticated detection apparatus and equipment and can be used for on-site detection in remote places. This procedure should be quick, sensitive, and precise, and it should not necessitate complicated instrumentation.

With the discovery of CRISPR/Cas-based systems, it is possible to develop an accurate, fast and convenient diagnostic test. Multiple pathogens can currently be detected utilizing RPA or ERA in combination with Cas12a, including mycoplasmas, ASFV, PRRSV, and SARS-CoV-2. The test can be completed in less than 30 min, with the results visible under UV light. The technique is extremely sensitive, being capable of detecting a single copy of genomic DNA with a sensitivity that is comparable to or better than that of qPCR (B. Wang et al., 2019; Bai et al., 2019; X. Wang et al., 2020). The sensitivity of a nucleic acid detection approach based on CRISPR-Cas12 is substantially higher than that of traditional PCR, RT-qPCR, RPA, or LAMP. Many detection methods have been reported for PPV infection,

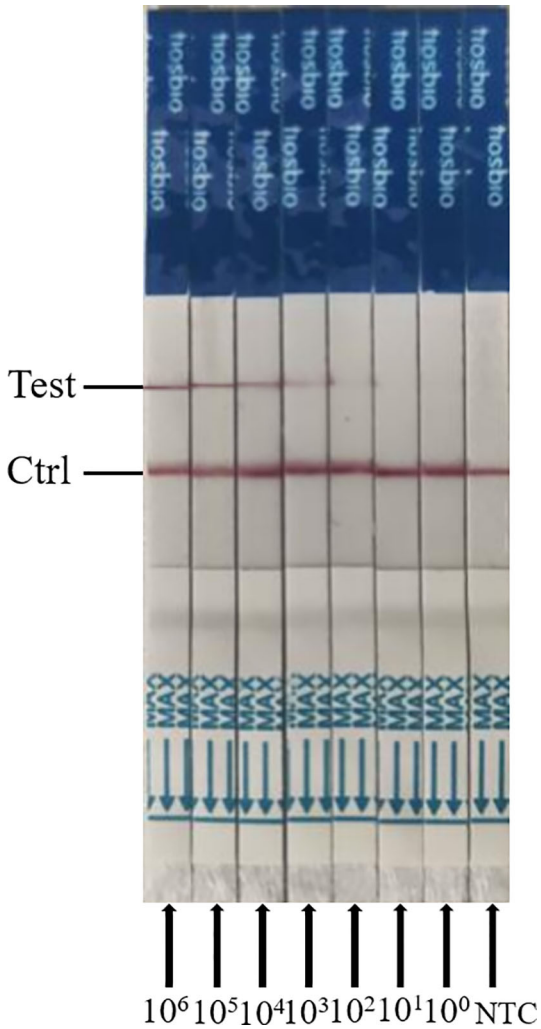

FIGURE 6 | Analytical sensitivity results of ERA-CRISPR/Cas12a/LFD for the plasmid; 10^6 to 10^0 indicate tests with 3.75×10^6 to 3.75 copies/μL recombinant plasmid as a template. NTC indicates a test with RNase-free ddH_2O as a template.

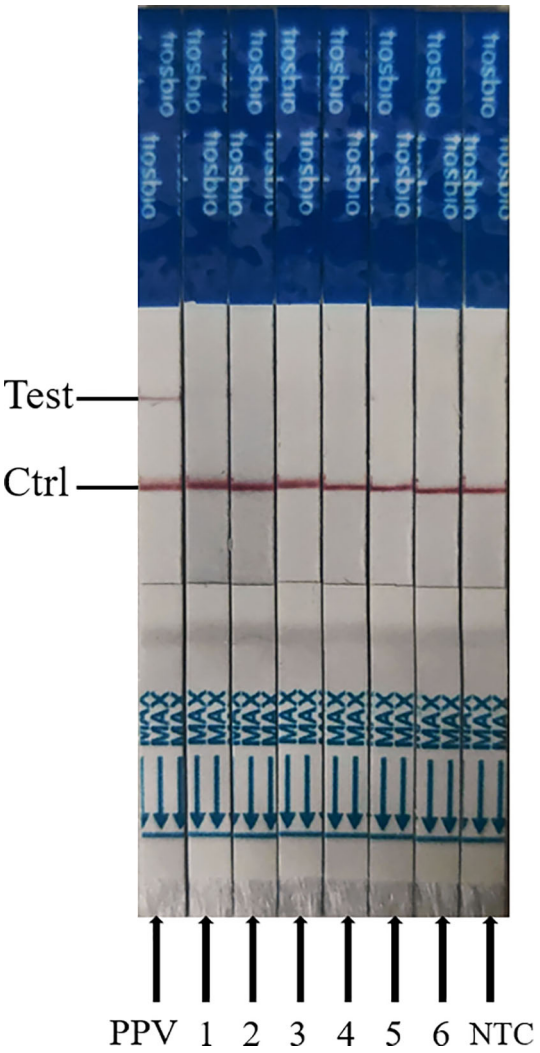

FIGURE 7 | Analytical specificity result of the ERA-CRISPR/Cas12a assay. From left to right, the test samples are positive samples of PPV; 1, PPV-2; 2, PCV3; 3, porcine pseudorabies live vaccine (PRV, HB-98 strain); 4, swine fever live vaccine (CSFV, AV1412 strain); 5, porcine epidemic diarrhea live vaccine (PEDV, ZJ08 strain); 6, porcine reproductive and respiratory syndrome live vaccine (PRRSV, R98 strain); NTC, negative control of RNase-free ddH_2O.

including the LAMP and real-time RPA assay (J.-c. Wang et al., 2017; Zhao et al., 2020). The ERA-CRISPR/Cas12a/LFD method developed in this study has higher or equivalent sensitivity to the above methods. The method has no cross-reactivity with other viruses and can specifically detect PPV.

In this study, three pairs of primers were designed for the conserved sequence VP2 of PPV and a rapid detection method of ERA-CRISPR/Cas12a/LFD with a detection limit of 3.75×10^2 copies was established. The testing of clinical samples (liver, spleen and kidney) using ERA-CRISPR/Cas12a/LFD and qPCR showed consistent results between the two approaches, with a positive rate of 26.7% for PPV, demonstrating the practicality and accuracy of the mechanism. The lateral flow dipstick technique was faster, the results were easy to read, and no professional operation was required. The combination of the

TABLE 2 | Comparison of qPCR and CRISPR/Cas12a/LFD results for clinical samples.

Assay	Number of samples		Total	Diagnostic accuracy
	Positive	Negative		
CRISPR/Cas12a/LFD Judgment	4	11	15	26.7%
qPCR Result	4	11	15	

qPCR and CRISPR/Cas12a/LFD represent quantitative real-time polymerase chain reaction, reverse-transcription recombinase-aided amplification coupled with lateral flow dipstick, respectively.

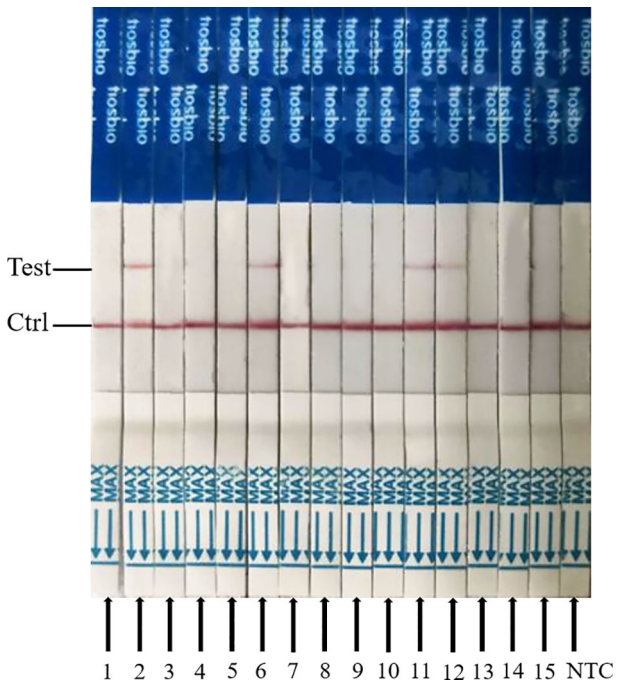

FIGURE 8 | Clinical sample results of ERA-CRISPR/Cas12a combined with ERA analysis. 1–15 indicate different clinical samples; NTC, negative control of RNase-free ddH_2O.

CRISPR/Cas12a and the lateral flow dipstick technique make this experiment not only rapid, sensitive, and accurate, but also intuitive. This is the first report of PPV detection using CRISPR/Cas12a and LFD, and this approach can be applied to the field detection of PPV in resource-poor areas, which is of high practical value for PPV prevention and control. In summary, this study established a rapid, accurate, simple and intuitive ERA-CRISPR/Cas12a/LFD assay for the specific detection of PPV.

DATA AVAILABILITY STATEMENT

The original contributions presented in the study are included in the article/supplementary material. Further inquiries can be directed to the corresponding author.

ETHICS STATEMENT

This animal study was reviewed and approved by the Committee on the Ethics of Animal Care and Use at Anhui Agriculture University (Anhui, China). Written informed consent was obtained from the individuals' and minors' legal guardians/ next of kin, for the publication of any potentially identifiable images or data included in this article.

AUTHOR CONTRIBUTIONS

All authors contributed to the article and approved the submitted version. JW, YL and KY designed the research and analyzed the data. XS, YS, KQ and JT provided resources. JW, YL, YC and QL performed the experiments and wrote the manuscript.

FUNDING

This work was supported financially by Application of supporting technology and poverty alleviation demonstration of ecological breeding of native black pig in contiguous poverty-stricken area of Dabie Mountains, Anhui (201907d06020016) and 2020 University Excellent Talents Support Program (gxyqZD2020009).

REFERENCES

Bai, J., Lin, H., Li, H., Zhou, Y., Liu, J., Zhong, G., et al. (2019). Cas12a-Based On-Site and Rapid Nucleic Acid Detection of African Swine Fever. *Front. Microbiol.* 10. doi: 10.3389/fmicb.2019.02830

Caprioli, A., McNeilly, F., McNair, I., Lagan-Tregaskis, P., Ellis, J., Krakowka, S., et al. (2006). PCR Detection of Porcine Circovirus Type 2 (PCV2) DNA in Blood, Tonsillar and Faecal Swabs From Experimentally Infected Pigs. *Res. Veterinary Sci.* 81 (2), 287–292. doi: 10.1016/j.rvsc.2006.01.001

Chen, H.-Y., Li, X.-K., Cui, B.-A., Wei, Z.-Y., Li, X.-S., Wang, Y.-B., et al. (2009). A TaqMan-Based Real-Time Polymerase Chain Reaction for the Detection of Porcine Parvovirus. *J. Virological Methods* 156 (1-2), 84–88. doi: 10.1016/j.jviromet.2008.10.029

Chen, H.-t., Zhang, J., Yang, S.-h., Ma, L.-n., Ma, Y.-p., Liu, X.-t., et al. (2010). Rapid Detection of Porcine Parvovirus DNA by Sensitive Loop-Mediated Isothermal Amplification (Vol 158, Pg 100, 2009). *J. Virological Methods* 163 (1), 166–166. doi: 10.1016/j.jviromet.2009.09.001

Deng, J., Li, X., Zheng, D., Wang, Y., Chen, L., Song, H., et al. (2018). Establishment and Application of an Indirect ELISA for Porcine Circovirus 3. *Arch. Virol.* 163 (2), 479–482. doi: 10.1007/s00705-017-3607-7

Ellis, J. A., Bratanich, A., Clark, E. G., Allan, G., Meehan, B., Haines, D. M., et al. (2000). Coinfection by Porcine Circoviruses and Porcine Parvovirus in Pigs With Naturally Acquired Postweaning Multisystemic Wasting Syndrome. *J. Veterinary Diagn. Invest.* 12 (1), 21–27. doi: 10.1177/104063870001200104

Green, M. R., and Sambrook, J. (2018). Touchdown Polymerase Chain Reaction (PCR). *Cold Spring Harbor Protoc.* 2018 (5), 350–53. doi: 10.1101/pdb.prot095133

Guk, K., Keem, J. O., Hwang, S. G., Kim, H., Kang, T., Lim, E.-K., et al. (2017). A Facile, Rapid and Sensitive Detection of MRSA Using a CRISPR-Mediated DNA FISH Method, Antibody-Like Dcas9/sgRNA Complex. *Biosensors Bioelectronics* 95, 67–71. doi: 10.1016/j.bios.2017.04.016

Huang, C. J., Hung, J. J., Wu, C. Y., and Chien, M. S. (2004). Multiplex PCR for Rapid Detection of Pseudorabies Virus, Porcine Parvovirus and Porcine Circoviruses. *Veterinary Microbiol.* 101 (3), 209–214. doi: 10.1016/j.vetmic.2004.04.007

Jiang, Y., Shang, H., Xu, H., Zhu, L., Chen, W., Zhao, L., et al. (2010). Simultaneous Detection of Porcine Circovirus Type 2, Classical Swine Fever Virus, Porcine Parvovirus and Porcine Reproductive and Respiratory Syndrome Virus in Pigs by Multiplex Polymerase Chain Reaction. *Veterinary J.* 183 (2), 172–175. doi: 10.1016/j.tvjl.2008.11.016

Kamstrup, S., Langeveld, J., Botner, A., Nielsen, J., Schaaper, W. M., Boshuizen, R. S., et al. (1998). Mapping the Antigenic Structure of Porcine Parvovirus at the Level of Peptides. *Virus Res.* 53 (2), 163–173. doi: 10.1016/s0168-1702(97)00145-7

Kennedy, S., Moffett, D., McNeilly, F., Meehan, B., Ellis, J., Krakowka, S., et al. (2000). Reproduction of Lesions of Postweaning Multisystemic Wasting Syndrome by Infection of Conventional Pigs With Porcine Circovirus Type 2 Alone or in Combination With Porcine Parvovirus. *J. Comp. Pathol.* 122 (1), 9–24. doi: 10.1053/jcpa.1999.0337

Li, S.-Y., Cheng, Q.-X., Liu, J.-K., Nie, X.-Q., Zhao, G.-P., and Wang, J. (2018). CRISPR-Cas12a has Both Cis- and Trans-Cleavage Activities on Single-Stranded DNA. *Cell Res.* 28 (4), 491–493. doi: 10.1038/s41422-018-0022-x

Li, L., Li, S., Wu, N., Wu, J., Wang, G., Zhao, G., et al. (2019). HOLMESv2: A CRISPR-Cas12b-Assisted Platform for Nucleic Acid Detection and DNA Methylation Quantitation. *ACS Synthetic Biol.* 8 (10), 2228–2237. doi: 10.1021/acssynbio.9b00209

Meszaros, I., Olasz, F., Csagola, A., Tijssen, P., and Zadori, Z. (2017). Biology of Porcine Parvovirus (Ungulate Parvovirus 1). *Viruses-Basel* 9 (12), 393. doi: 10.3390/v9120393

Mukama, O., Wu, J., Li, Z., Liang, Q., Yi, Z., Lu, X., et al. (2020). An Ultrasensitive and Specific Point-of-Care CRISPR/Cas12 Based Lateral Flow Biosensor for the Rapid Detection of Nucleic Acids. *Biosensors Bioelectronics* 159, 112143. doi: 10.1016/j.bios.2020.112143

Streck, A. F., Bonatto, S. L., Homeier, T., Souza, C. K., Goncalves, K. R., Gava, D., et al. (2011). High Rate of Viral Evolution in the Capsid Protein of Porcine Parvovirus. *J. Gen. Virol.* 92, 2628–2636. doi: 10.1099/vir.0.033662-0

Streck, A. F., Canal, C. W., and Truyen, U. (2015). Molecular Epidemiology and Evolution of Porcine Parvoviruses. *Infect. Genet. Evol.* 36, 300–306. doi: 10.1016/j.meegid.2015.10.007

Streck, A. F., and Truyen, U. (2020). Porcine Parvovirus. *Curr. Issues Mol. Biol.* 37, 33–45. doi: 10.21775/cimb.037.033

Terato, K., Do, C., Chang, J., and Waritani, T. (2016). Preventing Further Misuse of the ELISA Technique and Misinterpretation of Serological Antibody Assay Data. *Vaccine* 34 (39), 4643–4644. doi: 10.1016/j.vaccine.2016.08.007

Wang, J.-c., Liu, L.-b., Han, Q.-a., Wang, J.-f., and Yuan, W.-z. (2017). An Exo Probe-Based Recombinase Polymerase Amplification Assay for the Rapid Detection of Porcine Parvovirus. *J. Virological Methods* 248, 145–147. doi: 10.1016/j.jviromet.2017.06.011

Wang, B., Wang, R., Wang, D., Wu, J., Li, J., Wang, J., et al. (2019). Cas12aVDet: A CRISPR/Cas12a-Based Platform for Rapid and Visual Nucleic Acid Detection. *Analytical Chem.* 91 (19), 12156–12161. doi: 10.1021/acs.analchem.9b01526

Wang, X., Zhong, M., Liu, Y., Ma, P., Dang, L., Meng, Q., et al. (2020). Rapid and Sensitive Detection of COVID-19 Using CRISPR/Cas12a-Based Detection With Naked Eye Readout, CRISPR/Cas12a-NER. *Sci. Bull.* 65 (17), 1436–1439. doi: 10.1016/j.scib.2020.04.041

Wu, R., Wen, Y., Huang, X., Wen, X., Yan, Q., Huang, Y., et al. (2014). First Complete Genomic Characterization of a Porcine Parvovirus 5 Isolate From China. *Arch. Virol.* 159 (6), 1533–1536. doi: 10.1007/s00705-013-1948-4

Xu, Y. G., Cui, L. C., Wang, H. W., Huo, G. C., and Li, S. L. (2013). Characterization of the Capsid Protein VP2 Gene of a Virulent Strain NE/09 of Porcine Parvovirus Isolated in China. *Res. Veterinary Sci.* 94 (2), 219–224. doi: 10.1016/j.rvsc.2012.09.003

Yu, X., Shi, L., Lv, X., Yao, W., Cao, M., Yu, H., et al. (2015). Development of a Real-Time Reverse Transcription Loop-Mediated Isothermal Amplification Method for the Rapid Detection of Porcine Epidemic Diarrhea Virus. *Virol. J.* 12, 76. doi: 10.1186/s12985-015-0297-1

Zhao, K., Hu, R., Ni, J., Liang, J., He, X., Du, Y., et al. (2020). Establishment of a Porcine Parvovirus (PPV) LAMP Visual Rapid Detection Method. *J. Virological Methods* 284, 113924. doi: 10.1016/j.jviromet.2020.113924

Conflict of Interest: The authors declare that the research was conducted in the absence of any commercial or financial relationships that could be construed as a potential conflict of interest.

Publisher's Note: All claims expressed in this article are solely those of the authors and do not necessarily represent those of their affiliated organizations, or those of the publisher, the editors and the reviewers. Any product that may be evaluated in this article, or claim that may be made by its manufacturer, is not guaranteed or endorsed by the publisher.

frontiers | Frontiers in Cellular and Infection Microbiology

ORIGINAL RESEARCH
published: 26 May 2022
doi: 10.3389/fcimb.2022.884430

Development of a Cleaved Probe-Based Loop-Mediated Isothermal Amplification Assay for Rapid Detection of African Swine Fever Virus

Songqi Wang[1†], Haiyan Shen[2†], Qijie Lin[1], Jun Huang[3], Chunhong Zhang[2], Zhicheng Liu[2], Minhua Sun[2], Jianfeng Zhang[2], Ming Liao[2], Yugu Li[1] and Jianmin Zhang[1*]*

[1] Key Laboratory of Zoonoses Prevention and Control of Guangdong Province; The Research Center for African Swine Fever Prevention and Control; College of Veterinary Medicine, South China Agricultural University, Guangzhou, China, [2] Maoming Branch Center of Guangdong Laboratory for LingNan Modern Agricultural Science and Technology; Key Laboratory of Livestock Disease Prevention of Guangdong Province, Scientific Observation and Experiment Station of Veterinary Drugs and Diagnostic Techniques of Guangdong Province, Ministry of Agriculture and Rural Affairs, Institute of Animal Health, Guangdong Academy of Agricultural Sciences, Foshan, China, [3] College of Life Science and Engineering, Foshan University, Guangzhou, China

African Swine Fever (ASF), caused by African swine fever virus (ASFV), is a highly contagious and lethal viral disease of pigs. However, commercial vaccines are not yet available, and neither are drugs to prevent or control ASF. Therefore, rapid, accurate on-site diagnosis is urgently needed for detection during the early stages of ASFV infection. Herein, a cleaved probe-based loop-mediated isothermal amplification (CP-LAMP) detection method was established. Based on the original primer sets, we targeted the ASFV 9GL gene sequence to design a probe harboring a ribonucleotide insertion. Ribonuclease H2 (RNase H2) enzyme activity can only be activated when the probe is perfectly complementary, resulting in hydrolytic release of a quencher moiety, and consequent signal amplification. The method displayed robust sensitivity, with copy number detection as low as 13 copies/μL within 40 min at constant temperature (62°C). Visualization of the fluorescence product was employed using a self-designed 3D-printed visualization function cassette, and the CP-LAMP method achieved specific identification and visual detection of ASFV. Moreover, coupling the dual function cassette and smartphone quantitation makes the CP-LAMP assay first user-friendly, cost-effective, portable, rapid, and accurate point-of-care testing (POCT) platform for ASFV.

Keywords: African swine fever virus, rapid detection, RNase H2, CP-LAMP, point-of-care testing, smartphone quantitation

OPEN ACCESS

Edited by:
Muhammad Munir, Lancaster University, United Kingdom

Reviewed by:
Omnia Khaleel, Lancaster University, United Kingdom
Bin Zhou, Nanjing Agricultural University, China

***Correspondence:**
Yugu Li
liyugu@scau.edu.cn
Jianmin Zhang
jmzhang@scau.edu.cn

[†]These authors have contributed equally to this work

Specialty section:
This article was submitted to Clinical Microbiology, a section of the journal Frontiers in Cellular and Infection Microbiology

Received: *26 February 2022*
Accepted: *25 April 2022*
Published: *26 May 2022*

Citation:
Wang S, Shen H, Lin Q, Huang J, Zhang C, Liu Z, Sun M, Zhang J, Liao M, Li Y and Zhang J (2022) Development of a Cleaved Probe-Based Loop-Mediated Isothermal Amplification Assay for Rapid Detection of African Swine Fever Virus. Front. Cell. Infect. Microbiol. 12:884430. doi: 10.3389/fcimb.2022.884430

INTRODUCTION

African swine fever (ASF), an acute, hemorrhagic, virulent disease caused by ASV virus (ASFV), affects domestic pigs and wild boar (Normile, 2018; Ma et al., 2020). ASFV infection is characterized by rapid onset and a mortality rate near 100% for the most acute infections, depending on the viral strain (Galindo and Alonso, 2017). ASF has a devastating economic impact on the global pig industry (He et al., 2020; Yoon et al., 2020). Currently, there are no effective drugs or commercial vaccines to prevent and/or control ASF. Hence, a rapid on-site method is urgently needed for ASFV detection during the early stages of ASFV infection.

The World Organization for Animal Health currently recommends viral isolation, antigen detection, and molecular diagnostic methods for ASFV (Sánchez-Vizcaíno and Mur, 2013). However, viral isolation is laborious and ill-suited to in-field practices, while the presence of antibodies can disrupt antigen detection (Cadenas-Fernández et al., 2019). For ASFV detection, conventional and real-time PCR methods are considered the most reliable (King et al., 2003; Fernández-Pinero et al., 2013), but they are not sufficiently sensitive, and they cannot achieve quantitative analysis of small quantities of virus DNA during amplification. Real-time fluorescence quantitative PCR (qPCR) has been applied for testing ASFV, which can achieve quantitative analysis at low concentrations of samples using standard sample templates. However, these two methods required laboratory-based equipment and advanced expertise.

Loop-mediated isothermal amplification (LAMP) is a highly specific, simple, sensitive, and rapid technique for pathogen detection (Tomita et al., 2008). In LAMP assays, the target DNA or RNA template is amplified under isothermal conditions (60–65°C) using a DNA polymerase possessing strong strand displacement activity, and a set of primers that recognizes six distinct genomic regions. LAMP does not require expensive equipment, making it potentially ideal for clinical field testing. In addition, The LAMP assay results can be visualized with intercalating dyes such as ethidium bromide and SYBR Green (Tomita et al., 2008), or complexometric calcein (Hill et al., 2008) and hydroxyl naphthol blue (HNB) (Goto et al., 2009), a fluorescent metal indicator, under a UV lamp. However, distinguishing weak color changes from negative reactions is challenging, increasing the risk of inaccurately interpreting the results, especially at low sample concentrations. LAMP results can be judged quantitatively using real-time thermocyclers that detect fluorescence, or a real-time turbidimeter (Hill et al., 2008). However, LAMP cannot achieve quantification through analysis of color changes of fluorescent intercalating dyes.

To overcome these limitations, we aimed to develop a rapid, sensitive, cleaved probe-based LAMP (CP-LAMP) detection method. In this method based on traditional LAMP, we replaced one primer with a loop primer probe containing a ribonucleotide insertion; only when the base sequence perfectly matches the DNA-RNA mutant target can it be cleaved by the enzyme RNase H2. When the reporter fluorophore and the quencher fluorophore of the loop primer probe are separated, the fluorescent signal is generated, which can be read by a real-time thermocycler. Our method can detect ASFV quantitatively based on a standard curve, and it does not require addition of separate dyes, which effectively avoids contamination and false-positive results. With the help of a portable self-designed 3D-printed visualization function cassette to read the results, detection of ASFV is made more convenient for clinical diagnosis, and it meets the requirements of POCT.

MATERIALS AND METHODS

Primer Design

Sequence data from publicly accessible databases were used to generate consensus sequences by aligning the genomes of ASFV isolates. Primers were designed based on the 9GL gene sequence of ASFV isolate Pig/HLJ/2018 (GenBank: MK333180.1), which is highly conserved, and targeted for specific primer design using Primer Explorer V5. All oligonucleotide primers and probes used in this research were synthesized by Sangon Biotech (Shanghai) Co., Ltd. (Shanghai, China).

Standard Plasmid

The 9GL gene was chemically synthesized by Sangon Biotech (Shanghai) Co., Ltd., and inserted into the pUC57 plasmid (herein referred to as pUC57-9GL). The resulting construct was transformed into *Escherichia coli* DH5α cells, then extracted using an Endo-free Plasmid Mini Kit (D6950, Omega Bio-tek, USA) according to the manufacturer's instructions. Plasmid concentrations were measured by spectrophotometry, converted to copy numbers, and plasmid were used as templates for sensitivity assays.

CP-LAMP Reaction Conditions

In-tube CP-LAMP reactions consisted of a 25 μL reaction mixture containing 8 U of Bst 2.0 DNA polymerase, 100 μmol $MgSO_4$, 2.5 μL of 10× buffer (New England Biolabs Inc.), 0.1 U/μL RNase H2 Enzyme (catalog no. 11-02-12-01, Integrated DNA Technologies), 4 μL of dNTPs (TransGenBiotech), and 2.5 μL of DNA sample. Mineral oil was applied to the surface to prevent contamination before lid closure. The reaction procedure was performed at 1 cycle/min for 60 cycles using a CFX96 Touch Real-time PCR Detection System (Bio-Rad). The CP-LAMP assay could be completed in less than 40 min at 62°C, and the reaction was monitored using a real-time PCR instrument.

Specificity of CP-LAMP

Genomic DNA from African swine fever virus (ASFV), porcine circovirus type 2 (PCV2), pseudorabies virus (PRV), and porcine parvovirus (PPV) was used to evaluate the specificity of the CP-LAMP method. Total RNA from classic swine fever virus (CSFV), transmissible gastroenteritis virus (TGEV), porcine reproductive respiratory syndrome virus (PRRSV), and porcine epidemic diarrhea virus (PEDV) was extracted and reverse-transcribed into cDNA for use in specific testing.

Sensitivity of CP-LAMP

To evaluate the limit-of-detection (LOD) of the ASFV CP-LAMP assay, a 10-fold dilution series of pUC57-9GL in deionized water ranging from 1.3×10^6 to 1.3 copies/μL was prepared. Each solution was tested in triplicate in a 96-well PCR plate and heated at 62°C for 40 min. Finally, experimental data were used to establish a standard curve.

Stability and Repeatability of CP-LAMP

To measure the repeatability of this method, standard solutions of plasmid pUC57-9GL in the range of 1.3×10^6 to 1.3×10^2 copies/μL were used as templates. Under the same conditions, CP-LAMP amplification was performed and each dilution tested in triplicate. Finally, the coefficient of variation (CV) was calculated according to its cycle threshold (Ct) value to evaluate the repeatability of the measurement.

Comparison of CP-LAMP With Conventional PCR (For Diagnostic Sensitivity)

Diagnostic performance was evaluated by testing 61 DNA samples provided by the Research Center for African Swine Fever Prevention and Control, South China Agricultural University, Guangzhou, People's Republic of China. The CP-LAMP assay performance was directly compared with the conventional PCR amplification and TaqMan probe real-time PCR of ASFV (King et al., 2003; McKillen et al., 2010).

For the PCR assay, we performed as the Chinese national standard: Diagnostic techniques for African Swine Fever (GB/T 18648-2020). The primers were designed to target the conserved region of ASFV B646L gene, F-PPA-1: 5'-AGTTATGGGAAAC CCGACCC-3', R-PPA-2: 5'-CCCTGAATCGGAGCATCCT-3', the primer concentration was 10μM, and the amplification band was 257 bp. The conventional PCR was performed in a 20μL reaction volume containing 10 μL Premix Taq, 1 μL each primer, 6 μL H_2O and 2 μL of the genomic DNA. The tube was sealed, and centrifuged briefly. Positive, negative, and blank controls were included for each time of the conventional PCR performed. Thermal cycling involved a 95°C pre-denaturation step for 10 min, followed by 40 cycles of denaturation at 95°C for 15 s, annealing at 62°C for 30 s, extension at 72°C for 30 s, and a final extension at 72°C for 7 min. For PCR amplification product electrophoresis, 5 μL of 6 × loading buffer was added to each PCR product, mixed, and 8 μL was run on a 2% agarose gel prepared with 1 × TAE buffer, and electrophoresed for 30–40 min. After electrophoresis, the agarose gel was placed in a gel imager to observe the results.

Assembly of the 3D-Printed Visualization Function Cassette for Detection

We prepared a hand-held portable cassette device box 122 mm long, 82 mm wide, and 70 mm deep in previous work (Wen et al., 2021). The box is powered by rechargeable portable lithium batteries, which are connected in series to eight light-emitting diodes (LEDs) with an emission peak of 495 nm. When energized, the light source passes through a 495 nm band-pass filter between the LED lamp and the centrifuge tube, and illuminates the reaction solution at 495 nm, causing the fluorescent group to emit light. In order to facilitate observation and eliminate the overlap of excitation light and emission light, a plane reflector with a 45°C angle was placed on the opposite side of the tube body, and the reaction result graph can be obtained using a mobile phone.

RESULTS

Primer Design, Optimization, and establishment of the Basic Reaction System

Optimal CP-LAMP primers were selected by aligning the sequences of ASFV 9GL genes from the from NCBI database to identify the highly-conserved region for primer design. Five sets of candidate primers were selected and synthesized (**Table 1**). Moreover, we targeted this fragment of the ASFV 9GL gene to design a new reporter dye and a quencher-modified allelic discrimination cleaved probe with a ribonucleotide insertion (**Figure 1** and **Table 1**). Upon perfect matching with the ribonucleotide mutant site, the RNase H2 hydrolytic mechanism is activated, and release of the quencher generates an amplified signal. Conversely, a signal is not generated with mismatching ribonucleotides. Thus, robust specific detection of the ASFV 9GL gene was achieved.

Based on our previous report (Shen et al., 2020), we successfully set up a basic reaction system using standard plasmids. The reaction system contained 2.5 μL of buffer (10×), 1.5 μL of $MgSO_4$, 4 μL of dNTPs, 8 U/μL of Bst 2.0 WarmStart DNA polymerase (1 μL), 0.1 U/μL of RNase H2 Enzyme (0.3 μL), 0.3 μL of probe (10 μM), 4 μL of FIP/BIP primer (10 μM), 0.5 μL of F3/B3 primer (10 μM), 1.5 μL of loop primer (10 μM), and 2.5 μL of DNA sample. The mixture was made up to 25 μL with deionized water. The ASFV standard plasmid was successfully detected with good repeatability and reaction efficiency (**Figure 2A**). In order to facilitate the clinical testing, we use a self-designed 3D-printed visualization function cassette to establish the point-of-care testing (POCT) platform for ASFV. After the CP-LAMP reaction, the tubes containing the reaction mixtures were placed in the cassette and the results can be visualized using a smartphone (**Figure 2B**).

To optimize the reaction temperature of the CP-LAMP assay, reaction mixtures were tested from 60 to 64°C at 1°C intervals for

TABLE 1 | Primers and probe information of the CP-LAMP assay.

Name	Sequence (5'→3')
F3	GCCGGTTATTTACGTTGTT
B3	TTTCAGACGCTCCTAGCT
FIP	CACGCCTTTTCGTATCTTACAAAAACGAAGGTCCAGTACTGAAAG
BIP	CTGGTGCATGGCAGAGACTCAAGAAAAATATGAAGCCATCCA
LF	ACATTAAACAACTCGGAGGA
probe	FAM-ACATTAAACAACTC***G***(RNA)GAGGA-BHQ1

The bold and underline letter indicates that the base is a ribonucleotide.

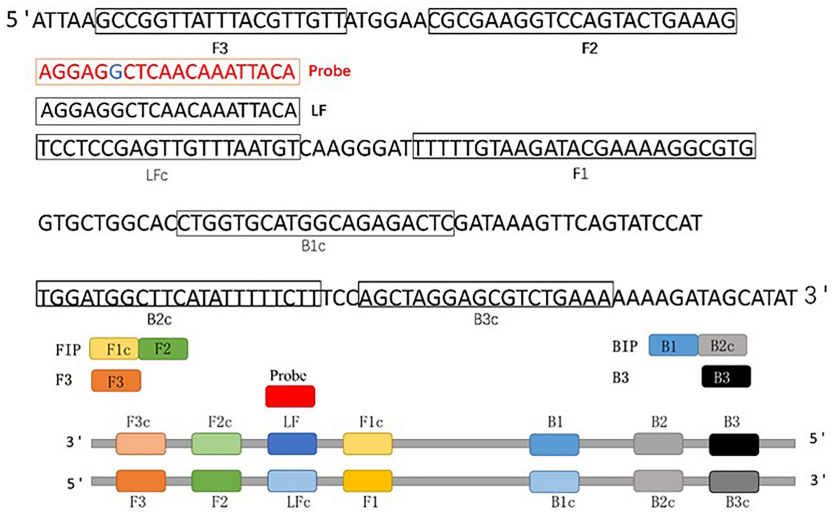

FIGURE 1 | Schematic diagram of the 9GL gene showing the position and composition of ASFV CP-LAMP primers and probe. F3, forward outer primer (F3); B3, backward outer primer; FIP (F1c+F2), forward inner primer; BIP (B1+B2c), backward inner primer; LF, loop forward primer; Probe, cleaved probe.

60 min. There was optimal reaction efficiency and amplification efficiency at 62°C, hence this temperature was chosen for subsequent testing (**Figure 3**).

To confirm the optimal reaction duration of the CP-LAMP assay, fluorescence values were compared and analyzed throughout the entire reaction, and values peaked then tended to remain constant after 40 min. Based on amplification efficiency and total detection time, a 40 min reaction duration was considered most appropriate.

Specificity of Test Results

Genomic DNAs or cDNAs of ASFV, PRV, PCV2, PPV, CSFV, PRRSV TGEV and PEDV were determined by CP-LAMP to evaluate the specificity. As shown in **Table 2** and **Figure 4**, reaction systems containing genomic DNA of ASFV gave excellent signal in the assay, while reaction systems containing DNAs or cDNAs from the other seven pathogens did not generate detectable signals. Therefore, the CP-LAMP assay displayed good specificity, and only amplified the 9GL gene DNA of ASFV.

Detection Limit of Test Results

Sensitivity testing of CP-LAMP was performed by using the real-time PCR instrument, and the results showed that plasmid concentrations from 1.3×10^6 copies/μL to 1.3 copies/μL were amplified successfully (**Figure 5**). Therefore, the detection limit was 13 copies/μL, analysis could be completed within 40 min, the standard curve equation was y = -1.7326x + 26.289 (R^2 = 0.9831), and there was an excellent correlation between copy number the reaction duration. Moreover, the results observed by the 3D-printed visualization function cassette are consistent with the results observed by real-time PCR instrument. In all, these results demonstrated that the CP-LAMP assay established in this study to detect ASFV was a sensitive probe-based real-time LAMP method.

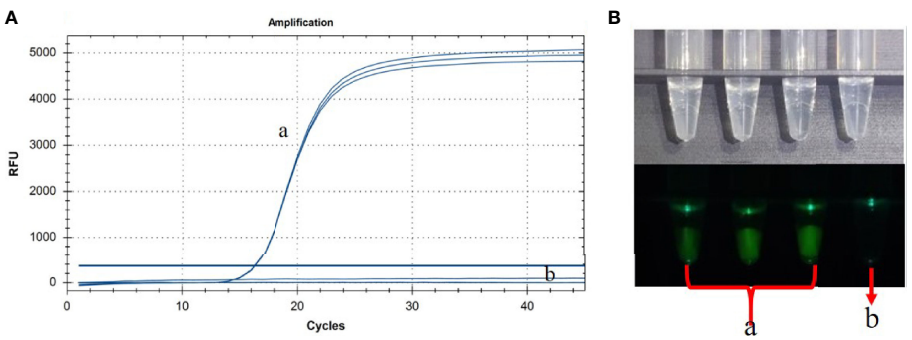

FIGURE 2 | Basic reaction system was performed in real-time PCR instrument **(A)** and the results were observed using 3D-printed visualization function cassette **(B)**. (a) ASFV standard plasmid (in triplicate test). (b) Negative control.

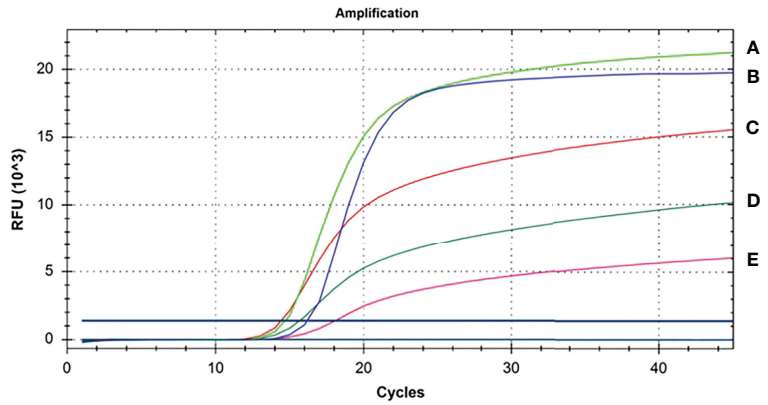

FIGURE 3 | Temperature optimization results. **(A)** 61°CC. **(B)** 60°CC, **(C)** 62°CC, **(D)** 64°CC, **(E)** 63°CC.

TABLE 2 | Specificity of the CP-LAMP assay.

Pathogen	ASFV	PRV	PCV2	PPV	CSFV	PRRSV	PEDV	TGEV
Result	+	–	–	–	–	–	–	–

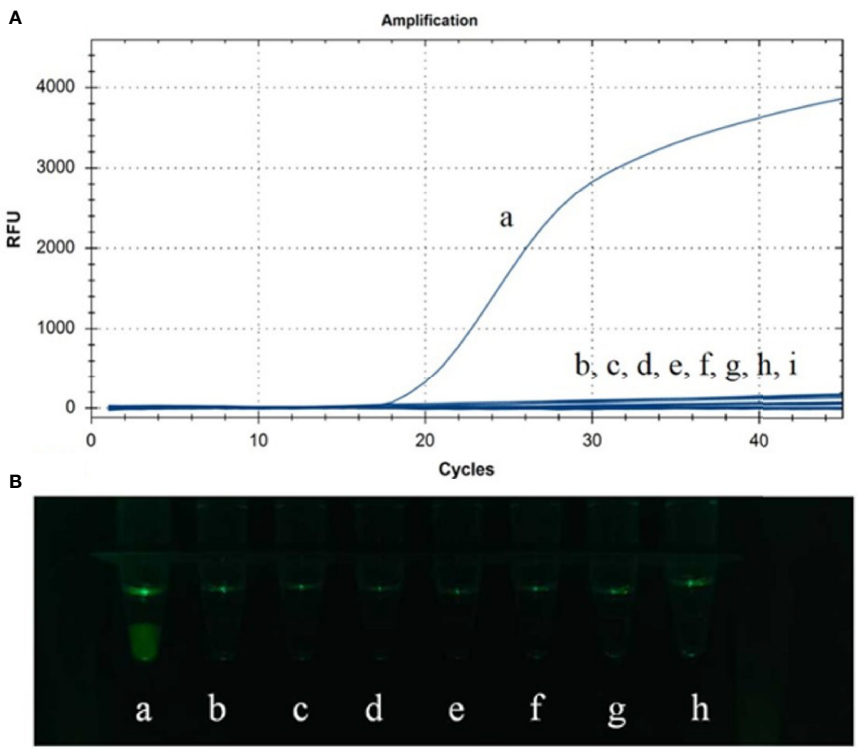

FIGURE 4 | Specificity analysis was performed in real-time PCR instrument **(A)** and observed by the 3D-printed visualization function cassette **(B)**. (a) ASFV. (b) PRV. (c) PCV2. (d) CSFV. (e) PRRSV. (f) PPV. (g) PEDV. (h) TGEV. (i) Negative control.

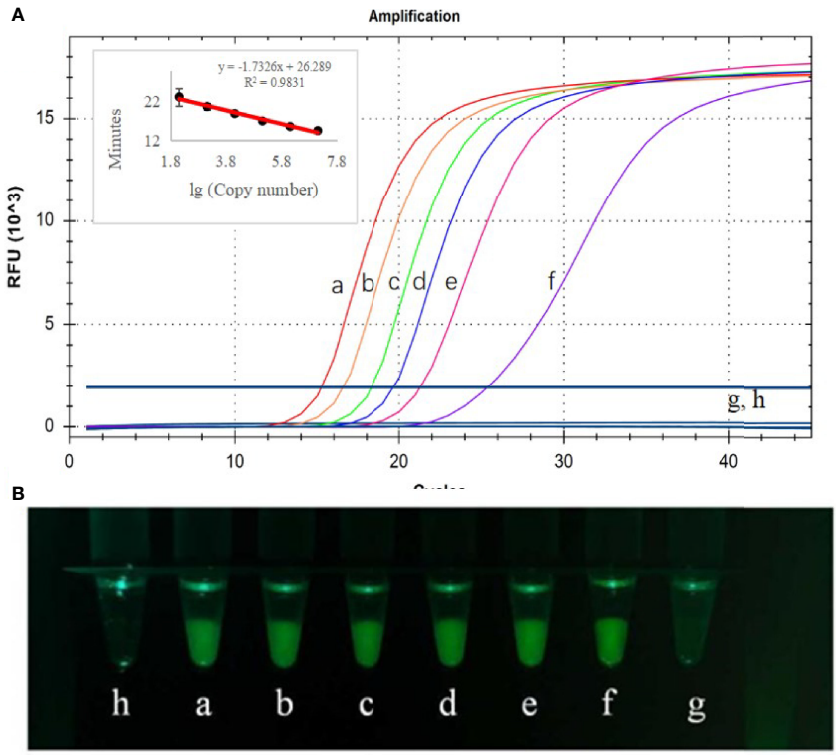

FIGURE 5 | Detection limit analysis used the real-time PCR instrument **(A)** and observed by the 3D-printed visualization function cassette **(B)**. CP-LAMP was used tested using ASFV plasmid diluted to various concentrations. (a) 1.3×10^6 copies/μL. (b) 1.3×10^5 copies/μL. (c) 1.3×10^4 copies/μL. (d) 1.3×10^3 copies/μL. (e) 1.3×10^2 copies/μL. (f) 1.3×10^1 copies/μL. (g) 1.3×10^0 copies/μL. (h) Negative control.

Repeatability of Test Results

In the same laboratory, using the same instrument, each sample was replicated three times over a short period of time. The CV values of three repeated experiments were all less than 0.05 (**Table 3**), indicating that the method had good reproducibility.

Application of CP-LAMP to Clinical Samples

To assess the practical application of the CP-LAMP method, 61 DNA samples were used to test CP-LAMP. A total of 13 samples were detected as positive by traditional PCR methods, while 48 samples were negative. By comparison, 17 samples were detected as positive by the CP-LAMP method, 13 of which were detected as positive by both traditional PCR and CP-LAMP methods, but the other four samples were only detected as positive by the CP-LAMP method (**Table 4**). Thus, CP-LAMP achieved a superior detection rate compared with traditional PCR, and no positive samples were missed. Meanwhile, partial visualization results of clinical samples using the 3D-printed visualization function cassette are shown in **Figure 6**.

TABLE 3 | Reproducibility of the CP-LAMP method.

Plasmid concentration (copies/μL)	Intra-assay coefficient of variation	Inter-assay coefficientof variation
1.3×10^6	3.01%	1.98%
1.3×10^5	1.96%	0.11%
1.3×10^4	4.20%	0.83%
1.3×10^3	3.41%	1.87%
1.3×10^2	4.54%	0.58%

DISCUSSION

Since the first ASF outbreak in China in August 2018, the diseases has spread to almost 32 provinces, and huge numbers of pigs have been culled to halt further expansion, which has had a devastating impact on both pork production and food security (Li and Tian, 2018). Currently, neither an efficacious vaccine nor effective control strategies are available. Thus, a rapid, facile, and accurate on-site detection method is essential to help control the epidemic and minimize losses. In the present study, we established a CP-LAMP detection method for this purpose. The ASFV CP-LAMP method achieved fast, efficient, and specific amplification at a constant temperature (62°C) in a short time (within 40 min) using a DNA polymerase possessing high strand displacement activity (Yang et al., 2018). Furthermore, it achieved excellent detection performance without the need for advanced instrumentation or technological expertise (Mori and Notomi, 2020), hence it has

TABLE 4 | Detection of suspected clinical ASFV samples.

Number of Samples	Traditional PCR		CP-LAMP		TaqMan probe real-time PCR	
	Positive	Negative	Positive	Negative	Positive	Negative
61	13	48	17	44	17	44

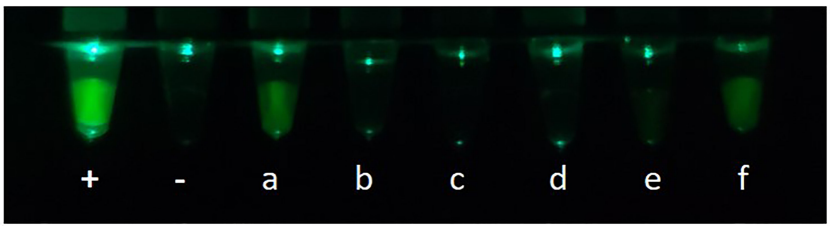

FIGURE 6 | Partial visualization results of clinical samples using the 3D-printed visualization function cassette: +, Positive control; -, Negative control; (a–f) are clinical samples.

the potential to be developed into a simple-to-use on-site molecular assay for diagnosis of ASFV in the field.

In the CP-LAMP ASFV detection method, based on the original primer sets, we targeted the 9GL gene sequence by designing a new fluorophore quencher-labeled cleaved probe with a ribonucleotide insertion; RNase H2 is only activated when the probe perfectly matches the mutant target, leading to the hydrolytic release of a quencher moiety, and consequently an amplified signal (Shen et al., 2020). Our CP-LAMP reaction can be measured in real time using a simple thermocycler to quantify fluorescence; it does not require any additional fluorescent intercalating dyes. Based on a 10-fold dilution series of positive plasmid solutions and their corresponding amplification curves, a standard curve equation was established. There was an excellent correlation between copy number and reaction duration, and the equation could be used for accurate quantification of unknown samples. A LAMP assay using EvaGreen as reported previously (Wang et al., 2020), but this method only achieved objective real-time detection, not quantitative detection. Another study reported an ASFV detection method that combined LAMP and image processing with the hue-saturation-value (HSV) color model. The colorimetric results of this LAMP assay can be used for semi-quantitative analysis of ASFV following HSV color space transformation (Yu et al., 2021).

Our CP-LAMP assay accurately detected ASFV without cross-reacting with other swine viruses, which demonstrates its high specificity. Furthermore, our CP-LAMP method only requires adding a fluorophore quencher-labeled probe, similar to the conventional LAMP method, and the other primer sets and dosage of reagents do not change. This makes is perfect for the highly sensitive standard LAMP strategy. Sensitivity analysis showed that the minimum detectable copy number was 13 copies/μL.

Compared with other methods, our method is more sensitive than traditional PCR assays for detection of ASFV DNA in field samples (Atuhaire et al., 2014). Moreover, the sensitivity of our CP-LAMP method is higher than that of the conventional LAMP assay (copy number = 330) (James et al., 2010), similar to a semi-quantitative colorimetric LAMP method (Yu et al., 2021) and a one-step visual LAMP assay using neutral red dye (Wang et al., 2021). Moreover, quantitative detection by CP-LAMP can be performed on an isothermal real-time instrument rather than a thermocycler, greatly decreasing costs for clinical use. In addition to real-time quantitative detection, we also used a home-made 3D-printed visualization function cassette for detection (**Figure 6**). Furthermore, a mobile phone can be used to both read the results and upload the data. Thus, our succinct operation process meets the needs of on-site diagnosis, and it may be applicable to other pathogens.

In summary, our method achieved real-time, quantitative, and sensitive detection of ASFV by replacing one primer with a probe without adding fluorescent intercalating dyes. The entire detection process can be completed under closed-tube conditions following a one-step sample addition process. Thus, our CP-LAMP detection platform achieves cost-effective, user-friendly, rapid, portable, and accurate POCT for ASFV.

DATA AVAILABILITY STATEMENT

The original contributions presented in the study are included in the article/supplementary material. Further inquiries can be directed to the corresponding authors.

ETHICS STATEMENT

In this study, 61 DNA samples were provided by the Research Center for African Swine Fever Prevention and Control, South China Agricultural University, Guangzhou, China, which did not involve the isolation and identification of ASFV from samples of

relevant sources. It did not include animal research and human research, and there were no ethical issues related to living animals and human. Ethics approval was not needed for this study from the Committee on the Ethics of Animal Experiments of South China Agricultural University, according to the Constitution on the Ethics of Animal Experiments of South China Agricultural University [Hua-nong-ban (2014)23hao], and the guidelines of our institution.

AUTHOR CONTRIBUTIONS

SW: Conceptualization, Methodology, Investigation, Visualization, Writing – original draft, Writing – review and editing. HS: Conceptualization, Writing – review and editing, Supervision. QL: Cassette design, Software. JH: Data curation, Formal analysis. CZ: Visualization, Resources. ZL: Data curation. MS: Data curation. JZ (8th author): Formal analysis. ML: Resources, Supervision, Project administration. YL: Validation, Writing – review & editing. JZ (11th author): Writing – review and editing, Supervision, Project.

FUNDING

This work was supported by the Key-Area Research and Development Program of Guangdong Province (2019B0 20211005), the Special Topic on Emergency Prevention and Control of African Classical Swine Fever in Guangdong Province (2019B020211003), the Independent Research and Development Projects of Maoming Laboratory (2021ZZ003), the Special Fund for Scientific Innovation Strategy-construction of High Level Academy of Agriculture Science-Prominent Talents (R2020PY-JC001), and the Science and Technology Planning Project of Guangdong Province (2020A1515010950, 2021A1515011125).

REFERENCES

Atuhaire, D. K., Af Ayoa, M., Ochwo, S., Katiti, D., Mwiine, F. N., Nanteza, A., et al. (2014). Comparative Detection of African Swine Fever Virus by Loop-Mediated Isothermal Amplification Assay and Polymerase Chain Reaction in Domestic Pigs in Uganda. *Afr. J. Microbiol. Res.* 8 (23), 2322–2328. doi: 10.5897/AJMR2014.6848

Cadenas-Fernández, E., Sánchez-Vizcaíno, J. M., Pintore, A., Denurra, D., Cherchi, M., Jurado, C., et al. (2019). Free-Ranging Pig and Wild Boar Interactions in an Endemic Area of African Swine Fever. *Front. Vet. Sci.* 6. doi: 10.3389/fvets.2019.00376

Fernández-Pinero, J., Gallardo, C., Elizalde, M., Robles, A., Gómez, C., Bishop, R., et al. (2013). Molecular Diagnosis of African Swine Fever by a New Real-Time PCR Using Universal Probe Library. *Transbound Emerg. Dis.* 60 (1), 48–58. doi: 10.1111/j.1865-1682.2012.01317.x

Galindo, I., and Alonso, C. (2017). African Swine Fever Virus: A Review. *Viruses* 9 (5):103. doi: 10.3390/v9050103

Goto, M., Honda, E., Ogura, A., Nomoto, A., and Hanaki, K. (2009). Colorimetric Detection of Loop-Mediated Isothermal Amplification Reaction by Using Hydroxy Naphthol Blue. *Biotechniques* 46 (3), 167–172. doi: 10.2144/000113072

He, Q., Yu, D., Bao, M., Korensky, G., Chen, J., Shin, M., et al. (2020). High-Throughput and All-Solution Phase African Swine Fever Virus (ASFV) Detection Using CRISPR-Cas12a and Fluorescence Based Point-of-Care System. *Biosens Bioelectron* 154, 112068. doi: 10.1016/j.bios.2020.112068

Hill, J., Beriwal, S., Chandra, I., Paul, V. K., Kapil, A., Singh, T., et al. (2008). Loop-Mediated Isothermal Amplification Assay for Rapid Detection of Common Strains of Escherichia Coli. *J. Clin. Microbiol.* 46 (8), 2800–2804. doi: 10.1128/jcm.00152-08

James, H. E., Ebert, K., McGonigle, R., Reid, S. M., Boonham, N., Tomlinson, J. A., et al. (2010). Detection of African Swine Fever Virus by Loop-Mediated Isothermal Amplification. *J. Virol. Methods* 164 (1-2), 68–74. doi: 10.1016/j.jviromet.2009.11.034

King, D. P., Reid, S. M., Hutchings, G. H., Grierson, S. S., Wilkinson, P. J., Dixon, L. K., et al. (2003). Development of a TaqMan PCR Assay With Internal Amplification Control for the Detection of African Swine Fever Virus. *J. Virol. Methods* 107 (1), 53–61. doi: 10.1016/s0166-0934(02)00189-1

Li, X., and Tian, K. (2018). African Swine Fever in China. *Vet. Rec* 183 (9), 300–301. doi: 10.1136/vr.k3774

Ma, J., Chen, H., Gao, X., Xiao, J., and Wang, H. (2020). African Swine Fever Emerging in China: Distribution Characteristics and High-Risk Areas. *Prev. Vet. Med.* 175, 104861. doi: 10.1016/j.prevetmed.2019.104861

McKillen, J., McMenamy, M., Hjertner, B., McNeilly, F., Uttenthal, Å., Gallardo, C., et al. (2010). Sensitive Detection of African Swine Fever Virus Using Real-Time PCR With a 5′ Conjugated Minor Groove Binder Probe. *J. Virol Methods* 168 (1), 141–146. doi: 10.1016/j.jviromet.2010.05.005

Mori, Y., and Notomi, T. (2020). Loop-Mediated Isothermal Amplification (LAMP): Expansion of its Practical Application as a Tool to Achieve Universal Health Coverage. *J. Infect. Chemother.* 26 (1), 13–17. doi: 10.1016/j.jiac.2019.07.020

Normile, D. (2018). Arrival of Deadly Pig Disease Could Spell Disaster for China. *Science* 361 (6404), 741. doi: 10.1126/science.361.6404.741

Sánchez-Vizcaíno, J. M., and Mur, L. (2013). African Swine Fever Diagnosis Update. *Dev. Biol. (Basel)* 135, 159–165. doi: 10.1159/000189240

Shen, H., Wen, J., Liao, X., Lin, Q., Zhang, J., Chen, K., et al. (2020). A Sensitive, Highly Specific Novel Isothermal Amplification Method Based on Single-Nucleotide Polymorphism for the Rapid Detection of Salmonella Pullorum. *Front. Microbiol.* 11. doi: 10.3389/fmicb.2020.560791

Tomita, N., Mori, Y., Kanda, H., and Notomi, T. (2008). Loop-Mediated Isothermal Amplification (LAMP) of Gene Sequences and Simple Visual Detection of Products. *Nat. Protoc.* 3 (5), 877–882. doi: 10.1038/nprot.2008.57

Wang, Y., Dai, J., Liu, Y., Yang, J., Hou, Q., Ou, Y., et al. (2021). Development of a Potential Penside Colorimetric LAMP Assay Using Neutral Red for Detection of African Swine Fever Virus. *Front. Microbiol.* 12. doi: 10.3389/fmicb.2021.609821

Wang, D., Yu, J., Wang, Y., Zhang, M., Li, P., Liu, M., et al. (2020). Development of a Real-Time Loop-Mediated Isothermal Amplification (LAMP) Assay and Visual LAMP Assay for Detection of African Swine Fever Virus (ASFV). *J. Virol. Methods* 276, 113775. doi: 10.1016/j.jviromet.2019.113775

Wen, J., Gou, H., Wang, S., Lin, Q., Chen, K., Wu, Y., et al. (2021). Competitive Activation Cross Amplification Combined With Smartphone-Based Quantification for Point-of-Care Detection of Single Nucleotide Polymorphism. *Biosens Bioelectron* 183, 113200. doi: 10.1016/j.bios.2021.113200

Yang, Q., Domesle, K. J., and Ge, B. (2018). Loop-Mediated Isothermal Amplification for Salmonella Detection in Food and Feed: Current Applications and Future Directions. *Foodborne Pathog. Dis.* 15 (6), 309–331. doi: 10.1089/fpd.2018.2445

Yoon, H., Hong, S. K., Lee, I., Yoo, D. S., Jung, C. S., Lee, E., et al. (2020). Clinical Symptoms of African Swine Fever in Domestic Pig Farms in the Republic of Korea. *Transbound Emerg. Dis.* 67, 2245–2248 doi: 10.1111/tbed.13552

Yu, L. S., Chou, S. Y., Wu, H. Y., Chen, Y. C., and Chen, Y. H. (2021). Rapid and Semi-Quantitative Colorimetric Loop-Mediated Isothermal Amplification

Detection of ASFV *via* HSV Color Model Transformation. *J. Microbiol. Immunol. Infect.* 54 (5), 963–970. doi: 10.1016/j.jmii.2020.08.003

Conflict of Interest: The authors declare that the research was conducted in the absence of any commercial or financial relationships that could be construed as a potential conflict of interest.

Publisher's Note: All claims expressed in this article are solely those of the authors and do not necessarily represent those of their affiliated organizations, or those of the publisher, the editors and the reviewers. Any product that may be evaluated in this article, or claim that may be made by its manufacturer, is not guaranteed or endorsed by the publisher.

Advantages of publishing in Frontiers

OPEN ACCESS
Articles are free to read for greatest visibility and readership

FAST PUBLICATION
Around 90 days from submission to decision

HIGH QUALITY PEER-REVIEW
Rigorous, collaborative, and constructive peer-review

TRANSPARENT PEER-REVIEW
Editors and reviewers acknowledged by name on published articles

Frontiers
Avenue du Tribunal-Fédéral 34
1005 Lausanne | Switzerland

Visit us: www.frontiersin.org
Contact us: frontiersin.org/about/contact

REPRODUCIBILITY OF RESEARCH
Support open data and methods to enhance research reproducibility

DIGITAL PUBLISHING
Articles designed for optimal readership across devices

FOLLOW US
@frontiersin

IMPACT METRICS
Advanced article metrics track visibility across digital media

EXTENSIVE PROMOTION
Marketing and promotion of impactful research

LOOP RESEARCH NETWORK
Our network increases your article's readership